New Insights into Pyrogenic Carbon by an Improved Benzene Polycarboxylic Acid Molecular Marker Method

Dissertation

zur

Erlangung der naturwissenschaftlichen Doktorwürde
(Dr. sc. nat.)

vorgelegt der

Mathematisch-naturwissenschaftlichen Fakultät

der

Universität Zürich

von

Daniel B. Wiedemeier

aus

Würenlos AG

Promotionskomitee

Prof. Dr. Michael W.I. Schmidt (Vorsitz)

Prof. Dr. Guido L.B. Wiesenberg

Prof. Dr. Willy Tinner

Dr. Jens Leifeld

Zürich, 2014

Table of Contents

Abbreviations

BC	Black Carbon
BPCA	Benzene Polycarboxylic Acids
B3CA, B4CA, B5CA, B6CA	BPCAs with 3, 4, 5 or 6 carboxylic groups, respectively
C	Carbon
CV	Coefficient of Variation
EA	Elemental Analysis
GC	Gas Chromatography
HPLC	High Pressure Liquid Chromatography
HTT	Highest Heating Treatment
LC	Liquid Chromatography
MIR	Mid-Infrared
NEXAFS	Near Edge X-Ray Absorption Fine Structure
NMR	Nuclear Magnetic Resonance
OC	Organic Carbon
PAH	Polycyclic Aromatic Hydrocarbons
PyC	Pyrogenic Carbon
PyOM	Pyrogenic Organic Matter
SOC	Soil Organic Carbon
TOC	Total Organic Carbon

Summary

Due to its persistence, pyrogenic carbon (PyC) is ubiquitous in the environment and its abundance might even increase with the projected increase in global wildfire activity and the continued burning of fossil fuel. PyC is also increasingly produced from the industrial pyrolysis of organic wastes, which yields charred soil amendments (biochar). Moreover, the emergence of nano-technology may also result in the release of PyC-like compounds to the environment. It is thus a high priority to detect, characterize and quantify these charred, carbonaceous materials in order to further investigate their properties and role in the environment.

This thesis describes the improvement and consolidation of the benzene polycarboxylic acid (BPCA) molecular marker method for PyC research. First, the method was thoroughly improved with respect to universal applicability, simpler handling, better reproducibility and smaller required sample amounts. In a next step, the improved method was applied in the context of two case studies to further illuminate its relevance and plausibility for PyC quantification in environmental research. In a third step, we tested the improved BPCA method's suitability for isolation and compound-specific isotopic (^{13}C, ^{14}C) analysis of PyC. Finally, we conducted two methodological studies including various other PyC methods to assess the BPCA method's potential for PyC characterization.

We could show that the improved BPCA method is an extremely useful and versatile tool for PyC research. It now affords highly robust estimates of PyC quantity in any kind of environmental sample materials while only requiring minimal sample amounts and significantly reduced analysis time. The improved BPCA method consequently yielded very insightful and plausible results when it was first applied in the context of two environmental case studies: For wildfire reconstructions, the method demonstrated its sensitivity to very small sedimentary PyC particles, thus providing interesting additional information to the conventional microscopic charcoal method. Similarly, it robustly assessed relevant differences in soil PyC contents of two adjacent ecosystems in the case of a soil carbon turnover study. On top of these first successful applications, the improved BPCA procedure was found to be perfectly suitable for compound-specific isotopic analysis of PyC, which considerably broadens the scope of the here presented method. Finally, the BPCA method was successfully embedded in the context of various PyC characterization techniques and it demonstrated its particular usefulness for the assessment of aromatic features in PyC.

The improved BPCA method now fully exploits the potential of its molecular marker approach for PyC research, which turns it into one of the most versatile PyC methods available to date. The method is expected to yield exciting insights about pyrogenic materials across different scientific disciplines. Examples for its use include the investigation of PyC in different soil fractions, illuminating the stabilization mechanisms of fire-derived organic matter or the assessment of fire residues in sediments, leading to a better understanding of pyrogeography.

Zusammenfassung

In der Natur ist pyrogener Kohlenstoff (PyC) sehr weit verbreitet aufgrund seiner stabilen Eigenschaften und der daraus resultierenden langen Verweilzeiten. Zudem dürfte der Anteil von PyC künftig durch häufigere Vegetationsbrände und dem grossskaligen Verbrennen von fossilen Energieträgern noch zunehmen. Pyrogener Kohlenstoff wird auch bei der Verkohlung von organischen Abfällen hergestellt, die als Biokohlen zur Verbesserung der Bodeneigenschaften und zur Kohlenstoffspeicherung immer häufiger dem Boden zugeführt werden. Schliesslich stellt das Aufkommen der Nanotechnologie eine weitere Quelle dar, die PyC ähnliche Verbindungen in die Umwelt freisetzen könnte. Aus all diesen Gründen ist es enorm wichtig, diese pyrogenen Substanzen zu detektieren, zu charakterisieren und zu quantifizieren, damit wir Einsichten über ihre Eigenschaften und ihr Verhalten in der Natur erhalten.

Diese Dissertation beschreibt die Verbesserung und Konsolidierung einer Methode, die Benzol Polycarboxylische Säuren (BPCA) als molekulare Marker für PyC nutzt. Zuerst wurde die Methode selbst gründlich verbessert in Bezug auf universelle Anwendbarkeit, einfachere Durchführung, verbesserte Reproduzierbarkeit und kleinere Probemengen. In einem nächsten Schritt wurde die verbesserte BPCA Methode im Kontext zweier Umweltfallstudien angewandt um ihre Relevanz und Plausibilität für die PyC Forschung zu prüfen. In einem dritten Schritt wurde untersucht, ob sich die verbesserte BPCA Methode für die Isolierung und komponentenspezifische Isotopenanalyse von PyC eignet. Schliesslich führten wir noch zwei methodische Studien unter Einbezug von weiteren PyC Methoden durch um das Potenzial der BPCA Methode für die PyC Charakterisierung zu evaluieren.

Wir konnten zeigen, dass die verbesserte BPCA Methode ein extrem nützliches und vielseitiges Instrument für die PyC Forschung darstellt. Die Methode ermöglicht nun hochrobuste Abschätzungen von PyC Mengen in allen möglichen Umweltproben währendem die erforderlichen Probemengen und der Analyseaufwand signifikant reduziert werden konnten. Daraufhin wurden in zwei Fallstudien auch äusserst plausible und relevante Daten erhoben, die zur Rekonstruktion der Feuergeschichte und zum Verständnis des Bodenkohlenstoffumsatzes einen wesentlichen Beitrag leisteten. Die verbesserte BPCA Methode eignet sich zudem tatsächlich hervorragend für die komponentenspezifische Isotopenanalyse von PyC, was ihre Anwendungsmöglichkeiten nochmals deutlich erweitert. Schliesslich wurde die BPCA Methode auch erfolgreich mit anderen PyC Charakterisierungsmethoden in Verbindung gebracht. In diesem Rahmen konnte sie ihre Nützlichkeit zur Erfassung von aromatischen Merkmalen in PyC erfolgreich unter Beweis stellen.

Die verbesserte BPCA Methode deckt nun das Potenzial dieses molekularen Marker Ansatzes umfassend ab, was sie zum jetzigen Zeitpunkt zu einer der vielseitigsten PyC Methoden überhaupt macht. Damit kann die in dieser Dissertation entwickelte Methode einen wichtigen Beitrag zur Forschung an PyC in unterschiedlichsten Disziplinen leisten.

Mögliche Anwendungsbereiche sind beispielsweise die Erforschung von PyC in verschiedenen Bodenfraktionen, was Aufschluss über die Stablisierungsmechanismen von PyC geben könnte oder aber die verfeinerte Messung von Feuerrückständen in Sedimenten, was zu neuen Einsichten im Feld der Pyrogeographie führen dürfte.

Part A - Synopsis

This is a cumulative thesis, based on five individual studies. In part A, the main findings of the individual studies are summarized and an outlook for future research is given. Further results and more detailed discussion can be found in part B, presenting the individual studies that are published in, or submitted to, international peer-reviewed journals.

1. Introduction

1.1. Fire, combustion and pyrogenic carbon (PyC)

Fire, or more generally, combustion, is a rapid oxidation process that produces a suite of different chemical products (Torero, 2013). In a complete combustion process, biomass or fossil fuel is converted into CO_2, H_2O and inorganic residues (ash). However, under local or temporal oxygen limitations, combustion becomes incomplete and pyrolysis takes place, which produces a solid organic residue known as char (Shafizadeh, 1982). These charred residues are also referred to as pyrogenic organic matter (PyOM) and mainly consist of pyrogenic carbon (PyC) or, synonymously, black carbon (BC) (Simoneit, 1984; Goldberg, 1985; Preston and Schmidt, 2006).

Charring processes are omnipresent and can be part of both, natural and anthropogenic combustion (Schmidt and Noack, 2000; Scott et al., 2014). Wildfires are an important natural process, intrinsic to most ecosystems, which produces a significant quantity of PyC each year (Tinner et al., 1999; Forbes et al., 2006; Preston and Schmidt, 2006; Bowman et al., 2009; Krawchuk et al., 2009). Similarly, the burning of fossil fuel for energy production in industry and transport presents an important anthropogenic source of PyC (Bond et al., 2004; Cao et al., 2006; Bond et al., 2013) . Both sources contribute to the ubiquity of PyC in the environment: PyC is present in the air, in the form of aerosols (Ramanathan and Carmichael, 2008; Bond et al., 2013), in water as particulate or dissolved organic matter (Dittmar and Koch, 2006; Dittmar, 2008; Ziolkowski and Druffel, 2010), as well as in ice cores (McConnell et al., 2007; Ming et al., 2008), soils (Glaser et al., 1998; Knicker, 2011) and sediments (Masiello and Druffel, 1998; Gustafsson et al., 2001; Sánchez-García et al., 2013) in sizes varying from m to nm (e.g. large charred tree trunk after a forest fire or nano-scale soot particles that escape a diesel engine exhaust).

The ubiquity of PyC in the environment is not only due to large production rates but also to its long persistence and relative stability against degradation (Marschner et al., 2008; Kuzyakov et al., 2009). Although exact turnover times have not yet been established, and may depend upon specific environmental conditions (Schmidt et al., 2011; Singh et al., 2012b), it is clear that PyC is less readily decomposed into CO_2 than most other forms of organic carbon (Santos et al., 2012; Kuzyakov et al., 2014). This observation has an important implication for the global C cycle: As charred materials store PyC for a relatively long time, they sequester C in organic forms that would otherwise be rapidly respired as CO_2, thus reducing atmospheric greenhouse gas concentrations over time (Kuhlbusch, 1998; Liang et al., 2008).

Besides the climate mitigating aspect, chars have further environmentally relevant properties. Their high porosity, large surface area and negative surface charge can immobilize hazardous compounds (Beesley et al., 2011) and improve soil fertility (Biederman and Harpole, 2013). As an example, the fertile Anthropogenic Dark Earth soils within

infertile Ferralsols in the Amazon basin are attributed to indigenous charring practices of organic wastes in pre-Columbian times (Glaser and Birk, 2012). The recognition of chars as a potentially beneficial soil amendment led to the emerging field of so-called biochar technology (Lehmann and Joseph, 2009), which is a modern implementation of this old concept: Organic wastes are charred in kilns producing bioenergy as well as biochar, with which C can be sequestered and soil properties improved (Lehmann et al., 2006; Meyer et al., 2011).

Biochar will likely be produced on large scales in the coming years and thus significantly increase PyC abundance in soils (Marris, 2006). Moreover, the occurrence of wildfires (cf. Figure 1) and the burning of fossil fuels are also projected to remain high over the course of the 21th century, continuously contributing large quantities of PyC to the environment (Bond et al., 2004; Flannigan et al., 2013; Kelly et al., 2013). Another increasingly important source of PyC is likely to be nanotechnology that also uses PyC-like compounds (Hoet et al., 2004; Ziolkowski and Druffel, 2009a). It is thus crucial to detect, characterize and quantify these pyrogenic materials accurately in order to investigate their properties and understand their role in the environment with respect to e.g. carbon cycle (Schmidt and Noack, 2000) , soil properties (Sohi et al., 2010), radiative effects in the atmosphere (Ramanathan and Carmichael, 2008) or health hazards (Boffetta et al., 1997; Wilcke, 2000; Koelmans et al., 2006; Lam et al., 2006). A better assessment of PyC will also enable us to better appreciate PyC records as a way to reconstruct paleofire histories (Conedera et al., 2009) and anthropogenic pollution of the past (Meyers, 2003; Louchouarn et al., 2006) or to evaluate archeological artifacts (Ascough et al., 2010; Bird and Ascough, 2012) .

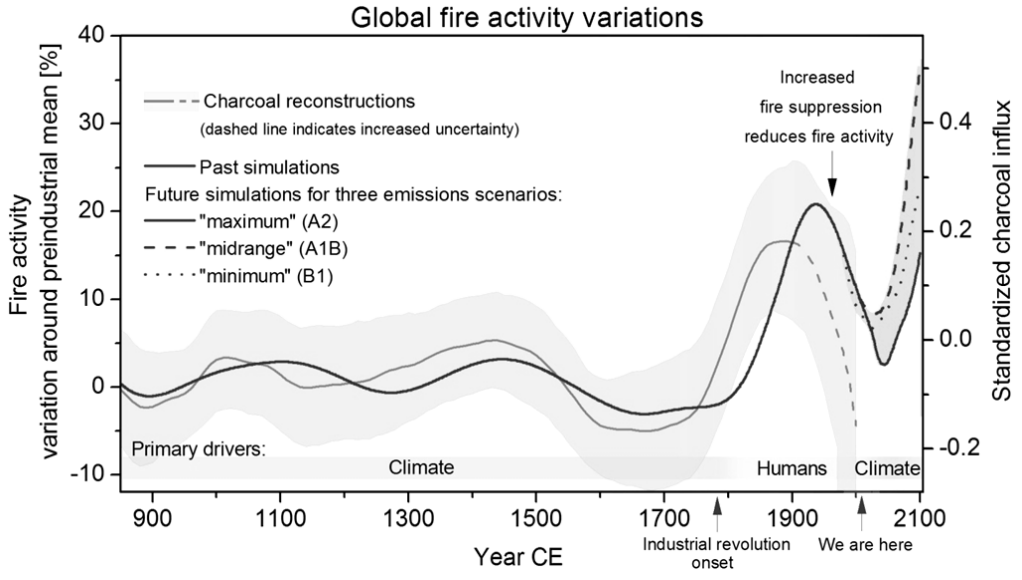

Figure 1: Reconstructions of fire activity based on sedimentary charcoal records shows fire history over the last millennium (gray). Modeled fire activity (black), based on climatic and ecological factors, closely matches the reconstruction data and predicts increasing fire activity for the near future. The magnitude of increased fire activity in this model is dependent on greenhouse gas emission scenarios. Source: Pechony and Shindell (2010).

1.2. Methods for PyC detection, quantification, characterization and isolation

PyC includes a large variety of very different materials, sharing the fact that they are combustion-derived (Masiello, 2004). Determining factors for any combustion product are i) the precursor material and ii) the combustion conditions, such as highest heating temperature (HTT), heating duration or oxygen availability (Lehmann and Joseph, 2009; Singh et al., 2012a). PyC is thus best understood with the concept of the 'combustion continuum' (Figure 2) that describes the change of typical physico-chemical properties over a range of combustion conditions, showing the variety of possible PyC products (Hedges et al., 2000; Masiello, 2004; Conedera et al., 2009).

	combustion continuum			
	uncharred biomass	slightly charred biomass	charcoal	soot and graphitic black carbon → graphite
		combustion residues		condensates
properties, characteristics or parameters	typical value, range of values, and/or trend (shaded area)			
size	mm and larger	cm to micron		micron to submicron
formation temperature	<300 °C	200-600 °C		>500 °C
recognizability of plant structures	wood structure	altered wood structure		graphite-like structure
dominant shape		angular appearance		globular or spherical habit
difficulties in defining the origin of the particles	plant species	plant family or even genus		combustion process
chemical stability (inertia, reactivity)				
stability against thermal oxidation				
O/C ratio	0.6-0.4	0.4-0.2		<0.2
H/C ratio	1.2-0.8	0.8-0.4		<0.4
N concentration				?
aromaticity of chemical structure, fraction of Aryl C				
bulk density	0.3-0.8 g/cm^3	0.1-0.6 g/cm^3		0.7-1.1 g/cm^3
total surface area by nitrogen adsorption (BET method)	?	7-326 m^2/g		0.9-100 m^2/g
total pore volume by mercury porosimetry	0.5 cm^3/g	0.7-4 cm^3/g		1.1 cm^3/g
electrical resistivity	10^{16}-10^{2} Ω·cm	10^{8}-10^{-1} Ω·cm		10^{1}-10^{-3} Ω·cm
reflectance				
transport in suspension				
typical sedimentary distance from the source				
supposable residence time in intermediate sedimentary pools				

Figure 2. The combustion continuum, demonstrating the variety of PyC and a few of its properties. Source: Conedera et al. (2009), adapted from Hedges et al. (2000), Masiello (2004) and others.

Due to this large variety of PyC, it seems impossible to uniquely define it on a physico-chemical basis. However, one defining property of PyC is its aromatic C structure, which originates from the thermal treatment and increases with increasing thermal overprint (Lehmann and Joseph, 2009). It consists of at least two different aromatic C phases: i) an amorphous phase comprising randomly organized aromatic rings and ii) a crystalline phase, comprising condensed polyaromatic sheets that are turbostratically aligned (Franklin, 1951; Cohen-Ofri et al., 2006; Keiluweit et al., 2010). The high amount of these aromatic C structures in PyC is thought to largely determine its relatively high stability against degradation in the environment and contributes to its porous nature (Downie et al., 2009; Lehmann et al., 2009). The unique C aromatic features and resulting higher stability and porosity of PyC in comparison to unaltered biomass (cf. Figure 2) are also employed in methods that aim to detect, quantify, characterize and isolate these materials.

Pyrogenic materials have been investigated in many different scientific disciplines with various objectives. Sedimentary wildfire reconstruction in the field of natural history (Patterson et al., 1987; Conedera et al., 2009), the assessment of global C pools in biogeochemistry (Gonzalez-Perez et al., 2004; Schmidt et al., 2011) or the economical and ecological production of biochars for green technology (Manyà 2012; Schimmelpfennig and Glaser, 2012) are just a few examples. Given the different traditions of PyC research and the above discussed wide definition of PyC itself, it is not surprising that many different PyC methods have been developed over time. An overview of a few currently used PyC methods is given in Table 1. They are grouped according to their measurement principle: Physical techniques rely on the fact that PyC is a highly porous material, with lower density than other OM. The chemical and thermal techniques employ the characteristic stability of PyC to differentiate it from other forms of OM. In contrast, spectroscopic and molecular marker techniques investigate pyrogenic compounds (mostly forms of aromatic C) by looking at the chemical composition of organic matter.

Besides differences in cost, availability and required expertise, each method has its own strengths and weaknesses with respect to applicability. Some methods are limited to a certain part of the combustion continuum (Schmidt et al., 2001). The chemo-thermal oxidation method (CTO) (Gustafsson et al., 2001), for example, leaves much PyC undetected and is only sensitive to the most stable PyC particles, such as soot (Hammes et al., 2007). Sometimes combinations of different methods yield good solutions. It is for example obvious from Table 1 that the chemical oxidation methods generally provide suitable isolation of PyC from environmental matrices whereas spectroscopic techniques are a good choice to characterize pure or purified PyC. Thus, the two approaches are often used sequentially, with a classical example being the use of the UV oxidation procedure in combination with subsequent NMR analysis (Skjemstad et al., 1993; Skjemstad et al., 1999).

Table 1. A selection of some common PyC methods, listed according to their measurement principle. Depending on the individual method, detection (1) of PyC can be broad or limited to certain parts of the combustion continuum. Likewise, the methods show different suitability for quantification (2) of PyC in environmental matrices and the characterization (3) of pure PyC. Methods that are capable to isolate PyC (4) from e.g. soils and sediments are of special interest as they can lead to isotopic measurements of PyC in the environment. Source: Michael Bird, James Cook University, Australia (unpublished), modified.

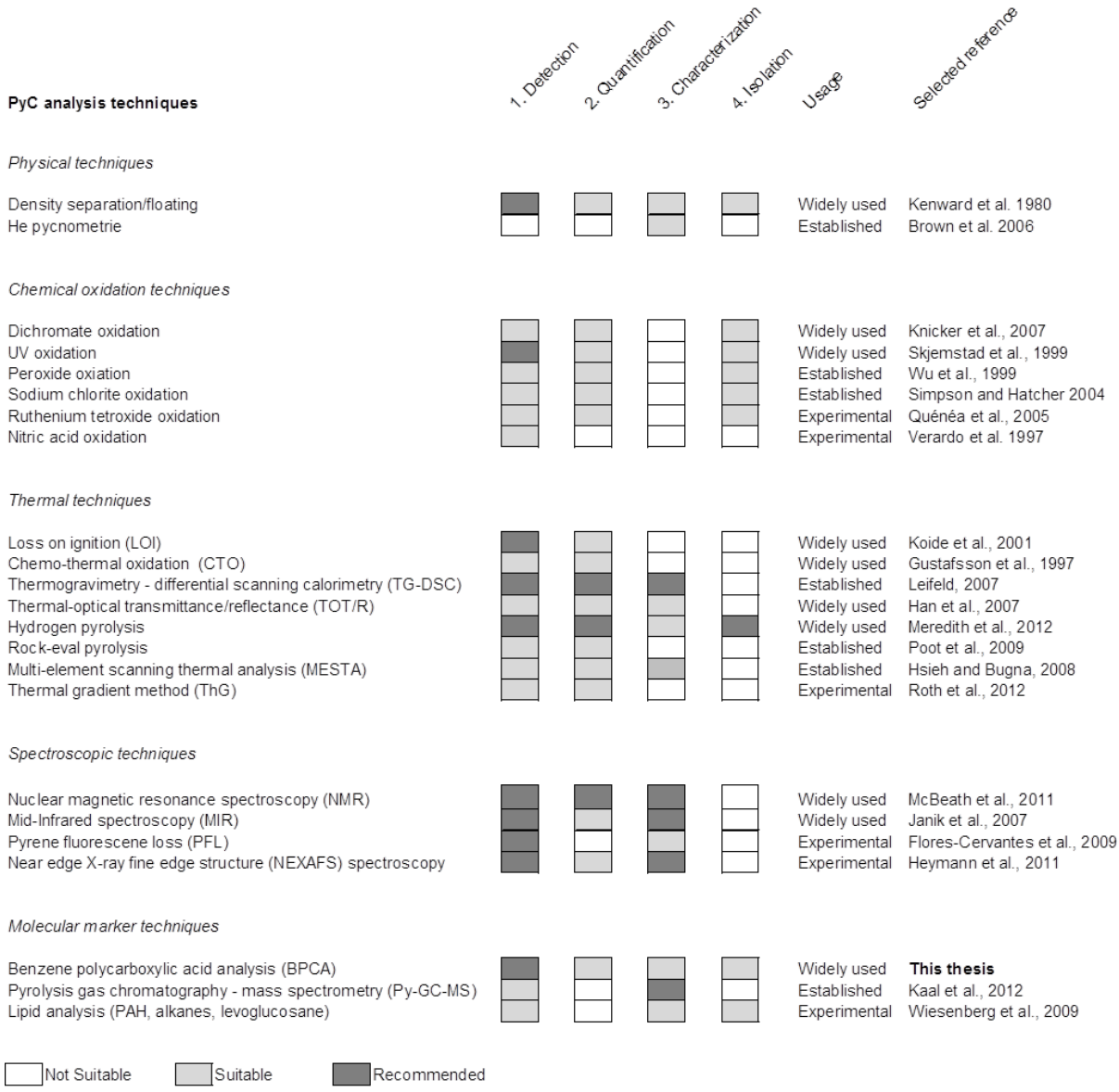

With respect to applicability, the molecular marker technique of benzene polycarboxylic acid (BPCA) analysis is potentially one of the most versatile methods. It targets the above discussed characteristic polyaromatic structures of PyC. However, due to their size and complexity, these large polyaromatic clusters are not directly assessable by chromatographic means. In order to chromatographically analyze such pyrogenic structures, PyC is first digested with nitric acid under high temperature and pressure, which breaks the large polyaromatic compounds down into its building blocks, the individual BPCAs (Glaser et al., 1998; Dittmar, 2008). The BPCAs are then, after a few purification steps, amenable to chromatographic analysis (Glaser et al., 1998; Brodowski et al., 2005). PyC is thus isolated and analyzed on a molecular level and can also be used to quantify PyC abundance in environmental compartments such as soils or sediments. The BPCA method additionally characterizes the investigated PyC when relative yields of B3-, B4-, B5- and B6CA are compared: The respective proportion of differently carboxylated BPCAs is linked to the size of the original polyaromatic clusters and is therefore indicative of PyC's quality (McBeath et al., 2011; Schneider et al., 2011). Moreover, the method is theoretically an ideal pre-procedure to analyse the C isotopic composition (^{13}C and ^{14}C) of PyC because the BPCAs derive directly from pure PyC clusters if no contamination is introduced during the procedure (Ziolkowski and Druffel, 2010; Coppola et al., 2013). Compound-specific isotopic analysis of PyC is of great interest (Bird and Ascough, 2012) as it can be used, e.g. to distinguish between the precursor biomass of chars in tropical regions (Roscoe et al., 2001; Wiedemeier et al., 2012), to derive the age of charred materials (Pessenda et al., 1996; Bird et al., 1999) or to trace PyC in C cycling studies with an isotopic label (Kuzyakov et al., 2009; Fang et al., 2014; Maestrini et al., 2014).

The original BPCA method using gas chromatography (GC) was first introduced by Glaser et al. (1998) and further developed over time by Brodowski et al (2005) and Schneider et al. (2010). Although the GC method has greatly supported PyC research for a long time (Glaser et al., 2000; Czimczik et al., 2005; Dai et al., 2005; Brodowski et al., 2007; Guggenberger et al., 2008; Hammes et al., 2008b), it exhibits several important drawbacks, e.g. laborious sample processing, poor reproducibility or the requirement of relatively large sample amounts. The necessary derivatization for GC furthermore leads to extraneous C contamination, which considerably complicates the highly desirable isotopic analyses of BPCAs (Coppola et al., 2013). Recently, it was shown that the BPCA procedure could be simplified for highly organic seawater or charcoal samples by analyzing the BPCAs on a high-performance liquid chromatography system ($HPLC_{organic}$) (Dittmar, 2008). Liquid chromatography does not require the time-consuming, external carbon-introducing and sometimes incomplete derivatization, which is necessary for the GC method. Although the $HPLC_{organic}$ method works well with highly organic samples (Schneider et al., 2011), BPCA analyses of more complex environmental materials proved to be difficult due to interference from organic and inorganic substances. Moreover, the $HPLC_{organic}$ method uses tetra-butylammonium bromide, an organic modifier that prohibits the use of mass spectrometry, also precluding much needed isotopic analyses of BPCAs.

This thesis aimed to develop a thoroughly improved and tested BPCA method that combines the universal applicability of the GC approach with the advantages of the $HPLC_{organic}$ method. In addition to an improved and simplified assessment of PyC in the environment, the aim was to make the method fully compatible with subsequent ^{13}C and ^{14}C analysis of BPCAs in order to entirely exploit the potential of the BPCA molecular marker approach. Such a versatile yet simple BPCA method is likely to become widely used, which is why we also further investigated the BPCA method's theoretical foundation and suitability for PyC quantification and characterization by putting it into a framework with a variety of other PyC methods.

2. Objectives

In detail, this thesis addresses the following research questions:

I. Can we improve the BPCA molecular marker method with respect to i) universal applicability, ii) simpler handling iii) better reproducibility and iv) smaller sample amounts? → Paper I.

Two approaches have been used to measure BPCA molecular markers: The GC protocol has been followed for environmental samples (e.g. soils or sediments (Glaser et al., 1998; Brodowski et al., 2005; Schneider et al., 2010)) while an $HPLC_{organic}$ approach has recently been proposed for purely organic samples (e.g. chars or dissolved organic matter (Dittmar, 2008; Schneider et al., 2011)). Both approaches have been continuously improved but a simple and thoroughly tested universal approach has not been developed yet. From a practical point of view, it is certainly desirable to have one method available, which is universally applicable, simple to implement and highly reproducible while requiring minimal sample amounts.

II. Is the improved BPCA method a suitable tool for environmental research? → Paper I and paper II.

While the improved BPCA method was tested thoroughly with reference PyC sample materials, the question remained whether it also yields plausible and relevant results when applied in environmental research. Two case studies, using specific sediment and soil samples with difficult matrices and partially very low C contents illuminated the plausibility and relevance of the improved BPCA method.

III. Can the improved BPCA molecular marker method lead to compound-specific ^{13}C and ^{14}C analysis of BPCAs? → Paper III

The possibility to measure C isotopic values directly on the BPCA molecular markers would largely extend the scope of the BPCA method. Molecular isotopic information of PyC would for example be crucial to distinguish between the char contributions of C3 versus C4 plants in tropical regions (^{13}C), to determine the age and turnover of charred materials in soils (^{14}C) or to trace labeled chars in the environment (^{13}C or ^{14}C) (Bird and Ascough, 2012). Although attempts have been made to measure C isotopic contents of BPCAs, they are either limited to only ^{13}C (Yarnes et al., 2011), suffer from laborious preparation that can introduce extraneous carbon (Ziolkowski and Druffel, 2010; Coppola et al., 2013) or are not compound-specific *sensu stricto* (Kuzyakov et al., 2014).

IV. How is the BPCA method linked to other PyC methods? → Paper IV and paper V.

There are many methods available for the chemical or physical characterization of PyC (cf. Table 1). Many of these methods are based on a direct or indirect assessment of the aromatic features of PyC, which are the defining property of chars on a chemical level (Lehmann and Joseph, 2009). The concept of the BPCA method to isolate the individual moieties of large polyaromatic clusters has been investigated before (Dittmar, 2008; Schneider et al., 2010; McBeath et al., 2011) but has not been put in a consistent framework with the assessments of other PyC methods. We thus further investigated how a suite of seven very different methods assessed the aromatic features in chars. Moreover, we conducted an in-depth comparison between the BPCA and the PAH method (Simoneit, 2002), one of the few other methods that is also based on a direct molecular marker approach of aromatic compounds.

3. Materials and methods

2.1. Environmental PyC reference materials (paper I)

A suite of previously characterized environmental PyC reference materials was employed for the BPCA method development and evaluation, including Aerosol (NIST Standard SRM 1649 – Urban Dust), Marine Sediment (NIST Standard SRM 1941b), Vertisol (Clay Soil), Chernozem (Silty Soil), Dissolved Organic Matter (DOM), Wood Charcoal (pyrolyzed *Castanea Sativa*), Grass Charcoal (pyrolyzed *Oryza Sativa*) and n-hexane soot (Hammes et al., 2006; Hammes et al., 2007; Hammes et al., 2008a).

2.2. Field samples (paper I and paper II)

The improved BPCA method was then applied in the framework of two environmentally relevant studies. The first one was geared towards wildfire reconstruction using sedimentary records of PyC. A 2.5 m long peatland core from Bega Swamp (Polach and Singh, 1980; Green et al., 1988) (NSW, Australia, 36° 32‘ 1.79‘‘ S, 49° 29‘ 55.12‘‘ E) was analyzed for this purpose. The second study investigating soil C turnover in an old-growth coast redwood forest (*Sequoia sempervirens*) and adjacent prairie (Califoria, USA, 41° 24' 25.92" N, 124° 1' 9.1194" W) used soil samples down to 110 cm depth.

2.3. Isotopic PyC reference materials (paper III)

For the validation of compound-specific isotopic analysis of BPCAs, two char samples were used with contrasting ^{14}C contents. One sample, called ‘Fossil Char’, with a very low ^{14}C content of 0.003 +/- 0.001 $F^{14}C$ and therefore an age of ca. 50 ka BP was from *in situ* charred trees in West-Central Sumatra (Alloway et al., 2004; Ascough et al., 2009). The above mentioned Wood Charcoal reference material (pyrolyzed *Castanea Sativa*) was taken as the modern analogue with high $F^{14}C$ values of 1.149 +/- 0.004 $F^{14}C$ and was termed ‘Modern Char’ (Hammes et al., 2006).

2.4. PyC thermosequences (paper IV and paper V)

The comparison of PyC characterization methods required materials that were pyrolyzed at different temperatures as aromatic features are thought to change with HTT (cf. Figure 2). We did not only systematically vary temperature (100 – 1000 °C) but also pyrolysis time (1h and 5h) and starting material (chestnut wood, pine wood, fescue grass and rice grass), thus producing 38 different char samples (Keiluweit et al., 2010; Schneider et al., 2011). These chars exhibit a wide range of properties, providing a diverse sample set for the comparison of PyC characterization methods and their assessment of aromatic features.

A much smaller sample set was employed for the in-depth analytical comparison of the BPCA and the PAH molecular marker approaches. In this case, thermosequences were produced from rye and maize straw with HTTs of 0, 300, 400 and 500 °C, respectively, and a pyrolysis time of 2 h, yielding 8 different chars (Rennert et al., 2008; Wiesenberg et al., 2009).

2.5. Improved BPCA method (paper I)

The improved BPCA method is conceptually based on the $HPLC_{organic}$ procedure (Dittmar, 2008). Important changes were introduced for the sample preparation after HNO_3 digestion and entirely different settings for chromatographic analysis were used. The use of mobile phases with a low pH and without an organic modifier was a crucial improvement for subsequent isotopic analysis of BPCAs (paper I). The improved BPCA method using HPLC was developed and tested thoroughly with respect to: i) universal applicability, ii) simple handling, iii) superior reproducibility and iv) minimizing sample amounts (Meyer, 2010).

2.6. Oxidation procedure and isotopic analysis of BPCAs (paper III)

Separated and collected BPCAs were oxidized into CO_2 as described by (Lang et al., 2012; Lang et al., 2013) to test the suitability of the improved BPCA method for compound-specific isotope analysis. The compound-specific ^{13}C isotopic signature of isolated BPCAs was then determined on a GasBench II on-line gas preparation and introduction system (Thermo Fisher Scientific, Bremen, Germany) coupled to a ConFlo IV interface and a Delta V Plus mass spectrometer (both Thermo Fisher Scientific). ^{14}C analysis, on the other hand, was carried out at the Laboratory for Ion Beam Physics of ETH Zürich, Switzerland using the MICADAS (mini carbon dating system) equipped with a gas ion source (Ruff et al., 2007; Synal et al., 2007; Wacker et al., 2013) that allows direct introduction of CO_2 into the gas ion source.

2.7. Other PyC methods that potentially detect aromatic features (paper IV and paper V)

A suite of seven PyC characterization methods was used to investigate PyC aromatic features (aromaticity and aromatic condensation) in detail: elemental analysis (Baldock and Smernik, 2002; Hammes et al., 2006), mid-infrared spectroscopy (MIR)(Wood, 1988; Moore and Owen, 2001), near-edge X-ray absorption fine structure spectroscopy (NEXAFS) (Francis and Hitchcock, 1992; Agren et al., 1995; Kuznetsova et al., 2001; Keiluweit et al., 2010), ^{13}C nucler magnetic resonance spectroscopy (NMR) (McBeath and Smernik, 2009; McBeath et al., 2011), lipid analysis (Wiesenberg et al., 2009; Wiesenberg et al., 2010), He pycnometry (Brown et al., 2006; Brewer et al., 2009), and, the improved BPCA method (paper I).

Moreover, a detailed study was conducted between the BPCA method and the other frequently used molecular marker technique for PyC: the polycyclic aromatic hydrocarbon (PAH) analysis. PAHs were extracted as described by (Wiesenberg et al., 2004; Wiesenberg et al., 2008; Wiesenberg et al., 2009).

2.8. Statistics

All data analysis was performed with the statistical software R (2011). In most cases, simple procedures such as linear regression (Stahel, 2011) or the coefficient of variation (CV) (Quan and Shih, 1996) were sufficient. However, in the case of the large dataset that was generated by the seven PyC characterization methods, multivariate techniques were required, including data imputation with the missForest algorithm (Stekhoven and Buehlmann, 2012) and principal component analysis (Gabriel, 1971; Mardia et al., 1979).

4. Results and discussion

4.1. Improvements of the BPCA molecular marker method

Analyzing a whole suite of environmental PyC reference materials with the improved BPCA procedure revealed its universal suitability for any kind of environmental samples. We achieved baseline separation with our modified sample pretreatment and improved chromatographic settings for all considered PyC materials (paper I). To the best of our knowledge, this has not been achieved before with liquid chromatography (Dittmar, 2008; Schneider et al., 2011; Yarnes et al., 2011) and thus presents an important achievement with respect to better BPCA quantification as well as better BPCA purification for subsequent isotopic analysis.

The improved BPCA method considerably simplified the sample pretreatment in comparison to the previous GC method and omitted two time-consuming steps (cf. paper I, supporting material). The trifluoracetic acid digestion (1) could be omitted, as the removal of polyvalent cations is not as much a concern with HPLC columns as with GC columns and is satisfactorily performed by the cation exchange resin. More importantly, the derivatization step (4) is not required anymore, which saves a lot of time and eliminates a chronic source of extraneous carbon introduction. The improved BPCA method is thus almost as fast to conduct as the $HPLC_{organic}$ method (2-3 days), only requiring minor purifying procedures such as a cation exchange and a solid phase extraction step. The quantitative recovery of BPCAs through the entire sample pretreatment was also found to be excellent as losses are small and constant over different sample amounts and very similar for the different BPCAs (paper I, supporting material).

Due to the simplified sample pretreatment, losses were minimized and the formerly poor reproducibility of the BPCA method was considerably improved (Figure 3). The average coefficient of variation (CV) (Quan and Shih, 1996) of 16 – 23 % for the GC method was lowered to a much more operational CV of 5 % in the case of the improved BPCA method (paper I). Interestingly, this leap forward in reproducibility was achieved without the need to use an internal standard, which was mandatory before in order to obtain decent reproducibility at all (Schneider et al., 2010). Instead, the improved BPCA method yielded perfectly reproducible results just using the external standard quantification approach (Meyer, 2010), which simplified the procedure even more (paper I, supporting material).

Corresponding to the improved and smoothed overall performance, the required sample amounts for PyC analysis could also be significantly reduced. In fact, the improved BPCA method still measured reliably within the linear measurement range using samples containing less than 1 mg TOC (paper I, supporting material). This fivefold decrease in required sample quantity will increasingly allow the use of the BPCA molecular marker approach for research projects with very limited sample amounts, e.g. from sediment cores or aerosol collectors (paper I).

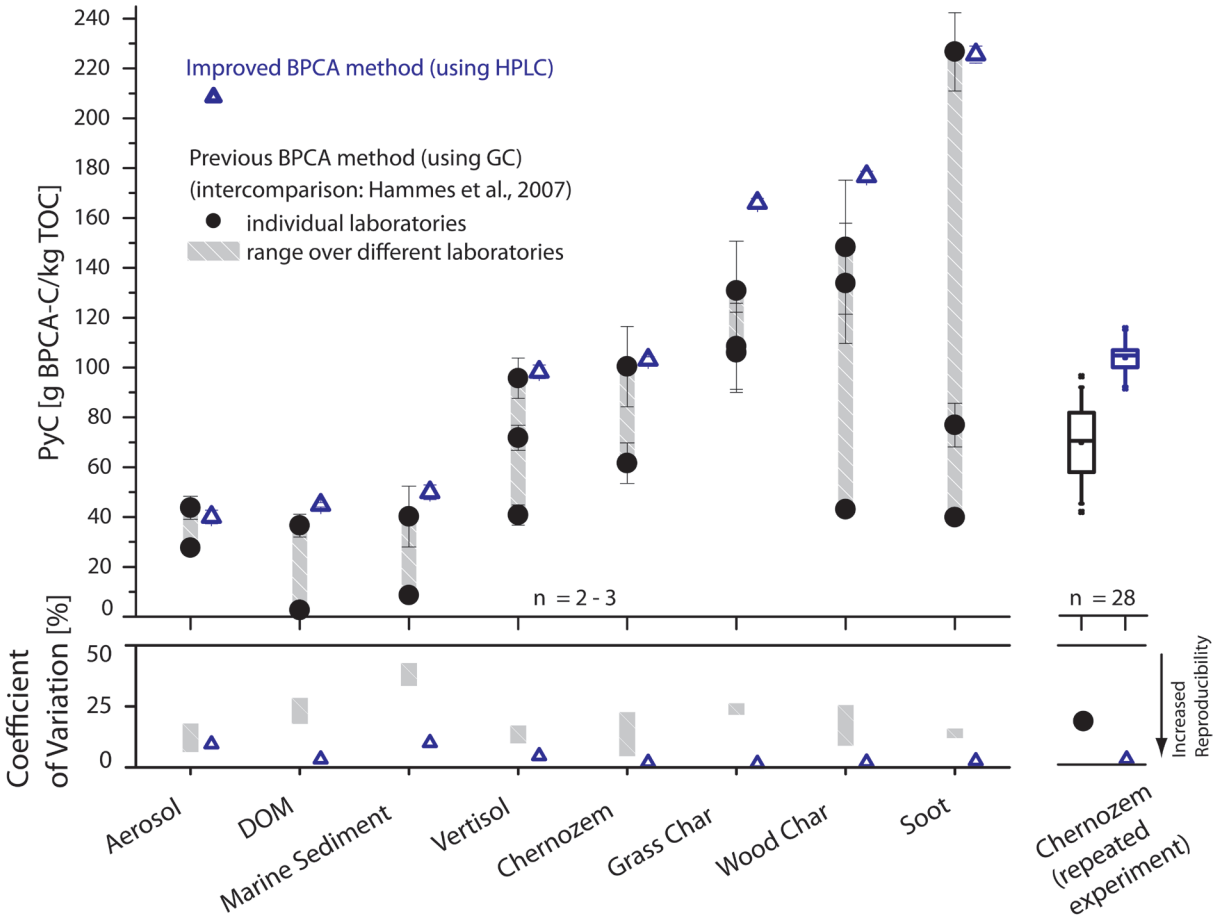

Figure 3. PyC measurements of different PyC reference materials with the improved BPCA (HPLC) method and the previously available BPCA (GC) method. Error bars for the improved BPCA approach are within symbol size and consequently, its reproducibility is much higher than for the previous BPCA method. This is also demonstrated by the HPLC method's much lower coefficient of variation in comparison to the GC method (bottom). Moreover, the HPLC method always detected the maximum amount of PyC (maximal BPCA yield) in the reference materials that was detected with the GC method across different laboratories (paper I). Note that comparison with the $HPLC_{organic}$ method was not possible as the $HPLC_{organic}$ method was only applicable to entirely organic sample materials.

4.2. Is the improved BPCA method a suitable tool for environmental research?

We here considered two case studies, which can also serve as a motivation for future applications of the improved BPCA method. Actually, the real strength of the BPCA approach lies in the broad detection and molecular characterization of PyC and slightly less in the exact quantification thereof (cf. Table 1). This is due to the fact that the BPCA method inherently underestimates total PyC contents: The method destroys large parts of the PyC polyaromatic structures in order to extract their BPCA building blocks, thus not quantitatively recovering all PyC (Glaser et al., 1998; Brodowski et al., 2005; Schneider et al., 2011). The BPCA approach hence provides a very conservative assessment of PyC quantity, which is not easily translated into realistic PyC contents. However, as the BPCA method consistently underestimates PyC contents and shows monotonic behavior with increasing PyC contents (cf. Figure 3), it is still a very helpful tool to compare PyC quantities on a relative basis.

The first case study concerned the use of the improved BPCA method in the emerging field of wildfire reconstruction (Power et al., 2008; Bowman et al., 2009; Conedera et al., 2009). Knowledge about past fire regimes is key to understand the present dynamics between ecosystems, climate, the anthroposphere and the carbon cycles (Graetz, 2003; Cordova et al., 2009) and to produce accurate fire scenarios for the future (Power et al., 2010). Fire frequency, severity and intensity has traditionally been reconstructed by palynological methods using radiometrically dated (^{14}C, ^{210}Pb, ^{137}Cs) sediment cores, in which charcoal was microscopically detected and counted (Clark, 1982; Clark and Hussey, 1996; Whitlock and Anderson, 2003). Interestingly, we found a strong correlation between the quantity of microscopically counted charcoal and the PyC quantity as detected by our BPCA method in the corresponding depth intervals of the Bega Swamp sediment (paper I). The relationship could be established as long as the BPCA method was applied to the same large, microscopically detectable particle size fraction (> 125 um), on which charcoal was counted. However, when the BPCA method was applied to the bulk sediment material, which includes much smaller particles, the data from the two approaches differed largely from each other (Figure 4). These findings highlight two important implications: i) The improved BPCA method yields a robust proxy for char quantities in environmental samples of very complex composition and ii) the BPCA molecular marker approach also provides char quantities in environmental media with small particles sizes, where microscopic methods reach their limits (paper I).

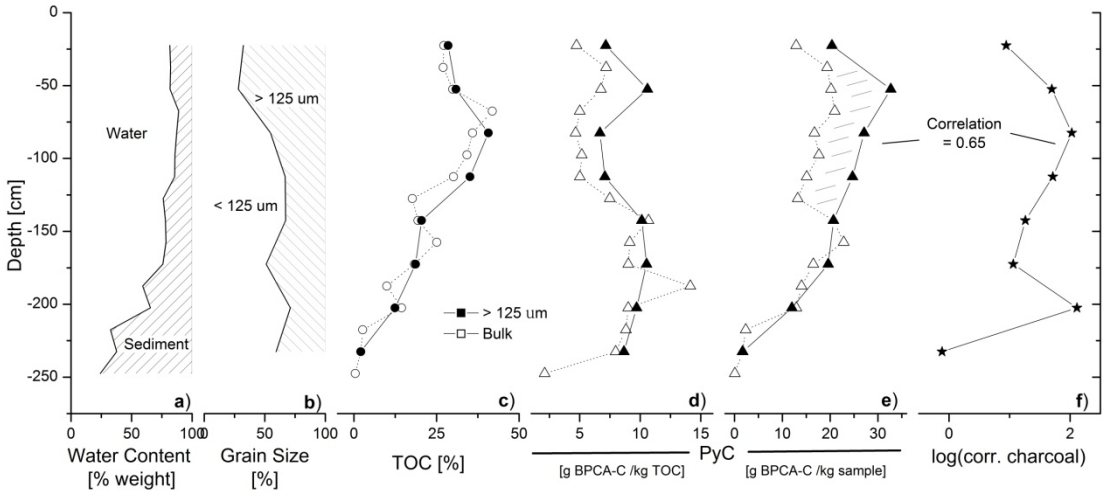

Figure 4. Bega Swamp core characteristics with respect to water content (a), grain size (b), TOC (c), PyC (d and e) and charcoal counts (f). Empty symbols show the values for the bulk sediment while filled symbols represent the values for the fraction >125 µm. Analytical errors for TOC (n = 2) and PyC (n = 3) are smaller than symbol size while charcoal counts were not replicated. A correlation between BPCA-based PyC measurements and microscopically counted charcoal is apparent, if both is measured on the large size fraction >125 µm (paper I).

The second case study was located in the field of soil C cycling (Janzen, 2004). Soils store approximately 2/3 of terrestrial C and thus constitute an enormous C pool of ca. 1.500 Gt C, where even slight changes may have important climatic consequences (Batjes, 1996). It is thus crucial to understand the processes that control the soil organic carbon (SOC) residence times. Various mechanisms have been proposed that can stabilize SOC. These include physical protection of SOC through occlusion within aggregates and pores, chemical protection through interaction with mineral surfaces or the selective preservation of chemically recalcitrant compounds (Lützow et al., 2006; Marschner et al., 2008). Moreover, preservation of SOC is increasingly understood as a complex system of different processes, depending on ecosystem properties (Schmidt et al., 2011). However, the importance of production, cycling and decomposition of PyC in soils across different ecosystems has not yet been assessed systematically and largely remains a mistery (Schmidt et al., 2011). In our study, we thus compared SOC stocks of two adjacent, yet very contrasting ecosystems: The old-growth coast redwood (*Sequoia sempervirens*) forest of Northern California (Sillett and Pelt, 2007) and its adjacent grassland prairie (Veirs et al., 1987). Redwood forests store more carbon in aboveground biomass than any other ecosystem, are among the most productive plant species on earth and produce large amounts of litter, which is known to be rather resistant against decay due to high amounts of polyphenolics such as tannin and lignin (Hättenschwiler and Vitousek, 2000). The prairie, in contrast, exhibits lower productivity and more decomposable litter than the redwood forest (Veirs et al., 1987). Since both ecosystems reside on the same parent material and within the same climate, it was hypothesized that the redwood forests soils would store more and older carbon due to higher recalcitrance of the

plant litter input. However, we observed considerably higher and older carbon stocks in the prairie soil, indicating longer SOC residence times in the prairie than in the redwood forest (paper II). Unfortunately, PyC quantification in the two soils using NMR was difficult due to interference with aromatic compounds of the plant litter input. With the help of the improved BPCA method, however, we could show that one of the main differences between the redwood and the prairie SOC was their respective proportion in PyC. The prairie being the more fire-prone ecosystem comprised about 2.5 times as much PyC in its soils in comparison to the redwood SOC. The larger amount of PyC in the prairie with its higher stability in the environment in comparison to other SOC was estimated to explain about 40 % of the observed difference between the SOC stocks of the two ecosystems (paper II). Thus, two major implications can be drawn from this study: i) the improved BPCA method is a helpful and robust tool for PyC estimation when quantification with other PyC methods becomes difficult and ii) compound-specific radioisotopic analysis of BPCAs could yield even more insights into the hypothesized long residence times of PyC.

4.3. The improved BPCA molecular marker method for compound-specific ^{13}C and ^{14}C analysis.

As mentioned before, compound-specific ^{13}C and ^{14}C analysis of PyC is highly desirable for many research fields (Bird and Ascough, 2012). However, isolation of pure PyC from environmental samples for subsequent ^{13}C and ^{14}C analysis is challenging as even minor amounts of contamination can result in large errors (Shah and Pearson, 2007; Ziolkowski and Druffel, 2009b; Coppola et al., 2013). From this point of view, the strictly conservative assessment of PyC by the BPCA molecular marker approach is beneficial. The BPCA approach targets exclusively the polyaromatic structures of PyC, which is in contrast to most other methods. It therefore does not rely on how well interfering materials are removed, as for example in the case of the chemical oxidation methods (cf. Table 1).

Using BPCAs is thus a very promising approach to analyze isotopes on PyC. However, previous BPCA methods were based on the GC procedure and consequently introduced extraneous C during the derivatization process, which complicated isotopic measurements considerably (Ziolkowski and Druffel, 2010; Coppola et al., 2013). The improved BPCA method circumvents this source of contamination as BPCAs are isolated and purified entirely in the liquid phase (paper I). For subsequent isotopic measurements, we then chemically oxidized the purified BPCAs into CO_2 in a gas tight vial, according to a recently published oxidation method (Lang et al., 2012; Lang et al., 2013).

This procedure proved to be simple and fast. When tested with the two isotopic PyC reference materials of Fossil and Modern Char, we could show that purified B5- and B6CA samples containing 20 – 30 ug C are sufficient for the two chars' successful isotopic analysis (Figure 5). The possibility to sequentially analyze ^{13}C and ^{14}C of purified BPCAs from the

same vial is furthermore very cost-efficient if both isotopic compositions are of interest (paper III). However, the improved BPCA method could potentially also be coupled to subsequent on-line oxidation and isotope-ratio monitoring instrumentation, which could further minimize labor, time and contamination (paper I).

The successful, compound-specific isotopic analysis of the two PyC reference materials further highlights the validity of the improved BPCA method and considerably enlarges its scope. Besides its use in PyC turnover and apportionment research, radiocarbon dating of very small fire residues, e.g. of a thin soot film on archeological pottery, might be possible with this approach. The method is thus likely to be of high value across many different scientific disciplines (paper III).

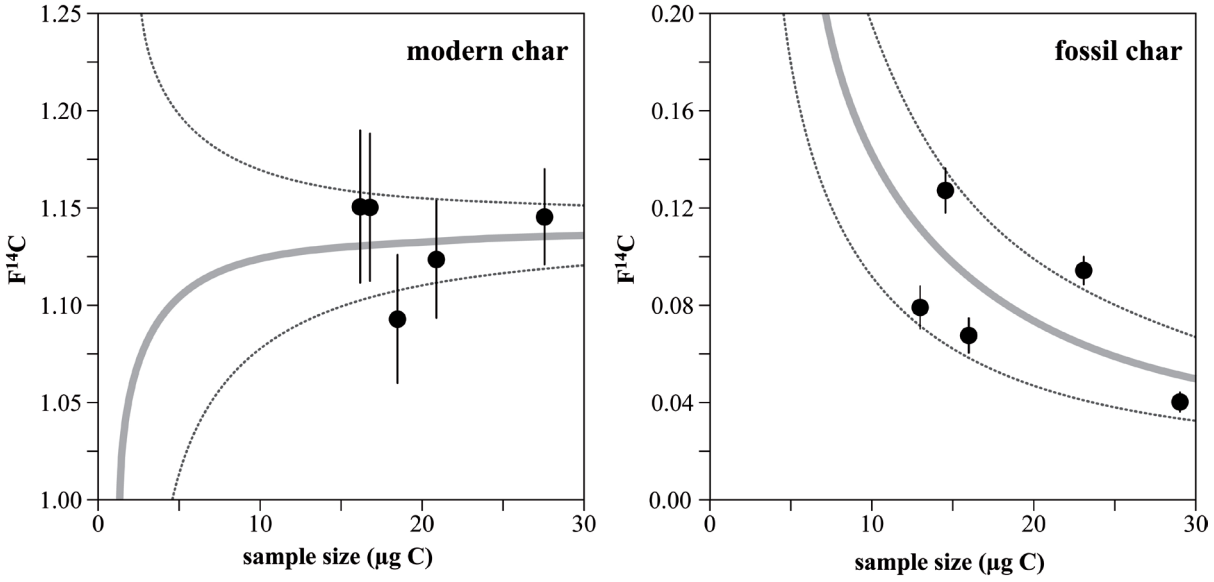

Figure 5. Radiocarbon values for B5CA and B6CA isolated from the Modern (left) and Fossil Char (right). The given error is composed of corrections for instrumental AMS background and the blank for wet oxidation. The solid gray line represents an idealized line for the mixture of the real $F^{14}C$ value of sample and the determined mean external contamination (paper III).

4.4. Linkages between the BPCA approach and other PyC methods

The BPCA approach has already been systematically tested and compared to other PyC methods with respect to the detection of PyC in environmental materials (Hammes et al., 2007) and its detection performance across the combustion continuum (Schneider et al., 2010). However, there has been much less intercomparison between different methods with respect to characterization of pure PyC (McBeath et al., 2011). We therefore investigated the improved BPCA method's potential for PyC characterization by comparing it with a variety of other common PyC characterization methods, including elemental analysis, MIR

spectroscopy, NEXAFS spectroscopy, ^{13}C NMR spectroscopy, lipid analysis and He pycnometry. We explored the similarities and differences between these methods by applying them on the same set of pure PyC materials, consisting of 38 different chars. The main aim was to examine if the characteristic aromatic C features of chars can be assessed by the different methods. These aromatic features are essential for the environmental properties of PyC and are conceptualized as aromaticity (i.e. the total proportion of aromatic C including amorphous and crystalline C phases (McNaught and Wilkinson, 1997)) and as aromatic condensation (i.e. the proportion of the condensed aromatic C only (McBeath et al., 2011)). While some of the methods are thought to assess only one of these aromatic features (e.g. He pycnometry indicating aromatic condensation with its density approach), other methods can potentially assess both aromatic features using different measures (e.g. BPCAs indicating both aromaticity and aromatic condensation with its molecular marker approach). As the methods use very different approaches and measure in widely different units, comparison of the obtained data was not straightforward. Therefore, we used multivariate statistical methods such as principal component analysis and multiple linear regression to analyze similarities and differences between the methods and their measures (paper IV).

We could observe a clear distinction between measures that assess aromaticity and those that assess the degree of aromatic condensation. The differentiation was sharp and resulted in two distinct trends with HTT: aromaticity increased sharply from 200 °C on, reaching maximum values at 500 – 600 °C, and stayed constant at the maximum with higher HTT (Figure 6). Aromatic condensation, on the other hand, increased smoothly from 300 °C on, reaching highest values at 1000 °C (paper IV). This congruent pattern of the different methods despite their largely different approaches was exciting to observe as it has four important implications. Firstly, i) the fundamental C aromatic features of chars can be assessed with a variety of methods and differently acquired data, e.g. from different research groups and laboratories can be compared. Consequently, ii) as these aromatic features have been linked to PyC's stability in the environment (Keiluweit et al., 2010; Harvey et al., 2012), the C sequestration potential of PyC may be assessable by various methods. Moreover, iii) pyrolysis temperature of unknown PyC may be reconstructed because aromaticity and aromatic condensation are functions of HTT. And finally, iv) the improved BPCA method performed very well, closely reproducing the trends of aromaticity and aromatic condensation and even providing both measures simultaneously (paper IV).

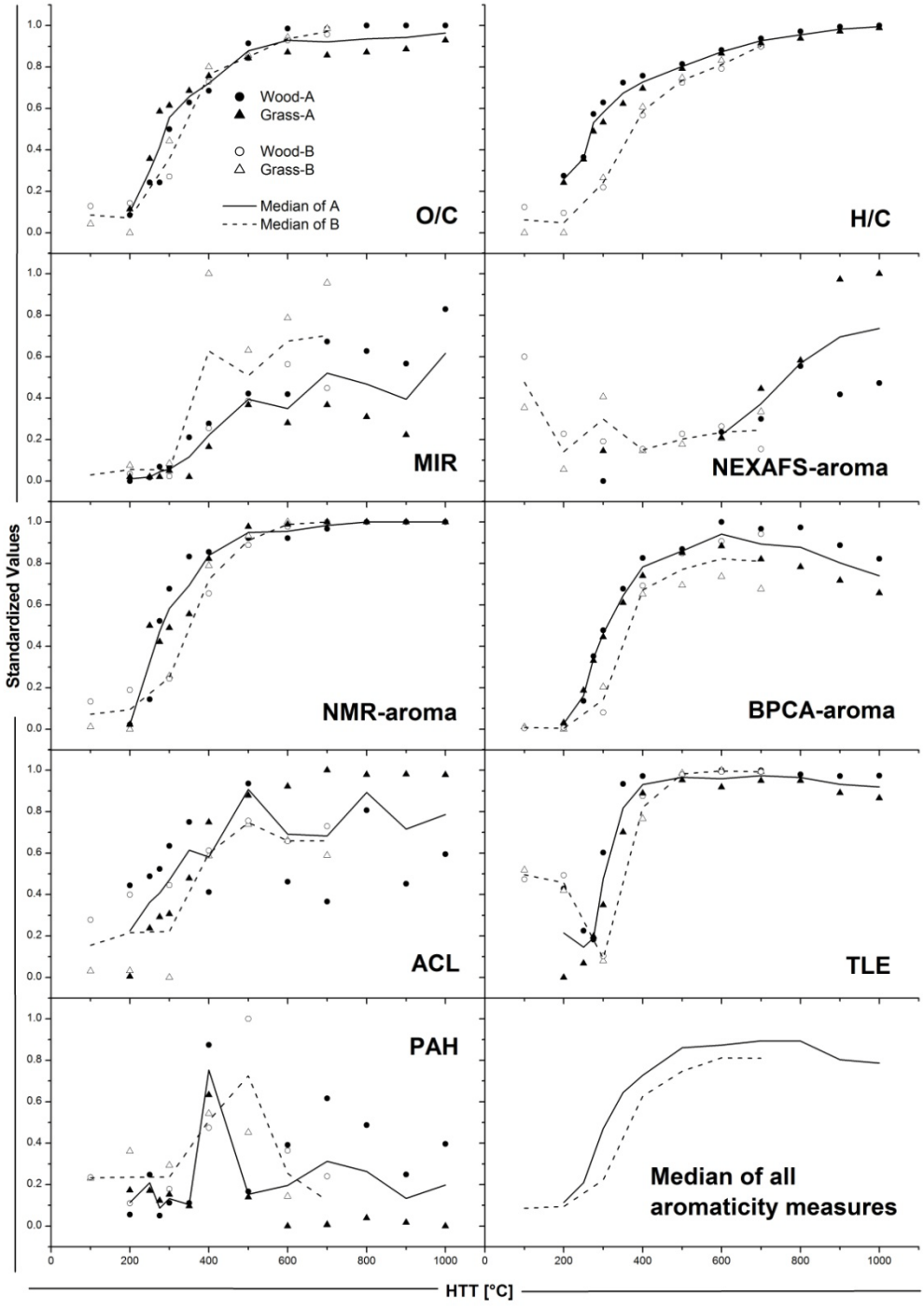

Figure 6. Char aromaticity as measured via nine different measures. The median of all the measures is shown at the lower right corner and thus describes the typical trend in aromaticity with HTT across a variety of 38 different chars (paper IV).

The large-scale intercomparison exercise also revealed differences between the BPCA method and the only other commonly used molecular marker-based PyC method: the PAH analysis (Simoneit, 2002; Denis et al., 2012). While the BPCA approach targets the large polyaromatic clusters of PyC, PAH analysis focuses on the much smaller pyrogenic polyaromatic moieties, which mostly comprise less than six condensed rings. PAH have frequently been used as tracers for combustion products in the environment because these small compounds are relatively volatile (Simoneit, 2002; Yunker et al., 2002; Bucheli et al., 2004). Moreover PAH analysis has recently received much attention in the context of biochar applications. Due to the mutagenic and carcinogenic properties of PAH, biochar applications with high PAH concentrations could be of environmental concern (Hale et al., 2012; Quilliam et al., 2013). We thus further investigated the link between the BPCA and PAH analysis in order to illuminate the similarities and differences of the two PyC molecular marker approaches. The aim was to test if the conceptually feasible overlap between the small aromatic PAH moieties and the larger, condensed polyaromatic structures, as indicated by BPCAs, can be assessed. Rye and maize straws and their analogues charred at 300, 400 and 500 °C, respectively, were thus analyzed with both methods. Moreover, we also measured BPCAs directly on the lipid extracts, on which PAHs were analyzed, and on the respective extraction residues, too.

We found that PAH analysis can also yield information about the increasingly condensed nature of PyC with increasing HTT (paper V). Moreover, we observed a significant relationship between the two methods when the BPCA analysis was directly applied on the same lipid extract, on which PAH were measured: The proportion of B3CA in the lipid extract, indicative of small polyaromatic clusters was logarithmically linked to the PAH concentration of the sample. The theory-based link between the two molecular marker approaches could thus be empirically established on real char samples (paper V). However, no relationship could be established when both methods were applied directly on the bulk chars according to their normal protocol, as the BPCA analysis was then not limited to the lipid fraction only. The study significantly contributed to the understanding of the two molecular marker approaches, which both target a part of the characteristic aromatic features of PyC. It showed their complementarity with respect to the characterization of PyC and further corroborated the BPCA method's underlying assumptions (paper V).

5. Conclusions

I. Can we improve the BPCA molecular marker method with respect to i) universal applicability, ii) simpler handling iii) better reproducibility and iv) smaller sample amounts? → Paper I.

The improved BPCA method, using a completely revised HPLC procedure, indeed merges the universal applicability of the GC approach with the benefits of the $HPLC_{organic}$ approach: The method provides baseline separation of BPCAs in all analyzed materials while sample preparation was substantially simplified (2-3 day vs. 4-5 days before) and reproducibility significantly improved (CV of 5 % vs. CV of 16-23 % before). Moreover, the improved BPCA method requires much smaller sample quantities (reduced by at least a factor of 5), which will now allow the use of the BPCA molecular marker approach in a variety of new research projects where sample amounts are strictly limited, e.g. assessing PyC in deep sea sediments or ice core materials.

II. Is the improved BPCA method a suitable tool for environmental research? → Paper I and paper II.

Besides the systematic method evaluation in the laboratory, the improved BPCA method has already produced plausible and relevant assessments of PyC in two environmental studies, using highly complex samples in very small amounts. In particular, the method was shown to be a good proxy for char as detected by microscopic means in a sediment core. Additionally it has the large advantage of being sensitive to even the smallest fire-residues in environmental media, where microscopic methods reach their limits. This is of fundamental importance as previous observations have shown that most PyC is usually found in the smallest size fractions (< 53 μm). The improved BPCA method also produced robust PyC estimates in a study where complex SOC composition prohibited the use of another state-of-the-art PyC quantification method (^{13}C NMR). In this case, it considerably contributed to the understanding of the C cycle in two different ecosystems, highlighting the importance of wildfires for the long-term stabilization of SOC in the form of PyC.

III. Can the improved BPCA molecular marker method lead to compound-specific ^{13}C and ^{14}C analysis of BPCAs? → Paper III

We tested a simple, fast and cost-efficient oxidation procedure subsequent to the improved BPCA method, with which we were able to reliably analyze the isotopic (^{13}C and ^{14}C) content of BPCA molecular markers. The successful compound-specific isotopic analysis of the BPCA markers further confirms the validity of the improved BPCA method and

simultaneously enlarges its scope tremendously. PyC isotopic analysis as presented in this thesis is likely to be a highly useful tool across scientific disciplines, including environmental or archeological sciences.

IV. How is the BPCA method linked to other PyC methods? → Paper IV and paper V.

By conducting a large-scale comparative study of different PyC characterization methods, we could show that aromaticity and aromatic condensation are intrinsic PyC features that are assessable by various methods. The study supports the comparison of differently acquired data within a consistent framework that relates aromaticity and aromatic condensation with HTT. Besides estimates of chars' environmental stability, the concept can also help to reconstruct the HTT of unknown chars. The BPCA method seems particularly suited for PyC characterization of this kind, as it simultaneously yields precise measures of both aromatic features. Moreover, the BPCA method was successfully linked to the methodologically related PAH method. The empricially established correlations between the two molecular marker approaches for PyC further corroborated their respective underlying assumptions and emphasized their complementarity in PyC research.

6. Perspectives

The thesis presents an entirely refined BPCA method, which now fully exploits the potential of this molecular marker approach for PyC research. The improved BPCA method consolidates the strengths of previous BPCA methods in just one procedure and is simple to employ. Its main features are (cf. Figure 7): (1) Broad detection of PyC over the combustion continuum, (2) robust and reproducible estimation of PyC quantity in any kind of environmental sample materials and (3) simultaneous qualitative information about the PyC, such as its aromaticity and aromatic condensation. Moreover, it now allows (4) the uncontaminated isolation of PyC on a compound-specific level and thus isotopic analysis (^{13}C, ^{14}C) of pure PyC with a very high precision. With all these features, the improved BPCA method became probably the most versatile PyC method available to date, whose underlying assumptions are well constrained and have been continuously tested against other methods.

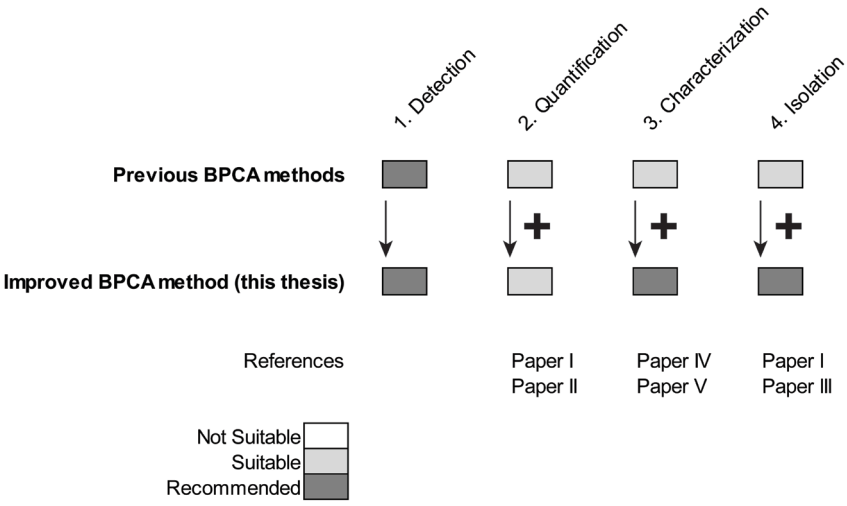

Figure 7. Schematic representation of how the BPCA method was improved during this thesis. The broad detection (1) over the whole PyC continuum is inherent to the BPCA approach and thus was not changed. In contrast, all other features of the BPCA method (2 – 4) were significantly improved, turning it into one of the most versatile PyC methods available (cf. Table 1). Quantification of PyC (2) with the BPCA method was possible before but is now much simpler and more reproducible. However, the inherent underestimation of PyC by the BPCA approach leads to the fact that other methods may still be more recommended for absolute quantification of PyC (cf. Part A section 4.2.). Characterization of PyC (3) by BPCAs was also done before but is now much better embedded in the context of other methods (cf. Part A section 4.4). Finally, uncontaminated isolation of PyC (4) by ultra-pure BPCAs was greatly improved, turning the improved BPCA method into one of the most recommended methods for isotopic analysis of PyC (cf. Part A section 4.3).

The improved BPCA method should thus yield interesting insights about pyrogenic materials across different scientific disciplines. Potential topics include:

Quantification, characterization and source apportionment of sedimentary wildfire residues

The improved BPCA analysis can be used on sedimentary archives to complement existing wildfire histories, which are based on the charcoal counting and pollen analysis approach (Whitlock, 2002). In particular, the BPCA-based assessment of PyC can yield interesting insights about the smallest size fraction of sediments, where microscopic methods reach their limits. The ^{13}C isotopic signature of the BPCA molecular markers can be used to infer the source of the PyC in tropical regions, as trees (C3 plants) exhibit a lower $\delta^{13}C$ ratio than herbaceous plants (C4) at these latitudes (Fry, 2006; Bird and Ascough, 2012). Additionally, the ^{14}C signature from the compound-specific isotopic analysis of PyC can be highly informative of the fire-residue's age and depositional pathways (Bird and Ascough, 2012).

Illuminating PyC stabilization mechanisms in soils and sediments

As PyC was found to be relatively stable in soils and sediments, it is of great interest to know more about the chemical, physical and biological mechanisms that lead to the observed persistence of PyC. With the help of the improved BPCA method, individual (size and/or density) fractions of soil and sediment material can be investigated for PyC quantity and quality, illuminating the mechanisms for its stability. Additionally, turnover times of PyC in soil and sediment fractions can be better constrained using the compound-specific analysis of BPCAs in field and laboratory experiments alike.

Estimating fluxes of PyC between different environmental compartments

Another major contribution towards a global budget of PyC comes from the systematic investigation of PyC fluxes across environmental compartments. Little is known, for example, about the pathways of PyC from terrestrial compartments to rivers, lakes, oceans and their sediments by fluvial and aerial transport (Preston and Schmidt, 2006). The improved BPCA method is a suitable tool to assess these PyC fluxes that usually occur in extremely low concentrations as the method only requires very small sample amounts.

Characterization and environmental assessments of biochars and nano-particles

PyC-like materials are increasingly and intentionally produced for agricultural purposes (biochar) or high-tech applications (nano-particles) and need to be carefully examined for their potential environmental impact (Ziolkowski and Druffel, 2009a; Hilber et al., 2012). The improved BPCA method is an ideal tool for the characterization of these materials, especially in combination with other methods, such as PAH analysis. It can also contribute to trace these materials in the environment, e.g. by using isotopically labeled samples and compound-specific isotopic analysis of BPCAs.

References

Agren, H., Vahtras, O., Carravetta, V., 1995. Near-edge core photoabsorption in polyacenes - model molecules for graphite. Chemical Physics 196, 47-58.

Alloway, B.V., Pribadi, A., Westgate, J.A., Bird, M., Fifield, L.K., Hogg, A., Smith, I., 2004. Correspondence between glass-FT and ^{14}C ages of silicic pyroclastic flow deposits sourced from Maninjau caldera, west-central Sumatra. Earth and Planetary Science Letters 227, 121-133.

Ascough, P.L., Bird, M.I., Brock, F., Higham, T.F.G., Meredith, W., Snape, C.E., Vane, C.H., 2009. Hydropyrolysis as a new tool for radiocarbon pre-treatment and the quantification of black carbon. Quaternary Geochronology 4, 140-147.

Ascough, P.L., Bird, M.I., Scott, A.C., Collinson, M.E., Cohen-Ofri, I., Snape, C.E., Le Manquais, K., 2010. Charcoal reflectance measurements: Implications for structural characterization and assessment of diagenetic alteration. Journal Of Archaeological Science 37, 1590-1599.

Baldock, J., Smernik, R., 2002. Chemical composition and bioavailability of thermally altered Pinus resinosa (Red pine) wood. Organic Geochemistry 33, 1093-1109.

Batjes, N.H., 1996. Total carbon and nitrogen in the soils of the world. European Journal of Soil Science 47, 151-163.

Beesley, L., Moreno-Jiménez, E., Gomez-Eyles, J.L., Harris, E., Robinson, B., Sizmur, T., 2011. A review of biochars' potential role in the remediation, revegetation and restoration of contaminated soils. Environmental Pollution 159, 3269-3282.

Biederman, L.A., Harpole, W.S., 2013. Biochar and its effects on plant productivity and nutrient cycling: a meta-analysis. GCB Bioenergy 5, 202-214.

Bird, M.I., Ascough, P.L., 2012. Isotopes in pyrogenic carbon: A review. Organic Geochemistry 42, 1529-1539.

Bird, M.I., Ayliffe, L.K., Fifield, L.K., Tumey, C.S.M., Cresswell, R.G., Barrows, T.T., David, B., 1999. Radiocarbon dating of "old" charcoal using a wet oxidation, stepped-combustion procedure. Radiocarbon 41, 127-140.

Boffetta, P., Jourenkova, N., Gustavsson, P., 1997. Cancer risk from occupational and environmental exposure to polycyclic aromatic hydrocarbons. Cancer Causes & Control 8, 444-472.

Bond, T.C., Doherty, S.J., Fahey, D.W., Forster, P.M., Berntsen, T., Deangelo, B.J., Flanner, M.G., Ghan, S., Kärcher, B., Koch, D., Kinne, S., Kondo, Y., Quinn, P.K., Sarofim, M.C., Schultz, M.G., Schulz, M., Venkataraman, C., Zhang, H., Zhang, S., Bellouin, N., Guttikunda,

S.K., Hopke, P.K., Jacobson, M.Z., Kaiser, J.W., Klimont, Z., Lohmann, U., Schwarz, J.P., Shindell, D., Storelvmo, T., Warren, S.G., Zender, C.S., 2013. Bounding the role of black carbon in the climate system: A scientific assessment. Journal of Geophysical Research D: Atmospheres 118, 5380-5552.

Bond, T.C., Streets, D.G., Yarber, K.F., Nelson, S.M., Woo, J.H., Klimont, Z., 2004. A technology-based global inventory of black and organic carbon emissions from combustion. Journal of Geophysical Research D: Atmospheres 109.

Bowman, D.M.J.S., Balch, J.K., Artaxo, P., Bond, W.J., Carlson, J.M., Cochrane, M.A., D'Antonio, C.M., DeFries, R.S., Doyle, J.C., Harrison, S.P., Johnston, F.H., Keeley, J.E., Krawchuk, M.A., Kull, C.A., Marston, J.B., Moritz, M.A., Prentice, I.C., Roos, C.I., Scott, A.C., Swetnam, T.W., van der Werf, G.R., Pyne, S.J., 2009. Fire in the Earth System. Science 324, 481-484.

Brewer, C., Schmidt Rohr, K., Satrio, J., Brown, R., 2009. Characterization of biochar from fast pyrolysis and gasification systems. Environmental progress & sustainable energy 28, 386-396.

Brodowski, S., Amelung, W., Haumaier, L., Zech, W., 2007. Black carbon contribution to stable humus in German arable soils. Geoderma 139, 220-228.

Brodowski, S., Rodionov, A., Haumaier, L., Glaser, B., Amelung, W., 2005. Revised black carbon assessment using benzene polycarboxylic acids. Organic Geochemistry 36, 1299-1310.

Brown, R.A., Kercher, A.K., Nguyen, T.H., Nagle, D.C., Ball, W.P., 2006. Production and characterization of synthetic wood chars for use as surrogates for natural sorbents. Organic Geochemistry 37, 321-333.

Bucheli, T.D., Blum, F., Desaules, A., Gustafsson, Ö., 2004. Polycyclic aromatic hydrocarbons, black carbon, and molecular markers in soils of Switzerland. Chemosphere 56, 1061-1076.

Cao, G., Zhang, X., Zheng, F., 2006. Inventory of black carbon and organic carbon emissions from China. Atmospheric Environment 40, 6516-6527.

Clark, J.S., Hussey, T.C., 1996. Estimating the mass flux of charcoal from sedimentary records: Effects of particle size, morphology, and orientation. Holocene 6, 129-144.

Clark, R.L., 1982. Point count estimation of charcoal in pollen preparations and thin sections of sediments. Pollen et Spores 24, 523-536.

Cohen-Ofri, I., Weiner, L., Boaretto, E., Mintz, G., Weiner, S., 2006. Modern and fossil charcoal: aspects of structure and diagenesis. Journal Of Archaeological Science 33, 428-439.

Conedera, M., Tinner, W., Neff, C., Meurer, M., Dickens, A.F., Krebs, P., 2009. Reconstructing past fire regimes: methods, applications, and relevance to fire management and conservation. Quaternary Science Reviews 28, 555-576.

Coppola, A.I., Ziolkowski, L.A., Druffel, E.R.M., 2013. Extraneous carbon assessments in radiocarbon measurements of black carbon in environmental matrices. Radiocarbon 55, 1631-1640.

Cordova, C.E., Harrison, S.P., Mudie, P.J., Riehl, S., Leroy, S.A.G., Ortiz, N., 2009. Pollen, plant macrofossil and charcoal records for palaeovegetation reconstruction in the Mediterranean-Black Sea Corridor since the Last Glacial Maximum. Quaternary International 197, 12-26.

Czimczik, C.I., Schmidt, M.W.I., Schulze, E.D., 2005. Effects of increasing fire frequency on black carbon and organic matter in Podzols of Siberian Scots pine forests. European Journal of Soil Science 56, 417-428.

Dai, X., Boutton, T.W., Glaser, B., Ansley, R.J., Zech, W., 2005. Black carbon in a temperate mixed-grass savanna. Soil Biology and Biochemistry 37, 1879-1881.

Denis, E.H., Toney, J.L., Tarozo, R., Scott Anderson, R., Roach, L.D., Huang, Y., 2012. Polycyclic aromatic hydrocarbons (PAHs) in lake sediments record historic fire events: Validation using HPLC-fluorescence detection. Organic Geochemistry 45, 7-17.

Dittmar, T., 2008. The molecular level determination of black carbon in marine dissolved organic matter. Organic Geochemistry 39, 396-407.

Dittmar, T., Koch, B.P., 2006. Thermogenic organic matter dissolved in the abyssal ocean. Marine Chemistry 102, 208-217.

Downie, A., Crosky, A., Munroe, P., 2009. Physical Properties of Biochar, in: Lehmann, J., Joseph, S. (Eds.), Biochar for Environmental Management: Science and Technology. Earthscan, London, UK, pp. 13-32.

Fang, Y., Singh, B., Singh, B.P., Krull, E., 2014. Biochar carbon stability in four contrasting soils. European Journal of Soil Science 65, 60-71.

Flannigan, M., Cantin, A.S., De Groot, W.J., Wotton, M., Newbery, A., Gowman, L.M., 2013. Global wildland fire season severity in the 21st century. Forest Ecology and Management 294, 54-61.

Flores-Cervantes, D.X., Reddy, C.M., Gschwend, P.M., 2009. Inferring black carbon concentrations in particulate organic matter by observing pyrene fluorescence losses. Environmental Science and Technology 43, 4864-4870.

Forbes, M.S., Raison, R.J., Skjemstad, J.O., 2006. Formation, transformation and transport of black carbon (charcoal) in terrestrial and aquatic ecosystems. Science of the Total Environment 370, 190-206.

Francis, J.T., Hitchcock, A.P., 1992. Inner-shell spectroscopy of a para-benzoquinone, hydroquinone, and phenol - distinguishing quinoid and benzenoid structures. Journal of Physical Chemistry 96, 6598-6610.

Franklin, R.E., 1951. Crystallite growth in graphitizing and non-graphitizing carbons. Proceedings of the Royal Society of London Series A 209, 196-218.

Fry, B., 2006. Stable isotope ecology. Springer New York.

Gabriel, K.R., 1971. The biplot graphic display of matrices with application to principal component analysis. Biometrika 58, 453-467.

Glaser, B., Balashov, E., Haumaier, L., Guggenberger, G., Zech, W., 2000. Black carbon in density fractions of anthropogenic soils of the Brazilian Amazon region. Organic Geochemistry 31, 669-678.

Glaser, B., Birk, J.J., 2012. State of the scientific knowledge on properties and genesis of Anthropogenic Dark Earths in Central Amazonia (terra preta de Índio). Geochimica et Cosmochimica Acta 82, 39-51.

Glaser, B., Haumaier, L., Guggenberger, G., Zech, W., 1998. Black carbon in soils: the use of benzenecarboxylic acids as specific markers. Organic Geochemistry 29, 811-819.

Goldberg, E.D., 1985. Black carbon in the environment: properties and distribution. Wiley, New York.

Gonzalez-Perez, J.A., Gonzalez-Vila, F.J., Almendros, G., Knicker, H., 2004. The effect of fire on soil organic matter - a review. Environment International 30, 855-870.

Graetz, R.D., 2003. The charcoal sink of biomass burning on the Australian continent in: Graetz, R.D., Skjemstad, J.O. (Eds.), CSIRO Atmospheric Research technical paper (Online) 64. CSIRO Atmospheric Research, Aspendale.

Green, D., Singh, G., Polach, H., Moss, D., Banks, J., Geissler, E.A., 1988. A Fine-Resolution Palaeoecology and Palaeoclimatology from South-Eastern Australia. Journal of Ecology 76, 790-806.

Guggenberger, G., Rodionov, A., Shibistova, O., Grabe, M., Kasansky, O.A., Fuchs, H., Mikheyeva, N., Zrazhevskaya, G., Flessa, H., 2008. Storage and mobility of black carbon in permafrost soils of the forest tundra ecotone in Northern Siberia. Global Change Biology 14, 1367-1381.

Gustafsson, Ö., Bucheli, T.D., Kukulska, Z., Andersson, M., Largeau, C., Rouzaud, J.N., Reddy, C.M., Eglinton, T.I., 2001. Evaluation of a protocol for the quantification of black carbon in sediments. Global Biogeochemical Cycles 15, 881-890.

Gustafsson, Ö., Haghseta, F., Chan, C., Macfarlane, J., Gschwend, P.M., 1997. Quantification of the dilute sedimentary soot phase: Implications for PAH speciation and bioavailability. Environmental Science and Technology 31, 203-209.

Hale, S.E., Lehmann, J., Rutherford, D., Zimmerman, A.R., Bachmann, R.T., Shitumbanuma, V., O'Toole, A., Sundqvist, K.L., Arp, H.P.H., Cornelissen, G., 2012. Quantifying the total and bioavailable polycyclic aromatic hydrocarbons and dioxins in biochars. Environmental Science & Technology 46, 2830-2838.

Hammes, K., Schmidt, M.W.I., Smernik, R.J., Currie, L.A., Ball, W.P., Nguyen, T.H., Louchouarn, P., Houel, S., Gustafsson, O., Elmquist, M., Cornelissen, G., Skjemstad, J.O., Masiello, C.A., Song, J., Peng, P., Mitra, S., Dunn, J.C., Hatcher, P.G., Hockaday, W.C., Smith, D.M., Hartkopf-Froeder, C., Boehmer, A., Luer, B., Huebert, B.J., Amelung, W., Brodowski, S., Huang, L., Zhang, W., Gschwend, P.M., Flores-Cervantes, D.X., Largeau, C., Rouzaud, J.N., Rumpel, C., Guggenberger, G., Kaiser, K., Rodionov, A., Gonzalez-Vila, F.J., Gonzalez-Perez, J.A., de la Rosa, J.M., Manning, D.A.C., Lopez-Capel, E., Ding, L., 2007. Comparison of quantification methods to measure fire-derived (black/elemental) carbon in soils and sediments using reference materials from soil, water, sediment and the atmosphere. Global Biogeochemical Cycles 21, GB3016.

Hammes, K., Smernik, R., Skjemstad, J., Herzog, A., Vogt, U., 2006. Synthesis and characterisation of laboratory-charred grass straw (Oryza saliva) and chestnut wood (Castanea sativa) as reference materials for black carbon quantification. Organic Geochemistry 37, 1629-1633.

Hammes, K., Smernik, R.J., Skjemstad, J.O., Schmidt, M.W.I., 2008a. Characterisation and evaluation of reference materials for black carbon analysis using elemental composition, colour, BET surface area and ^{13}C NMR spectroscopy. Applied Geochemistry 23, 2113-2122.

Hammes, K., Torn, M., Lapenas, A., Schmidt, M., 2008b. Centennial black carbon turnover observed in a Russian steppe soil. Biogeosciences 5, 1339-1350.

Han, Y.M., Cao, J.J., Chow, J.C., Watson, J.G., An, Z.S., Jin, Z.D., Fung, K.C., Liu, S.X., 2007. Evaluation of the thermal/optical reflectance method for discrimination between char- and soot-EC. Chemosphere 69, 569-574.

Harvey, O., Kuo, L.-J., Zimmerman, A., Louchouarn, P., Amonette, J., Herbert, B., 2012. An index-based approach to assessing recalcitrance and soil carbon sequestration potential of engineered black carbons (biochars). Environmental Science & Technology 46, 1415-1421.

Hättenschwiler, S., Vitousek, P.M., 2000. The role of polyphenols in terrestrial ecosystem nutrient cycling. Trends in Ecology & Evolution 15, 238-243.

Hedges, J.I., Eglinton, G., Hatcher, P.G., Kirchman, D.L., Arnosti, C., Derenne, S., Evershed, R.P., Kögel-Knabner, I., De Leeuw, J.W., Littke, R., Michaelis, W., Rullkötter, J., 2000. The

molecularly-uncharacterized component of nonliving organic matter in natural environments. Organic Geochemistry 31, 945-958.

Heymann, K., Lehmann, J., Solomon, D., Schmidt, M.W.I., Regier, T., 2011. C 1s K-edge near edge X-ray absorption fine structure (NEXAFS) spectroscopy for characterizing functional group chemistry of black carbon. Organic Geochemistry 42, 1055-1064.

Hilber, I., Blum, F., Leifeld, J., Schmidt, H.P., Bucheli, T.D., 2012. Quantitative determination of PAHs in biochar: A prerequisite to ensure its quality and safe application. Journal of Agricultural and Food Chemistry 60, 3042-3050.

Hoet, P.H.M., Brüske-Hohlfeld, I., Salata, O.V., 2004. Nanoparticles - Known and unknown health risks. Journal of Nanobiotechnology 2.

Hsieh, Y.P., Bugna, G.C., 2008. Analysis of black carbon in sediments and soils using multi-element scanning thermal analysis (MESTA). Organic Geochemistry 39, 1562-1571.

Janik, L.J., Skjemstad, J.O., Shepherd, K.D., Spouncer, L.R., 2007. The prediction of soil carbon fractions using mid-infrared-partial least square analysis. Australian Journal of Soil Research 45, 73-81.

Janzen, H.H., 2004. Carbon cycling in earth systems - A soil science perspective. Agriculture, Ecosystems and Environment 104, 399-417.

Kaal, J., Schneider, M.P.W., Schmidt, M.W.I., 2012. Rapid molecular screening of black carbon (biochar) thermosequences obtained from chestnut wood and rice straw: A pyrolysis-GC/MS study. Biomass and Bioenergy 45, 115-129.

Keiluweit, M., Nico, P.S., Johnson, M.G., Kleber, M., 2010. Dynamic molecular structure of plant biomass-derived black carbon (biochar). Environmental Science & Technology 44, 1247-1253.

Kelly, R., Chipman, M.L., Higuera, P.E., Stefanova, I., Brubaker, L.B., Hu, F.S., 2013. Recent burning of boreal forests exceeds fire regime limits of the past 10,000 years. Proceedings of the National Academy of Sciences of the United States of America 110, 13055-13060.

Kenward, H.K., Hall, A.R., Jones, A.K.G., 1980. A tested set of techniques for the extraction of plant and animal macrofossils from waterlogged archaeological deposits. Science and Archaeology 22, 3-15.

Knicker, H., 2011. Pyrogenic organic matter in soil: Its origin and occurrence, its chemistry and survival in soil environments. Quaternary International 243, 251-263.

Knicker, H., Müller, P., Hilscher, A., 2007. How useful is chemical oxidation with dichromate for the determination of "Black Carbon" in fire-affected soils? Geoderma 142, 178-196.

Koelmans, A.A., Jonker, M.T.O., Cornelissen, G., Bucheli, T.D., Van Noort, P.C.M., Gustafsson, O., 2006. Black carbon: The reverse of its dark side. Chemosphere 63, 365-377.

Koide, R.T., Petprakob, K., Peoples, M., 2011. Quantitative analysis of biochar in field soil. Soil Biology and Biochemistry 43, 1563-1568.

Krawchuk, M.A., Moritz, M.A., Parisien, M.A., Van Dorn, J., Hayhoe, K., 2009. Global pyrogeography: The current and future distribution of wildfire. PLoS ONE 4.

Kuhlbusch, T.A.J., 1998. Black Carbon and the Carbon Cycle. Science 280, 1903-1904.

Kuznetsova, A., Popova, I., Yates, J.T., Bronikowski, M.J., Huffman, C.B., Liu, J., Smalley, R.E., Hwu, H.H., Chen, J.G.G., 2001. Oxygen-containing functional groups on single-wall carbon nanotubes: NEXAFS and vibrational spectroscopic studies. Journal of the American Chemical Society 123, 10699-10704.

Kuzyakov, Y., Bogomolova, I., Glaser, B., 2014. Biochar stability in soil: Decomposition during eight years and transformation as assessed by compound-specific ^{14}C analysis. Soil Biology and Biochemistry 70, 229-236.

Kuzyakov, Y., Subbotina, I., Chen, H., Bogomolova, I., Xu, X., 2009. Black carbon decomposition and incorporation into soil microbial biomass estimated by ^{14}C labeling. Soil Biology and Biochemistry 41, 210-219.

Lam, C.W., James, J.T., McCluskey, R., Arepalli, S., Hunter, R.L., 2006. A review of carbon nanotube toxicity and assessment of potential occupational and environmental health risks. Critical Reviews in Toxicology 36, 189-217.

Lang, S., Bernasconi, S., Frueh Green, G., FrÃ¼h Green, G., 2012. Stable isotope analysis of organic carbon in small (μg C) samples and dissolved organic matter using a GasBench preparation device. Rapid Communications in Mass Spectrometry 26, 9-16.

Lang, S.Q., Früh-Green, G.L., Bernasconi, S.M., Wacker, L., 2013. Isotopic ($\delta^{13}C$, $\Delta^{14}C$) analysis of organic acids in marine samples using wet chemical oxidation. Limnology and Oceanography: Methods 11, 161-175.

Lehmann, J., Czimczik, C., Laird, D., Sohi, S., 2009. Stability of biochar in soil, in: Lehmann, J., Joseph, S. (Eds.), Biochar for environmental management: science and technology. Earthscan: London, UK, pp. 183-206.

Lehmann, J., Gaunt, J., Rondon, M., 2006. Bio-char sequestration in terrestrial ecosystems - A review. Mitigation and Adaptation Strategies for Global Change 11, 403-427.

Lehmann, J., Joseph, S., 2009. Biochar for Environmental Management - An Introduction, in: Lehmann, J., Joseph, S. (Eds.), Biochar for Environemental Management: Science and Technology. Earthscan, London, UK, pp. 1-12.

Leifeld, J., 2007. Thermal stability of black carbon characterised by oxidative differential scanning calorimetry. Organic Geochemistry 38, 112-127.

Liang, B., Lehmann, J., Solomon, D., Sohi, S., Thies, J.E., Skjemstad, J.O., Luizão, F.J., Engelhard, M.H., Neves, E.G., Wirick, S., 2008. Stability of biomass-derived black carbon in soils. Geochimica et Cosmochimica Acta 72, 6069-6078.

Louchouarn, P., Chillrud, S.N., Houel, S., Yan, B., Chaky, D., Rumpel, C., Largeau, C., Bardoux, G., Walsh, D., Bopp, R.F., 2006. Elemental and Molecular Evidence of Soot- and Char-Derived Black Carbon Inputs to New York City's Atmosphere during the 20th Century. Environmental Science & Technology 41, 82-87.

Lützow, M.V., Kögel-Knabner, I., Ekschmitt, K., Matzner, E., Guggenberger, G., Marschner, B., Flessa, H., 2006. Stabilization of organic matter in temperate soils: Mechanisms and their relevance under different soil conditions - A review. European Journal of Soil Science 57, 426-445.

Maestrini, B., Herrmann, A.M., Nannipieri, P., Schmidt, M.W.I., Abiven, S., 2014. Ryegrass-derived pyrogenic organic matter changes organic carbon and nitrogen mineralization in a temperate forest soil. Soil Biology and Biochemistry 69, 291-301.

Manyà , J., 2012. Pyrolysis for biochar purposes: a review to establish current knowledge gaps and research needs. Environmental Science & Technology 46, 7939-7954.

Mardia, K.V., Kent, J.T., Bibby, J.M., 1979. Multivariate analysis. Academic Press.

Marris, E., 2006. Putting the carbon back: Black is the new green. Nature 442, 624-626.

Marschner, B., Brodowski, S., Dreves, A., Gleixner, G., Gude, A., Grootes, P.M., Hamer, U., Heim, A., Jandl, G., Ji, R., Kaiser, K., Kalbitz, K., Kramer, C., Leinweber, P., Rethemeyer, J., Schaeffer, A., Schmidt, M.W.I., Schwark, L., Wiesenberg, G.L.B., 2008. How relevant is recalcitrance for the stabilization of organic matter in soils? Journal of Plant Nutrition and Soil Science 171, 91-110.

Masiello, C.A., 2004. New directions in black carbon organic geochemistry. Marine Chemistry 92, 201-213.

Masiello, C.A., Druffel, E.R.M., 1998. Black carbon in deep-sea sediments. Science 280, 1911.

McBeath, A., Smernik, R., Plant, E., 2011. Determination of the aromaticity and the degree of aromatic condensation of a thermosequence of wood charcoal using NMR. Organic Geochemistry 42, 1194-1202.

McBeath, A.V., Smernik, R.J., 2009. Variation in the degree of aromatic condensation of chars. Organic Geochemistry 40, 1161-1168.

McConnell, J.R., Edwards, R., Kok, G.L., Flanner, M.G., Zender, C.S., Saltzman, E.S., Banta, J.R., Pasteris, D.R., Carter, M.M., Kahl, J.D.W., 2007. 20th-Century Industrial Black Carbon Emissions Altered Arctic Climate Forcing. Science 317, 1381-1384.

McNaught, A.D., Wilkinson, A., 1997. IUPAC. Compendium of Chemical Terminology., 2nd Edition. Blackwell Scientific Publications, Oxford.

Meredith, W., Ascough, P.L., Bird, M.I., Large, D.J., Snape, C.E., Sun, Y., Tilston, E.L., 2012. Assessment of hydropyrolysis as a method for the quantification of black carbon using standard reference materials. Geochimica et Cosmochimica Acta 97, 131-147.

Meyer, S., Glaser, B., Quicker, P., 2011. Technical, economical, and climate-related aspects of biochar production technologies: a literature review. Environmental Science & Technology 45, 9473-9483.

Meyer, V., 2010. Practical High-Performance Liquid Chromatography.

Meyers, P., 2003. Applications of organic geochemistry to paleolimnological reconstructions: a summary of examples from the Laurentian Great Lakes. Organic Geochemistry 34, 261-289.

Ming, J., Cachier, H., Xiao, C., Qin, D., Kang, S., Hou, S., Xu, J., 2008. Black carbon record based on a shallow Himalayan ice core and its climatic implications. Atmospheric Chemistry and Physics 8, 1343-1352.

Moore, A., Owen, N., 2001. Infrared spectroscopic studies of solid wood. Applied Spectroscopy Reviews 36, 65-86.

Patterson, W.A., Edwards, K.J., Maguire, D.J., 1987. Microscopic charcoal as a fossil indicator of fire. Quaternary Science Reviews 6, 3-23.

Pechony, O., Shindell, D.T., 2010. Driving forces of global wildfires over the past millennium and the forthcoming century. Proceedings of the National Academy of Sciences of the United States of America 107, 19167-19170.

Pessenda, L.C.R., Aravena, R., Melfi, A.J., Telles, E.C.C., Boulet, R., Valencia, E.P.E., Tomazello, M., 1996. The use of carbon isotopes (^{13}C,^{14}C) in soil to evaluate vegetation changes during the holocene in Central Brazil. Radiocarbon 38, 191-201.

Polach, H., Singh, G., 1980. Contemporary ^{14}C levels and their significance to sedimentary history of Bega Swamp, New South Wales. Radiocarbon 22, 398-409.

Poot, A., Quik, J.T.K., Veld, H., Koelmans, A.A., 2009. Quantification methods of Black Carbon: Comparison of Rock-Eval analysis with traditional methods. Journal of Chromatography A 1216, 613-622.

Power, M.J., Marlon, J., Ortiz, N., Bartlein, P.J., Harrison, S.P., Mayle, F.E., Ballouche, A., Bradshaw, R.H.W., Carcaillet, C., Cordova, C., Mooney, S., Moreno, P.I., Prentice, I.C.,

Thonicke, K., Tinner, W., Whitlock, C., Zhang, Y., Zhao, Y., Ali, A.A., Anderson, R.S., Beer, R., Behling, H., Briles, C., Brown, K.J., Brunelle, A., Bush, M., Camill, P., Chu, G.Q., Clark, J., Colombaroli, D., Connor, S., Daniau, A.L., Daniels, M., Dodson, J., Doughty, E., Edwards, M.E., Finsinger, W., Foster, D., Frechette, J., Gaillard, M.J., Gavin, D.G., Gobet, E., Haberle, S., Hallett, D.J., Higuera, P., Hope, G., Horn, S., Inoue, J., Kaltenrieder, P., Kennedy, L., Kong, Z.C., Larsen, C., Long, C.J., Lynch, J., Lynch, E.A., McGlone, M., Meeks, S., Mensing, S., Meyer, G., Minckley, T., Mohr, J., Nelson, D.M., New, J., Newnham, R., Noti, R., Oswald, W., Pierce, J., Richard, P.J.H., Rowe, C., Goni, M.F.S., Shuman, B.N., Takahara, H., Toney, J., Turney, C., Urrego-Sanchez, D.H., Umbanhowar, C., Vandergoes, M., Vanniere, B., Vescovi, E., Walsh, M., Wang, X., Williams, N., Wilmshurst, J., Zhang, J.H., 2008. Changes in fire regimes since the Last Glacial Maximum: an assessment based on a global synthesis and analysis of charcoal data. Climate Dynamics 30, 887-907.

Power, M.J., Marlon, J.R., Bartlein, P.J., Harrison, S.P., 2010. Fire history and the Global Charcoal Database: A new tool for hypothesis testing and data exploration. Palaeogeography, Palaeoclimatology, Palaeoecology 291, 52-59.

Preston, C.M., Schmidt, M.W.I., 2006. Black (pyrogenic) carbon: a synthesis of current knowledge and uncertainties with special consideration of boreal regions. Biogeosciences 3, 397-420.

Quan, H., Shih, W.J., 1996. Assessing Reproducibility by the Within-Subject Coefficient of Variation with Random Effects Models. Biometrics 52, 1195-1203.

Quénéa, K., Derenne, S., Gonzalez-Vila, F.J., Mariotti, A., Rouzaud, J.N., Largeau, C., 2005. Study of the composition of the macromolecular refractory fraction from an acidic sandy forest soil (Landes de Gascogne, France) using chemical degradation and electron microscopy. Organic Geochemistry 36, 1151-1162.

Quilliam, R.S., Rangecroft, S., Emmett, B.A., Deluca, T.H., Jones, D.L., 2013. Is biochar a source or sink for polycyclic aromatic hydrocarbon (PAH) compounds in agricultural soils? GCB Bioenergy 5, 96-103.

R, 2011. R: A language and environment for statistical computing. R Foundation for Statistical Computing.

Ramanathan, V., Carmichael, G., 2008. Global and regional climate changes due to black carbon. Nature Geoscience 1, 221-227.

Rennert, T., Kaufhold, S., Brodowski, S., Mansfeldt, T., 2008. Interactions of ferricyanide with humic soils and charred straw. European Journal of Soil Science 59, 348-358.

Roscoe, R., Buurman, P., Velthorst, E.J., Vasconcellos, C.A., 2001. Soil organic matter dynamics in density and particle size fractions as revealed by the $^{13}C/^{12}C$ isotopic ratio in a Cerrado's oxisol. Geoderma 104, 185-202.

Roth, P.J., Lehndorff, E., Brodowski, S., Bornemann, L., Sanchez-García, L., Gustafsson, Ö., Amelung, W., 2012. Differentiation of charcoal, soot and diagenetic carbon in soil: Method comparison and perspectives. Organic Geochemistry 46, 66-75.

Ruff, M., Wacker, L., Gaggeler, H.W., Suter, M., Synal, H.A., Szidat, S., 2007. A gas ion source for radiocarbon measurements at 200 kV. Radiocarbon 49, 307-314.

Sánchez-García, L., de Andrés, J.R., Gélinas, Y., Schmidt, M.W.I., Louchouarn, P., 2013. Different pools of black carbon in sediments from the Gulf of Cádiz (SW Spain): Method comparison and spatial distribution. Marine Chemistry 151, 13-22.

Santos, F., Torn, M.S., Bird, J.A., 2012. Biological degradation of pyrogenic organic matter in temperate forest soils. Soil Biology and Biochemistry 51, 115-124.

Schimmelpfennig, S., Glaser, B., 2012. One Step Forward toward Characterization: Some Important Material Properties to Distinguish Biochars. Journal of Environment Quality 41, 1001-1013.

Schmidt, M.W.I., Noack, A.G., 2000. Black carbon in soils and sediments: Analysis, distribution, implications, and current challenges. Global Biogeochemical Cycles 14, 777-793.

Schmidt, M.W.I., Skjemstad, J.O., Czimczik, C.I., Glaser, B., Prentice, K.M., Gelinas, Y., Kuhlbusch, T.A.J., 2001. Comparative analysis of black carbon in soils. Global Biogeochemical Cycles 15, 163-167.

Schmidt, M.W.I., Torn, M.S., Abiven, S., Dittmar, T., Guggenberger, G., Janssens, I.A., Kleber, M., Kogel-Knabner, I., Lehmann, J., Manning, D.A.C., Nannipieri, P., Rasse, D.P., Weiner, S., Trumbore, S.E., 2011. Persistence of soil organic matter as an ecosystem property. Nature 478, 49-56.

Schneider, M.P.W., Hilf, M., Vogt, U.F., Schmidt, M.W.I., 2010. The benzene polycarboxylic acid (BPCA) pattern of wood pyrolyzed between 200 °C and 1000 °C. Organic Geochemistry 41, 1082-1088.

Schneider, M.P.W., Smittenberg, R., Dittmar, T., Schmidt, M.W.I., 2011. Comparison of gas with liquid chromatography for the determination of benzenepolycarboxylic acids as molecular tracers of black carbon. Organic Geochemistry 42, 275-282.

Scott, A.C., Bowman, D.M.J.S., Bond, W.J., Pyne, S.J., Alexander, M.E., 2014. Fire on Earth: An Introduction. Wiley, New York.

Shafizadeh, F., 1982. Introduction to pyrolysis of biomass. Journal of Analytical and Applied Pyrolysis 3, 283-305.

Shah, S.R., Pearson, A., 2007. Ultra-microscale (5-25 μg C) analysis of individual lipids by ^{14}C AMS: Assessment and correction for sample processing blanks. Radiocarbon 49, 69-82.

Sillett, S.C., Pelt, R.V., 2007. Trunk reiteration promotes epiphytes and water storage in an old-growth redwood forest canopy. Ecological Monographs 77, 335-359.

Simoneit, B.R.T., 1984. Organic matter of the trophosphere - III. Characterization and sources of petroleum and pyrogenic residues in aerosols over the western United States. Atmospheric Environment 18, 51-67.

Simoneit, B.R.T., 2002. Biomass burning -- a review of organic tracers for smoke from incomplete combustion. Applied Geochemistry 17, 129-162.

Simpson, M.J., Hatcher, P.G., 2004. Determination of black carbon in natural organic matter by chemical oxidation and solid-state ^{13}C nuclear magnetic resonance spectroscopy. Organic Geochemistry 35, 923-935.

Singh, B.P., Cowie, A.L., Smernik, R.J., 2012a. Biochar carbon stability in a clayey soil as a function of feedstock and pyrolysis temperature. Environmental Science & Technology 46, 11770-11778.

Singh, N., Abiven, S., Torn, M.S., 2012b. Fire-derived organic carbon in soil turns over on a centennial scale. Biogeosciences 9, 2847-2857.

Skjemstad, J.O., Janik, L.J., Head, M.J., MacClure, S.G., 1993. High energy ultraviolet photo-oxidation: a novel technique for studying physically protected organic matter in clay- and silt-sized aggregates. Journal of Soil Science 44, 485-499.

Skjemstad, J.O., Taylor, J.A., Smernik, R.J., 1999. Estimation of charcoal (char) in soils. Communications in Soil Science and Plant Analysis 30, 2283-2298.

Sohi, S.P., Krull, E., Lopez-Capel, E., Bol, R., 2010. Chapter 2 - A Review of Biochar and Its Use and Function in Soil, in: Donald, L.S. (Ed.), Advances in Agronomy. Academic Press, pp. 47-82.

Stahel, W., 2011. The R-Function regr for an Augmented Regression Analysis. ETH Zürich, Zürich.

Stekhoven, D., Buehlmann, P., 2012. MissForest--non-parametric missing value imputation for mixed-type data. Bioinformatics 28, 112-118.

Synal, H.A., Stocker, M., Suter, M., 2007. MICADAS: A new compact radiocarbon AMS system. Nuclear Instruments and Methods in Physics Research, Section B: Beam Interactions with Materials and Atoms 259, 7-13.

Tinner, W., Hubschmid, P., Wehrli, M., Ammann, B., Conedera, M., 1999. Long-term forest fire ecology and dynamics in southern Switzerland. Journal of Ecology 87, 273-289.

Torero, J.L., 2013. An Introduction to Combustion in Organic Materials, Fire Phenomena and the Earth System. John Wiley & Sons, pp. 1-13.

Veirs, S.D., Unit, C.N.P.R.S., Parks, C.D.o., Recreation, 1987. Vegetation Studies of Elk Prairie, Prairie Creek Redwoods State Park, Humboldt County, California. Cooperative Park Studies Unit, National Park Service, Redwood National Park.

Verardo, D.J., 1997. Charcoal analysis in marine sediments. Limnology and Oceanography 42, 192-197.

Wacker, L., Fahrni, S.M., Hajdas, I., Molnar, M., Synal, H.A., Szidat, S., Zhang, Y.L., 2013. A versatile gas interface for routine radiocarbon analysis with a gas ion source. Nuclear Instruments and Methods in Physics Research Section B: Beam Interactions with Materials and Atoms 294, 315-319.

Whitlock, C., 2002. Charcoal as a fire proxy. Developments in Paleoenvironmental Research 3, 75-97.

Whitlock, C., Anderson, R.S., 2003. Fire history reconstructions based on sediment records from lakes and wetlands, in: Veblen, T.T., Baker, W.L., Montenegro, G., Swetnam, T.W. (Eds.), Fire and climatic change in temperate ecosystems of the western Americas. Springer, New York, pp. 3-31.

Wiedemeier, D.B., Bloesch, U., Hagedorn, F., 2012. Stable forest–savanna mosaic in north-western Tanzania: local-scale evidence from $\delta^{13}C$ signatures and ^{14}C ages of soil fractions. Journal of Biogeography 39, 247-257.

Wiesenberg, G.L.B., Gocke, M., Kuzyakov, Y., 2010. Fast incorporation of root-derived lipids and fatty acids into soil – evidence from a short term multiple pulse labelling experiment. Organic Geochemistry 41, 1049-1055.

Wiesenberg, G.L.B., Lehndorff, E., Schwark, L., 2009. Thermal degradation of rye and maize straw: lipid pattern changes as a function of temperature. Organic Geochemistry 40, 167-174.

Wiesenberg, G.L.B., Schmidt, M.W.I., Schwark, L., 2008. Plant and soil lipid modifications under elevated atmospheric CO2 conditions: I. Lipid distribution patterns. Organic Geochemistry 39, 91-102.

Wiesenberg, G.L.B., Schwark, L., Schmidt, M.W.I., 2004. Improved automated extraction and separation procedure for soil lipid analyses. European Journal of Soil Science 55, 349-356.

Wilcke, W., 2000. Polycyclic aromatic hydrocarbons (PAHs) in soil — A review. Journal of Plant Nutrition and Soil Science 163, 229-248.

Wood, D.J., 1988. Characterization of charcoals by drift. Mikrochimica Acta 2, 167-169.

Wu, Q., Blume, H.P., Beyer, L., Schleuß, U., 1999. Method for characterization of inert organic carbon in urbic anthrosols. Communications in Soil Science and Plant Analysis 30, 1497-1506.

Yarnes, C., Santos, F., Singh, N., Abiven, S., Schmidt, M.W.I., Bird, J.A., 2011. Stable isotopic analysis of pyrogenic organic matter in soils by liquid chromatography–isotope-ratio mass spectrometry of benzene polycarboxylic acids. Rapid Communications in Mass Spectrometry 25, 3723-3731.

Yunker, M.B., Macdonald, R.W., Vingarzan, R., Mitchell, R.H., Goyette, D., Sylvestre, S., 2002. PAHs in the Fraser River basin: a critical appraisal of PAH ratios as indicators of PAH source and composition. Organic Geochemistry 33, 489-515.

Ziolkowski, L., Druffel, E., 2010. Aged black carbon identified in marine dissolved organic carbon. Geophysical Research Letters 37, L16601.

Ziolkowski, L.A., Druffel, E.R.M., 2009a. The feasibility of isolation and detection of fullerenes and carbon nanotubes using the benzene polycarboxylic acid method. Marine Pollution Bulletin 59, 213-218.

Ziolkowski, L.A., Druffel, E.R.M., 2009b. Quantification of extraneous carbon during compound specific radiocarbon analysis of black carbon. Analytical Chemistry 81, 10156-10161.

Part B - Publications

Paper I

Improved assessment of pyrogenic carbon quantity and quality in environmental samples by high-performance liquid chromatography

Published as:

Wiedemeier, D.B., Hilf, M.D., Smittenberg, R.H., Haberle, S.G., Schmidt, M.W.I., 2013. Improved assessment of pyrogenic carbon quantity and quality in environmental samples by high-performance liquid chromatography. Journal of Chromatography A 1304, 246-250.

Author contributions:

D.B.W. designed and conducted the study, analyzed the data and wrote the paper. M.D.H. and R.H.S. gave conceptual and technical support. S.G.H. provided the peatland core and charcoal counts and M.W.I.S. designed the study and gave conceptual advice.

Abstract

The analysis of pyrogenic carbon (PyC) in environmental samples is of great interest, e.g. for carbon cycle assessment, (bio-)char characterization and palaeoenvironmental or archaeological reconstruction. Here, an HPLC method (HPLC) is presented that reproducibly quantifies Benzene Polycarboxylic Acids (BPCA) as molecular markers for PyC in various kinds of environmental samples. It operates at low pH without requiring an organic modifier and was thoroughly tested with PyC reference materials and a peatland core that served as a feasibility and plausibility check. Compared to the established gas chromatography (GC) method, the HPLC method results in higher BPCA quantification reproducibility by showing a significantly smaller coefficient of variation (HPLC: 5 %, GC: 16 – 23 %). It works well with small sample amounts, as for instance from sediment cores and aerosol collectors, and requires less sample preparation work than the GC method. Moreover, the here presented HPLC method facilitates ^{13}C and ^{14}C analyses on PyC from environmental samples.

Introduction

Pyrogenic carbon (PyC) is the solid residue of incomplete biomass combustion and can persist in the environment for a long time [1-2]. It is, therefore, ubiquitously found in different environmental matrices, e.g. in soil, sediment, water or as an aerosol [3-5]. Its accurate quantification is of great interest because its slow turnover has implications for the global carbon budget [6]. In addition, PyC affects the atmospheric radiative budget [5] and is a constituent of many anthropogenic nanoparticles [7]. Many different methods have been developed for PyC detection and quantification [6,8-9] because PyC is not a defined chemical structure but rather a continuum of thermally altered biomass [6,10]. The benzene polycarboxylic acids (BPCA) analysis [4,11-13] is a molecular marker method that has been shown to yield conservative estimates of PyC quantity in different environmental matrices and was able to quantify PyC over a broad range of the combustion continuum [8]. Moreover, the BPCA method yields additional information about PyC quality, such as its degree of aromaticity and aromatic condensation, which is related to the temperature of pyrolysis [14-15]. Since the method is based directly on molecular separation, it also allows the further analysis of isolated PyC molecular compounds to determine their isotopic composition, including ^{13}C and ^{14}C [16-17].

The BPCA method employs nitric acid to break down the PyC polymers into a suite of BPCA monomers, which are then purified and chromatographically analyzed. This last step is commonly done by gas chromatography (GC) [11-13]. The amount of detected BPCAs in a sample then serves as an estimate of its PyC content. Recently, it was shown that the procedure could be simplified for highly organic seawater or charcoal samples by analyzing the BPCAs on a high-performance liquid chromatography system ($HPLC_{organic}$) [4,15]. Liquid chromatography does not require the time-consuming, external carbon-introducing and sometimes incomplete derivatization, which is necessary for the GC method (a technical overview is given in the supplementary material).

Although the $HPLC_{organic}$ method works well with highly organic samples, analyses of more complex environmental matrices proved difficult due to interference from organic and inorganic substances. Moreover, the $HPLC_{organic}$ method runs at pH 8 and uses tetrabutylammonium bromide, an organic modifier that prohibits the potential use of mass spectrometry, including isotope analyses. It is possible to use ion exchange chromatography [17] in order to circumvent this issue at high pH, but this approach unfortunately suffers from laborious sample preparation and tedious solvent and column maintenance.

Here, we present an improved HPLC method (HPLC) that is able to reproducibly separate and quantify BPCAs in complex environmental matrices with varying amounts and types of organic matter contents as well as in highly organic samples. Its low pH allows separation without an organic modifier and the use of the here described mobile phases is favorable for subsequent isotopic analysis of BPCAs. Environmental PyC reference materials were measured for comparing the HPLC method with the previous GC method. To test for

plausibility, we analyzed a peatland core from a location that is known for its wide range of organic matter and charcoal contents.

Materials and Methods

Environmental PyC reference materials

A suite of PyC reference materials from a previous intercomparison exercise [8,18] was used to compare HPLC and GC quantification of BPCAs. In particular, Aerosol (NIST Standard SRM 1649b - Urban Dust), Marine Sediment (NIST Standard SRM 1941b), Vertisol (Clay Soil), Chernozem (Silty Soil), Dissolved Organic Matter (DOM), Wood Charcoal (pyrolyzed *Castanea Sativa*), Grass Charcoal (pyrolyzed *Oryza Sativa*) and *n*-hexane soot were analyzed.

In order to compare the HPLC method with the previous GC method, their respective intra-laboratory reproducibility was quantitatively assessed with the coefficient of variation (CV) [19] by measuring the environmental PyC materials in replicates (Table 1).

Peatland core

Bulk core analyses

A 2.5 m long core was taken at Bega Swamp [20-21] (NSW, Australia, 36 ° 32 ' 1.79 " S, 149 ° 29 ' 55.12 " E) and was split in 5 cm sections. The material within sections was homogenized and then taken for charcoal analyses (wet) or BPCA analyses (dried).

Charcoal Counting on the fraction >125 µm

A standardized macrocharcoal (> 125 µm) counting procedure [22-23] was carried out in each depth interval. Charcoal pieces were counted [number of pieces / wet volume aliquot] but PyC was reported as concentration [g BPCA-C / g dry material], and thus cannot be compared directly. In order to correct for the water mass loss due to drying, the charcoal counts were normalized by the factor f, as explained below. Furthermore, the logarithmic distribution of the charcoal counts was corrected. Both corrections helped to produce more comparable measures for the presence of charcoal, either reported as counts or as BPCA-based PyC concentrations (equation 1).

$$\log\left\{Charcoal\ counts\ \left[\frac{pieces}{aliquot}\right] * f\right\} \propto Pyrogenic\ carbon\ \left[\frac{BPCA-C\ [g]}{dry\ sample\ weight\ [g]}\right] \quad \text{(equation 1)}$$

where: $f = \frac{1}{dry\ sample\ weight\ [g]}$

BPCA analyses with the HPLC method

For the here presented HPLC method, we weighed dried and milled samples containing approximately > 1 mg TOC and digested the samples directly with nitric acid (65%, 8 h at 170 °C). The resulting solution, containing the BPCAs, was filtrated over ashless cellulose filters. The solution was further cleaned by a cation exchange resin and freeze dried to remove the acid. The freeze-dried residue was then redissolved in methanol/water (1:1) and eluted over a C18 solid phase extraction cartridge (Supelco, U.S.A.) to remove apolar compounds, after which it was dried again and transferred to the HPLC vials in ultrapure water.

Chromatographic BPCA separation was carried out with an Agilent 1290 Infinity HPLC system (Santa Clara, U.S.A.), equipped with an Agilent Poroshell 120 SB-C18 column (100 mm x 4.6 mm). Mobile Phase A consisted of orthophosphoric acid (Sigma-Aldrich, U.S.A) dissolved in water and buffered with NaH_2PO_4 (Sigma-Aldrich, U.S.A) to a pH-value of 1.2. Pure acetonitrile (Scharlau, Spain) was used as the mobile phase B (c.f. supplementary data for mixing gradients). Alternatively, a purely aqueous gradient to pH = 4.7 can be used if it is important to work without organic solvents, e.g. for subsequent on-line oxidation to perform carbon isotopic analyses on the BPCAs (supplementary data). Figure 1 depicts the retention times of the BPCA target components for three different samples. A photo diode array detector (DAD) was used for peak identification (absorbance spectra 190 – 400 nm), in concert with retention times of BPCA standards. The 240 nm and 216 nm wavelengths (slit width: 8 nm) were used to record the chromatograms for subsequent quantification.

HPLC method evaluation

We tested the HPLC method further in-depth with respect to (I) quantification of BPCAs, (II) required sample quantities and (III) recoveries of BPCAs after the simplified pretreatment steps prior to HPLC injection.

For the chromatographic quantification of the BPCAs (I), we compared the more reliable standard addition quantification approach with the less laborious external standard quantification approach [24]. The two approaches yielded essentially the same results in case of the matrix containing Chernozem reference sample (supplementary data), suggesting that the simpler external standard quantification is suitable for the HPLC method.

The linearity of the HPLC method (II) was evaluated by measuring two reference matrix samples (Chernozem, Vertisol) with differing sample amounts. Quantification was linear, even when working with less than 100 mg of soil sample (supplementary data), corresponding to roughly 1 mg of organic carbon per sample.

Recovery of the BPCAs (III) after pretreatment (cation exchange resin, solid phase extraction, transfer and handling) was assessed by treating well-known amounts of BPCA standard solutions (Sigma-Aldrich, U.S.A) the same way as the samples. No systematic proportional

error was observed (supplementary data), i.e. the recovery is independent from the amount of sample or its BPCA content. There is, however, a small systematic constant error (< 14 μg) for all BPCAs, which is probably due to losses during handling.

Results and Discussion

HPLC-BPCA method for environmental samples (HPLC)

The HPLC sample pretreatment procedure and separation technique allowed baseline separation of all BPCA target components in all the analyzed environmental samples (e.g. Fig 1). Thus, it also represents an improvement compared to previous HPLC methods (e.g. $HPLC_{organic}$) because, to the best of our knowledge, no baseline separation of all BPCAs has been achieved with liquid chromatography before [15,17].

The HPLC method resulted in a more consistent quantification of PyC reference materials as compared to the well-established GC method. In a repeated experiment, the Chernozem reference sample was measured multiple times (n = 28) in our laboratory using both the GC [13] and the HPLC procedure. The HPLC method showed a much smaller coefficient of variation (CV = 6 %) compared to the GC method (CV = 22 %), translating into better reproducibility (Fig 2, right side). The improved intra-laboratory reproducibility of the HPLC method versus the GC method was further confirmed when we compared the replicated (n = 2 - 3) PyC-values of eight reference materials analyzed with both methods (Fig 2). The samples had been analyzed by two to three different laboratories using the GC method [8] with a respective mean intra-laboratory CV of 16 - 23 % (min: 6 %, max: 43 %; Fig 2, bottom). In contrast, the HPLC method showed a mean intra-laboratory CV of only 5 % (min: 1 %, max: 10 %) and thus a much better intra-laboratory measurement reproducibility.

The BPCA yields also showed a consistent pattern between the HPLC and the GC method: The HPLC method always detected an amount that was at least equal to the maximum detected by the other laboratories using the GC method. In the case of the two charcoal standards, the HPLC method detected even slightly more than the maximum of the GC measurements. It seems, therefore, that the HPLC method always captures the maximal yields of BPCA, resulting in a lower variation of the replicates.

These results are in agreement with a previous GC-$HPLC_{organic}$ comparison using almost purely organic (char) samples [15]. Higher reproducibility and yields of the $HPLC_{organic}$ method were, at that time, attributed to fewer losses during sample handling and possibly the omission of the trifluoracetic acid and the derivatization step (cf. supplementary data). This probably also holds true in the case of the environmental matrix samples measured with the presented HPLC method.

The here presented HPLC method has additional advantages over the GC method. While it requires less sample material per measurement, higher sample throughput is achieved

because of the simplified sample preparation and reduced chromatographic analysis time. Additionally, entirely prepared samples can now be stored in the vials for at least three months, which is useful in case of intermittent instrument access, or repeat measurements made later. In the GC protocol, samples had to be laboriously preprocessed immediately before measurement (cf. supplementary data).

PyC in the peatland core

We considered the Bega Swamp peatland core to be an ideal test sample for the HPLC method because it spans a wide range of TOC contents (0.4 % – 42 % TOC), and because its wildfire history is well known [25]. Although TOC contents varied widely, chromatographic separation of BPCAs was excellent and PyC could be reliably quantified throughout the whole core.

The PyC quantification revealed very plausible site characteristics. Normalizing the PyC content to dry sample mass (Fig 3e) mirrored the overall trend of TOC because the PyC/TOC ratio stayed relatively constant. However, in contrast to the TOC, the PyC values deviated between the bulk sediment and the > 125 μm fraction for the layers above *ca.* 130 cm (Fig 3e, striped area). The grain sizes > 125 μm, were enriched in PyC in these upper layers. When we additionally consider the fact that the large grain size fraction (> 125 μm) dominates the upper part of the sediment (Fig 3b), it becomes evident that the majority of total PyC in the upper part of the peatland must have consisted of relatively large particles. The size distribution of fire residue particles in sediments is often used to reconstruct the distance of past fire events [26-28]. Thus, the larger pyrogenic particles present in the upper 130 cm indicate more local fires in the last *ca.* 4000 years [20], which appears very plausible because it coincides with the onset of drier conditions and the expansion of the *Eucalyptus*/*Casuarina* forest at this site [25].

Without venturing too far into the large field of wildfire reconstructions (e.g. Conedera et al. [29]), we aimed for an additional, simple plausibility check: Does the BPCA method detect similar quantities of fire residues to the charcoal count method for the same sample? The two measures capture two different aspects of charcoal (particle count vs. molecular mass concentration) and cannot be compared directly (section 2.2.2). Still, both values basically show a similar pattern for the peatland core (Fig 3e/f). Since BPCAs are a molecular marker for charcoal [11], correlation between the charcoal count data and the molecular marker can be expected, confirming the plausibility of the BPCA measurements obtained with the HPLC method presented above.

Conclusion and Outlook

The presented HPLC method for various kinds of environmental samples requires less sample material than the widely used GC method and is thus particularly suitable for small samples, e.g. from sediment cores or aerosol collectors. Despite the reduction of sample amounts and the simplification of sample pretreatment, the HPLC method still showed higher reproducibility and very plausible PyC values as compared to the commonly used GC method or when applied to samples from a peatland site.

The BPCA isolation and separation method applied here (HPLC) can be used to purify individual BPCA for subsequent radiocarbon analyses (unpublished results). Moreover, when the method is set up with a pH gradient as shown above, it is possible to measure the ^{13}C of the PyC-derived BPCAs by on-line isotope-ratio monitoring. Besides PyC quantity and quality, the PyC isotopic information may yield valuable supplementary information about the burned biomass fuel and its age. Thus, the field of possible applications for the HPLC method is large and includes paleo-environmental reconstructions using sediment cores, the investigation of archaeological artifacts, or biochar and soil carbon studies.

Acknowledgements

We thank Janelle Stevenson for her help with the Bega Swamp samples, Guido L. B. Wiesenberg, Maximilian P. W. Schneider and Marco Griepentrog for constructive discussions on our manuscript and Ivan Woodhatch for a language check.

Table 1.The environmental PyC reference materials that were used for the comparison of the HPLC method with the GC method. Chernozem and Vertisol were also used for the HPLC method evaluation (chromatographic quantification approach and linearity). The GC data from the different laboratories come from Hammes et al. [8,18] and the GC data from the repeated experiment were partially published in Schneider et al. [13].

PyC Reference Material	Number of Replicates			
	HPLC	GC		
	our lab	our lab	other lab 1	other lab 2
Aerosol	2	3	3	--
DOM	3	2	4	--
Marine Sediment	3	2	2	--
Vertisol	3	3	2	3
Chernozem	3	3	2	2
Grass Charcoal	2	3	2	2
Wood Charcoal	3	3	2	2
Soot	3	3	2	3
repeated experiment:				
Chernozem	28	28	--	--
HPLC method evaluation:				
Chernozem	22	--	--	--
Vertisol	9	--	--	--

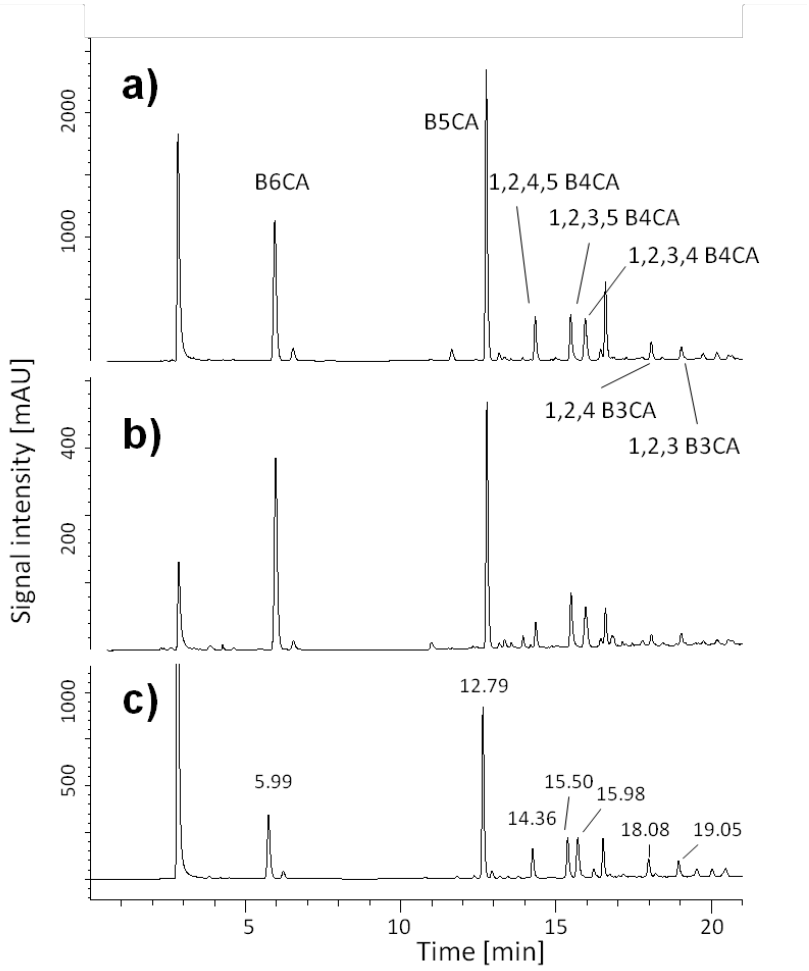

Figure 1. Chromatograms of nitric acid oxidation products according to the HPLC preparation and analysis method: a) Sediment from Bega Swamp in 80 – 85 cm depth, sieved to > 125 µm; b) Chernozem; c) Grass charcoal (*Oryza Sativa*). Baseline separation was achieved for all the BPCA target components (B6CA; B5CA; 1,2,4,5-, 1,2,3,5-, 1,2,3,4-B4CA; 1,2,4-, 1,2,3-B3CA) in all the analyzed samples.

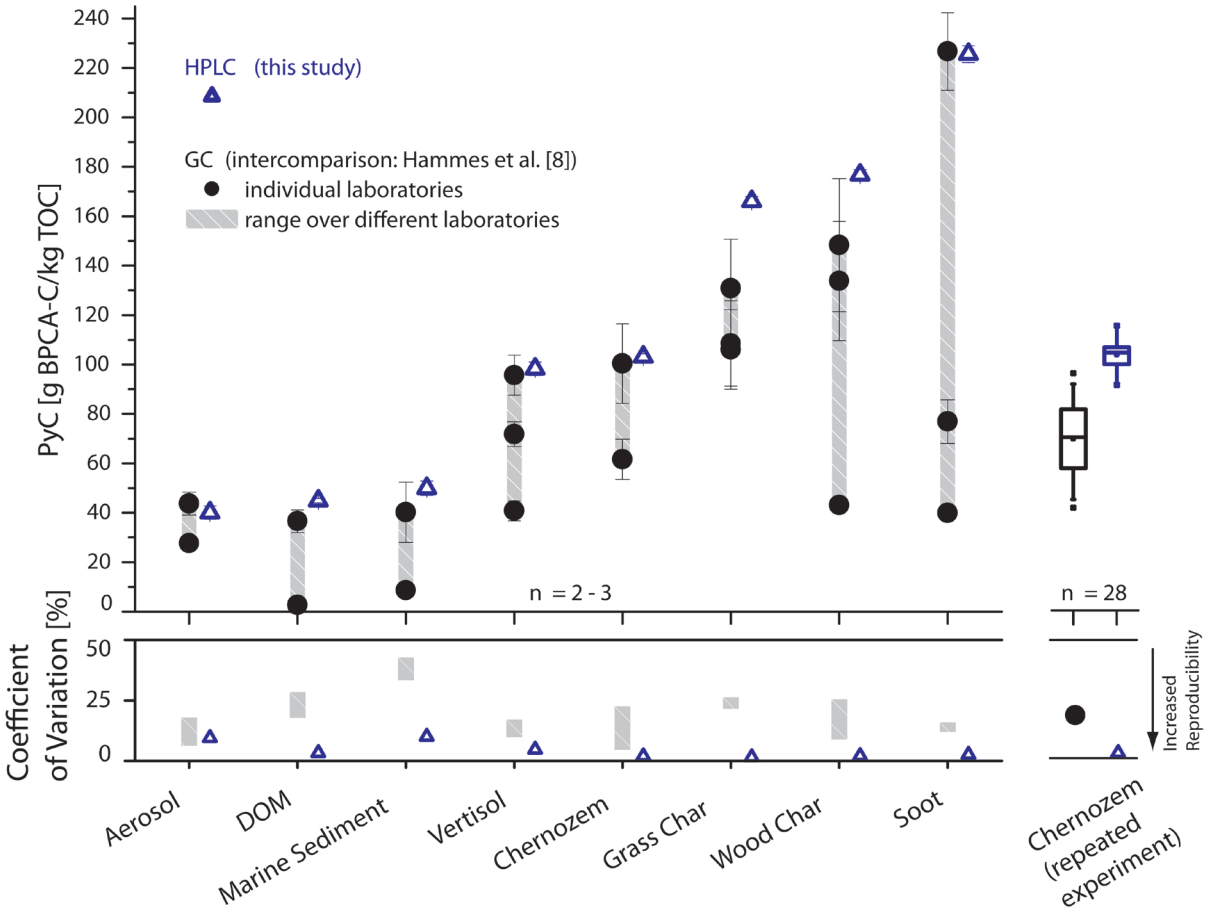

Figure 2. Replicated PyC measurements of different PyC reference materials with the HPLC and GC method. Error bars for the HPLC method are mostly smaller than symbol size. Triangles in this and the following figure represent PyC quantifications that were achieved with the HPLC method. Intra-laboratory measurement reproducibility was higher for the HPLC method than the GC method, as can be seen by the lower coefficient of variation. Moreover, the HPLC method always detected the maximum amount of PyC (maximal BPCA yield) in the reference materials that was detected with the GC method in the different laboratories.

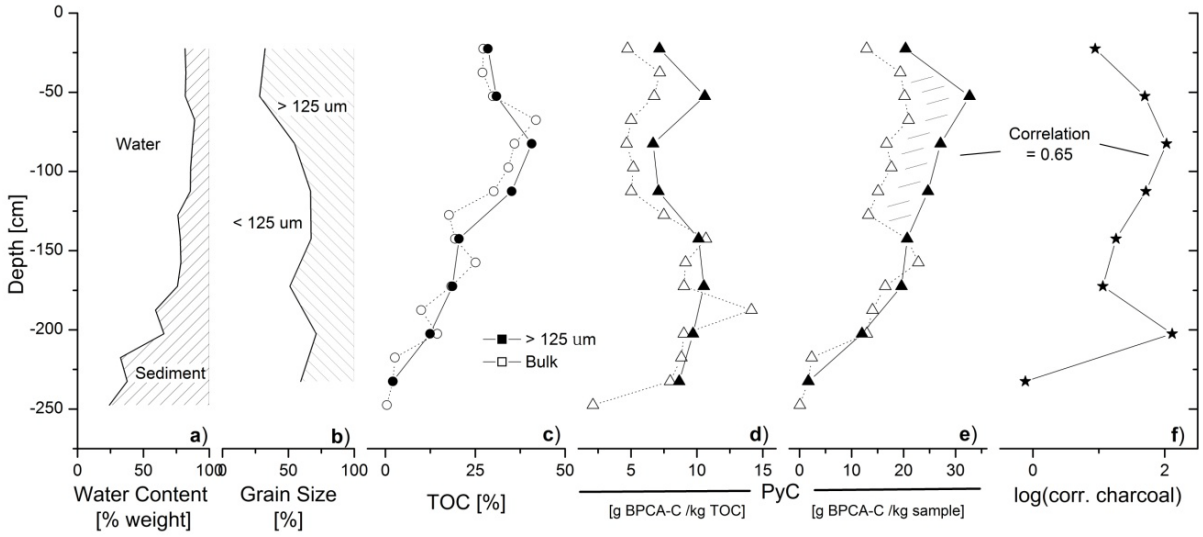

Figure 3. Bega Swamp core characteristics with respect to water content, grain size, TOC, PyC and charcoal counts. Empty symbols show the values for the bulk sediment while filled symbols represent the values for the fraction > 125 µm. Analytical errors for TOC (n = 2) and PyC (n = 3) are smaller than symbol size while charcoal counts were not replicated.

References

[1] E.D. Goldberg, Black carbon in the environment: properties and distribution, Wiley, New York, 1985.

[2] M.W.I. Schmidt, M.S. Torn, S. Abiven, T. Dittmar, G. Guggenberger, I.A. Janssens, M. Kleber, I. Kogel-Knabner, J. Lehmann, D.A.C. Manning, P. Nannipieri, D.P. Rasse, S. Weiner, S.E. Trumbore, Nature 478 (2011) 49.

[3] J.M. de la Rosa, L.S. García, J.R. de Andrés, F.J. González-Vila, J.A. González-Pérez, H. Knicker, Quaternary International 243 (2011) 264.

[4] T. Dittmar, Organic Geochemistry 39 (2008) 396.

[5] T.C. Bond, S.J. Doherty, D.W. Fahey, P.M. Forster, T. Berntsen, B.J. DeAngelo, M.G. Flanner, S. Ghan, B. Kärcher, D. Koch, S. Kinne, Y. Kondo, P.K. Quinn, M.C. Sarofim, M.G. Schultz, M. Schulz, C. Venkataraman, H. Zhang, S. Zhang, N. Bellouin, S.K. Guttikunda, P.K. Hopke, M.Z. Jacobson, J.W. Kaiser, Z. Klimont, U. Lohmann, J.P. Schwarz, D. Shindell, T. Storelvmo, S.G. Warren, C.S. Zender, Journal of Geophysical Research: Atmospheres (2013) n/a.

[6] C.A. Masiello, Marine Chemistry 92 (2004) 201.

[7] L.A. Ziolkowski, E.R.M. Druffel, Marine Pollution Bulletin 59 (2009) 213.

[8] K. Hammes, M.W.I. Schmidt, R.J. Smernik, L.A. Currie, W.P. Ball, T.H. Nguyen, P. Louchouarn, S. Houel, Ö. Gustafsson, M. Elmquist, G. Cornelissen, J.O. Skjemstad, C.A. Masiello, J. Song, P.a. Peng, S. Mitra, J.C. Dunn, P.G. Hatcher, W.C. Hockaday, D.M. Smith, C. Hartkopf-Fröder, A. Böhmer, B. Lüer, B.J. Huebert, W. Amelung, S. Brodowski, L. Huang, W. Zhang, P.M. Gschwend, D.X. Flores-Cervantes, C. Largeau, J.-N. Rouzaud, C. Rumpel, G. Guggenberger, K. Kaiser, A. Rodionov, F.J. Gonzalez-Vila, J.A. Gonzalez-Perez, J.M. de la Rosa, D.A.C. Manning, E. López-Capél, L. Ding, Global Biogeochem. Cycles 21 (2007) GB3016.

[9] A. Poot, J.T.K. Quik, H. Veld, A.A. Koelmans, Journal of Chromatography A 1216 (2009) 613.

[10] M.W.I. Schmidt, A.G. Noack, Global Biogeochemical Cycles 14 (2000) 777.

[11] B. Glaser, L. Haumaier, G. Guggenberger, W. Zech, Organic Geochemistry 29 (1998) 811.

[12] S. Brodowski, A. Rodionov, L. Haumaier, B. Glaser, W. Amelung, Organic Geochemistry 36 (2005) 1299.

[13] M.P.W. Schneider, M. Hilf, U.F. Vogt, M.W.I. Schmidt, Organic Geochemistry 41 (2010) 1082.

[14] A. McBeath, R. Smernik, E. Plant, Organic Geochemistry 42 (2011) 1194.

[15] M.P.W. Schneider, R.H. Smittenberg, T. Dittmar, M.W.I. Schmidt, Organic Geochemistry 42 (2011) 275.

[16] L. Ziolkowski, E. Druffel, Geophysical Research Letters 37 (2010).

[17] C. Yarnes, F. Santos, N. Singh, S. Abiven, M.W.I. Schmidt, J.A. Bird, Rapid Communications in Mass Spectrometry 25 (2011) 3723.

[18] K. Hammes, R.J. Smernik, J.O. Skjemstad, M.W.I. Schmidt, Applied Geochemistry 23 (2008) 2113.

[19] H. Quan, W.J. Shih, Biometrics 52 (1996) 1195.

[20] H. Polach, G. Singh, Radiocarbon 22 (1980) 398.

[21] D. Green, G. Singh, H. Polach, D. Moss, J. Banks, E.A. Geissler, Journal of Ecology 76 (1988) 790.

[22] R.L. Clark, Pollen et Spores 24 (1982) 523.

[23] C. Whitlock, R.S. Anderson, in T.T. Veblen, W.L. Baker, G. Montenegro, T.W. Swetnam (Editors), Fire and climatic change in temperate ecosystems of the western Americas, Springer, New York, 2003, p. 3.

[24] V. Meyer, Practical High-Performance Liquid Chromatography, 2010.

[25] T.H. Donders, S.G. Haberle, G. Hope, F. Wagner, H. Visscher, Quaternary Science Reviews 26 (2007) 1621.

[26] W.A. Patterson, K.J. Edwards, D.J. Maguire, Quaternary Science Reviews 6 (1987) 3.

[27] J.S. Clark, J. Lynch, B.J. Stocks, J.G. Goldammer, Holocene 8 (1998) 19.

[28] P.E. Higuera, M.E. Peters, L.B. Brubaker, D.G. Gavin, Quaternary Science Reviews 26 (2007) 1790.

[29] M. Conedera, W. Tinner, C. Neff, M. Meurer, A.F. Dickens, P. Krebs, Quaternary Science Reviews 28 (2009) 555.

Supplementary Material

The commonly used GC method for environmental samples, the $HPLC_{organic}$ method for highly organic samples and the here presented HPLC method for various environmental samples. Note that Yarnes et al. [17] presented an ion exchange chromatography approach that is not listed here.

Nr	Work step/description	GC-BPCA	$HPLC_{organic}$-BPCA (only for highly organic samples)	HPLC-BPCA
		Glaser et al. (1998), Brodowski et al. (2005), Schneider et al. (2010)	Dittmar (2008), Schneider et al. (2011)	this study
1	Sample preparation before HNO_3 digestion	Trifluoracetic acid (TFA) digestion (4 h at 105 °C), filtration: collect sample on glass fiber filter(GF 6, Schleicher and Schuell, Dassel, Germany) and rinse wih excess of water, dry (2 h at 40 °C)		
2	HNO_3 digestion, conversion to BPCA	2 ml 65% HNO_3 (8 h at 170 °C in oven)	2 ml 65% HNO_3 (8 h at 170 °C in oven)	2 ml 65% HNO_3 (8 h at 170 °C in oven)
	Solid to acid ratio, mg C ml^{-1}	1-25	1-2.5	1-25
3	Sample preparation after HNO_3 digestion	Filtration over ashless cellulose filter (589/3, 110 mm diameter, Schleicher and Schuell, Dassel, Germany) into 10 ml volumetric flasks, fill up with deionized water	Drying at 60 °C under N_2 stream and dissolution in methanol/water (1:3), further dilution with mobile phase A	Filtration over ashless cellulose filter (589/3, 110 mm diameter, Schleicher and Schuell, Dassel, Germany) into 50 ml volumetric flasks, fill up with deionized water
		Addition of internal standard phtalic acid, cleaning with cation exchange resin (Dowex 50 W X 8, 200-400 mesh, Fluka, Steinheim, Germany), freeze drying for acid removal, transfer to GC vials with four times 1 ml methanol		Cleaning with cation exchange resin (Dowex 50 W X 8, 200-400 mesh, Fluka, Steinheim, Germany), freeze drying for acid removal.
				Redissolution in methanol/water (1:1), cleaning through solid phase extraction tubes (DSC-18, Supelco, USA), drying and transfer to LC vial in ultrapure water
4	Derivatization	100 µl BSTFA + TMCS, 100 µl pyridine (2 h at 80 °C + storage for 24 h)		
5	Chromatographic analysis			
	Mobile phase A	He	Ortho phosphoric acid (50%) 1 ml l^{-1} Tetrabutylammonium bromide (TBAB) 2g l^{-1} - Dissolved in water - Adjusted to pH 8 by slowly adding 1 M NaOH	Ortho phosphoric acid (85%) 25 ml l^{-1} - Dissolved in water - Buffered with NaH_2PO_4 (ca. 250 mg l^{-1}) - target value pH 1.2
	Mobile phase B	-	Mobile phase A + 75% MeOH	Acetonitrile
	Injection volume	1 µl	20 µl	1 µl
	Injections per sample replicate	2	1	1
	Flow rate	0.8 ml min^{-1}	0.18 ml min^{-1}	0.4 ml min^{-1}
	Column temperature	100-300 °C	16 °C	15 °C
	Column/quantification	Agilent DB-5 (50 m, diameter 0.2 mm)/flame ionization detector (FID)	Waters Atlantis T3 3µm (150 mm, diameter 2.1 mm)/ UV absorption at 240 nm	Agilent Poroshell 120 SB-C18 (100 mm, diameter 4.6 mm)/ UV absorption at 240 nm
	Identification	Retention time, GC-MS	Retention time, absorbance spectra 220-380 nm	Retention time, absorbance spectra 190-400 nm
	Quantification	External standards of BPCAs with correction for losses by Internal Standard	External standards of BPCAs	External standards of BPCAs
A	Storage for remeasurements	after filtration (Step 3), acid extract diluted with water, < 1 month	not tested	after transfer to LC vial (Step 3), dissolved in ultrapure water, ready for LC injection, > 3 months
B	Approximate preparation time per sample batch	4-5 days	2-3 days	2-3 days

Mobile Phase mixing gradients (A: orthophosphoric acid buffered with NaH_2PO_4 to a pH-value of 1.2; B: pure acetonitrile) used for the HPLC method for various environmental sample materials.

Time [min]	Mobile phase B [vol %]
0	0.5
5	0.5
25.9	30
26	95
28	95
28.1	0.5
30	0.5

If the aim is to minimize the introduction of external carbon (e.g. for subsequent ^{13}C or ^{14}C measurements of the separated BPCAs), purely aequeous mobile phases with a pH gradient can be used:

A: 40 ml H_3PO_4 (85%) l^{-1} (target pH: 1.12)

B: 1560 mg NaH_2PO_4 l^{-1} (target pH: 4.7)

Time [min]	Mobile phase B [vol %]
0	1
5	1
10	35
18	100
31	100
31.1	1
35	1

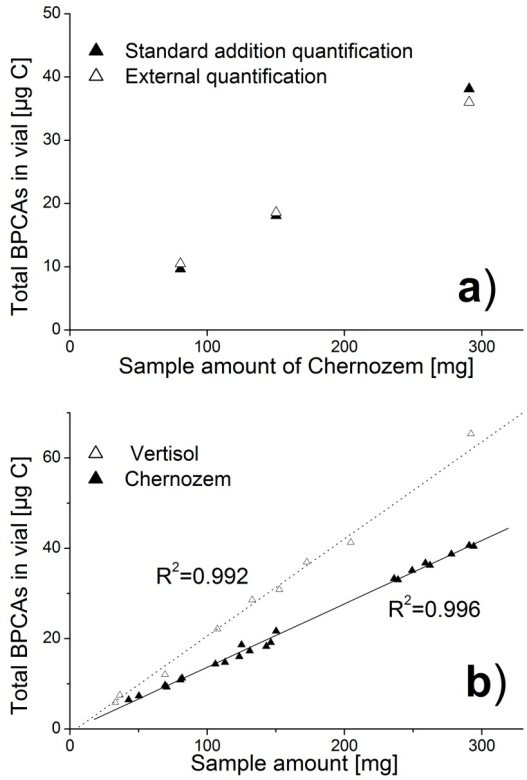

The less laborious external standard quantification yields the same BPCA quantity as the standard addition quantification in a Chernozem for three different sample amounts (a). Linearity of the HPLC method with differing sample amounts for two soil samples: In these two cases, less than 100 mg soil sample (less than 1 mg TOC) is required for a reliable BPCA quantification in the linear measurement range (b).

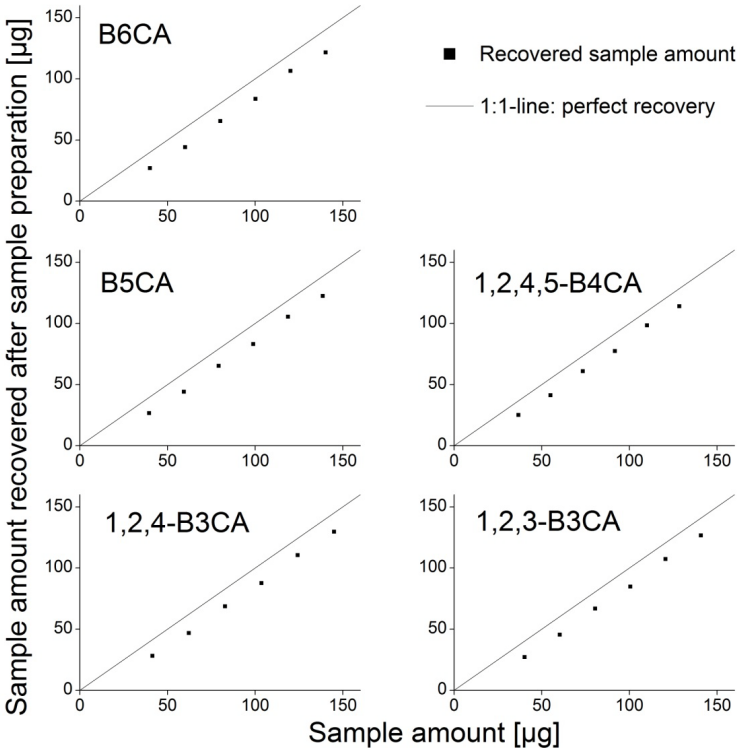

Quantitative recovery of BPCA standards after the sample preparation steps. Losses are small and constant over different sample amounts and very similar for the different BPCA.

Paper II

Contrasting belowground carbon budgets for coast redwood forest and adjacent prairie

Submitted as:

McFarlane, K.J., Mambelli, S., Porras, R.C., Wiedemeier, D.B., Murphy, L., Orans, K., Dawson, T.E., Torn, M.S., Contrasting belowground carbon budgets for coast redwood forest and adjacent prairie. Journal of Geophysical Research: Biogeosciences (in review).

Author contributions:

K.J.M, S.M., K.O., T.E.D. and M.S.T designed the study and conducted field work. R.C.P., S.M, L.M. and K.O. performed soil texture, pH, C/N and root analysis. D.B.W. performed BPCA analysis. K.J.M. performed ^{14}C measurements, data analysis and wrote the paper. S.M., R.C.P., D.B.W., T.E.D. and M.S.T provided input into the drafting and final version of the manuscript.

Abstract

Old-growth coast redwood (*Sequoia sempervirens*) forests store more carbon in aboveground biomass per area than any ecosystem, in trees that are among the oldest, largest, and most productive plant species on earth. Moreover, redwood litter is known to be resistant to decay, a result of high levels of aromatic compounds in the tissues. In contrast, little is known about belowground carbon storage or turnover in these forests. We tested the hypothesis that an old-growth redwood stand would have more, and older, soil organic carbon than an adjacent prairie having lower productivity and more decomposable litter. We measured soil carbon stocks to 110 cm depth in a redwood stand and coastal prairie in Prairie Creek Redwoods State Park and used physical soil fractionation and radiocarbon measurements to estimate soil organic matter turnover times. Total soil carbon stocks were higher in prairie (350 Mg C ha^{-1}) than in redwood (277 Mg C ha^{-1}) even with the forest O-horizon included. Differences between ecosystems in soil C and N concentrations and stocks, and C:N ratios were observed for the top 50 cm only, suggesting that the influence of the different litter types did not extend deeper. Contrary to what was expected, bulk soil and dense-fraction ^{14}C values indicated shorter carbon turnover times under redwood. Lower soil carbon stocks and faster turnover in the old-growth forest compared to the prairie suggests that properties of aboveground litter, despite the immense contrast between the ecosystems, are not a dominant control on soil carbon dynamics at these sites.

Introduction

Old-growth coast redwood trees (*Sequoia sempervirens*) are among the world's largest and longest-lived trees, capable of living over 2000 years thanks to their ability to tolerate shade, resistance to fungi, and resilience to fire and flood events [*Sawyer and Largent*, 2000]. This longevity allows for the development of complex canopy and root structures [*Stone and Vasey*, 1968; *Sawyer and Largent*, 2000; *Sillett and Van Pelt*, 2007]. Furthermore, old-growth coast redwoods are highly productive, with increasing wood production with age [*Sillett et al.*, 2010] as well as producing large amounts of aboveground litter [*Pillers and Stuart*, 1993]. In addition to being large in size and highly productive, redwoods are known for highly aromatic tissues that are resistant to decomposition by fungi [*Anderson et al.*, 1968], a characteristic that contributes to large accumulations of carbon in detrital material [*Busing and Fujimori*, 2005]. Despite the importance of old-growth redwood forests to carbon storage in aboveground biomass, little is known about belowground carbon storage and cycling in these ecosystems.

Coastal prairie provides a striking contrast to old-growth redwood forest in terms of plant stature and canopy structure, but the two ecosystems exist in close proximity to one another throughout much of the redwood range. Both ecosystem types are fire tolerant or fire adapted. Where measured, grasslands and prairies have considerable amounts of black carbon (char or charcoal, produced by incomplete burning of biomass), particularly those on dark colored high organic matter soils (Mollisols or Chernozems) because they tend to have had high fire frequencies or been maintained as grassland by fire [*Schmidt and Noack*, 2000; *Glaser and Amelung*, 2003; *Hammes et al.*, 2008]. The importance of soil aggregation to soil organic matter (SOM) storage in grasslands and prairies has also been widely reported [*Ewing et al.*, 2006; *Pérès et al.*, 2013] and attributed to dense root systems [*Young et al.*, 1998; *De León-González et al.*, 2007], although largely in the context of agriculturally relevant plant species such as rye grass (*Lolium perenne*) or maize [*Tisdall and Oades*, 1979; *Watteau et al.*, 2006].

Old-growth redwood forest and coastal prairie differ substantially in their carbon inputs. The role of litter inputs as a control in SOM storage and cycling, primarily through the regulation of litter decomposition, has been well studied [*Zhang et al.*, 2008; *Prescott*, 2010]. Polyphenolics such as tannin and lignin, present in relatively high amounts in redwood tissues and litter, decrease initial decomposition rates of litters containing high amounts of them and can form secondary metabolites and additional complexes with proteins, enzymes, and other compounds that further inhibit decomposition [*Horner et al.*, 1988; *Berg*, 2000; *Hättenschwiler and Vitousek*, 2000]. Positive correlations between soil carbon storage and polyphenolic and other chemically resistant compounds in litter have been reported [*Marín-Spiotta et al.*, 2008; *Ostertag et al.*, 2008; *Montané et al.*, 2010] and accumulations of organic matter as a result of polyphenol regulation of decomposition have been observed [*Northup et al.*, 1998]. In contrast, litter from grasses and other prairie plants contain high amounts of cellulose and other polysaccharides and lower amounts of lignin, tannin, and waxes

compared to tree leaf litter [*Marín-Spiotta et al.*, 2008; *Ostertag et al.*, 2008; *Osono et al.*, 2013; *Zhang et al.*, 2013], which tend to decompose more quickly than litter from trees and woody shrubs [*Castro et al.*, 2010]. Different plant tissues also decompose at different rates, with needles, leaves, and shoots decomposing faster than roots [*Bird and Torn*, 2006; *Ostertag et al.*, 2008; *Ziter and MacDougall*, 2012], finer diameter roots decomposing more quickly than coarser diameter roots [*W Wang et al.*, 2014], and leaves and needles decomposing faster than woody tissues [*Edmonds*, 1990]. Black carbon consists primarily of aromatic C compounds [*Schmidt and Noack*, 2000], which similarly to lignin and other polyphenols have slower initial decay rates than most direct plant inputs. Thus, differences in the litter chemistry, carbon allocation above- and belowground, root morphology and phenology, and black carbon inputs between forests and prairies may lead to differences in soil carbon storage and dynamics between these ecosystems.

Several other factors besides plant litter inputs influence soil carbon storage and cycling. These include climate, which strongly influences plant productivity and microbial decomposition, and soil characteristics, which influence physic-chemical protection of soil carbon. For example, globally soil carbon content increases with increasing precipitation and decreasing temperature [*Post et al.*, 1982] and with increasing clay content [*Jobbágy and Jackson*, 2000]. Soil parent materials and development are also important controls over soil carbon storage and cycling; for example soil reactive Fe and/or Al oxyhydroxides are correlated with higher stocks of soil carbon and longer turnover times [*Torn et al.*, 1997; *Massiello et al.* 2004; *Rasmussen et al.*, 2006].

We assessed the importance of the type of carbon inputs on soil carbon storage and cycling in an old-growth coast redwood stand and an adjacent coastal prairie with the same macroclimate and parent material by measuring soil carbon storage, distribution, and turnover to 110 cm depth. We hypothesized that if plant litter inputs were the primary control on soil carbon storage and dynamics, the redwood forest would have more, and older, soil organic carbon than the prairie with lower productivity and more decomposable litter, and that differences in soil carbon would be more pronounced near the surface where plant litter inputs are concentrated. We determined carbon storage and ^{14}C-based turnover times of soil density fractions to examine how storage and cycling differed in free particulate, aggregate occluded, and mineral associated fractions. We also quantified root biomass and black carbon. In addition to exploring these influences on carbon cycling, we present the first soil carbon and soil ^{14}C inventory to be published for old growth redwood forest.

Methods

Study Area

This study was conducted at Prairie Creek Redwoods State Park in northwestern California (Lat: 41.45 / Long: -124.05). The study area is characterized by very deep soils formed in alluvium from mixed sedimentary sources. The Franciscan Assemblage is the underlying geologic formation. The region has a Mediterranean climate with cool, wet winters and warm, dry summers. Mean annual precipitation is 1709 mm and mean annual temperature is 11°C (Western Regional Climate Center 2010, http://www.wrcc.dri.edu/cgi-bin/cliMAIN.pl?ca6498). Both the redwood forest and prairie sites were located east of Prairie Creek on alluvial deposits derived from mixed sources to the north (redwood forest) and south (prairie) of Boyes Creek. The sites are within approximately 550 m of one another.

The redwood forest is dominated by old-growth coast redwood (*Sequoia sempervirens*) with bigleaf maple (*Acer macrophyllum* Pursh.), western buckthorn (*Rhamnus purshiana)*, Douglas Fir (*Pseudotsuga menziesii* (Mirb.) Franco), western hemlock (*Tsuga heterophylla)*, and California bay laurel (*Umbellularia californica* Nutt.) also present. Understory vegetation includes Western sword fern (*Polystichum munitum (Kaulf.) Presl.*), salal (*Gaultheria shallon*), huckleberry (*Vaccinium ovatum Pursh.*), and redwood sorel (*Oxalis oregana Nutt.*) [Sillet and Van Pelt, 2007]. Soils at the redwood forest are coarse loamy Inceptisols of the Mystery Soil Series.

The prairie study plots were located in the northeastern portion of Boyes Prairie, a natural prairie resulting from poorly drained soils that become waterlogged in winter and dry rapidly in spring and summer favoring dry season dormant grasses and herbs [*Veirs*, 1987]. The prairie was present when the first European American settlers arrived around 1830 [*Veirs*, 1987] and was extensively grazed from approximately 1885 to 1923 when the park was established. Grazing by wild elk continues. Previous vegetation surveys found the prairie to be dominated by perennial grasses including non-native sweet vernalgrass (*Anthoxanthus odoratum*) and meadow grass (*Agrostis alba*) with California oatgrass (*Danthonia californica*), Kentucky bluegrass (*Poa pratensis*), velvet grass (*Holcus lanatus*), sedges (*Carex* sp.), false dandelion (*Hypochoeris radicata*), ribwort plantain (*Plantago lanceolata*), bracken fern (*Pteridium aquilinum*), orchard grass (*Dactilis glomerata*), Pacific dewberry (*Rubus vitifolius*), and Rosaceae also present [Veirs, 1987; Stassia Samuels, personal communication, 2011]. Soils are mapped as Ferndale Series (fine-loamy Entisols) at the prairie site.

Both sites were subject to fires historically, but the prairie was subject to prescribed fire in 1983, 1991, 1994, 1996, 2000, and 2005 (Stassia Samuels, personal communication, 2011). For fires where burn severity was surveyed, fires were uniform and light severity resulting in lightly burned vegetation (foliage partly to completely consumed, some plants still standing, bases of plants not deeply burned) and scorched (litter partially blackened, duff nearly unchanged) to unburned substrates (Stassia Samuels, personal communication, 2011).

Prescribed fire has not altered the plant community of the prairie from its pre-1983 composition [Viers1987; Stassia Samuels, personal communication, 2011].

Field Sampling

Samples were collected from the redwood forest and prairie in July 2009. At the redwood forest, seven plots were randomly selected from a 0.2 ha area. At the prairie, a 50 m sampling transect was established and samples collected from five plots along the redwood forest and prairie transects, respectively. More cores were collected at the redwood forest than the prairie because we expected greater spatial variability in the redwood forest than the prairie. From each redwood plot, forest floor samples were collected using a 25 cm x 25 cm sampling frame. All material inside the frame was collected down to the mineral soil surface. When possible, the Oi horizon was separated from the Oe/Oa horizon. Further separation of the Oe from the Oa was not possible. Results for O horizon are for all plots with Oe/Oa and Oi mathematically combined for plots where separation of Oi from Oe/Oa was possible. From each prairie plot, standing biomass was harvested from within a 25 cm x 25 cm sampling frame to the mineral soil surface. From each plot at each site, mineral soil cores were collected using a hammer-driven 7.5 cm diameter, 10 cm long corer from the following depths: 0–10 cm, 10–20 cm, 20–30 cm, 30–50 cm, 50–70 cm, 70–90 cm, 90–110 cm. At both sites, a gravelly layer was encountered at 110 cm that could not be sampled using the coring device (driving the corer deeper was difficult and samples fell out of corer during retrieval).

Soil samples were weighed at field moisture and sieved to 2 mm. Large roots and root branches were also removed from soil and saved for determination of root biomass (described below). A subsample of bulk soil (<2 mm) was dried at 105°C to determine moisture content and allow for the calculation of fine-fraction bulk density. The bulk soil for a given depth interval of each core was split in half using the cone and quarter subsampling method to ensure each split was representative of the whole core interval. One half of the soil from each core depth interval was air dried and used for soil chemistry and fractionation (described below). The other half was frozen until it could be processed for root biomass. Forest floor samples were dried at 55°C to constant mass and finely ground for C and N analysis.

Bulk density and soil carbon and nitrogen concentrations were measured for all depths and all plots (described below). Three cores from each site were selected for isotopic analysis and density fractionation. To capture spatial variability within each ecosystem, we chose to do these procedures on every other core for each site (cores 1, 3, and 5 for the prairie and cores 2, 4, and 6 for the redwoods).

Aboveground litterfall was collected in the redwood forest using eight 0.135 m^2 litter traps that were placed along our soil sampling transect in early October 2008. All litter from within the traps was collected in November 2008 and late April 2009. Litter was dried at 60°C,

sorted by type, and weighed. Litter from the 2009 collection was analyzed for C and N analysis (see details below). Previous litterfall measurements at the site showed little or no litterfall occurring during summer months (Vanessa Boukili, personal communication, 2007). Aboveground litterfall was scaled up to g m^{-2} y^{-1} by assuming similar litterfall rates in May and June to litterfall rates measured for October through April and assuming no litterfall July–September.

Fine Root Biomass

Fine roots (<2 mm diameter) from all mineral soil depths at each site were hand picked and sorted into classes. Roots were separated from the mineral soil using a combination of dry and wet sieving. Small root fragments were picked, sorted, and kept moist by immersing the samples in tap water. For the prairie, roots were picked from the same 3 cores used for soil density fractionation and isotopic analyses and sorted into 3 root diameter size classes: < 0.25 mm, 0.25-0.50 mm, and 0.50-2.0 mm. For the redwood forest, roots < 0.25 mm in diameter were virtually non-existent, so roots were only sorted into <0.25-0.50 mm and 0.50-2.0 mm diameter classes. Because variability in the amount of roots in the redwoods was higher than that in the prairie, we picked and sorted roots from 6 cores to provide more accurate estimates of root biomass than was attained with only 3 cores. In addition, we thought the redwood forest might include an ecologically significant pool of dead roots, so a subset of samples were additionally sorted into live and dead roots using tensile strength and root morphology. Roots were thoroughly cleaned with tap water, dried at 55 °C and weighed. A subset of roots were ground and analyzed for carbon and nitrogen concentrations.

Soil Density Fractionation

Sieved soil samples from 0–10 cm and 50–70 cm depth from three redwood forest and three prairie cores were fractionated into free light (fLF), occluded light (oLF), and dense (DF) density fractions [*Swanston et al.*, 2005; *McFarlane et al.*, 2013]. fLF comprises free particulate organic matter, oLF contains light density organic matter that was occluded in aggregate structures, and DF includes mineral-associated organic matter. Briefly, low C/N sodium polytungstate (SPT-0, TC Tungsten Compounds) adjusted to a density of 1.65 g cm^{-3} was used to separate soil based on density. First, SPT was added to soil, the sample gently inverted to wet soil, and the floating material (fLF) was aspirated and rinsed with Nanopure H_2O on a 0.8 μm polycarbonate filter. To disperse aggregates, sediment remaining at the bottom of the bottle was then mixed in SPT for 1 min at 1700 rpm using a desktop mixer (G3U05R, Lightnin, New York, NY) and sonicated in an ice bath for 1.5 min at maximum power and 70 % pulse for a total input of 100 J ml^{-1} (Branson 450 Sonifier, Danbury, CT). The floating material (oLF) was then aspirated and rinsed in the same manner as the fLF. The

remaining sediment, the DF, was rinsed three times by aspirating the supernatant, adding 150 ml Nanopure H_2O, shaking vigorously, and centrifuging the mixture for 20 minutes at 3500 rpm. The DF was rinsed a fourth time as described previously except that it was centrifuged 1 hour at 4000 rpm to encourage suspended particles to settle. After rinsing, all fractions were washed into aluminum weighing tins and dried at 55°C until standing water had evaporated at which point they were dried at 105°C for 48 hours. Fractions were then weighed, ground, and prepared for chemical and isotopic analysis.

Sample Analysis

Soil texture and pH were determined for all seven depths for the three cores used for density fractionation. Soil texture was measured using the micropipette method [*Miller and Miller*, 1987; *Burt et al.*, 1992]. Bulk soil pH was measured in water and 0.01M $CaCl_2$ at a 1:1 soil:solution ratio [*Thomas*, 1996]. Plant material, litterfall, and soil C and N concentrations were determined using a Carlo Erba Elantech elemental analyzer at UC-Berkeley.

Samples of O horizons, bulk soil, and soil fractions for the three cores at each site selected for isotopic analysis were measured for ^{14}C on the Van de Graaff FN accelerator mass spectrometer (AMS) at the Center for AMS at Lawrence Livermore National Laboratory. Samples were prepared for ^{14}C measurement by sealed-tube combustion to CO_2 in the presence of CuO and Ag and then reduced onto iron powder in the presence of H_2 [*Vogel et al.*, 1984]. Aliquots of CO_2 were analyzed for ^{13}C at the Department of Geological Sciences Stable Isotope Laboratory, University of California Davis (GVI Optima Stable Isotope Ratio Mass Spectrometer). $\delta^{13}C$ is reported relative to V-PDB. Measured ^{13}C values were used to correct for mass-dependent fractionation. Radiocarbon content is reported in $\Delta^{14}C$ notation, had an average AMS precision of 3 ‰, and was corrected for ^{14}C decay since 1950 [*Stuiver and Polach*, 1977].

The amount of pyrogenic carbon (PyC) was determined by analyzing benzene polycarboxylic acids (BCPA) molecular markers by high-preformance liquid chromatography (HPLC) at the University of Zurich [*Wiedemeier et al.*, 2013]. This method has several benefits including small sample size requirements, high reproducibility, and sensitivity over a broad range of the combustion continuum [*Masiello*, 2004]. However, it is conservative measure of total black C. Most commonly, a multiplier or 2.27 is used to convert BPCA-C to total black C [from *Glaser et al.*, 1998], but this number may still be conservative [*Brodowski et al.*, 2005]. Therefore, these results should be considered a low-end estimate of black C content in our study soils.

Soil Carbon Turnover Modeling

Mean turnover times were calculated for all redwood forest O horizons (n=7) and for bulk soils at all depths and density fractions from 0-10 and 50-70 cm depths for three cores from each site. To determine turnover time, we used a time-dependent steady-state model [*Torn et al.*, 2009; *McFarlane et al.*, 2013]. This model calculates the $\Delta\ ^{14}C$ of a given carbon pool over time and varies turnover time to match measured $\Delta\ ^{14}C$. New carbon inputs to soil were assumed to have the $\Delta\ ^{14}C$ value of the current atmosphere. For density fractions, a three-pool model was used to determine turnover times of all three fractions simultaneously using the mass balance of carbon and amount of ^{14}C as additional constraints. Annual atmospheric $^{14}CO_2$ values through 2007 were compiled from several sources [*Graven et al.*, 2012; *Hua and Barbetti*, 2004; *Levin and Kromer*, 2004; *Stuiver et al.*, 1998]. Values for 2008 and 2009 are annual average $^{14}CO_2$ measured at Niwot Ridge (Brian LaFranchi, personal communication, 2012) and were 46.6 ‰ and 43.2 ‰, respectively.

The model has several assumptions, which are described in *Torn et al.*, 2009. Most importantly, it assumes steady state conditions and uses atmospheric ^{14}C values with a 1-year time lag for the ^{14}C content of new carbon inputs. The model also assumes all inputs come from recently fixed plant carbon (i.e., carbon does not cycle from one depth or fraction into another). This is likely an appropriate time lag for aboveground inputs in the prairie, but perennial roots and most inputs in the redwood forest are probably older [*Gaudinski et al.*, 2009, 2010]. Thus, turnover times may be most accurately interpreted as being for the ecosystem rather than the individual carbon pool. In addition, turnover times are only equal to mean residence times when pools are well mixed with a homogenous distribution as well as in steady state. This is certainly not the case for bulk soils, which are comprised of a mixture of individual pools with a range of turnover times. Therefore, we urge our readers to interpret bulk turnover times as a relative indicator of ecosystem residence time rather than a precise estimate of MRT [see *Torn et al.*, 2009].

In some cases, ^{14}C values allowed for two modeled solutions of turnover time, one corresponding to the increasing and one corresponding to the decreasing side of the atmospheric "bomb curve" [*e.g., Trumbore et al.*, 1996; *Trumbore*, 2000]. This was only the case for O horizons in the redwood forest and for a few (4 out of 36) density fractions. For fractions that had two solutions for only one of the plots, we assumed that the solution closest in value to the singular solution found for the other replicate plots was the correct turnover time. For O horizons in the redwood forest, we used O horizon carbon stocks and litterfall values to identify the most likely solution assuming steady state conditions and using the identity that turnover time equals stock over input rate at steady state as a constraint.

Data Analysis

Differences in bulk soil and root variables between ecosystems and with depth were tested using analysis of variance with repeated measures for depth using Linear Mixed Effects Models (lme) in the Non-Linear Mixed Effects Models (nlme) in R 2.14.1 [*Pinheiro et al.,* 2011; *R Development Core Team,* 2011]. Correlation analysis was conducted to determine if soil texture, pH, or black carbon content should be considered as covariates for soil carbon concentration, ^{14}C, or turnover time, but these variables were significantly correlated with site and depth and therefore could not be included as covariates in the statistical model. Soil density fraction data were analyzed in the same manner but with density fraction included as a factor in the model in addition to ecosystem type and depth. All main factor and interaction effects were tested at $\alpha = 0.05$ for soil variables. We report main and interaction effects for root variables at $\alpha = 0.1$ because high variability resulted in a reduced sensitivity to ecologically significant differences between sites. Interaction effects were investigated using the Phia Package [*Rosario-Martinez,* 2012]. A priori hypotheses tests were conducted using the Contrasts package [*Kuhn*, 2011] with $\alpha = 0.05$. When necessary for ad hoc interpretation of three-way interactions, multiple comparisons were made with a Tukey adjustment using the Multcomp Package [*Hothorn, et al.*, 2008] with $\alpha = 0.1$ to compensate for the large number of multiple pairwise comparisons included in the test that were not of interest (out of 56, only 22 were of interest). All results are reported as means followed by one standard deviation.

Results

Aboveground Biomass, Litter, and Fine Roots

Aboveground biomass in the prairie in July 2008 was 10.42 ± 1.81 Mg ha^{-1} (Table 1, consisted almost entirely of grasses (97 ± 6 % by mass), and was mostly dead or senesced material (91± 2 % by mass). We did not measure aboveground biomass in the old-growth redwood forest. *Sillet and Van Pelt* [2007] reported an estimate of total living aboveground biomass in the same forest stand of 4283 Mg ha^{-1}, 95 % of which was redwood, meaning that there was over 400 times as much as in the prairie. Aboveground litterfall in the redwood forest was 7.80 ± 1.61 Mg ha^{-1} yr^{-1}, which was similar to litterfall measured in previous years (7.31 Mg ha^{-1} yr^{-1}, Vanessa Boukili, personal communication, 2012). Redwood litterfall consisted mainly of needles (81% by mass). Prairie aboveground biomass had higher N concentration, lower C concentration, and lower C:N ratio than aboveground litter from the redwood forest ($p < 0.01$, Table 1).

Fine root biomass was highly variable and the distribution of roots with depth and between size classes differed considerably between sites (Figure 1). Total fine root biomass (< 2 mm in diameter) to 110 cm in the prairie (7.8 ± 4.4 Mg root ha^{-1}, n=3) was less than half that in the

redwood forest (17.9 ± 7.8 Mg root ha^{-1}, n=6, p = 0.03), but variability at both sites was high. Fine root biomass declined with depth at both sites, but the pattern differed somewhat with a more consistent decline in the prairie (Figure 1).

Prairie roots were sorted into three diameter classes, < 0.25 mm, 0.25-0.5 mm, and 0.5-2 mm. Distribution of root biomass among size classes did not change significantly with depth and, averaged across all depths, 38 % of all fine roots were < 0.25 mm in diameter, 46 % were 0.25-0.5 mm, and 16 % were 0.5-2.0 mm in diameter (Figure 1). Virtually no roots <0.25 mm were found from the redwood forest, so roots were sorted into two size classes: 0.25-0.5 mm and 0.5 mm-2.0 mm. In contrast to the prairie, most of the fine root biomass in the redwood forest was in the 0.5-2 mm size class (86 % averaged across depths) with a small portion of roots <0.50 mm in diameter (14 % on average). A subset of redwood root samples was sorted into live and dead roots. On average, 42 % of fine roots from the redwood forest were live root biomass while 58 % were necromass. There were no differences in live vs dead root biomass with depth or between size classes.

A subset of roots was analyzed for carbon and nitrogen concentrations. Redwood roots had consistently higher N concentrations (1.04 ± 0.12 %) than did prairie roots (0.66 ± 0.21 %) (p=0.07), but C concentrations and C:N ratios were similar between sites. At both sites, roots 0.5-2 mm in diameter had lower N concentrations (by about 0.2 % N) and higher C:N ratios than did roots smaller than 0.5 mm (p<0.01), but C concentrations did not differ amongst different size classes. Redwood root C and N concentrations did not differ between live and dead roots.

Root biomass and carbon concentrations were scaled up to mass per unit area using measured bulk density to provide fine root carbon stocks for each site. Total fine root stocks to 110 cm were small compared to soil stocks and were lower in the prairie (3.34 ± 1.88 Mg C ha^{-1} and 0.05 ± 0.02 Mg N ha^{-1}) than redwood forest (7.06 ± 3.30 Mg C ha^{-1} and 0.16 ± 0.08 Mg N ha^{-1}, p = 0.03).

Bulk Soil Characteristics

Bulk soil pH was acidic for both ecosystems, and was slightly higher in the redwood forest than the prairie for the surface 40 cm (p < 0.01, Table 2). Soil texture analysis showed that soils in the prairie tended to be finer textured than soils in the redwood forest, with higher clay contents in the prairie below 50 cm and higher sand contents in the redwood forest throughout the profile (p < 0.01, Table 2). Soil bulk density increased with depth at both sites although it increased more sharply with depth in the prairie than in the [redwood] forest (p < 0.01, Table 2). Similarly, mineral soil carbon and nitrogen concentrations declined with depth at both sites, but at a faster rate in prairie than redwood forest (p < 0.01, Figure 2). Prairie soils had roughly 3 percentage points higher carbon concentrations and 0.3 percentage points higher nitrogen concentrations than redwood forest soils in the top 30 cm (p < 0.01), but

values at the two sites converged and were not different from one another below 50 cm depth. C:N ratios also declined with depth ($p < 0.01$), were higher in the redwood forest than the prairie for all depths by about one-third ($p < 0.01$), and ranged from 14 at the surface to 8 at depth in the prairie and from 18 at the surface to 13 at depth in the redwood forest.

O horizons from 5 of the 7 redwood forest plots were separated into Oi and Oe/Oa horizons. For these plots, total forest floor mass was 50 % in the Oi and 50 % in the Oe/Oa horizons (data not shown). Oi layers had greater carbon concentrations (47 %) and higher C:N ratios (57) than Oe/Oa layers (32 % C; C:N ratio = 39), but nitrogen concentrations were similar at 0.8 % ($\alpha = 0.01$, data not shown). Total forest floor carbon and nitrogen stocks were also evenly split with approximately 50 % in the Oi and the remaining 50 % in the Oe/Oa horizon.

Mineral soil carbon and nitrogen stocks (on a per cm depth basis to account for deeper depth intervals below 30 cm) declined with depth at both sites ($p < 0.01$) and were higher at the prairie than the redwood forest to 50 cm depth ($\alpha = 0.05$ or 0.01, Figure 3). Total stocks to 110 cm, including O horizons for the redwood forest, were smaller in the redwood forest (277 ± 36 Mg C ha^{-1} and 16 ± 1 Mg N ha^{-1}) than the prairie (350 ± 31 Mg C ha^{-1} and 28 ± 2 Mg N ha^{-1} $p < 0.01$). For the 5 redwood forest plots for which O horizon were separated into Oi and Oe/Oa layers, Oi and Oe/Oa horizons each contributed 50 % of the total O horizon mass and N stock, while 59 % of total O horizon C was in Oi layers (Table 2).

At both sites, bulk soil $\delta^{13}C$ values increased with depth while $\Delta^{14}C$ values decreased with depth, ($p < 0.01$, Figure 4). Bulk soil $\delta^{13}C$ and $\Delta^{14}C$ values were lower in the prairie than the redwood forest for all mineral soil depths sampled (alpha=0.05). Redwood forest O horizon $\delta^{13}C$ was -28.2 ± 0.4 ‰, $\Delta^{14}C$ was 92 ± 14 ‰, and these values did not differ between Oi and Oe/Oa horizons (data not shown).

We determined bulk soil turnover times for the three cores at each site that were analyzed for bulk soil ^{14}C (Figure 4). Consistent with our observation of more depleted $\Delta^{14}C$ values in the prairie than redwood forest, turnover times for prairie bulk mineral soil carbon pools were much longer than those for redwood forest soils (Figure 4). This difference was smaller at the surface (231 years) and more pronounced with depth (over 5000 years at 90-110 cm depth) as turnover times in the prairie increased more steeply with depth than did turnover times in the prairie. The organic horizon in the redwood forest provided the only bulk soil samples that yielded two solutions for turnover time based on ^{14}C values, 9 ± 2 years and 95 ± 15 years. Both of these solutions are shorter than the mean turnover time determined for 0-5 cm bulk mineral soil (131 ± 15 years). Based on the size of the O horizon carbon pools and litterfall rates measured at the site, we concluded that the shorter solution is more likely, resulting in turnover times of 7–9 years for the redwood forest floor.

We measured the amount of black carbon in a subset of bulk soil samples at each of our sites to assess the importance of fire residues in soil carbon storage and cycling in them. Black carbon content per mass of soil decreased with depth in the prairie from 7 g BCPA-C kg $soil^{-1}$ for 0-10 cm depth to 2 g BCPA-C kg $soil^{-1}$ for 50-70 cm depth ($p < 0.05$, Figure 5-a), but was

not affected by depth in the redwood forest where it averaged 2 g BCPA-C kg soil^{-1} for all depths measured. It was higher in the prairie than in the redwood forest for surface soils although it was similar between sites at depths greater than 30 cm ($p < 0.05$, Figure 5-a). When normalized to the amount of carbon in the soil, black carbon content was higher in the prairie throughout the profile ($p < 0.01$) and increased slightly with depth at both sites ($p = 0.03$, Figure 5-b).

Soil Fractions

Carbon concentrations were higher for light fractions (about 34 %) than DF (about 4 %), regardless of site or depth ($p < 0.01$, Table 3). In the prairie, oLF carbon concentrations were slightly higher than those for fLF (39 % and 28 %, respectively, $p < 0.01$). Soil fraction carbon concentrations only differed by site for 0-10 cm fLF, and in this case, carbon concentrations were 23 % in the prairie and 34 % in the redwood forest ($p < 0.01$). Depth only influenced fLF and DF carbon concentrations in the prairie, increasing fLF carbon concentrations to 32 % ($p < 0.01$) and decreasing DF carbon concentrations from nearly 9 % at the surface to less than 2 % at depth ($p = 0.02$).

In general, nitrogen concentrations were higher for light fractions than DF, but the magnitude of the effect depended strongly on depth and site (three-way interaction $p < 0.01$). The 0-10 cm oLF from the prairie had a much higher nitrogen concentration (2.3 %) than any of the other fractions from any site or depth. Nitrogen concentrations tended to be higher in the prairie than the redwood forest, though this difference was larger at the surface and largest for oLF (Table 3). Nitrogen concentrations decreased with depth regardless of site and fraction, but the slope of N versus depth was steepest in the prairie oLF and DF ($p < 0.05$).

C:N ratios increased with depth for fLF and oLF (by about 17), but not for DF ($p < 0.01$). C:N ratios of fLF and oLF were similar, regardless of site or depth, but C:N ratios of both light fractions were higher than C:N ratios of DF and this difference was more pronounced at depth and in the prairie compared to the redwood forest ($p < 0.01$). C:N ratios for fLF and oLF were about 14 units lower in the prairie than redwood forest ($p<0.01$), reflecting higher N concentrations in the prairie, but DF had similar C:N ratios at both sites.

During soil density fractionation, some amount of soil carbon and nitrogen is dissolved in SPT solution or during water rinses and is lost from the solid sample [*McFarlane et al.*, 2010, 2013]. In this study, the SPT- or water-mobilized fraction amounted to 2-9 % of bulk soil carbon and 0-4 % of bulk soil nitrogen depending on site and depth. Results below are calculated as a proportion of the total carbon and nitrogen recovered following density fractionation.

Fraction N and C stocks declined with depth ($p < 0.01$, Figure 6). DF stocks were larger in the prairie regardless of depth ($p <0.01$), but light fraction stocks did not differ by site. The

distribution of carbon and nitrogen amongst fractions as a proportion of the total carbon or nitrogen recovered differed between sites and changed with depth (significant three-way interaction, $p \leq 0.01$, Figure 6). At both sites, DF contained most of the soil carbon (79-91 %, $p < 0.01$) and nitrogen (84-97 %, $p < 0.01$) and the proportion of total soil carbon and nitrogen contained in DF increased with depth ($p < 0.1$). This increase with depth was larger in the prairie than redwood forest and accompanied by a coincident decrease in fLF with depth in the prairie and decrease in oLF in the redwood forest ($p < 0.1$). In the 0-10 cm depth, oLF contained a larger proportion of soil carbon (21 %) and soil nitrogen (10 %) in the redwood forest compared to the prairie (5 % of soil carbon and 4 % of soil nitrogen) ($p < 0.01$). In contrast, fLF contained a larger portion of soil carbon and nitrogen in the prairie (17 % of soil carbon and 12 % of soil nitrogen) than redwood forest (8 % of soil carbon and 4 % of soil nitrogen) ($p < 0.03$).

Similar to the bulk soil, fraction$\delta^{13}C$ values became less depleted with depth, and the effect was larger in prairie (2 ‰) than in redwood forest (0.4 ‰) and in oLF (1.7 ‰) and HF (1.3 ‰) than fLF (0.5 ‰) on average ($p < 0.01$, Table 3). Soil fraction $\delta^{13}C$ values were more depleted in the prairie than redwood forest at the surface, but sites did not differ at depth ($p < 0.01$). DF $\delta^{13}C$ values were less depleted than those for fLF and oLF by 1.5 ‰ at the surface and about 0.9 ‰ at depth ($p < 0.01$), while$\delta^{13}C$ values for fLF and oLF were similar regardless of depth.

As with bulk soil, fraction $\Delta^{14}C$ values declined with depth (Table 3). However, this decline was less pronounced in fLF at both sites, which declined 185 ‰, than oLF and DF, which declined 430 and 320 ‰, respectively ($p < 0.01$), and was more pronounced in prairie (379 ‰) than in redwood forest (246 ‰, $p = 0.02$). In the top 10 cm, $\Delta^{14}C$ values did not differ amongst fractions, but in the 50-70 cm depth fLF $\Delta^{14}C$ values were higher than those for oLF or DF ($p < 0.01$) and DF were higher than those for oLF ($p = 0.05$) although variability was high. In addition, $\Delta^{14}C$ values were similar between sites at the surface, but in the 50-70 cm depth were higher in redwood forest than in prairie ($p < 0.01$). Trends in soil fraction turnover times were consistent with those for $\Delta^{14}C$ values in that turnover times increased with depth at both sites ($p < 0.01$, Table 3). On average, this increase in turnover times was largest for oLF, smallest for fLF, and more pronounced in prairie than redwood forest (Table 3). Turnover times between soil fractions were similar at the surface, but at 50-70 cm depth fLF turnover times were shorter than those for DF and oLF ($p < 0.01$) and DF turnover times were shorter than those for oLF ($p < 0.01$). Turnover times between sites were also similar at the surface, but at 50-70 cm depth turnover times in prairie were longer than those in redwood forest ($p < 0.01$).

Discussion

In interpreting the differences in turnover times between our study sites, it is helpful to place them in the context of other studied ecosystems. Our results for redwood forest bulk soil turnover times fall within the range of those reported for temperate deciduous forests for similar depths [*Gaudinski et al.*, 2000; *McFarlane et al.*, 2013] and Hawaiian forests of similar soil age [*Torn et al.*, 1997]. Turnover times for for density fractions for redwood forest reported here also fall within the range of those reported for other temperate forests [*Crow et al.*, 2007; *McFarlane et al.*, 2013]. We observed similar turnover times for density fractions in surface and subsurface soils for our redwood forest as implied by similar $\Delta^{14}C$ values reported for two *Pinus ponderosa* forests in the Sierra Nevada [*Rasmussen et al.,* 2005]. However, others have reported shorter turnover times (some < 100 y) for fLF in surface soils from other western coniferous forests [*Trumbore et al.,* 1996; *Crow et al.*, 2007; Castanha et al., 2008]. Strikingly similar bulk soil turnover times to our redwood forest were reported for an old-growth conifer forest in the western Sierra Nevada for O horizon and 0-20 and 20-45 cm bulk mineral soil [*Wang et al.*, 1999], but the same study reported much shorter turnover times for bulk soils from a Sierran annual grassland than we determined for our prairie. A shorter turnover time for stable SOM in surface soil from tallgrass prairie at Konza Prairie Research Natural Area in Kansas than that observed for our prairie has also been reported [*Frank et al.*, 2012], although these turnover times were longer than those we observed for our redwood forest. Others have also reported ^{14}C signatures for bulk soils that were less depleted than measurements from our prairie soils, suggesting shorter SOM turnover times than our prairie for an Iowa prairie and cropland [*Harden et al.,* 2002] and in grasslands on ancient marine terraces about 170 km south of our study location [*Masiello et al.*, 2004]. In contrast, turnover times for bulk soils in our prairie are within the range reported for profiles from a Russian Steppe soil [*Torn et al.*, 2002]. In summary, it seems that in general, our observed turnover times for the redwood forest are similar to observations from other forests but for the prairie, we observed longer turnover times than reported for most other prairies and grasslands where similar research has been conducted.

We observed longer C turnover times in bulk soils and density fractions in prairie than in old-growth redwood forest and those differences increased with depth along the soil profile. Longer C turnover times in prairie imply longer residence time for carbon that enters the plant/soil system and that the rate of carbon loss through decomposition and microbial respiration is lower in the prairie, because of soil conditions that limit microbial activity, chemical inaccessibility of litter and SOM, or physic-chemical protection of SOM.

We did not measure soil microbial biomass or activity at our sites. However, at sites with inhibited microbial activity as a result of extreme conditions such as anoxia or freezing temperatures, undecomposed and partly decomposed organic inputs tend to accumulate [e.g., *Rapalee et al.*, 1998; *Gorham*, 1991], but we do not see evidence for this type of accumulation in our prairie. In contrast, ^{13}C-NMR measurements suggest that prairie SOM is more microbially processed than redwood forest SOM (Mambelli et al., manuscript in

preparation, 2014). Second, chemical recalcitrance of litter inputs is an unlikely explanation for slower decomposition in the prairie for several reasons. Surface litter inputs in grasslands decompose more quickly than those in coniferous forests in general [*D Zhang et al.*, 2008] and indications are that redwood litter in particular contains high amounts of phenolic compounds that retard decomposition [*Horner et al.*, 1988; *Berg*, 2000; *Hättenschwiler and Vitousek*, 2000]. In addition, we found that aboveground litter from the old-growth redwood forest had lower N concentrations and higher C:N ratios than aboveground biomass in the prairie, suggesting that initial decay of redwood litter would be slower, all else equal. Furthermore, the chemical composition and decomposability of surface litter inputs has little influence on the decomposition rate and dynamics of SOM in subsurface horizons [*Schmidt et al.*, 2011]. Others have observed higher lignin concentrations in fine roots in forest than grassland [*Zhang et al.*, 2013]. It is this difference in chemistry that likely explains the higher N concentrations found in redwood fine-roots compared to prairie roots in this study and reported by others comparing root N concentrations in forests and adjacent grassland [*Steinaker and Wilson*, 2005]. In addition, if plant litter inputs were controlling soil carbon turnover times through the inhibition of decomposition, we would expect differences in turnover times to be more evident near the surface where litter inputs are concentrated. In contrast, we observed turnover times near the surface to be somewhat similar between sites, while the differences became more pronounced with depth. Consequently, longer turnover times (and larger soil carbon stocks) in the prairie are not likely a result of inhibited microbial activity or inherent chemical recalcitrance of plant litter inputs at this site.

In addition to plant litter inputs, our sites have been influenced by fire and associated inputs of black carbon. The BCPA analyses suggest that the prairie had approximately 2.4 times as much black carbon as the redwood forest, consistent with observations of high black carbon contents in grasslands and prairies around the world [*Schmidt et al.*, 1999; *Hammes et al.*, 2008]. Black carbon appears to decompose more slowly than plant inputs of litter or wood [cite incubation studies], but as fast as or faster than slow-cycling SOM fractions [*Hammes et al.*, 2008; *Singh et al.*, 2012]. If it is more stable than other SOM pools, black carbon may contribute to longer turnover times in the prairie than redwood forest, although to what degree is unclear. Few studies have quantified turnover times of black carbon and reported values vary widely from millennial timescales [*Schmidt and Noack*, 2000; *Skjemstad et al.*, 1996; *Kuzyakov et al.*, 2014] to centuries [*Hammes et al.*, 2008; *Singh et al.*, 2012].

Alternatively, soil carbon turnover could be slower in prairie than redwood forest because prairie soil conditions impart more physic-chemical protection than soils in redwood forest. One of the primary mechanisms for reducing the rate of microbial decay of SOM is the formation of organo-mineral complexes [*Oades*, 1988; *Lehmann et al.*, 2007]. The density and/or stability of these complexes appear to be greater in soils with higher clay content, possibly because higher surface area results in a greater capacity for adsorption of organic matter on mineral surfaces [*Oades*, 1988; *Mayer*, 1994], and in soils with higher concentrations of Fe and Al oxides and hydroxides [*Torn et al.*, 1997; *Masiello et al.*, 2004]. Prairie soils were

finer textured, with higher silt content throughout the profile and higher clay content at depth, than those in redwood forest, Although soils at both sites were derived from the same parent materials, higher soil moisture, due to less drainage and/or evapotranspiration, and lower pH at the prairie site may favor more rapid weathering of primary minerals and the formation of secondary metal oxide mineral phases and clays. Over time such differences in chemical weathering could lead to important differences in texture, mineralogy, and reactivity between the soils at our two sites.

In addition, SOM occlusion with soil aggregates can slow microbial decay by making that SOM physically inaccessible [*Lützow et al.*, 2006]. The role of aggregates in protecting SOM has been reported to be particularly important in agricultural, prairie, and grassland soils [*Ewing et al.*, 2006; *De León-González et al.*, 2007; *Pérès et al.*, 2013]. In both prairie and redwood forest, oLF had longer turnover times than HF or fLF. This trend has been reported by others [e.g., *Rasmussen et al.*, 2005; *McFarlane et al.*, 2013] and suggests that occlusion or interaction with aggregates can result in long-term stabilization.

Black carbon, more abundant in the prairie than the redwood forest, interacts with minerals [*Eckmeier et al.*, 2010; *Cusack et al.*, 2012;] and has been found within microaggregate soil fractions [*Brodowski et al.*, 2006]. Furthermore, Brodowski *et al.*, [2006] speculated that black carbon could contribute to the formation and stabilization of microaggregates, enhancing stabilization of SOM along with black carbon. Nevertheless, we conclude that aggregation and SOM occlusion were not primary drivers of long-term stabilization or of site differences because only a very small fraction of the total SOM was isolated in the oLF (Figure 6) and we did not find more SOM associated with oLF in the prairie than redwood forest.

In addition to observing longer turnover times in the prairie than redwood forest, we also report larger carbon and nitrogen stocks in the prairie. Soil carbon stock results from the balance between carbon inputs and carbon loss, where loss is primarily through decomposition and subsequent heterotrophic respiration. Thus, larger carbon stocks at the prairie than the redwood forest could result from higher carbon input rates, slower carbon loss through decomposition, or both. Standing aboveground biomass in the prairie at the time of sampling can be used as a proxy for aboveground litter inputs as the majority of the vegetation in the prairie is dry season grasses, which reach their peak biomass or start senescing by early summer. As such, we found the total dry mass of aboveground biomass in the prairie to be slightly higher than annual aboveground litterfall in the redwood forest. However, when these values are converted to carbon fluxes (by multiplying by carbon concentration), they were similar, suggesting similar aboveground carbon input rates between ecosystems.

Growing evidence suggests that belowground inputs through root turnover and rhizosphere deposition are more important carbon sources to soils than aboveground litter [*Clemmensen et al.*, 2013]. We did not quantify belowground input rates, but root biomass in the prairie was less than half that in the redwood forest. The few direct comparisons of litter production

between paired prairie and forest report similar annual litter input rates (sum of above- and belowground) in aspen forest and nearby grassland, although in forest roots represented a greater portion of total litter inputs and occurred at greater depths [*Steinaker and Wilson*, 2005]. At the same site, fine root turnover time, mortality rate, and biomass were lower in grassland than forest, although total root length was higher in grassland than forest [*Pärtel and Wilson*, 2002]. Along successional stages following agricultural abandonment, mature secondary forests had higher fine root productivity and belowground carbon inputs than grasslands [*Zhang et al.*, 2013]. In addition, fine roots tend to have different morphologies in prairies versus forests, with a tendency towards longer, smaller diameter roots in prairies [*Jackson et al.*, 1997], which is consistent with the observation of higher total root length despite lower root biomass in grasslands in the previously mentioned study. Furthermore, differences in root morphology, phenology, and function may result in differences in the chemical composition, decomposition, and exudation of roots between forest and prairie. Fine-root decomposition has been observed to be faster in grassland than in forest [*Zhang et al.*, 2013]. In addition to higher root biomass, much shorter turnover times for fLF in deep soils in the redwood forest than prairie support higher rates of root-C inputs to deep soils in the redwood forest while fresh plant inputs may be more limited to near-surface soils in the prairie.

In addition to plant inputs, fire residues may be an important source of C to soils [*Schmidt et al.*, 2011]. Expressing the black carbon content in our soils as a stock (Figure 5-a), the difference in black carbon between the prairie and redwood forest accounts for at least 19 % of the difference in mineral-soil carbon stocks (Figure 6) between sites. The BCPA method provides a conservative measure of black carbon, so this estimate should be considered a minimum. With the commonly used conversion factor of 2.23, BPCA would be estimated to explain 38 % of the difference between sites. Furthermore, differences between sites in black C content (Figure 5-a) are more pronounced at the surface where prairie carbon stocks are higher than those in redwood forest.

We did not account for all C stocks in the redwood forest. Measuring coarse root biomass is sufficiently destructive that it was not permitted in the old-growth forest. We also did not quantify coarse woody debris although old-growth redwood forests tend to have large amounts of coarse woody debris [*Busing and Fujimori*, 2005]; reported values across different sites range from 10-280 Mg ha^{-1} [see *Sawyer et al.*, 2000 and references therin]. Considering only living aboveground biomass, there is about seven times more C in aboveground tree biomass than in the forest floor and mineral soil in the redwood forest [*Sillett et al.*, 2010]. Thus, despite storing less carbon in soil, this old-growth redwood forest stores much more carbon in the ecosystem as a whole than does the adjacent prairie.

Summary and Conclusion

In summary, we observed soil C stocks to 110 cm depth of 277 Mg C ha^{-1} in an old-growth redwood forest and 350 Mg C ha^{-1} in a coastal prairie with similar climate and parent materials. Fine root C stocks were more than twice as large in the redwood forest as the prairie, but were small compared to the amount of C stored in soil. Radiocarbon-based turnover times for bulk soils ranged from about 130 y for surface soils to 3100 y at depth in the redwood forest and from about 360 y at the surface to 8600 y at depth in the prairie.

Despite similar or higher productivity, higher abundance of tannins, lignin, and other complex compounds in litter, and much higher aboveground biomass, soils in the redwood forest contained lower carbon stocks and had faster overall carbon turnover times compared to an adjacent prairie. Differences in black C stocks accounted for about 20–40 % of the difference in total C stocks. We conclude that differences in soil carbon storage and turnover in these sites of contrasting litter inputs but similar macroclimate and parent material is influenced more by plant root inputs, fire residues, and soil properties than by the chemistry of plant litter.

Acknowledgements

All reported data are kept internally on LBNL servers with daily backup, and are available upon request with the customary limitations. We thank Alex Morales for help during field collection, Abe Rohilla and Paloma Cuartero for help with laboratory and fieldwork, and Cristina Castanha and Melissa Payton for assistance in the laboratory. We also thank Stassia Samuels and Leonel Arguello at the Redwood National and State Parks for information on site history. Vanessa Boukili conducted preliminary research on litterfall at our redwood forest site. This work was supported in part by the Director, Office of Science, Office of Biological and Environmental Research, Climate and Environmental Science Division, of the U.S. Department of Energy under Contract No. DE-AC02-05CH11231 to Lawrence Berkeley National Laboratory as part of the Terrestrial Ecosystem Science Program.A part of this work was performed under the auspices of the U.S. Department of Energy by Lawrence Livermore National Laboratory under Contract DE-AC52-07NA27344 (release number). S. Mambelli would like to thank the Save-the-Redwoods League for providing her with additional funding.

Table 1. Aboveground Biomass and Litter Input

Site		Mass (Mg ha^{-1})	C (%)	N(%)
Prairie	Aboveground Biomass	10.42 ± 1.81	44.12 ± 0.31	0.79 ± 0.06
Redwood	Aboveground Biomass	4283*	NA	NA
	Total Annual Litterfall	7.80 ± 1.61	48.83 ± 0.45	0.58 ± 0.05

* From Sillett and Van Pelt, 2007.

Table 2. General Soil Characteristics. Values are means followed by one standard deviation.

Site	Horizon/ Depth (cm)	Texture (% sand/silt/clay)	pH_w	pH_{CaCl2}	O Horizon Mass ($g\ m^{-2}$) or Mineral Soil Bulk Density ($g\ cm^{-3}$)
Prairie	0–10 cm	10/89/1	4.9 ± 0.1	4.1 ± 0.2	0.58 ±.58
	10–20 cm	8/91/1	4.9 ± 0.0	4.1 ± 0.1	0.72 ±.72
	20–30 cm	8/90/2	5.0 ± 0.1	4.2 ± 0.1	0.94 ±.94
	30–50 cm	6/86/8	5.1 ± 0.1	4.3 ± 0.0	0.92 ±.92
	50–70 cm	12/66/22	5.1 ± 0.2	4.3± 0.0	1.20 ±.20 0
	70–90 cm	18/57/26	5.1 ± 0.2	4.3 ± 0.1	1.48 ±.48
	90–110 cm	20/55/25	5.2 ± 0.2	4.3 ± 0.1	1.64 ±.64
Redwood	O (total)	NA	NA	NA	3647 ±61059
	Oi	NA	NA	NA	2078 ±078
	Oe/Oa	NA	NA	NA	2078 ±078
	0–10 cm	31/68/1	5.3 ± 0.1	4.8 ± 0.1	0.59 ±.59
	10–20 cm	31/67/2	5.4 ± 0.1	4.7 ± 0.2	0.70 ±.70
	20–30 cm	33/65/2	5.3 ± 0.1	4.6 ± 0.3	0.86 ±.86
	30–50 cm	34/63/3	5.1 ± 0.2	4.5 ± 0.2	0.91 ±.0.20
	50–70 cm	38/56/7	5.0 ± 0.1	4.4 ± 0.2	0.94 ±.94
	70–90 cm	42/49/10	5.0 ± 0.1	4.4 ± 0.1	1.27 ±.27
	90–110 cm	48/40/12	5.1 ± 0.1	4.4 ± 0.1	0.97 ±.97

Table 3. Soil fraction C and N concentration, isotopes, and turnover times for 0-10 and 50–70 cm depths. Values are means followed by one standard deviation (n = 3).

Site	Horizon/ Depth (cm)	Fraction	C (%)	N (%)	$\delta^{13}C$ (‰)	$\Delta^{14}C$ (‰)	τ (y)
Prairie	0–10	fLF	23.1 ± 1.1	1.3 ± 0.1	-28.7 ± 0.4	63 ± 15	138 ± 28
		oLF	36.8 ± 0.5	2.3 ± 0.1	-28.7 ± 0.3	31 ± 10	212 ± 30
		DF	8.9 ± 1.3	0.7 ± 0.1	-27.6 ± 0.4	-2 ± 18	341 ± 87
	50–70	fLF	32.1 ± 2.7	0.9 ± 0.1	-27.3 ± 0.4	-197 ± 170	2416 ± 2192
		oLF	40.8 ± 3.0	1.1 ± 0.1	-26.5 ± 0.1	-505 ± 54	8359 ± 1667
		DF	1.4 ± 0.4	0.1 ± 0.0	-25.3 ± 0.2	-344 ± 35	4294 ± 667
Red-wood	0–10	fLF	34.0 ± 3.3	1.0 ± 0.2	-27.0 ± 0.5	44 ± 26	183 ± 66
		oLF	35.9 ± 2.0	1.1 ± 0.1	-27.5 ± 0.4	25 ± 22	235 ± 71
		DF	5.1 ± 0.6	0.4 ± 0.0	-25.3 ± 0.5	82 ± 13	106 ± 16
	50–70	fLF	32.7 ± 2.0	0.7 ± 0.0	-27.4 ± 0.2	-67 ± 75	816 ± 630
		oLF	38.4 ± 4.8	0.8 ± 0.1	-26.3 ± 0.1	-302 ± 163	3944 ± 2501
		DF	1.5 ± 0.1	0.1 ± 0.0	-24.9 ± 0.2	-218 ± 69	2377 ± 937

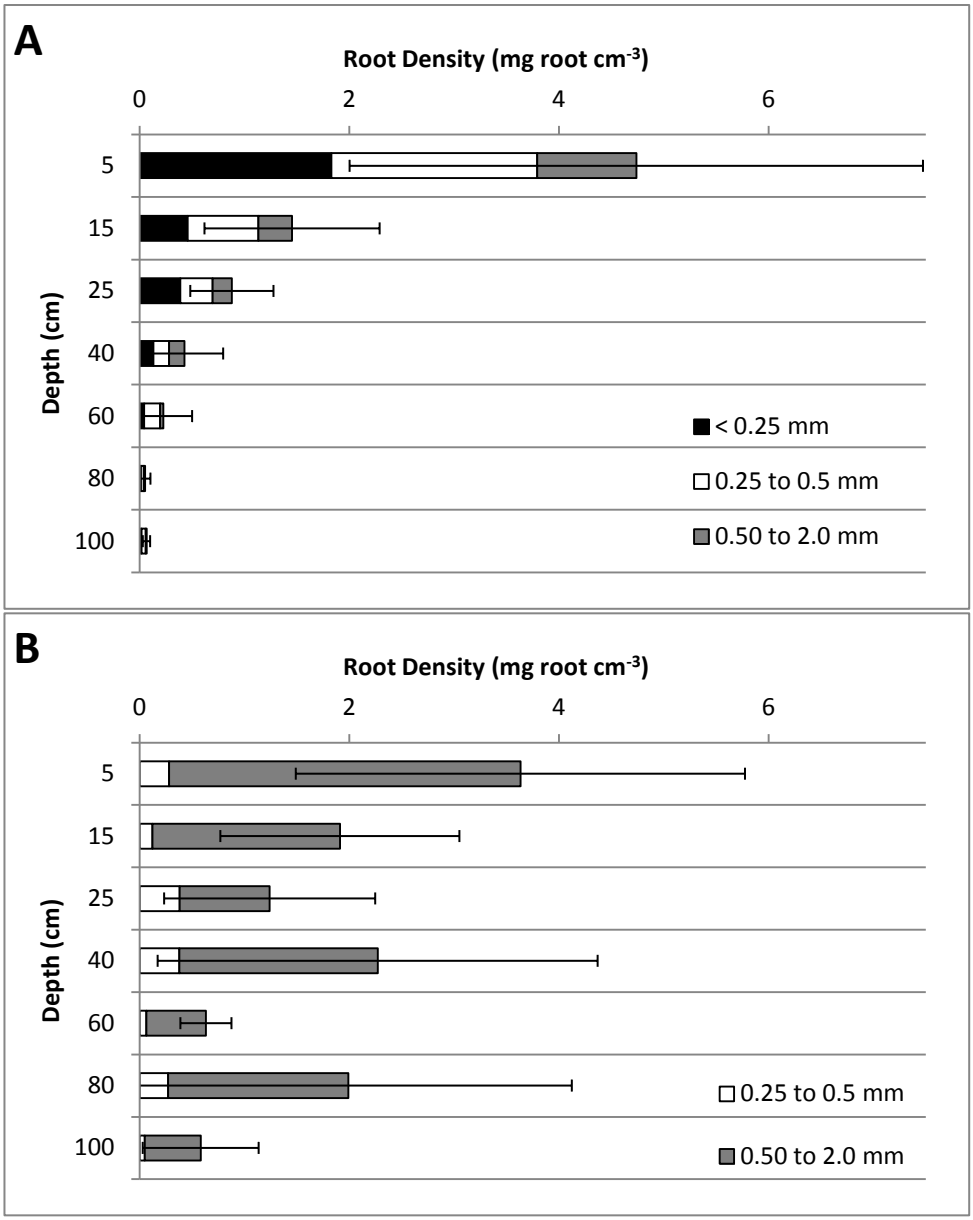

Figure 1. Fine root biomass in Coastal Prairie (A) and Redwood Forest (B). Data are means ± 1 standard deviation of the total mean with n = 3 for the prairie and 6 for the redwood forest.

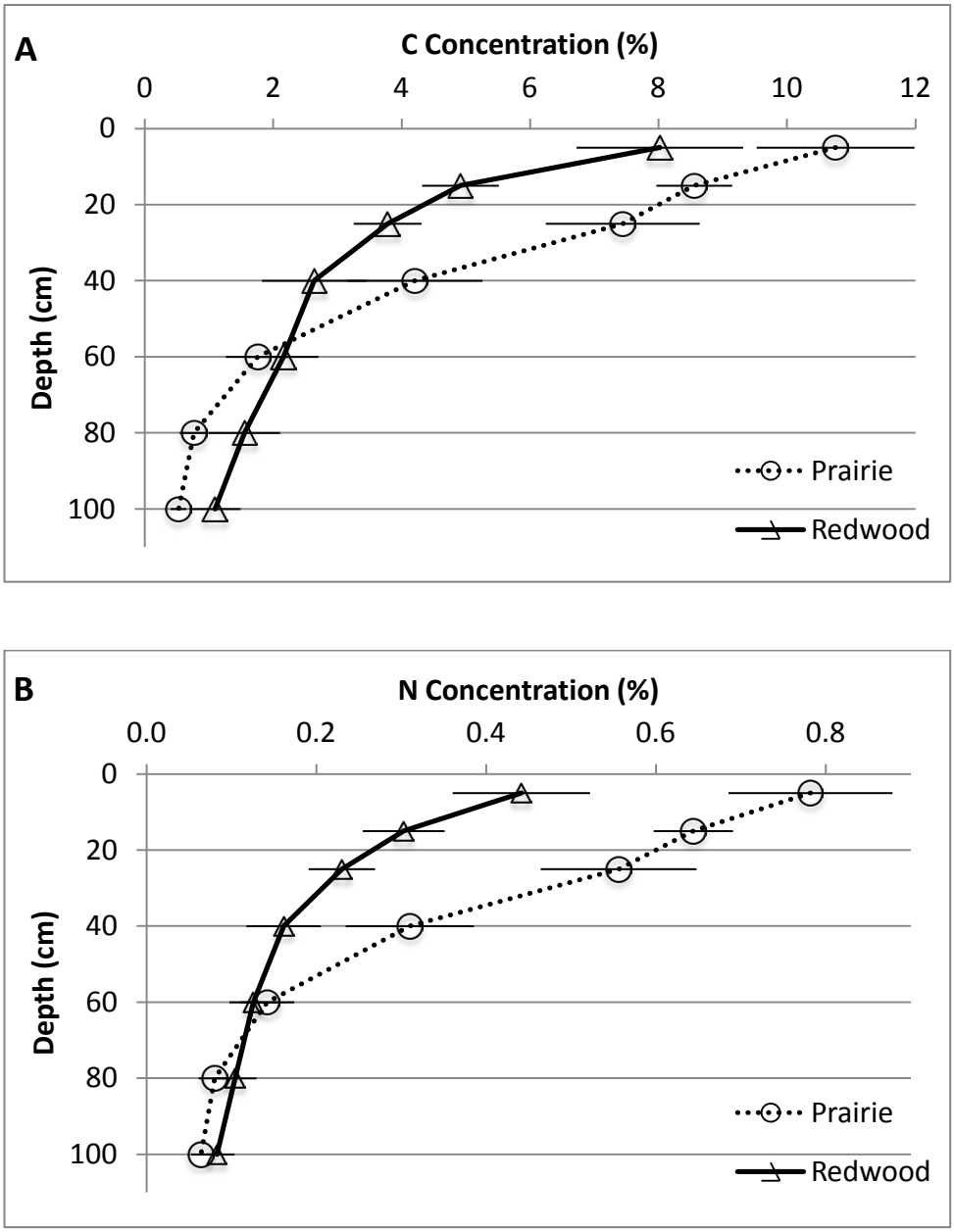

Figure 2. Bulk soil carbon (A) and nitrogen (B) concentrations in Coastal Prairie and Redwood Forest (n = 5 for Prairie and 7 for Redwood). Depth is middle of depth increment. Data are means ± 1 standard deviation.

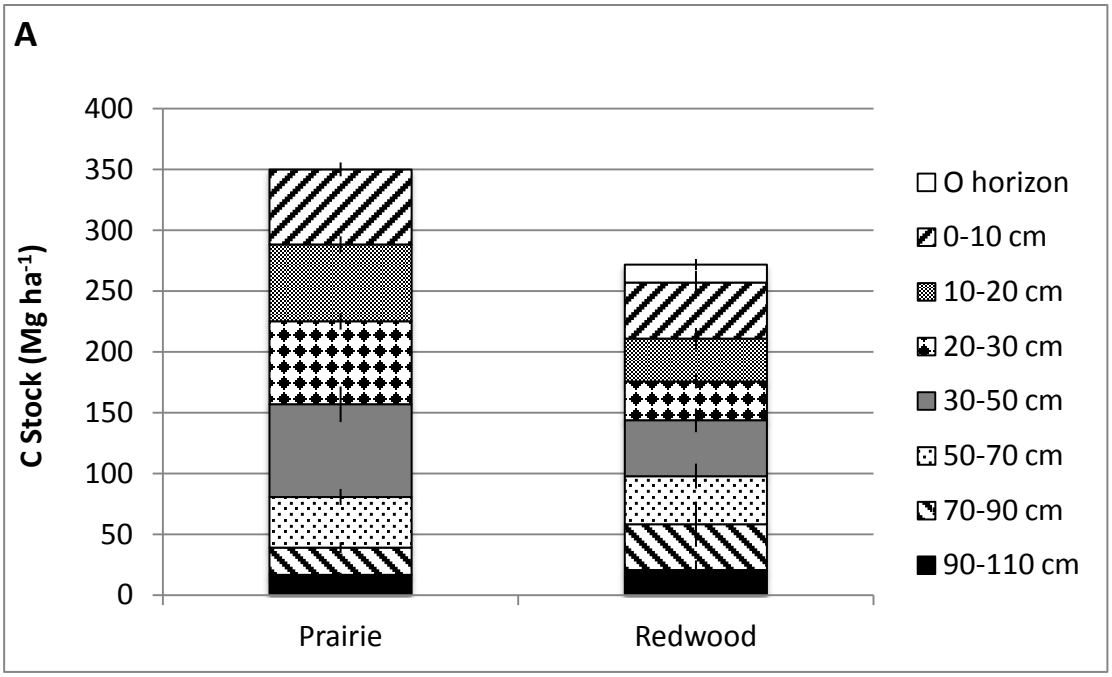

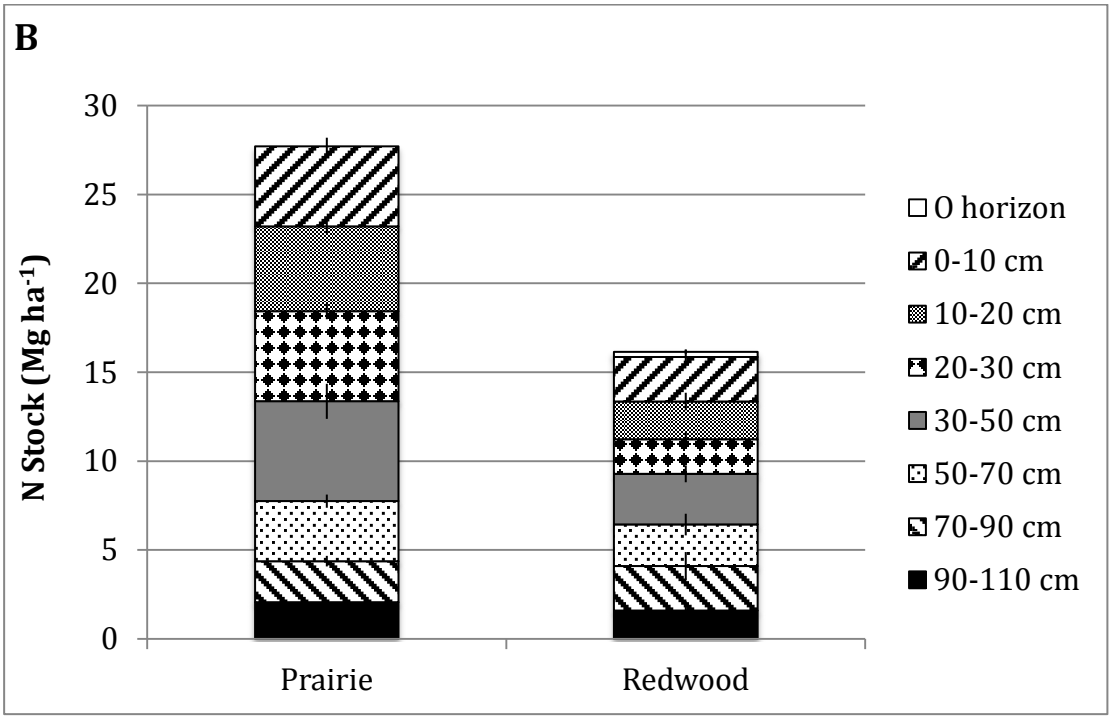

Figure 3. Bulk soil carbon (A) and nitrogen (B) stocks in Coastal Prairie and Redwood Forest (n = 5 for Prairie and 7 for Redwood). Data are means ± 1 standard deviation.

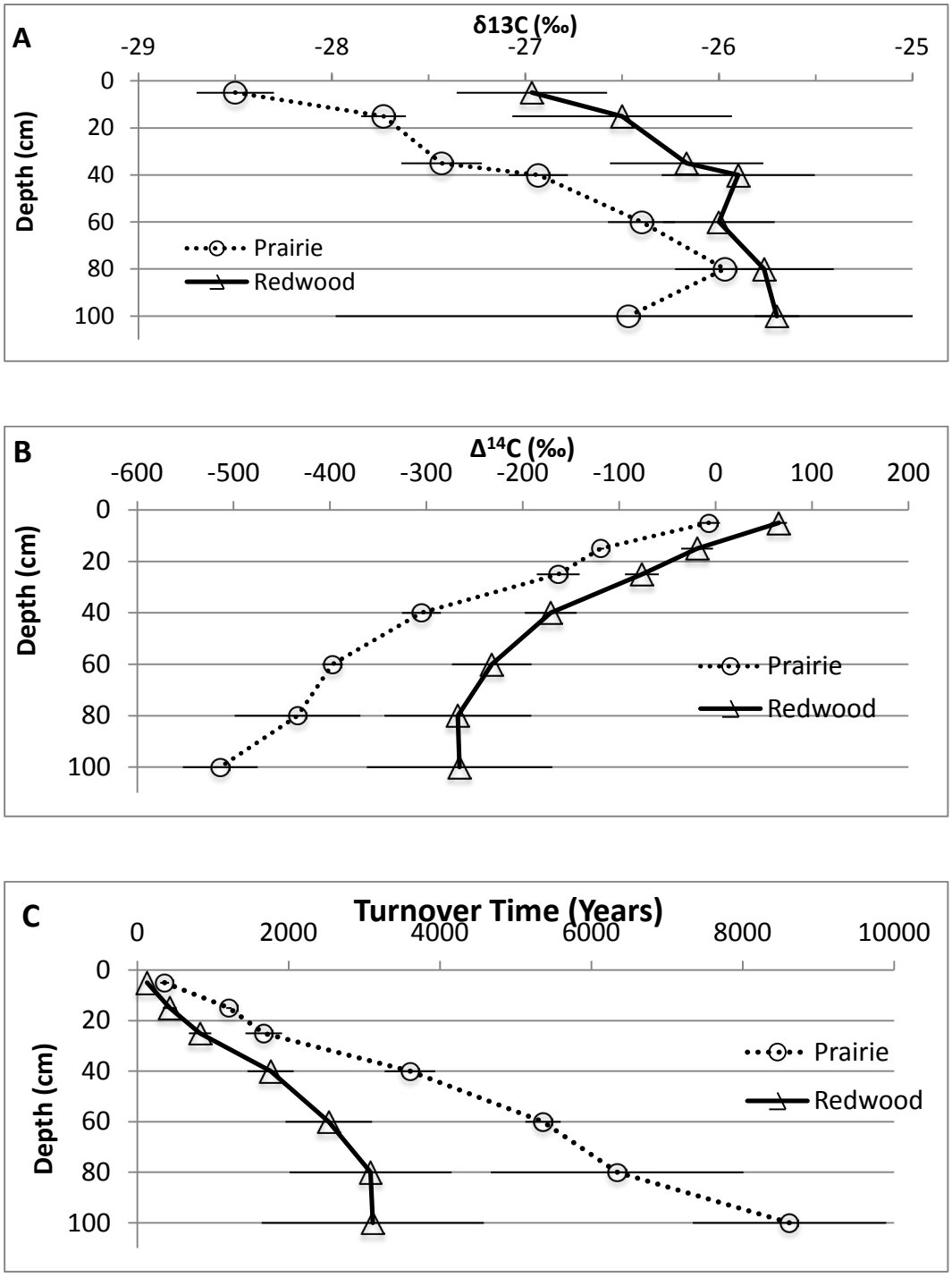

Figure 4. (A) Bulk mineral soil ^{13}C, (B) ^{14}C, and (C) mean turnover time in Coastal Prairie and Redwood Forest (n = 3 for Prairie and 3 for Redwood). Depth is middle of depth increment. Data are means ± 1 standard deviation.

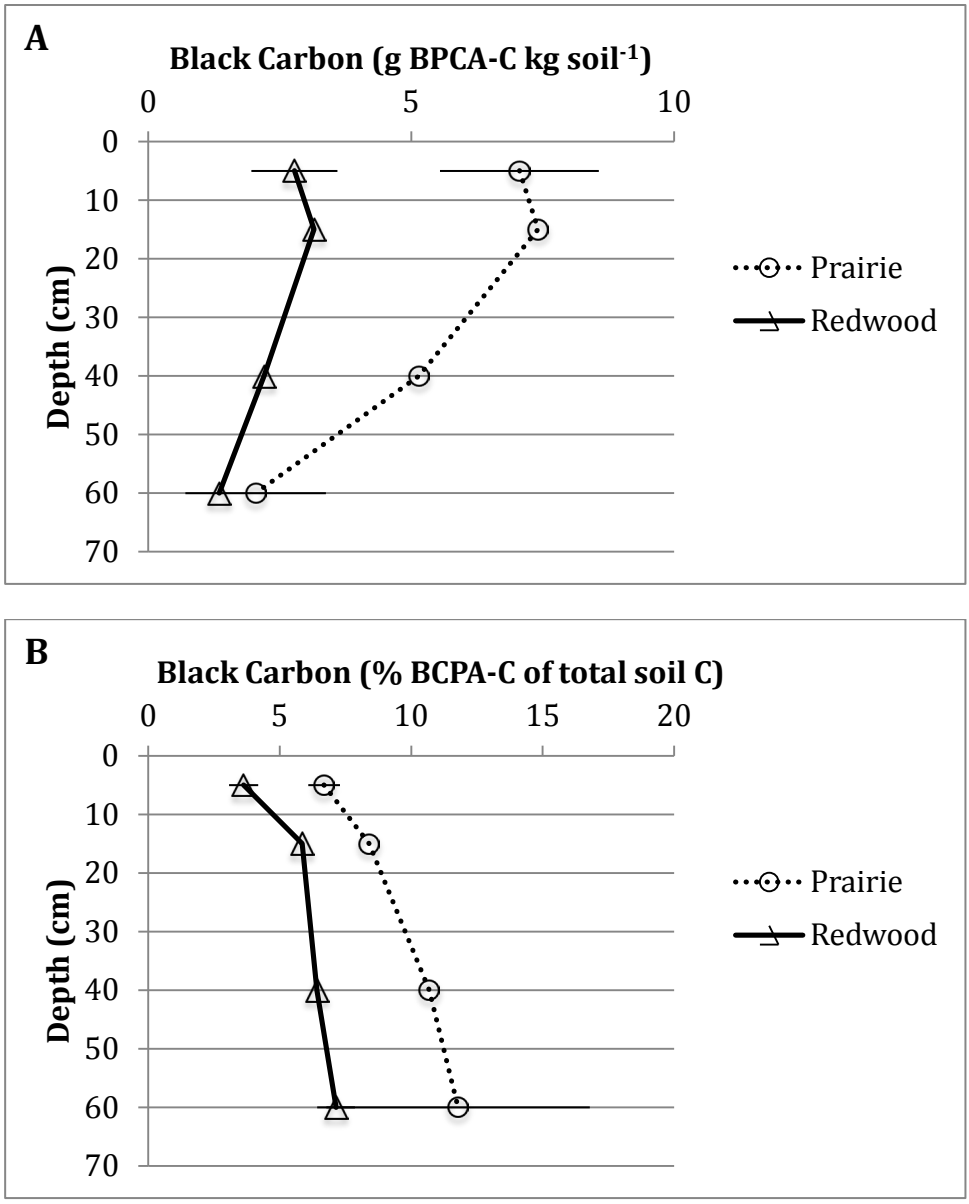

Figure 5. Black carbon content in bulk soils from coastal prairie and redwood forest determined by BCPA expressed (A) per soil mass and (B) as a percentage of total soil carbon mass. Depth is middle of depth increment. Data are means ± 1 standard deviation for 0–10 cm and 50–70 cm depths, where n=3 plots for each site. N = 1 plot for each site for intermediate depths.

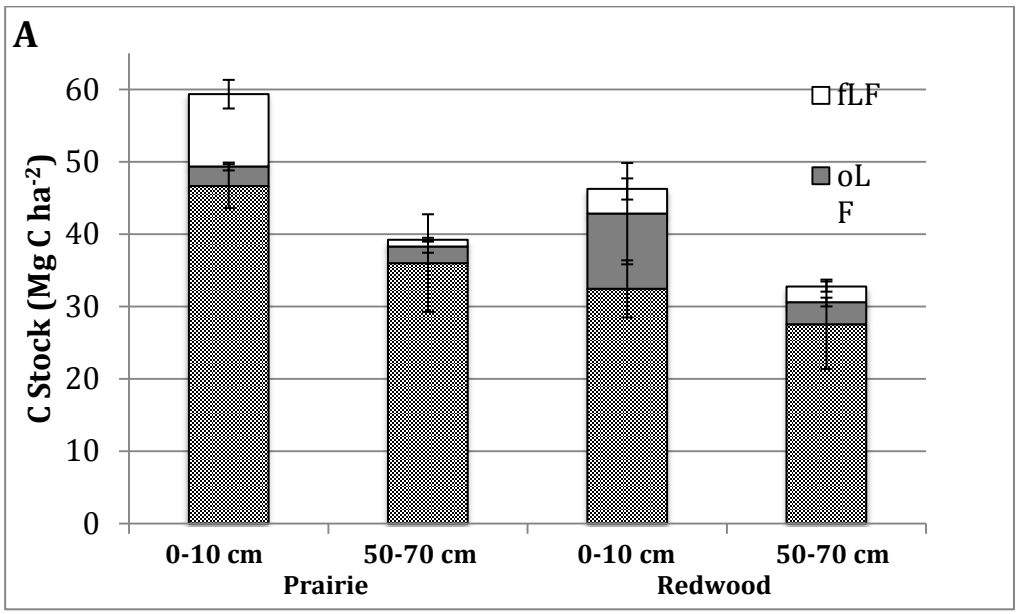

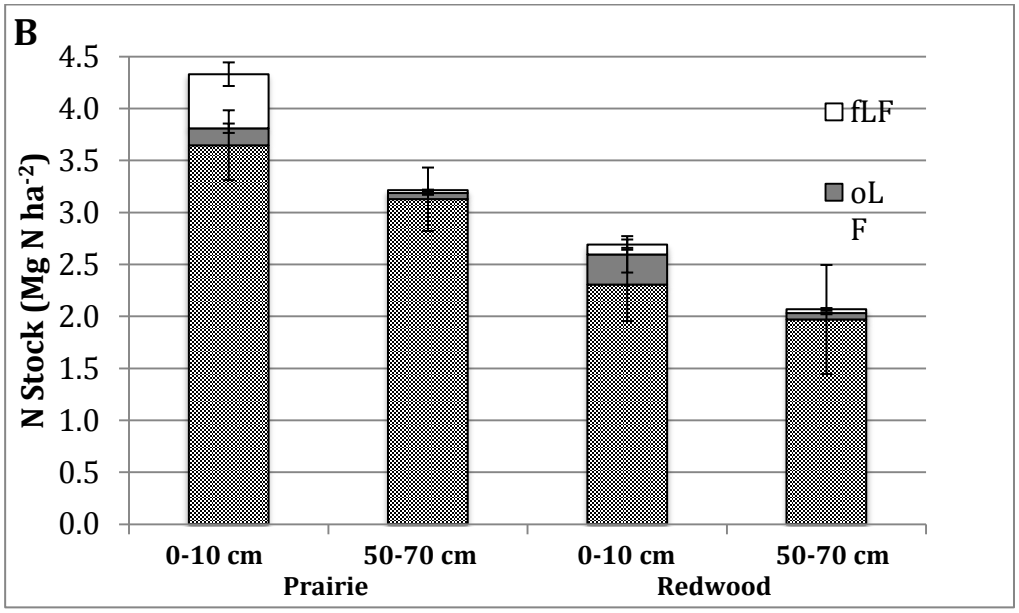

Figure 6. Carbon (A) and Nitrogen (B) distribution in density fractions from coastal prairie and redwood forest. Data are means ± 1 standard deviation of the total mean. N = 3.

References

Anderson, A. B., R. Riffer, and A. Wong (1968), Chemistry of the genus sequoia—VI: On the cyclitols present in heartwood of sequoia sempervirens, *Phytochemistry*, 7(10), 1867–1870, doi:10.1016/S0031-9422(00)86661-3.

Berg, B. (2000), Litter decomposition and organic matter turnover in northern forest soils, *Forest Ecol. Manag.*, 133(1-2), 13–22.

Bird, J. A., and M. S. Torn (2006), Fine roots vs. needles: a comparison of ^{13}C and ^{15}N dynamics in a ponderosa pine forest soil, *Biogeochemistry*, (79), 361–382.

Brodowski, S., A. Rodionov, L. Haumaier, B. Glaser, and W. Amelung (2005), Revised black carbon assessment using benzene polycarboxylic acids, *Org. Geochem.*, 36(9), 1299–1310, doi:10.1016/j.orggeochem.2005.03.011.

Brodowski, S., B. John, H. Flessa, and W. Amelung (2006), Aggregate-occluded black carbon in soil, *Eur. J. Soil Sci.*, 57(4), 539–546, doi:10.1111/j.1365-2389.2006.00807.x.

Burt, R., T. Reinsch, and W. Miller (1992), A micro-pipette method for water dispersible clay, *Commun. Soil Sci. Plan.*, 24, 2531–2544.

Busing, R. T., and T. Fujimori (2005), Biomass, production and woody detritus in an old coast redwood (Sequoia sempervirens) forest, *Plant Ecol.*, 177(2), 177–188, doi:10.1007/s11258-005-2322-8.

Castanha, C., S. Trumbore, and R. Amundson (2008), Methods of Separating Soil Carbon Pools Affect the Chemistry and Turnover Time of Isolated Fractions, *Radiocarbon*, 50(1), 83–97.

Castro, H., C. Fortunel, and H. Freitas (2010), Effects of land abandonment on plant litter decomposition in a Montado system: relation to litter chemistry and community functional parameters, *Plant Soil*, 333(1-2), 181–190, doi:10.1007/s11104-010-0333-2.

Clemmensen, K. E., A. Bahr, O. Ovaskainen, A. Dahlberg, A. Ekblad, H. Wallander, J. Stenlid, R. D. Finlay, D. A. Wardle, and B. D. Lindahl (2013), Roots and Associated Fungi Drive Long-Term Carbon Sequestration in Boreal Forest, *Science*, 339(6127), 1615–1618, doi:10.1126/science.1231923.

Crow, S. E., C. W. Swanston, K. Lajtha, J. R. Brooks, and H. Keirstead (2007), Density fractionation of forest soils: Methodological questions and interpretation of incubation results and turnover time in an ecosystem context, *Biogeochemistry*, *85*, 69–90.

Cusack, D. F., O. A. Chadwick, W. C. Hockaday, and P. M. Vitousek (2012), Mineralogical controls on soil black carbon preservation, *Global Biogeochem. Cycles*, *26*(2), GB2019, doi:10.1029/2011gb004109.

De León-González, F., M. C. Gutiérrez-Castorena, M. C. A. González-Chávez, and H. Castillo-Juárez (2007), Root-aggregation in a pumiceous sandy soil, *Geoderma*, *142*(3–4), 308–317, doi:10.1016/j.geoderma.2007.08.023.

De Rosario-Martinez, H (2012), phia: Post-Hoc Interaction Analysis, R package version 0.1-0. http://CRAN.R-project.org/package=phia

Eckmeier, E., M. Egli, M. W. I. Schmidt, N. Schlumpf, M. Nötzlic, N. Minikus-Stary, and F. Hagedorn (2010), Preservation of fire-derived carbon compounds and sorptive stabilisation promote the accumulation of organic matter in black soils of the Southern Alps, *Geoderma*, *159*, 147–155, doi:10.1016/j.geoderma.2010.07.006.

Edmonds, R. L. (1990), Organic matter decomposition in western United States forests, in *Management and Productivity of Western-Montane Forest Soils*, edited by A. E. Harvey and L. F. Neuenschwander, pp. 118–128, USDA-FS Intermountain Research Station, Boise, ID.

Ewing, S. A., J. Sanderman, W. T. Baisden, Y. Wang, and R. Amundson (2006), Role of large-scale soil structure in organic carbon turnover: Evidence from California grassland soils, *J. Geophys. Res.-Biogeo.*, *111*(G3), G03012, doi:10.1029/2006jg000174.

Frank, D. A., A. W. Pontes, and K. J. McFarlane (2012), Controls on Soil Organic Carbon Stocks and Turnover Among North American Ecosystems, *Ecosystems*, 15(4), 604–615, doi:10.1007/s10021-012-9534-2.

Gaudinski, J. B., S. E. Trumbore, E. A. Davidson, and S. Zheng (2000), Soil carbon cycling in a temperate forest: radiocarbon-based estimates of residence times, sequestration rates and partitioning fluxes, *Biogeochemistry*, 51, 33–69.

Gaudinski, J. B., M. S. Torn, W. J. Riley, C. Swanston, S. E. Trumbore, J. D. Joslin, H. Majdi, T. E. Dawson, and P. J. Hanson (2009), Use of stored carbon reserves in growth of temperate tree roots and leaf buds: analyses using radiocarbon measurements and modeling, *Glob. Change Biol.*, 15, 992–1014, doi:doi: 10.1111/j.1365-2486.2008.01736.x.

Gaudinski, J. B., M. S. Torn, W. J. Riley, T. E. Dawson, J. D. Joslin, and H. Majdi (2010), Measuring and modeling the spectrum of fine-root turnover times in three forests using isotopes, minirhizotrons, and the Radix model, *Global Biogeochem. Cycles*, 24(3), GB3029, doi:10.1029/2009GB003649.

Glaser, B. and W. Amelung (2003), Pyrogenic carbon in native grassland soils along a climosequence in North America, *Global Biogeochem. Cycles*, *17*(2), 1064, doi:10.1029/2002gb002019.

Glaser, B., L. Haumaier, G. Guggenberger, and W. Zech (1998), Black carbon in soils: the use of benzenecarboxylic acids as specific markers, *Org. Geochem.*, 29(4), 811-819, doi:10.1016/S0146-6380(98)00194-6.

Gorham, E. (1991), Northern Peatlands: Role in the Carbon Cycle and Probable Responses to Climatic Warming, *Ecol. Appl.*, *1*(2), 182-195, doi:10.2307/1941811.

Graven, H. D., T. P. Guilderson, and R. F. Keeling (2012), Observations of radiocarbon in CO2 at La Jolla, California, USA 1997-2007: Analysis of the long-term trend, *J. Geophys. Res.*, *117*(D2), D02302, doi:10.1029/2011jd016533.

Hammes, K., M. S. Torn, A. G. Lapenas, and M. W. I. Schmidt (2008), Centennial black carbon turnover observed in a Russian steppe soil, *Biogeosciences*, *5*(5), 1339-1350, doi:10.5194/bg-5-1339-2008.

Harden, J. W., T. L. Fries, and M. J. Pavich (2002), Cycling of Beryllium and Carbon through hillslope soils in Iowa, *Biogeochemistry*, *60*(3), 317-336, doi:10.1023/a:1020308729553.

Hättenschwiler, S., and P. M. Vitousek (2000), The role of polyphenols in terrestrial ecosystem nutrient cycling, *Trends Ecol. Evol.*, *15*(6), 238-243.

Hothorn, T, Frank Bretz and Peter Westfall (2008). Simultaneous Inference inGeneral Parametric Models. *Biometrical J.*, 50(3), 346–363.

Horner, J. D., J. R. Gosz, and R. G. Cates (1988), Carbon-based plant secondary metabolites in decomposition in terrestrial ecosystems, *Am. Nat.*, 132(6), 869–883.

Hua, Q. and M. Barbetti (2004), Review of tropospheric bomb ^{14}C data for carbon cycle modeling and age calibration purposes, *Radiocarbon*, 46(3), 1273–1298.

Jackson, R. B., H. A. Mooney, and E.-D. Schulze (1997), A global budget for fine root biomass, surface area, and nutrient contents, *P. Natl. Acad. Sci. USA*, 94(14), 7362–7366.

Jobbágy, E. G. and R. B. Jackson (2000), The vertical distribution of soil organic carbon and its relation to climate and vegetation, *Ecol. Appl.*, 10(2), 423–436.

Kuzyakov, Y., I. Bogomolova, and B. Glaser (2014), Biochar stability in soil: Decomposition during eight years and transformation as assessed by compound-specific ^{14}C analysis, *Soil. Biol. Biochem.*, 70, 229–236, doi:10.1016/j.soilbio.2013.12.021.

Kuhn, M., S. Weston, J. Wing and J. Forester (2011), Contrast: A collection of contrast methods. R package version 0.17, http://CRAN.R-project.org/package=contrast.

Lehmann, J., J. Kinyangi, and D. Solomon (2007), Organic matter stabilization in soil microaggregates: Implications from spatial heterogeneity of organic carbon contents and carbon forms, *Biogeochemistry*, 85, 45–57.

Levin, I. and B. Kromer (2004), The tropospheric $^{14}CO_2$ level in mid-latitudes of the northern hemisphere (1959-2003), *Radiocarbon*, 46(3), 1261–1272.

Lützow, M. v., I. Kögel-Knaber, K. Erkschmitt, E. Matzner, G. Guggenberger, B. Marschner, and H. Flessa (2006), Stabilization of organic matter in temperate soils: mechanisms and their relevance under different soil conditions - a review, *Eur. J. Soil Sci.*, *57*, 426–445.

Marín-Spiotta, E., C. W. Swanston, M. S. Torn, W. L. Silver, and S. D. Burton (2008), Chemical and mineral control of soil carbon turnover in abandoned tropical pastures, *Geoderma*, *143*, 49–62.

Masiello, C. A. (2004), New directions in black carbon organic geochemistry, *Mar. Chem.*, *92*, 201–213, doi:10.1016/j.marchem.2004.06.043.

Masiello, C. A., O. A. Chadwick, J. Southon, M. S. Torn, and J. W. Harden (2004), Weathering controls on mechanisms of carbon storage in grassland soils, *Global Biogeochem. Cycles*, *18*(4), GB4023, doi:10.1029/2004gb002219.

Mayer, L. M. (1994), Relationships between mineral surfaces and organic carbon concentrations in soils and sediments, *Chem. Geol.*, *114*(3–4), 347-363, doi:http://dx.doi.org/10.1016/0009-2541(94)90063-9.

McFarlane, K. J., S. H. Schoenholtz, R. F. Powers, and S. S. Perakis (2010), Soil organic matter stability in intensively managed ponderosa pine stands in California, *Soil Sci. Soc. Am. J.*, *73*, 1020–1032.

McFarlane, K. J., M. S. Torn, P. J. Hanson, R. C. Porras, C. W. Swanston, M. A. Callaham, Jr., and T. P. Guilderson (2013), Comparison of soil organic matter dynamics at five temperate deciduous forests with physical fractionation and radiocarbon measurements, *Biogeochemistry*, *112*, 457–476, doi:10.1007/s10533-012-9740-1.

Miller, W. and D. Miller (1987), A micropipette method for soil mechanical analysis, *Commun. Soil Sci. Plan.*, 18, 1–15.

Montané, F., J. Romanyà, P. Rovira, and P. Casals (2010), Aboveground litter quality changes may drive soil organic carbon increase after shrub encroachment into mountain grasslands, *Plant and Soil*, *337*(1-2), 151–165, doi:10.1007/s11104-010-0512-1.

Northup, R., R. Dahlgren, and J. McColl (1998), Polyphenols as Regulators of Plant-litter-soil Interactions in Northern California's Pygmy Forest: A Positive Feedback?, *Biogeochemistry*, *42*(1-2), 189–220, doi:10.1023/a:1005991908504.

Oades, J. M. (1988), The retention of organic matter in soils, *Biogeochemistry*, *5*, 35–70.

Osono, T., J.-i. Azuma, and D. Hirose (2013), Plant species effect on the decomposition and chemical changes of leaf litter in grassland and pine and oak forest soils, *Plant Soil*, 1–11, doi:10.1007/s11104-013-1993-5.

Ostertag, R., E. Marín-Spiotta, W. L. Silver, and J. Schulten (2008), Litterfall and decomposition in relation to soil carbon pools along a secondary forest chronosequence in Puerto Rico, *Ecosystems*, *11*, 701–714.

Pärtel, M., and S. D. Wilson (2002), Root dynamics and spatial pattern in prairie and forest, *Ecology*, *83*(5), 1199–1203.

Pérès, G., D. Cluzeau, S. Menasseri, J. F. Soussana, H. Bessler, C. Engels, M. Habekost, G. Gleixner, A. Weigelt, W. W. Weisser, S. Scheu, N. Eisenhauer (2013), Mechanisms linking plant community properties to soil aggregate stability in an experimental grassland plant diversity gradient, *Plant Soil*, *373*(1-2), 285–299, doi:10.1007/s11104-013-1791-0.

Pillers, M. D. and J. D. Stuart (1993), Leaf-litter accretion and decomposition in interior and coastal old-growth redwood stands, *Can. J. Forest Res.*, *23*(3), 552–557, doi:10.1139/x93-073.

Pinheiro, J., D. Bates, S. DebRoy, D. Sarkar, and the R Development Core Team (2011),

nlme: Linear and Nonlinear Mixed Effects Models, R package version 3.1-102.

Post, W. M., W. R. Emanuel, P. J. Zinke, and A. G. Stagenberger (1982), Soil carbon pools and world life zones, *Nature*, 298, 156–159.

Prescott, C. (2010), Litter decomposition: what controls it and how can we alter it to sequester more carbon in forest soils? *Biogeochemistry*, 101(1-3), 133–149, doi:10.1007/s10533-010-9439-0.

R Development Core Team (2011), R: A language and environment for statistical

Computing, R Foundation for Statistical Computing, Vienna, Austria, ISBN 3-900051-07-0, URL http://www.R-project.org.

Rapalee, G., S. E. Trumbore, E. A. Davidson, J. W. Harden, and H. Veldhuis (1998), Soil Carbon stocks and their rates of accumulation and loss in a boreal forest landscape, *Global Biogeochem. Cycles*, 12(4), 687–701, doi:10.1029/98gb02336.

Rasmussen, C. G., R. J. Southard, and W. R. Horwath (2006), Mineral control of organic carbon mineralization in a range of temperate conifer forest soils, *Glob. Change Biol.*, 12, 834–847.

Rasmussen, C. G., M. S. Torn, and R. J. Southard (2005), Mineral assemblage and aggregates control carbon dynamics in a California conifer forest, *Soil Sci. Soc. Am. J.*, 69, 1711–1721.

Sawyer J.O., S. C. Sillet, J. H. Popenoe, A. LaBanca, T. Sholars, D. L. Largent, R. F. Noss, and R. Van Pelt (2000), Characteristics of redwood forests., in *The redwood forest: history, ecology and conservation of the coast redwoods*, edited by R.F. Noss, pp. 39–79, Island Press, Washington, D.C.

Schmidt, M. W. I., and A. G. Noack (2000), Black carbon in soils and sediments: Analysis, distribution, implications, and current challenges, *Global Biogeochem. Cycles*, 14(3), 777–793, doi:10.1029/1999gb001208.

Schmidt, M. W. I., J. O. Skjemstad, E. Gehrt, and I. Kögel-Knabner (1999), Charred organic carbon in German chernozemic soils, *Eur. J. Soil Sci.*, 50(2), 351–365, doi:10.1046/j.1365-2389.1999.00236.x.

Schmidt, M. W. I., et al. (2011), Persistence of soil organic matter as an ecosystem property, *Nature*, 478(7367), 49–56.

Sillett, S. C. and R. Van Pelt (2007), Trunk reiteration promotes ephiphytes and water storage in an old-growth redwood forest canopy, *Ecol. Monogr.*, 77(3), 335–359, doi:10.1890/06-0994.1.

Sillett, S. C., R. Van Pelt, G. W. Koch, A. R. Ambrose, A. L. Carroll, M. E. Antoine, and B. M. Mifsud (2010), Increasing wood production through old age in tall trees, *Forest Ecol. Manag.*, 259(5), 976–994, doi:http://dx.doi.org/10.1016/j.foreco.2009.12.003.

Singh, N., S. Abiven, M. S. Torn, and M. W. I. Schmidt (2012), Fire-derived organic carbon in soil turns over on a centennial scale, *Biogeosciences*, 9(8), 2847–2857, doi:10.5194/bg-9-2847-2012.

Skjemstad, J., P. Clarke, J. Taylor, J. Oades, and S. Mcclure (1996), The chemistry and nature of protected carbon in soil, *Soil Research*, 34(2), 251–271, doi:10.1071/SR9960251.

Steinaker, D. F. and S. D. Wilson (2005), Belowground litter contributes to nitrogen cycling at a northern grassland-forest boundary, *Ecology*, 86(10), 2825–2833, doi:10.1890/04-0893.

Stone, E. C. and R. B. Vasey (1968), Preservation of coast redwood on alluvial flats, *Science*, 159(3811), 157-161, doi:10.1126/science.159.3811.157.

Stuiver, M. and H. A. Polach (1977), Reporting of C-14 data, *Radiocarbon*, 19, 355–363.

Stuiver, M., P. J. Reimer, and T. F. Braziunas (1998), High-precision radiocarbon age calibration for terrestrial and marine samples, *Radiocarbon*, 40(3), 1127–1151.

Swanston, C. W., M. S. Torn, P. J. Hanson, J. R. Southon, C. T. Garten, E. M. Hanlon, and L. Ganio (2005), Initial characterization of processes of soil carbon stabilization using forest stand-level radiocarbon enrichment, *Geoderma*, 128, 52– 62.

Thomas, G. W. (1996), Soil pH and Soil Acidity, in *Methods of Soil Analysis, Part 3, Chemical Methods,* edited by Soil Science Society of America and American Society of Agronomy, pp. 475–490, SSSA, Madison.

Tisdall, J., and J. Oades (1979), Stabilization of soil aggregates by the root systems of ryegrass, *Aust. J. Soil Res.*, 17(3), 429–441, doi:10.1071/SR9790429.

Torn, M. S., S. E. Trumbore, O. A. Chadwick, P. M. Vitousek, and D. M. Hendricks (1997), Mineral control of soil organic carbon storage and turnover, *Nature*, 389, 170–173.

Torn, M. S., A. G. Lapenis, A. Timofeev, M. L. Fischer, B. V. Babikov, and J. W. Harden (2002), Organic carbon and carbon isotopes in modern and 100-year-old-soil archives of the Russian steppe, *Glob. Change Biol*., 8, 941–953.

Torn, M. S., C. W. Swanston, C. Castanha, and S. E. Trumbore (2009), Storage and Tunover of Organic Matter, in *Soil, in Biophysico-Chemical Processes Involving Natural Nonliving Organic Matter in Environmental Systems*, edited by N. Senesi, B. Xing and P. M. Huang, pp. 219–272, John Wiley & Sons, Inc., Hoboken, New Jersey.

Trumbore, S. (2000), Age of soil organic matter and soil respiration: radiocarbon constraints on belowground C dynamics, *Ecol. Appl.,* 10(2), 399–411.

Trumbore, S. E., O. A. Chadwick, and R. Amundson (1996), Rapid exchange between soil carbon and atmospheric carbon dioxide driven by temperature change, *Science*, 272, 393–396, doi:10.1126/science.272.5260.393

Veirs, S. (1987), Vegetation studies of Elk Prairie, Prairie Creek Redwoods State Park, Humbolt County, California, Rep., Cooperative Park Studies Unit, Humbolt County, California.

Vogel, J. S., J. R. Southon, D. E. Nelson, and T. A. Brown (1984), Performance of catalytically condensed carbon for use in accelerator mass-spectrometry, *Nucl. Instrum. Meth. B*, *5*(2), 289–293, doi:10.1016/0168-583X(84)90529-9.

Wang, W., X. Zhang, N. Tao, D. Ao, W. Zeng, Y. Qian, and H. Zeng (2014), Effects of litter types, microsite and root diameters on litter decomposition in Pinus sylvestris plantations of northern China, *Plant Soil*, 374(1-2), 677–688, doi:10.1007/s11104-013-1902-y.

Wang, Y., R. Amundson, and S. Trumbore (1999), The impact of land use change on C turnover in soils, *Global Biogeochem. Cycles*, *13*(1), 47–57, doi:10.1029/1998gb900005.

Watteau, F., G. Villemin, G. Burtin, and L. Jocteur-Monrozier (2006), Root impact on the stability and types of micro- aggregates in silty soil under maize, *Eur. J. Soil Sci.*, *57*(2), 247–257, doi:10.1111/j.1365-2389.2005.00734.x.

Wiedemeier, D. B., M. D. Hilf, R. H. Smittenberg, S. G. Haberle, and M. W. I. Schmidt (2013), Improved assessment of pyrogenic carbon quantity and quality in environmental samples by high-performance liquid chromatography, *J. Chromatogr. A*, 1304, 246–250, doi:10.1016/j.chroma.2013.06.012.

Young, I. M., E. Blanchart, C. Chenu, M. Dangerfield, C. Fragoso, M. Grimaldi, J. Ingram, and L. J. Monrozier (1998), The interaction of soil biota and soil structure under global change, *Glob. Change Biol.*, *4*(7), 703–712, doi:10.1046/j.1365-2486.1998.00194.x.

Zhang, D., D. Hui, Y. Luo, and G. Zhou (2008), Rates of litter decomposition in terrestrial ecosystems: global patterns and controlling factors, *J. Plant Ecol.*, *1*(2), 85–93, doi:10.1093/jpe/rtn002.

Zhang, K., X. Cheng, H. Dang, C. Ye, Y. Zhang, and Q. Zhang (2013), Linking litter production, quality and decomposition to vegetation succession following agricultural abandonment, *Soil. Biol. Biochem.*, *57*(0), 803–813, doi:10.1016/j.soilbio.2012.08.005.

Ziter, C. and A. S. MacDougall (2012), Nutrients and defoliation increase soil carbon inputs in grassland, *Ecology*, *94*(1), 106–116, doi:10.1890/11-2070.1.

Paper III

Purification of fire derived markers for μg scale isotope analysis ($\delta^{13}C$,$\Delta^{14}C$) using high performance liquid chromatography (HPLC)

Published as:

Gierga, M., Schneider, M.P.W., Wiedemeier, D.B., Lang, S.Q., Smittenberg, R.H., Hajdas, I., Bernasconi, S., Schmidt, M.W.I., 2014. Purification of fire-derived markers for μg scale isotope analysis ($\delta^{13}C$, $\Delta^{14}C$) using high-performance liquid chromatography (HPLC). Organic Geochemistry (in press).

Author contributions:

The study was proposed by M.G., M.P.W.S., M.W.I.S., R.H.S. and S.M.B.; M.G. and M.P.W.S. carried out the experiments and data analysis. D.B.W., S.Q.L. and R.H.S. provided technical expertise for method development. I.H. carried out AMS analysis with solid graphite targets.

Abstract

Black carbon (BC) is the residue of incomplete biomass combustion. It is ubiquitous in nature and, due to its relative persistence, is an important factor in Earth's slow-cycling carbon pool. This resistant nature makes pure BC one of the most used materials for ^{14}C dating to elucidate its formation date or residence time in the environment. However, most BC samples cannot be physically separated from their matrices, precluding accurate ^{14}C values. Here we present a method for radiocarbon dating of the oxidation products of BC, benzene polycarboxylic acids, thereby circumventing interference from extraneous carbon. Individual compounds were isolated using high performance liquid chromatography (HPLC) and converted to CO_2 via wet chemical oxidation for ^{13}C and ^{14}C isotope analysis. A detailed assessment was performed to identify and quantify sources of extraneous carbon contamination with two process standards of distinct isotopic signatures. The average blank was 1.6 ± 0.7 μg C and had an average radiocarbon content of 0.90 ± 0.50 $F^{14}C$. We successfully analyzed the ^{14}C content of individual benzene polycarboxylic acids with a sample size as small as 20-30 μg C after correcting for the presence of the average blank. The combination of $\delta^{13}C$ and $F^{14}C$ analysis helps interpret the results and enables monitoring of extraneous carbon contribution in a fast and cost efficient way. Such a molecular approach to radiocarbon dating of BC residues enables the expansion of isotopic BC studies to samples that have either been too small or strongly affected by non-fire derived carbon.

Introduction

The solid residues of incomplete biomass combustion are generally summarized under the term black carbon (BC). It is ubiquitous in nature and can be found in the atmosphere, sediments, water and ice (Goldberg, 1985) and includes a continuum of combustion products ranging from slightly charred biomass to char and charcoal to highly condensed refractory soot (Hedges et al., 2000; Masiello, 2004). Fire derived components are of interest for the investigation of the global C cycle due to their relative persistence in the environment. It is widely accepted that BC contributes significantly to the Earth's slow-cycling C pool (Skjemstad et al., 1996, 2001; Schmidt et al., 2000; Preston and Schmidt, 2006; Knicker et al., 2008) and in models of soil organic matter (OM) turnover it is defined as a C pool with relatively high resistance to degradation (Skjemstad et al., 2004). It is also utilized in the reconstruction of fire history from geological records (e.g. Glaser et al., 2000; Carcaillet et al., 2002; Tinner et al., 2005). Similarly, pure charcoal is of importance for archeological research; in addition, the presence of BC at excavation sites allows precise determination of the age of the finds from ^{14}C analysis. Consequently, pieces of pure charcoal are one of the most targeted materials for ^{14}C dating in archaeological or geological research (Bird et al., 1999).

Nevertheless, the physicochemical properties and the biological stability of BC are poorly understood and even quantification is inherently difficult. One promising approach towards a better understanding and quantification of BC is a molecular method, the so-called 'BPCA method' introduced by Glaser et al. (1998). Benzene polycarboxylic acids (BPCAs) result from the digestion of BC with HNO_3 under high pressure and temperature, and can be analyzed using either gas chromatography (GC; Glaser et al., 1998) or high performance liquid chromatography (HPLC; Dittmar, 2008; Wiedemeier et al., 2013). The BPCAs derive unambiguously from BC and provide insight into the original BC at a molecular scale. In addition to being a quantifiable molecular proxy for the total amount of BC in a complex matrix, the relative distribution of individual BPCAs can provide further information. For example, a relatively high amount of highly carboxylated BPCAs such as mellitic acid (B6CA) and benzene pentacarboxylic acid (B5CA) is indicative of a high degree of condensation (Dittmar, 2008; Schneider et al., 2011). The numbers in the notation indicate the number of substituted carboxylic acid groups per benzene ring.

The radiocarbon signature of BPCAs has potential for elucidating the fate and source of BC in nature, as the concentration of ^{14}C in a BC sample can be directly related to its age or mean residence time. For recent BC samples, ^{14}C analysis allows source apportioning of the BC between fossil fuel derived charcoal that is depleted in ^{14}C ($F^{14}C$ 0) and burned modern biomass that reflects atmospheric radiocarbon content ($F^{14}C \geq 1$). On the whole, there is an essential advantage in determining the ^{14}C content of these specific biomarkers vs. dating of bulk BC samples (e.g. Ziolkowski and Druffel, 2009; Zimmerman, 2010; Yarnes et al., 2011). In particular, analysis of bulk samples frequently suffers from large uncertainty due to small sample size and the challenge in physically separating pure BC from interfering OM. For example, OM in soils and sediments is a complex mixture of compounds, which can range

from recently produced compounds to very old material (Hedges et al., 2000). The same is true for buried archaeological samples. The matrix of pottery can contain organic carbon-bearing clay closely associated with the charred residue, or organic carbon can be taken up from the burial environment, causing further interference.

Eglinton et al. (1996) introduced the concept of compound-specific radiocarbon analysis (CSRA) applied to certain solvent extractable lipids. The first application using the BPCA method to date BC on a molecular scale was by Ziolkowski and Druffel (2009a), who separated individual BPCAs using preparative GC, and achieved reliable results with reasonably low and constant blanks. Nevertheless, the method has several drawbacks. BPCAs must be treated to form GC-amenable derivatives, requiring the addition of external C. The authors applied trimethylsilyl-diazomethane as derivatization agent. Even though it has been reported to be more efficient than other derivatization protocols (Ziolkowski and Druffel, 2009b), it is known that losses can occur. This is also true for the most common derivatization technique, silylation with BSTFA (Schneider et al., 2011). Finally, a GC column has limited capacity, necessitating a number of injections to collect sufficient material for dating. Many of the problems can be circumvented by separating the BPCAs using HPLC (Dittmar, 2008; Wiedemeier et al., 2013).

In general, ^{14}C analysis is sensitive to any contribution from extraneous carbon (C_{ex}) added to the sample during the laboratory protocol. This is particularly true for ultra small scale samples containing < 30 μg C. Purification procedures for CSRA must therefore be designed to minimize and accurately quantify C_{ex} addition (Pearson et al., 1998; Shah and Pearson, 2007; Ziolkowski and Druffel, 2009a; Birkholz et al., 2013; Lang et al., 2013).

In this study we present a new approach for molecular scale ^{14}C analysis of fire-derived compounds on the basis of the separation of BPCAs using liquid chromatography (Wiedemeier et al., 2013) combined with a recent method of wet oxidation suitable for combined ^{13}C and ^{14}C isotope analysis (Lang et al., 2012, 2013). The method allows sample oxidation despite the presence of concentrated H_3PO_4, which is essential for achieving separation of the BPCAs with HPLC. The direct conversion of the BPCAs to CO_2 within a gas tight vial allows the sample gas to be subsampled for $\delta^{13}C$ analysis prior to injection for accelerator mass spectrometry (AMS).

We describe the successful purification of individual B5CAs and B6CAs followed by $\delta^{13}C$ and $F^{14}C$ analysis. A detailed blank assessment was carried out using direct and indirect approaches to assess the amount and the isotopic signature of C_{ex}. Two different types of charcoal were selected as standards. The first was an archaeological charcoal with a ^{14}C age > 50000 BP ($\leq$ 0.02 $F^{14}C$) and the second a modern charcoal ($\geq$ 1 $F^{14}C$) prepared from a recently cut tree. Together they represented the end members of ^{14}C analysis and thereby allowed a good evaluation of this new method for BC dating.

Experimental

The data were produced from two successive series of experiments. Both included HPLC isolation followed by wet oxidation, GC-isotope ratio mass spectrometry (GC-IRMS) and AMS measurements. All glassware was pre-heated to 450 °C for 5 h prior to use to remove organic contaminants. Ultra pure water was supplied from a MilliQ Advantage A10 system (Millipore, USA) and all chemicals were of the highest available grade and were tested for impurities before use.

Process standards

The archaeological charcoal sample ('fossil char') was from in situ charred trees sampled from paroxysmal flow deposits in the Maninjau caldera in West-Central Sumatra (Alloway et al., 2004). Its precise dating using conventional AMS demonstrated that it lacked ^{14}C and had an age of ca. 50 ka BP (Alloway et al., 2004; Ascough et al., 2009). The modern analog ('modern char') was produced from chestnut wood (*Castanea sativa*) from a single tree cut in a forest in Southern Switzerland. The wood was charred at 450 °C for 5 h under a N_2 atmosphere (Hammes et al., 2006).

The samples were of almost pure charcoal, one was recovered in-situ and the other was produced in the laboratory under controlled conditions, allowing the assumption that they were not significantly affected by interfering C-bearing material. Therefore the radiocarbon contents of the bulk samples were expected to be the same as that of the isolated BPCAs. Bulk subsamples were analyzed for ^{14}C content as solid targets at the Laboratory of Ion Beam Physics of the ETH Zürich, Switzerland after being sequentially extracted with acid and base reagents to remove contaminants from the surfaces. The so-called acid-base-acid (ABA) treatment is a standard cleaning procedure prior to ^{14}C analysis (Hajdas et al., 2004). The ^{14}C content of the fossil char was found to be 0.003 ± 0.001 $F^{14}C$ (ETH-50456). The modern char was produced from unaltered dried wood that had a ^{14}C content of 1.142 ± 0.004 $F^{14}C$ (ETH-50458) and its charred residue was almost identical at 1.149 ± 0.004 $F^{14}C$ (ETH-50457). These values were used as reference values.

Sample extraction and purification

Extraction and purification of BPCAs was carried out according to the protocol of Wiedemeier et al. (2013) with modifications to make it amenable for CSRA. In brief, 15-25 mg of the dried and milled sample was directly digested in a quartz tube with 2 ml HNO_3 (65 wt.% or 14.4 mol/l) at 170 °C for 8 h. After cooling, the aqueous solution was filtered over pre-rinsed quartz fiber filters. The extract was eluted over a cation exchange resin and freeze dried to remove water and acid. The dried residue was dissolved in MeOH/water (1:1, v/v)

and applied to a pre-conditioned C_{18} solid phase extraction cartridge to remove apolar components. Finally, the eluate was dried again using an Eppendorf concentrator system.

HPLC purification

Individual BPCAs were isolated using an Agilent 1290 Infinity UPLC instrument (Santa Clara, USA). Separation was achieved with an Agilent Poroshell 120-SB C_{18} column (4.6 × 100 mm, 2.7 μm pore size) using a gradient of diluted ortho H_3PO_4 buffered to pH 1.2 with NaH_2PO_4 (mobile phase A) and pure MeCN (mobile phase B). Compounds were detected with an Agilent 1290 Infinity diode array detector at 216 and 240 nm.

Extracted samples ('total digest') were diluted in ultra pure water to achieve a concentration of B5CA and B6CA of ca. 200 ± 50 ng C/ μl for HPLC injection. A small (1 μl) initial injection was made to quantify the peaks and assign retention times. Larger (5 μl) injections (10-30 in total) were then made for fraction collection. The mobile phase was collected during the time windows corresponding to the elution of the B5CA and B6CA compounds into pre-combusted glass vials with a time-programmed analytical fraction collector (Agilent 1260 AS-FC). The collected fractions were transferred to screw cap vials with borosilicate pipettes and dried under a stream of N_2 to remove all mobile phases with the exception of non-volatile H_3PO_4. Before drying, a small aliquot was re-injected on HPLC to assess the recovery and purity of the isolated compounds. Quantification was carried out with an external standard series that contained a mixture of commercially available BPCAs (Wiedemeier et al., 2013).

Wet oxidation

The compound-specific isotopic signature ($\delta^{13}C$, $F^{14}C$) of isolated BPCAs was determined with the methods described by Lang et al. (2012, 2013). Specifically, isolated and acidified samples were transferred to 12 ml gas tight vials, diluted with Milli-Q water to a total volume of 4 ml, and spiked with 0.75 ml supersaturated oxidizing solution (100 ml H_2O + 2.0 g $K_2S_2O_8$ + 200 μl 85% H_3PO_4). Vials were sealed using a standard cap with a butyl rubber septum and flushed with high purity He (grade 5.0, 99.999%) for 8 min at 125 ml/min to remove atmospheric CO_2 from the headspace. The output gas stream passed through a water trap to prevent backflow of atmospheric CO_2. Then, the vials were heated to 100 °C for 60 min to oxidize the BPCAs to CO_2. Samples were allowed to cool to room temperature overnight. Modern sucrose [Sigma Aldrich, P/N S7903, lot 090M02112V, $F^{14}C$ 1.053 ± 0.03 (ETH-47293)] and ^{14}C-free phthalic acid [Sigma Aldrich, P/N 80010, lot 1431342V, $F^{14}C \leq$ 0.0025 (ETH-42443)] were used to assess the addition of external carbonaceous material during oxidation and transfer. Both were oxidized and analyzed for $\delta^{13}C$ and $F^{14}C$.

Stable carbon isotope analysis ($\delta^{13}C$)

The stable carbon isotopic composition of the headspace CO_2 was measured with two approaches. For initial tests, we analyzed the C content of various blank samples to determine background values, while the isotopic composition was of secondary interest. These samples were analyzed on a GasBench II on-line gas preparation and introduction system (Thermo Fisher Scientific, Bremen, Germany) coupled to a ConFlo IV interface and a Delta V Plus mass spectrometer (both Thermo Fisher Scientific), allowing the accurate detection of C content and ^{13}C of samples as small as 5 μg C. As $\delta^{13}C$ analysis with the GasBench uses the majority of the CO_2, samples were also analyzed with a second method designed to preserve the majority of the CO_2 for ^{14}C analysis. In this approach, 100 μl of headspace gas was removed from the vials with a gastight syringe (Hamilton). The gas was injected into a gas chromatograph (Agilent 6890) with a split/splitless inlet and which was directly connected to a Delta V Plus via a ConFlo IV interface (both Thermo Fisher Scientific, Bremen, German). CO_2 was separated from interfering gases with a CP Poraplot Q column (27.5 m × 0.32 μm; 10 μm; Varian) maintained at 100 °C and a He flow rate of 2.0 ml/min.

The raw $\delta^{13}C$ values of each series of samples were corrected for fractionation effects between headspace and dissolved CO_2, as well for blank values and instrumental drift using standards of known composition (Lang et al., 2012). The amount of C was calculated by comparison with a dilution series of phthalic acid.

Radiocarbon analysis ($F^{14}C$)

Radiocarbon analysis was carried out at the Laboratory for Ion Beam Physics of ETH Zürich, Switzerland using the MICADAS (mini carbon dating system) equipped with a gas ion source (Ruff et al., 2007; Synal et al., 2007) that allows direct introduction of CO_2 from the headspace into the gas ion source. Detailed descriptions about the instrumentation can be found elsewhere (Lang et al., 2013; Wacker et al., 2013). In brief, sample CO_2 was removed from the vials by flushing with He and diverting the output over a magnesium perchlorate water trap to a trap containing X13 zeolite molecular sieve, which adsorbs CO_2 at room temperature. After trapping, a valve was toggled to connect the trap to a gas tight syringe, and the CO_2 was released by heating the zeolite to 450 °C. The amount of CO_2 in the syringe was detected pneumatically to allow dilution of the sample gas with He to 5 %, v/v CO_2 in He. This gas mixture was then pushed continuously out of the syringe into the ion source. Oxalic acid I (OX-1) gas was used as a modern standard (Stuiver and Polach, 1977) for normalization and fossil CO_2 gas served as a blank.

The raw data output was processed with the BATS software (Wacker et al., 2010) so that the results are reported as fraction modern ($F^{14}C$; Reimer et al., 2004) being corrected for instrumental background, standard normalization and evaluated for uncertainty. Further corrections for wet oxidation and purification of BPCAs are discussed below.

Results and Discussion

Isolation of individual BPCAs with HPLC

The first goal in method development was the definition of appropriate chromatographic conditions for providing sufficient amounts of the pure target compounds. BPCA concentrations in the total digests where determined following Wiedemeier et al. (2013). In both samples B6CA and B5CA represented ca. 80 % of the total quantified BPCA-C. For CSRA these two compounds provided the best conditions for successfully isolating and dating them. As a second step we injected as much as 1 µg C from each of the two target compounds and were still able to define robust retention times of the baseline separated peaks. Even though the column was slightly overloaded, no tailing of the target peaks to other fractions was observed (Fig. 1A) by re-injection of the eluent collected just before and after collection of the sample peak. The time window for fraction collection was set as narrow as possible to minimize the amount of potential co-eluting extraneous compounds and, especially, column bleed. Next to the quantified BPCAs a suite of other peaks are present (Fig 1A). These were other by-products of the digestion and were most likely nitrated BPCAs (Ziolkowski and Druffel, 2009b). We isolated B5CA and B6CA fractions from both process standards, the fossil and modern char, in 3 replicates, respectively. As a preliminary assessment of C_{ex}, aliquots of the collected fractions were re-injected; this did not show any UV-detectable contaminants (Fig. 1B). Fractions were typically collected and combined from 20 to 30 repeated injections. Sample recovery varied between 50 and 84% (Table 1). Losses might have occurred during fraction collection or during transfer and concentration of the individual fractions. We did not detect significant amounts of the target compounds in fractions collected subsequently after the time window for B6CA or B5CA, which suggests that no significant tailing occurred after passing the detector and before the fraction collector. As we considered it more important to avoid the collection of other peaks eluting shortly after the target compounds, we did not try to optimize the recovery widening the collection window, as soon as recovery exceeded 50%. Isotopic fractionation effects over the chromatographic peak were not expected for the ^{14}C content (Zencak et al., 2007). This can be explained by the fact that $F^{14}C$ values are corrected for isotopic fractionation, which is expected to occur during AMS analysis. It is also possible that losses occurred during the transfer and concentration of the collected sample volumes. Up to 15 ml of that aqueous solution had to be reduced to a final volume of 2 ml, resulting in a high concentration of H_3PO_4 as only water and MeCN were volatilized under N_2 flow.

Wet oxidation and $\delta^{13}C$ values

The wet oxidation method was originally designed to oxidize organic acids (Lang et al. 2012; 2013) but proved to be also suitable for BPCAs. The oxidation efficiency was tested by oxidizing a known amount of a benzene pentacarboxylic acid standard, with recovery always > 90%. Furthermore, no isotopic fractionation was observed when the $\delta^{13}C$ values of

the oxidized standard material were compared with the reference values obtained with total combustion of the bulk sample powder using elemental analysis (EA)-IRMS. Attempts to further optimize the oxidation parameters by varying temperature and reaction time did not result in improvement of recovery. Wet oxidation of a mellitic acid standard gave consistent results compared with the B5CA standard.

The final $\delta^{13}C$ values of each isolated B5CA or B6CA sample, as well of the entire digestion extracts are listed in Table 1. The values are corrected for fractionation effects between the liquid and gas phase and for process and instrumental background of the wet oxidation procedure itself, as described by Lang et al. (2012). In brief, the process blank was determined using oxidized ultra pure water with similar volumes to the samples. The peak area of these blanks averaged 0.55 ± 0.09 V·s (n = 3), which corresponds to a value near the limit of detection of ≤ 0.2 μg C. As these peaks were too small for reliable $\delta^{13}C$ values, the isotopic composition of the process blank was estimated indirectly by comparing the values for the oxidized phthalic acid standard samples with the known reference value. The $\delta^{13}C$ of the blanks is very sensitive, so it was individually calculated for each prepared series. The blanks were calculated to be -14.1 ± 1.1‰ for the first and -9.1 ± 1.1‰ for the second series. At first sight, there is a significant difference between the two blanks. It should be taken into account, however, that small differences detected with such small signals could lead to large differences in the $\delta^{13}C$ values for the blanks. The isotopic shift of ca. 5‰ for the blank results probably resulted from slightly changes in the quality of the chemicals in use, for instance the oxidizing reagent or the ultra pure water. This assumption is supported by the fact that the $\delta^{13}C$ values for the fire-derived compounds from the fossil and modern char showed no significant difference after being corrected for the blank value for the wet oxidation procedure (Table 1). The BPCAs had slightly lower $\delta^{13}C$ values than the total digests (Fig. 2), while B5CA was more negative than B6CA. These small differences may be the result of inhomogeneity of the parent material. Another explanation might be an incomplete collection of the chromatographic peak, as $\delta^{13}C$ values are much more sensitive to fractionation effects than $F^{14}C$ values (Zencak et al., 2007). The overall reproducibility (1σ) was ≤ 0.7‰. Even if this is slightly higher than the reported precision for the chemical oxidation method (≲ 0.4 ‰, Lang et al., 2012), the values are still satisfyingly accurate. With this technique, only a very small part of the isolated samples was used for stable isotope analysis in order to assure large enough samples for the AMS analysis. More accurate results could potentially be achieved by isolating a separate sample dedicated only to $\delta^{13}C$ using a GasBench device.

For the modern charcoal, we compared the isotopic composition of total digests and compound-specific $\delta^{13}C$ values with data from Yarnes et al. (2011), who successfully performed continuous flow ^{13}C analysis after separation of BPCAs using a laborious 2 h ion exchange chromatography method. The values of Yarnes et al. (2011) are shown in Fig. 2 for direct comparison with our results. Their results for B5CA and B6CA from the modern char were within the error of our results. Furthermore, we obtained values for the BPCA extract of

the modern char comparable to their value obtained using EA-IRMS analysis with the bulk sample. Compared with our distinct results the reported values by Yarnes et al. (2011) were systematically shifted by a value as small as -0.5‰, which is still in the range of the precision of both studies. This comparison demonstrates that our method for analyzing the $\delta^{13}C$ values of BPCAs is of high quality and can be performed on a very small aliquot of a sample whose main part is needed for CSRA.

Assessment of extraneous carbon

As mentioned above, radiocarbon analysis is more sensitive to the addition of extraneous C than $\delta^{13}C$ analysis (e.g. Shah and Pearson, 2007; Ziolkowski and Druffel, 2009a). It is therefore mandatory to minimize and precisely determine the contribution from C_{ex} to carry out an appropriate blank correction and obtain reliable radiocarbon values. Generally speaking, a measured $F^{14}C$ value is composed of a contribution from both the compound of interest and from C_{ex}. This can be expressed with the following mass balance equation:

$$F_T \cdot C_T = F_S \cdot C_S + F_{ex} \cdot C_{ex} \quad (1)$$

Where F is the $F^{14}C$ value and C the amount of carbon in µg. The subscript T refers to total as measured, S to sample and ex to extraneous. In order to solve the equation for F_S, the amount and radiocarbon content of C_{ex} need to be determined beforehand, given that $C_S = C_T - C_{ex}$.

There are several possible sources of contaminating C added to the sample. Considering the entire laboratory protocol, it might be taken up during the extraction and cleaning procedure ($C_{chemistry}$), the HPLC isolation (C_{HPLC}), the wet oxidation procedure (C_{ox}) and finally during the AMS analysis itself (C_{AMS}). Accordingly C_{ex} can be expressed as a sum of the following components: $C_{ex} = C_{chemistry} + C_{HPLC} + C_{ox} + C_{AMS}$. The most straightforward way to trace back to C_{ex} is to start at the end of the laboratory protocol, going back to the first steps.

C_{AMS}

The AMS instrumental background is routinely determined during each measurement campaign. As mentioned above, reported values are normalized using the results of small scale Ox-I standards and are corrected for small scale AMS blanks using the BATS software (Wacker et al., 2010). Because of this, C_{AMS} is not discussed further here. Accordingly, the subscript T ($F^{14}C_T$, C_T) indicates in the following that the raw values had already been corrected with the BATS software.

C_{ox}

The contribution of C_{ex} added during wet oxidation was calculated indirectly using two standards of known radiocarbon content (^{14}C-free phthalic acid and modern sucrose). With this method it is possible to assess separately two contaminant fractions. A detailed description of the method is given by Lang et al. (2013). As we adopted the approach for the assessment of $C_{chemistry}$ and C_{HPLC}, further information is given in the following section.

For the samples measured during the first campaign, we determined a small influence from a modern C_{ox} source, corresponding to 0.13 ± 0.04 µg C (n = 5), whereas the contribution from radiocarbon-dead C_{ox} corresponded to 0.85 ± 0.44 µg C (n = 5). In combination, this resulted in a total blank of 0.97 ± 0.44 µg C with a F^{14}C value of 0.13 ± 0.07. For the second measurement campaign, we were able to reduce the amount of C_{ox} via 0.07 ± 0.03 µg C modern C_{ox} and 0.45 ± 0.43 µg C of radiocarbon-dead material, i.e. a total of 0.52 ± 0.44 µg C_{ox} with 0.14 ± 0.13 F^{14}C. Evaluation of the first data set pointed to some sources of C_{ox} that could easily be reduced, especially for the reagent used for the wet oxidation. The reagent was recrystallized 2x in water before use during the second campaign. This resulted in a reduction of radiocarbon-dead C_{ox} of ca. 0.5 µg C per sample, while the average F^{14}C of C_{ox} remained comparable with the F_{ox} determined for the first campaign. The correction for C_{ox} was applied to all samples before determining $C_{chemistry}$ and C_{HPLC}. The corrected values are indicated as $C_{T'}$ and $F^{14}C_{T'}$ in the following.

$C_{chemistry}$ and *C_{HPLC}*

Initially, we directly collected and analyzed $C_{chemistry}$ and C_{HPLC}. Blank samples were run through the entire laboratory protocol except for radiocarbon dating. Another set of blanks was produced, performing only the HPLC step, omitting the extraction procedure. Because the total amount of extraneous C was very low, the number of injections and the duration of the fraction collection window were increased vs. regular sample fraction collection. The amount of C and its δ^{13}C values were determined by analyzing all material with the GasBench device (Table 2), which gives better accuracy than the GC option described above. For one sample, it was not possible to obtain a reliable δ^{13}C value, as the sample size was too small. The average blank that passed both extraction and HPLC contained 0.23 ± 0.12 µg $C_{chemistry+HPLC}$ ml^{-1} (n = 2), whereas C_{HPLC} showed an average of 0.22 ± 0.04 µg ml^{-1} (n = 5). This showed that the chemical extraction process ($C_{chemistry}$) did not significantly contribute to the amount of the sum of C_{ex} and could be assumed to be zero. Most likely, if any $C_{chemistry}$ were present, it would again be removed during the HPLC purification step to a level below the detection limit. The isotopic signatures of the C_{HPLC} replicates showed comparable values, within a relatively larger error due to the small sample sizes. The δ^{13}C value of C_{HPLC} averaged -29.5 ± 1.3‰ (Table 2), implying that the source of C_{ex} remained constant and that no unexpected and uncontrolled addition of C_{ex} occurred. Separate analysis of the aqueous eluent before usage showed that this was most probably the main source of C_{HPLC}, as it

already contained 0.3 ± 0.1 μg C/ml. Future efforts to reduce C_{HPLC} should therefore focus on the mobile phase in the HPLC step.

A strong relationship (R^2 0.91) existed between the collected volumes of C_{HPLC} and their C content (Fig. 3). The intercept of near zero suggests that any constant background was absent, while the slope (0.22 μg C ml^{-1}) of the linear regression represented the amount of C_{HPLC} eluting per ml eluent. Therefore, multiplying this value by the volume collected for a specific sample should give a preliminary estimate of C_{HPLC} for an individual sample, enabling calculation of F_{HPLC} for each sample. However, we discovered that this estimate was not accurate enough: calculated values of C_{HPLC} for individual samples ranged between 0.9 and 2.1 μg C, resulting in reasonable estimates for F_{HPLC} for some samples (Supplementary material), but also in non-natural values of $F_{HPLC} > 2$ for others. Interestingly, the averaged values for F_{HPLC} for each process standard were at the same level of a blank with a modern radiocarbon value ($F^{14}C \approx 1$).

It is also possible to determine the blank contribution (C_{HPLC}) and its radiocarbon signature (F_{HPLC}) indirectly. For this approach, C_{ex} needs to be assumed as a constant amount of carbon being added to each sample during sample preparation. It is based on the theoretical assumption that the F_{ex} would be composed of two pools characterized by opposite ^{14}C content (i.e. modern and ^{14}C-free). The combination of the results from two standards with that with opposite ^{14}C content then allows a mathematical solution for both unknowns, here C_{HPLC} and F_{HPLC}. It is a common approach to determine a theoretical contribution from modern C_{ex} ($F^{14}C = 1$) by use of a radiocarbon-dead ($F^{14}C = 0$) process standard and vice versa (Shah and Pearson, 2007; Ziolkowski and Druffel, 2009a; Lang et al., 2013). For this, Eq. 1 was re-arranged and modified:

$$C_{HPLC} = (F_{T'} \cdot C_{T'} - F_S \cdot C_S) / (F_{HPLC} - F_S) \quad (2)$$

Accordingly, a C_{HPLC} value for each replicate of fossil char was calculated assuming $F_{HPLC} = 1$ and similarly for the modern char, assuming $F_{HPLC} = 0$ (Table 3). To solve the equation the reference values from the bulk powder were used as F_S. The average modern C_{HPLC} based on the individual B5CAs and B6CAs from the fossil charcoal, was 1.4 ± 0.5 μg C (n = 5; Table 3). In contrast, the BPCAs isolated from the modern char sample were hardly affected (Fig. 3), resulting in an average contribution of ^{14}C-free C_{HPLC} of 0.2 ± 0.4 μg C.

While the subdivision of the amount of blank C into two pools is a convenient mathematical concept, in nature it is more likely that there is a single C pool with a distinct ^{14}C signature displaying a mean value of all various compounds. In order to determine more realistic values, C_{ex} and F_{ex} can be combined by addition of the two theoretical C_{ex} values and by calculating the weighted average of the two F_{ex} values:

$$F_{ex} = (F_{modern} \cdot C_{modern} + F_{dead} \cdot C_{dead}) / (C_{modern} + C_{dead}) \quad (3)$$

While the subscript *ex* can be substituted with the subscript describing the respective part of the sample preparation. Here, it resulted in C_{HPLC} = 1.6 ± 0.7 µg C with an average radiocarbon content F_{HPLC} of 0.90 ± 0.50 $F^{14}C$. This amount was satisfyingly low for samples with > 15 µg C. Consequently, a fossil source for C_{HPLC} can be excluded; nevertheless, it is hardly possible to directly identify the origin of C_{HPLC}. A significant change of F_{HPLC} during later measurements is though a clear indication for additional contribution of C_{HPLC}, in general.

Fig. 3 illustrates the size-dependent relationship of the radiocarbon content of the samples not corrected for C_{HPLC} vs. the theoretically modeled F_{HPLC} deduced from the mixture of a C_S with varying sample size and the constant C_{HPLC}. Note that the given data set does not show a significant dependence between the amounts of repeated injections (i.e. the amount of collected mobile phase) and C_{HPLC}. However, the opposite was concluded after direct analysis of C_{HPLC} (Fig. 3). This apparent contradiction can be attributed to the fact that the process samples were only collected over 20 to 30 injections, with a total of 4-12 ml (but mostly 6-8 ml), as opposed to the volume range of 8 up to 40 ml collected for the C_{HPLC} tests. In short, this volume range was too small for detection of a significant size dependence of C_{HPLC}. The correct radiocarbon content (F_S) values from the individual samples are listed in Table 3. There was no evidence for a significant difference in the $F^{14}C$ values between the B5CAs and B6CAs. Hence, replicate analyses of B5CAs and B6CAs from the same process standard were taken as equal. The 5 replicates of the modern charcoal sample give a mean $F^{14}C$ value of 1.142, with a standard deviation of 0.025, i.e. a precision of 2.2%. This value mirrors both the $F^{14}C$ of the digest (ETH-49860.1.1) and the reference analysis of the bulk material (ETH-50458). The individual samples exhibited values with a slightly greater uncertainty that in turn depended on the sample size and lower counting statistics. The largest sample containing 27 µg C had a precision of 2.9% and the smallest (16 µg C) a precision of 4.5%. Likewise, the F_S for the largest sample (ETH-49868.1.1) was also the one closest to the reference value. The same was true for the fossil charcoal standard being depleted in ^{14}C, even if no size dependent increase in precision is given for these duplicate values. The average F_S from 5 individual measurements was 0.001 ± 0.032. Samples with < 15 µg C were not analyzed, as demonstrated by Birkholz et al. (2013) that samples designated for CSRA and < 10 µg C are usually affected by C_{ex} to such an extent that no reliable results can be obtained. However, the data here demonstrate that sample amounts of 25 to 35 µg C are suitable for high precision analysis. Additional replicate analyses are still recommended so that possible outliers can be easily identified. In summary, the given uncertainty in an individual measurement is satisfactory for C turnover studies or C source apportion. For precise dating purposes a higher precision is usually required. Indeed, there is room for further minimization of C_{ex}, especially during the HPLC isolation procedure. Comparing the background level of organic C in the ultra-pure water used (i.e. in the aqueous HPLC solvent) with published references indicates that the system used for this study could be improved with better maintenance. Lang et al. (2012) reported that not more than 0.04 µg

C/ml were detected in the aquatic mobile phase. In contrast, a concentration of up to 0.3 μg C/ml was measured for the eluents used here.

Conclusions

We present a method to purify individual BPCAs as compound-specific biomarkers for BC, followed by the determination of $\delta^{13}C$ and $F^{14}C$. The combination of two measurements on the same sample reduces the efforts specified by an isolation protocol for the particular analysis. Furthermore, knowing both the $\delta^{13}C$ and $F^{14}C$ values for a sample helps interpret the results with respect to the impact of contamination that might be difficult to detect, especially when they have a different $\delta^{13}C$ value from the sample of interest. Another benefit is the possibility of monitoring the development of the general C_{ex} background in an easy and cost effective way. C content and its $\delta^{13}C$ value should give enough information and help avoid expensive radiocarbon analysis of contaminated samples. Finally the wet oxidation method avoids the problems encountered in the combustion of H_3PO_4-rich sample residues.

A constant addition of extraneous C to the isolated samples was identified. Nevertheless, a size dependent component C_{ex} cannot be excluded. This is especially true for much larger samples (> 50 μg C) that need to be isolated with a greater extent of injections (e.g. 100-150 injections to yield ca. 100 μg BPCA C). Contamination of 1.6 ± 0.2 μg C, with $F^{14}C$ 0.90 ± 0.14, was calculated. We have shown that the precision of individual measurements of samples with > 15 μg C is adequate for studies aimed at determining C turnover or source apportioning in soils and sediments. In addition, our data show that there is potential for also applying the method for dating purposes. Samples isolated in replicates each containing > 25 μg C should give values precise enough for an age determination of, for example, combustion residues on pottery or other samples with very fine charcoal that cannot be analyzed directly or BC that is mixed with other OM. Based on the experience from study, we recommend that process standards and blanks are determined regularly, as it is possible that C concentration in chemicals and/or solvent changes through time.

The method can also be applied to other marker compounds (e.g. B4CA or B3CA), although it might require minor tuning of the HPLC method to obtain a clean chromatographic separation of the target compounds. Additional improvements could include the use of a HPLC column with more capacity to reduce the number of injections required for isolation of sufficient material. This might lead to less C_{ex}, although the flow rate would need to be increased.

Acknowledgements

We would like to thank two anonymous reviewers for their constructive comments. Funding support from Swiss National Science Foundation (SNF) project Nr 200021-119950 / 200020-13484 and Nr 200020-131922, and also University of Zurich Forschungskredit Nr 57061004 Fellowship is gratefully acknowledged. We thank M. Hilf, C. McIntyre and L. Wacker for assistance with HPLC and AMS measurements. T. Eglinton generously donated funding for the AMS measurements. We also thank P. Ascough and M. Bird for donating the archaeological charcoal.

Associate Editor – M.J. Simpson

Table 1. Isolation of B5CA and B6CA from two process standards with HPLC, recovered mass as analyzed with HPLC and GC-IRMS and corresponding $\delta^{13}C$ values.

Sample	Compound	HPLC Injection	HPLC µg C[a]	HPLC Recovery	GC-IRMS µg C[b]	GC-IRMS $\delta^{13}C$ (‰)	Yarnes et al., 2011 $\delta^{13}C$ (‰)[c]
Fossil char	Digest				43.4	-23.8 ± 0.1	
	B6CA	20×5µl	22.3	76%	29.3	-25.5 ± 0.3	
	B6CA	30×5µl	35.2	80%	39.7	-24.5 ± 0.1	
	Avg. B6CA					-25.0 ± 0.7	
	B5CA	20×5µl	16.3	55%	17.2	-26.9 ± 0.3	
	B5CA	25×5µl	20.4	55%	21.7	-26.4 ± 0.3	
	B5CA	30×5µl	21.8	49%	22.9	-26.8 ± 0.2	
	Avg. B5CA					-26.7 ± 0.4	
Modern	Digest				17.7	-26.9 ± 0.2	-27.4[d]
	B6CA	20×5µl	19.9	74%	23.3	-27.9 ± 0.3	
	B6CA	25×5µl	28.6	84%	32.5	-28.1 ± 0.1	
	B6CA	25×5µl	25.9	76%	31.1	-27.1 ± 0.3	
	Avg. B6CA					-27.7 ± 0.5	-28.24 ± 0.36
	B5CA	20×5µl	19.7	50%	25.8	-28.4 ± 0.3	
	B5CA	25×5µl	30.6	62%	29.5	-27.7 ± 0.1	
	B5CA	25×5µl	25.3	52%	28.1	-29.0 ± 0.3	
	Avg. B5CA					-28.4 ± 0.6	-28.71 ± 0.36

[a] Determined by comparing sample peak areas with those from a dilution series of BPCA standards with known concentration;

[b] determined on amount of CO_2 generated during oxidation in the headspace of the vials, by comparing peak areas with those of a series of standards of known concentration;

[c] determined with ion chromatography IRMS;

[d] bulk sample analyzed with EA-IRMS.

Table 2. Direct assessment of C_{HPLC} (n.a.: not analyzed).

Sample	HPLC Collected ml	GC-IRMS µg C[a]	GC-IRMS µg /ml	GC-IRMS $\delta^{13}C$ (‰)
$C_{chem.+HPLC}$[b]	20		0.23 ± 0.12	n.a.
C_{HPLC}	40	9.7	0.24	-28.6 ± 0.1
C_{HPLC}	40	8.7	0.22	-28.5 ± 0.1
C_{HPLC}	8	2.2	0.28	n.a.
C_{HPLC}	30	5.2	0.17	-29.8 ± 0.1
C_{HPLC}	30	5.8	0.19	-31.4 ± 0.1
Avg. C_{HPLC}			0.22 ± 0.04	-29.5 ± 1.3

[a] Determined on amount of CO_2 generated during oxidation in the headspace of the vials, by comparing peak areas with those of a series of standards of known concentration;

[b] n = 2.

Table 3. Amount and radiocarbon content of isolated process standards B5CA and B6CA, calculated amount of external C (Cex) added to the related sample and residual $F^{14}C$ values after correction for the blank (FS).

Sample		$F_{T'}$ ($F^{14}C$) [a]	$C_{T'}$ (µg C)	*Calculated* C_{ex} (µg C)	*Corrected values* F_S ($F^{14}C$)[b]	Lab code
Fossil char	Bulk[c]				0.003 ± 0.001	ETH-50456
	Digest				0.010 ± 0.002	ETH-49849
	B6CA	0.094 ± 0.004	23.1 ± 0.5	2.1 ± 0.1	0.036 ± 0.025	ETH-50461
	B6CA	0.040 ± 0.003	29.0 ± 0.5	1.1 ± 0.1	-0.009 ± 0.019	ETH-49854
	B5CA	0.079 ± 0.006	13.0 ± 0.5	1.0 ± 0.1	-0.033 ± 0.045	ETH-50459
	B5CA	0.068 ± 0.005	16.0 ± 0.5	1.0 ± 0.1	-0.022 ± 0.036	ETH-50460
	B5CA	0.127 ± 0.007	14.5 ± 0.5	1.8 ± 0.1	0.034 ± 0.040	ETH-49859
Modern extraneous C ($F^{14}C$ = 1) addition:				1.4 ± 0.5	Avg. C_{ex}	
Modern char	Bulk[c]				1.142 ± 0.004	ETH-50458
	Digest				1.143 ± 0.020	ETH-49860
	B6CA	1.151 ± 0.025	16.2 ± 0.5	-0.1 ± 0.5	1.162 ± 0.074	ETH-50462
	B6CA	1.093 ± 0.021	18.5 ± 0.5	0.8 ± 0.5	1.102 ± 0.056	ETH-49864
	B6CA	1.124 ± 0.020	20.9 ± 0.5	0.3 ± 0.5	1.132 ± 0.056	ETH-50463
	B5CA	1.145 ± 0.019	27.6 ± 0.5	-0.1 ± 0.6	1.152 ± 0.034	ETH-49868
	B5CA	1.150 ± 0.024	16.8 ± 0.5	-0.1 ± 0.5	1.161 ± 0.071	ETH-50465
Radiocarbon dead extraneous C ($F^{14}C$ = 1)				0.2 ± 0.4	Avg. C_{ex}	

[a] Subscript *T'* indicates that values were corrected for instrumental background using the BATS program (Wacker, 2010) and for the wet oxidation procedure (Lang et al., 2013);

[b] subscript *S* indicated that values were corrected for mean modern or radiocarbon dead extraneous carbon addition occurring during the entire laboratory protocol. Please note that the fractions of 'bulk' and 'extract' required less corrections than those isolated by HPLC.

[c] ^{14}C values from bulk sample material were corrected for instrumental background using BATS software.

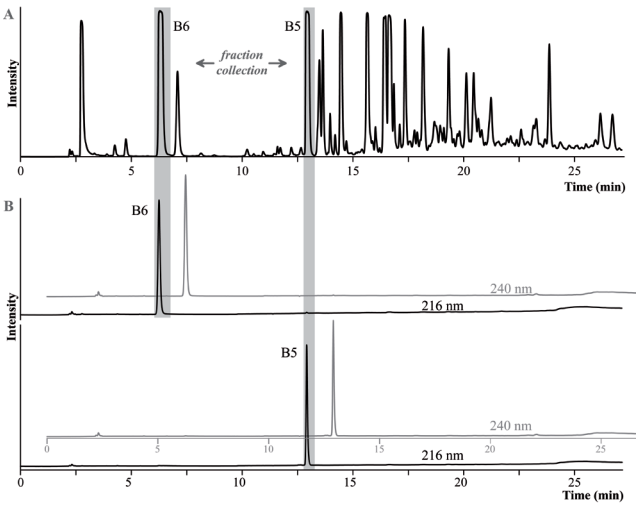

Figure 1. HPLC-DAD chromatogram from a 5 µl injection of a BPCA extract of modern char for fraction collection (A), and HPLC-DAD chromatograms of aliquots of purified B6CA and B5CA fractions detected at 216 and 240nm (B). Time windows for single peak collection of B6CA (B6) and B5CA (B5) are highlighted in the gray boxes.

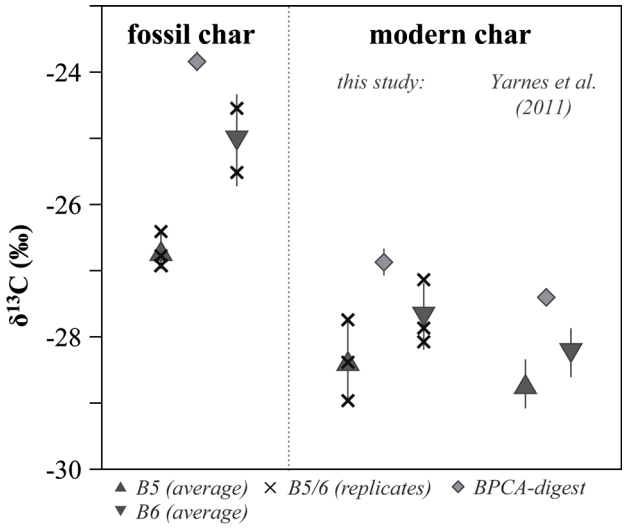

Figure 2. $\delta^{13}C$ values of individual B5CA and B6CA and of the whole BPCA digest of fossil (left) and modern char (right) measured in this study, and as published by Yarnes et al. (2011) for the modern char.

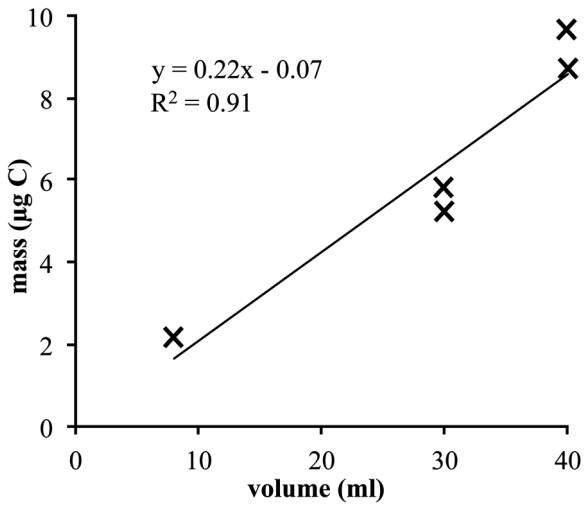

Figure 3. Mass of HPLC blank vs. volume of collected eluent.

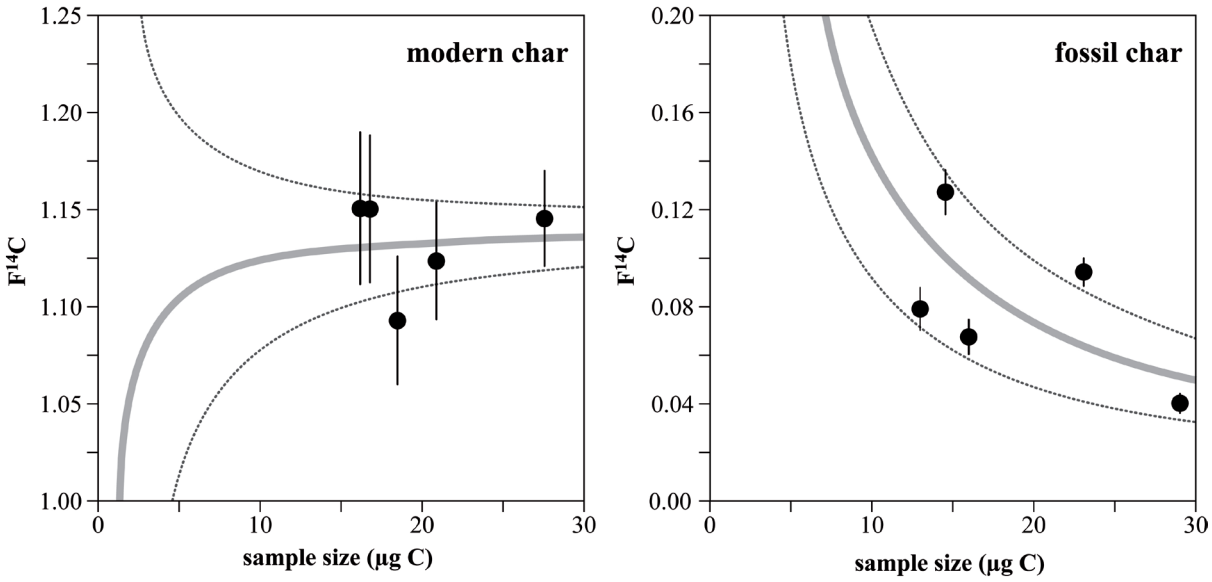

Figure 4. Radiocarbon values for B5CA and B6CA isolated from the modern (left) and fossil char (right). The given error is composed of corrections for instrumental AMS background and the blank for wet oxidation. The solid gray line represents an idealized line for the mixture of the real $F^{14}C$ value of sample and the determined mean external contamination.

References

Alloway, B.V., Pribadi, A., Westgate, J.A., Bird, M., Fifield, L.K., Hogg, A., Smith, I., 2004. Correspondence between glass-FT and ^{14}C ages of silicic pyroclastic flow deposits sourced from Maninjau caldera, west-central Sumatra. Earth and Planetary Science Letters 227, 121–133.

Ascough, P.L., Bird, M.I., Brock, F., Higham, T.F.G., Meredith, W., Snape, C.E., Vane, C.H., 2009. Hydropyrolysis as a new tool for radiocarbon pre-treatment and the quantification of black carbon. Quaternary Geochronology 4, 140–147.

Bird, M.I., Ayliffe, L.K., Fifield, L.K., Turney, C.S.M., Cresswell, R.G., Barows, T.T., David, B., 1999. Radiocarbon dating of "old" charcoal using a wet oxidation, stepped-combustion procedure. Radiocarbon 41, 127–140.

Birkholz, A., Smittenberg, R.H., Hajdas, I., Wacker, L., Bernasconi, S.M., 2013. Isolation and compound specific radiocarbon dating of terrigenous branched glycerol dialkyl glycerol tetraethers (brGDGTs). Organic Geochemistry 60, 9-19.

Carcaillet, C., Almquist, H., Asnong, H., Bradshaw, R.H.W., Carrión, J.S., Gaillard, M.-J., Gajewski, K., Haas, J.N., Haberle, S.G., Hadorn, P., Müller, S.D., Richard, P.J.H., Richoz, I., Rösch, M., Sánchez Goñi, M.F.S., Von Stedingk, H., Stevenson, A.C., Talon, B., Tardy, C., Tinner, W., Tryterud, E., Wick, L., Willis, K.J., 2002. Holocene biomass burning and global dynamics of the carbon cycle. Chemosphere 49, 845–863.

Dittmar, T., 2008. The molecular level determination of black carbon in marine dissolved organic matter. Organic Geochemistry 39, 396–407.

Eglinton, T.I., Aluwihare, L.I., Bauer, J.E., Druffel, E.R.M., McNichol, A.P., 1996. Gas chromatographic isolation of individual compounds from complex matrices for radiocarbon dating. Analytical Chemistry 68, 904–912.

Glaser, B., Balashov, E., Haumaier, L., Guggenberger, G., Zech, W., 2000. Black carbon in density fractions of anthropogenic soils of the Brazilian Amazon region. Organic Geochemistry 31, 669–678.

Glaser, B., Haumaier, L., Guggenberger, G., Zech, W., 1998. Black carbon in soils: the use of benzenecarboxylic acids as specifc markers. Organic Geochemistry 29, 811–819.

Goldberg, E.D., 1985. Black Carbon in the Environment. Properties and Distribution. Wiley, Chichester, UK.

Hajdas, I., Bonani, G., Thut, H., Leone, G., Pfenninger, R., Maden, C., 2004. A report on sample preparation at the ETH/PSI AMS facility in Zurich. Nuclear Instruments & Methods in Physics Research Section B-Beam Interactions with Materials and Atoms 223-224, 267–271.

Hammes, K., Smernik, R.J., Skjemstad, J.O., Herzog, A., Vogt, U.F., Schmidt, M.W.I., 2006. Synthesis and characterisation of laboratory-charred grass straw (*Oryza sativa*) and chestnut wood (*Castanea sativa*) as reference materials for black carbon quantification. Organic Geochemistry 37, 1629–1633.

Hedges, J.I., Eglinton, G., Hatcher, P.G., Kirchman, D.L., Arnosti, C., Derenne, S., Evershed, R.P., Kögel-Knabner, I., de Leeuw, J.W., Littke, R., Michaelis, W., Rullkötter, J., 2000. The molecularly-uncharacterized component of nonliving organic matter in natural environments. Organic Geochemistry 31, 945–958.

Knicker, H., Hilscher, A., González-Vila, F.J., Almendros, G., 2008. A new conceptual model for the structural properties of char produced during vegetation fires. Organic Geochemistry 39, 935–939.

Lang, S.Q., Bernasconi, S.M., Früh-Green, G.L., 2012. Stable isotope analysis of organic carbon in small (μg C) samples and dissolved organic matter using a GasBench preparation device. Rapid Communications in Mass Spectrometry 26, 9–16.

Lang, S.Q., Früh-Green, G.L., Bernasconi, S.M., Wacker, L., 2013. Isotopic ($\delta^{13}C$, $\Delta^{14}C$) analysis of organic acids in marine samples using wet chemical oxidation. Limnology and Oceanography: Methods 11, 161–175.

Masiello, C.A., 2004. New directions in black carbon organic geochemistry. Marine Chemistry 92, 201–213.

Pearson, A., McNichol, A.P., Schneider, R.J., von Reden, K.F., 1998. Microscale AMS ^{14}C measurement at NOSAMS. Radiocarbon 40, 61–75.

Preston, C.M., Schmidt, M.W.I., 2006. Black (pyrogenic) carbon: a synthesis of current knowledge and uncertainties with special consideration of boreal regions. Biogeosciences 3, 397–420.

Reimer, P.J., Brown, T.A., Reimer, R.W., 2004. Discussion: Reporting and calibration of post-bomb ^{14}C data. Radiocarbon 46, 1299–1304.

Ruff, M., Wacker, L., Gäggeler, H.W., Suter, M., Synal, H.A., Szidat, S., 2007. A gas ion source for radiocarbon measurements at 200 kV. Radiocarbon 49, 307–314.

Schmidt, M.W.I., Noack, A.G., 2000. Black carbon in soils and sediments: Analysis, distribution, implications, and current challenges. Global Biogeochemical Cycles 14, 777–793.

Schneider, M.P.W., Smittenberg, R.H., Dittmar, T., Schmidt, M.W.I., 2011. Comparison of gas with liquid chromatography for the determination of benzenepolycarboxylic acids as molecular tracers of black carbon. Organic Geochemistry 42, 275–282.

Shah, S.R., Pearson, A., 2007. Ultra-microscale (5–25 μg C) analysis of individual lipids by ^{14}C AMS: Assessment and correction for sample processing blanks. Radiocarbon 49, 69–82.

Skjemstad, J.O., Clarke, P., Taylor, J.A., Oades, J.M., McClure, S.G., 1996. The chemistry and nature of protected carbon in soil. Australian Journal of Soil Research 34, 251–271.

Skjemstad, J.O., Dalal, R.C., Janik, L.J., McGowan, J.A., 2001. Changes in chemical nature of soil organic carbon in Vertisols under wheat in south-eastern Queensland. Australian Journal of Soil Research 39, 343–359.

Skjemstad, J.O., Spouncer, L.R., Cowie, B., Swift, R.S., 2004. Calibration of the Rothamsted organic carbon turnover model (RothC ver. 26.3), using measurable soil organic carbon pools. Australian Journal of Soil Research 42, 79–88.

Stuiver, M., Polach, H.A., 1977. Discussion: Reporting of ^{14}C data. Radiocarbon 19, 355–363.

Synal, H.A., Stocker, M., Suter, M., 2007. MICADAS: A new compact radiocarbon AMS system. Nuclear Instruments & Methods in Physics Research Section B: Beam Interactions with Materials and Atoms 259, 7–13.

Tinner, W., Conedera, M., Ammann, B., Lotter, A.F., 2005. Fire ecology north and south of the Alps since the last ice age. The Holocene 15, 1214–1226.

Wacker, L., Christl, M., Synal, H.A., 2010. Bats: A new tool for AMS data reduction. Nuclear Instruments Methods in Physics Research Section B: Beam Interactions with Materials and Atoms 268, 976–979.

Wacker, L., Fahrni, S.M., Hajdas, I., Molnar, M., Synal, H.-A., Szidat, S., Zhang, Y.L., 2013. A versatile gas interface for routine radiocarbon analysis with a gas ion source. Nuclear Instruments and Methods in Physics Research Section B: Beam Interactions with Materials and Atoms 294, 315–319.

Wacker, L., Lippold, J., Molnár, M., Schulz, H., 2013. Towards radiocarbon dating of single foraminifera with a gas ion source. Nuclear Instruments and Methods in Physics Research Section B: Beam Interactions with Materials and Atoms 294, 307–310.

Wiedemeier, D.B., Hilf, M.D., Smittenberg, R.H., Haberle, S.G., Schmidt, M.W.I., 2013. Improved assessment of pyrogenic carbon quantity and quality in environmental samples by high-performance liquid chromatography. Journal of Chromatography A 1304, 246–250.

Yarnes, C., Santos, F., Singh, N., Abiven, S., Schmidt, M.W.I., Bird, J.A., 2011. Stable isotopic analysis of pyrogenic organic matter in soils by liquid chromatography-isotope-ratio mass spectrometry of benzene polycarboxylic acids. Rapid Communications in Mass Spectrometry 25, 3723–3731.

Zencak, Z., Reddy, C.M., Teuten, E.L., Xu, L., McNichol, A.P., Gustafsson, Ö., 2007. Evaluation of gas chromatographic isotope fractionation and process contamination by carbon in compound-specific radiocarbon analysis. Analytical Chemistry 79, 2042–2049.

Zimmerman, A.R., 2010. Abiotic and microbial oxidation of laboratory-produced black carbon (biochar). Environmental Science & Technology 44, 1295–1301.

Ziolkowski, L.A., Druffel, E.R.M., 2009a. Quantification of extraneous carbon during compound specific radiocarbon analysis of black carbon. Analytical Chemistry 81, 10156–10161.

Ziolkowski, L.A., Druffel, E.R.M., 2009b. The feasibility of isolation and detection of fullerenes and carbon nanotubes using the benzene polycarboxylic acid method. Marine Pollution Bulletin 59, 213–218.

Supplementary Material

Table A 1: Amounts and radiocarbon contents of the isolated process standards of the wet oxidation – phthalic acid and sucrose with the corresponding calculated amount of external C (C_{ex}) added to the standard, and the residual $F^{14}C$ values after correction for the blank (F_S).

Standard	*BATS output*		*Calculated*	*Corrected values*	**Lab code**
	F_T ($F^{14}C$) [a]	C_T (µg C)	C_{ex} (µg C)	F_S ($F^{14}C$)	
1st campaign					
Phthalic acid [b]	0.0140 ± 0.002	12.4 ± 0.5	0.14 ± 0.03	0.004 ± 0.004	ETH-49846.11.1
	0.0165 ± 0.003	13.4 ± 0.5	0.19 ± 0.04	0.007 ± 0.004	ETH-49846.12.1
	0.0078 ± 0.002	15.3 ± 0.5	0.08 ± 0.03	-0.001 ± 0.003	ETH-49846.17.1
	0.0083 ± 0.002	17.8 ± 0.5	0.10 ± 0.04	0.001 ± 0.003	ETH-49846.7.1
	0.0084 ± 0.002	21.0 ± 0.5	0.12 ± 0.03	0.002 ± 0.003	ETH-49846.13.1
Average addition of C_{ex} with $F^{14}C$ = 1:			**0.13 ± 0.04**		
Sucrose [c]	1.018 ± 0.012	17.4 ± 0.5	0.58 ± 0.88	1.070 ± 0.050	ETH-49845.2.1
	1.004 ± 0.011	21.5 ± 0.5	1.01 ± 0.95	1.045 ± 0.040	ETH-49845.1.1
	1.012 ± 0.012	21.7 ± 0.5	0.85 ± 0.96	1.053 ± 0.040	ETH-49845.3.1
	1.004 ± 0.012	23.4 ± 0.5	1.09 ± 1.00	1.042 ± 0.037	ETH-49845.4.1
	1.026 ± 0.012	27.3 ± 0.5	0.70 ± 1.09	1.059 ± 0.033	ETH-49845.12.1
Average addition of C_{ex} with $F^{14}C$ = 0:			**0.85 ± 0.44**		
2nd campaign					
Phthalic acid	0.0243 ± 0.007	3.7 ± 0.5	0.08 ± 0.03	0.005 ± 0.012	ETH-49846.23.1
	0.0049 ± 0.003	9.1 ± 0.5	0.02 ± 0.03	-0.003 ± 0.005	ETH-49846.31.1
	0.0080 ± 0.003	11.5 ± 0.5	0.06 ± 0.04	0.002 ± 0.004	ETH-49846.25.1
	0.0086 ± 0.003	13.8 ± 0.5	0.08 ± 0.04	0.003 ± 0.004	ETH-49846.26.1
	0.0080 ± 0.003	20.0 ± 0.5	0.11 ± 0.07	0.004 ± 0.004	ETH-49846.30.1
Average addition of C_{ex} with $F^{14}C$ = 1:			**0.07 ± 0.03**		
Sucrose	1.0016 ± 0.012	11.6 ± 0.5	0.57 ± 0.78	1.042 ± 0.066	ETH-49845.17.1
	1.0161 ± 0.013	12.4 ± 0.5	0.43 ± 0.79	1.054 ± 0.063	ETH-49845.18.1
	1.0359 ± 0.011	17.9 ± 0.5	0.29 ± 0.89	1.062 ± 0.044	ETH-49845.22.1
	1.0315 ± 0.010	24.0 ± 0.5	0.49 ± 1.00	1.051 ± 0.033	ETH-49845.20.1
Average addition of C_{ex} with $F^{14}C$ = 0:			**0.45 ± 0.43**		

[a] Subscript *T* indicates that values have been corrected for instrumental background using the program BATS (Wacker, 2010) and for the wet oxidation procedure (Lang et al., 2013), if required.

[b] The radiocarbon content of 1.053 ± 0.03 $F^{14}C$ was determined on the powdered phthalic acid standard by conventional AMS methods.

[c] The radiocarbon content of ≤ 0.0025 $F^{14}C$ was determined on the powdered sucrose standard by conventional AMS methods.

Table B 1: Amounts and radiocarbon contents of isolated process standards B5CA and B6CA, the volume of collected eluent of each sample and the calculated amount of external C (C_{ex}) and its radiocarbon content (F_{ex}), assuming that a C_{ex} of 0.22 ± 0.04 μg ml^{-1} elutes with the mobile phase.

Sample		F_T ($F^{14}C$) [a]	C_T (μg C)	*Collected* V_{el} (ml)	*Calculated* C_{ex} (μg C)	F_{ex} ($F^{14}C$)	Lab code
Fossil char	B6CA	0.094 ± 0.004	23.1 ± 0.2	4	0.9	2.4	ETH-50461.1.1
	B6CA	0.040 ± 0.003	29.0 ± 0.3	9	2.0	0.5	ETH-49854.1.1
	B5CA	0.079 ± 0.006	13.0 ± 0.2	4	0.9	1.1	ETH-50459.1.1
	B5CA	0.068 ± 0.005	16.0 ± 0.2	5	1.1	0.9	ETH-50460.1.1
	B5CA	0.127 ± 0.007	14.5 ± 0.3	12	2.6	0.7	ETH-49859.1.1
					Average F_{ex}	**1.1**	
Modern char	B6CA	1.151 ± 0.025	16.2 ± 0.2	6	1.3	1.2	ETH-50462.1.1
	B6CA	1.093 ± 0.021	18.5 ± 0.2	8	1.8	1.6	ETH-49864.1.1
	B6CA	1.124 ± 0.020	20.9 ± 0.2	8	1.8	0.8	ETH-50463.1.1
	B5CA	1.183 ± 0.023	22.0 ± 0.3	5	1.1	0.2	ETH-50464.1.1
	B5CA	1.145 ± 0.019	27.6 ± 0.3	5	1.1	1.1	ETH-49868.1.1
	B5CA	1.150 ± 0.024	16.8 ± 0.2	6	1.3	1.2	ETH-50465.1.1
					Average F_{ex}	**1.0**	

[a] Subscript *T* indicates that values have been corrected for instrumental background using the program BATS (Wacker, 2010) and for the wet oxidation procedure (Lang et al., 2013).

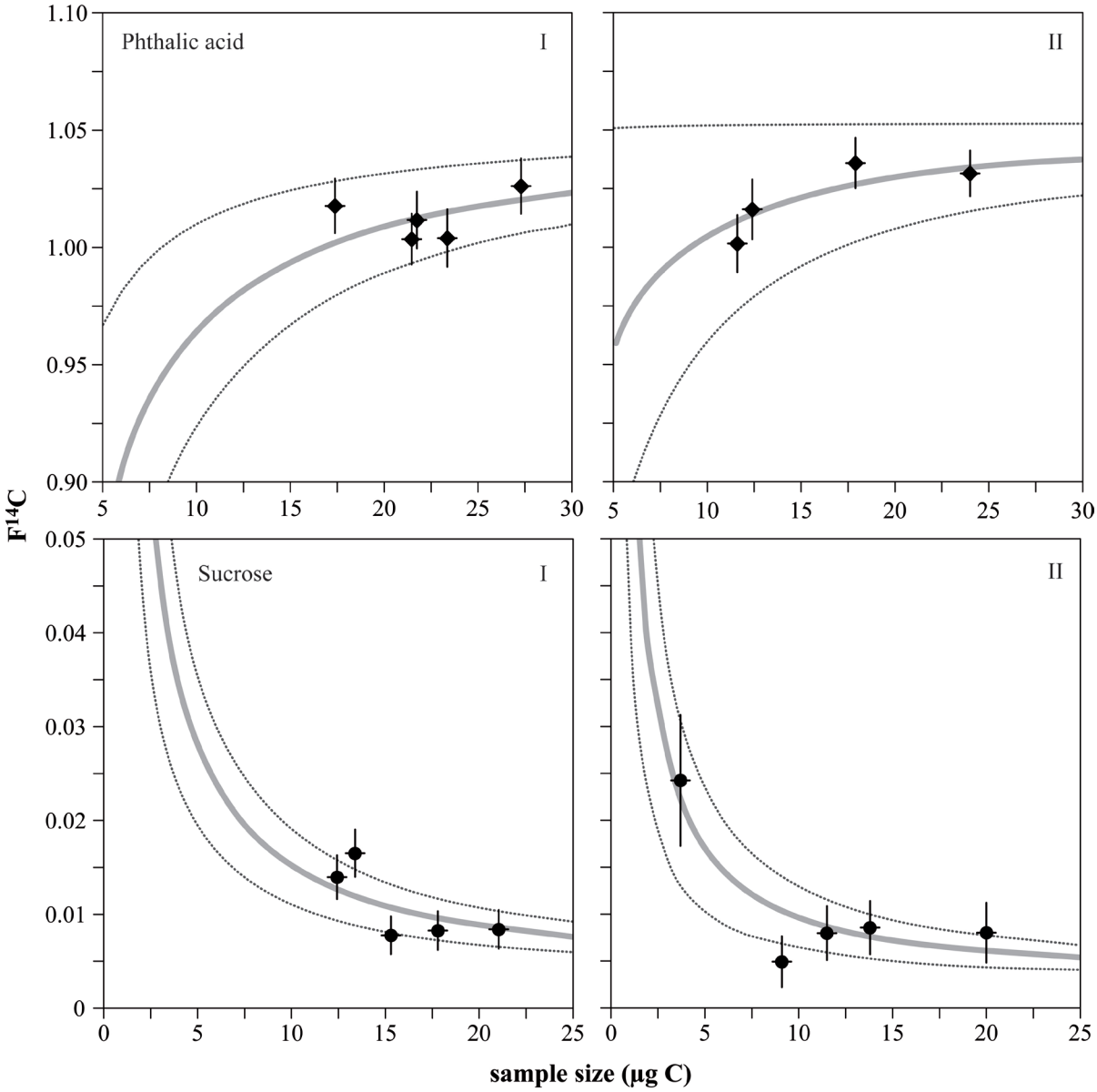

Figure A 1: Radiocarbon values of phthalic acid (above) and sucrose (below) after the wet oxidation procedure of both campaigns (I left, and II right). The given error bars derive only from corrections of instrumental AMS background and counting statistics. The solid grey line represents an idealized line of the mixture of the $F^{14}C$ value of the process standard and the mean external contamination of modern ($F^{14}C$ = 1, Phthalic acid) or radiocarbon dead ($F^{14}C$ = 0, Sucrose) carbon.

Paper IV

Aromaticity and degree of aromatic condensation of char

Submitted as:

Wiedemeier, D.B., Abiven, S., Hockaday, W.C., Keiluweit, M., Kleber, M., Pyle, L.A., Masiello, C.A., McBeath, A.V., Nico, P.S., Schneider, M.P.W., Smernik, R.J., Wiesenberg, G.L.B., Schmidt, M.W.I., 2014. Aromaticity and aromatic condensation of chars. Organic Geochemistry (in review).

Author contributions:

D.B.W. compiled and analyzed the data, and wrote the paper. M.W.I.S. conceived and coordinated the comparative study. Samples were provided by M.P.W.S., M.Ke. and M.Kl. Analysis was performed by S.A. (MIR), A.V.M., R.J.S. and W.C.H (NMR), M.Ke. and P.S.N. (NEXAFS), L.A.P. and C.A.M. (pycnometry), M.P.W.S. and A.V.M. (BPCA), G.L.B.W. (lipid analysis). All authors provided input into the drafting and the final version of the manuscript.

Abstract

The aromatic carbon structure is a defining property of chars and is often expressed with the help of two concepts: (i) aromaticity and (ii) degree of aromatic condensation. The varying extent of these two features is assumed to largely determine the relatively high persistence of charred material in the environment and is thus of interest for e.g. biochar characterizations or carbon cycle studies. Consequently, a variety of methods has been used to assess the aromatic structure of chars, which has led to interesting insights but has complicated the comparison of data acquired with different methods. We therefore used a suite of seven methods (EA, MIR spectroscopy, NEXAFS spectroscopy, ^{13}C NMR spectroscopy, BPCA analysis, lipid analyses and helium pycnometry) and compared 13 measurements from them using a diverse sample set of 38 chars. Our results demonstrate that most of the measurements could be categorized either into those which assess aromaticity or those which assess the degree of aromatic condensation. A variety of measurements, including inexpensive and simple ones, reproducibly captured the two aromatic features in question, and data from different methods could therefore be compared. Moreover, general patterns between the two aromatic features and the pyrolysis conditions were revealed, supporting reconstruction of the highest heat treatment temperature (HTT) of chars.

Introduction

Natural and anthropogenic chars have recently received much attention (Knicker, 2011; Glaser and Birk, 2012; Manyà 2012). Their role as important environmental constituents is increasingly being recognized; chars persist in soils and sediments, which has important implications for the global C budget (Schmidt and Noack, 2000) and they can exert beneficial properties on soils, improving fertility (Biederman and Harpole, 2013) and immobilizing hazardous compounds (Beesley et al., 2011). Moreover, anthropogenic chars (biochars) involve additional economic advantages; prudent biochar production can provide green energy, providing an interesting alternative to management of organic wastes (Meyer et al., 2011).

With increasing interest in the use of charred material, there is a growing need to characterize and classify the material accurately in order to improve understanding of its properties and behavior in the environment. A defining property of chars and of pyrogenic organic matter in general (Preston and Schmidt, 2006) is their aromatic C structure (Lehmann and Joseph, 2009), which is believed to consist of at least two different aromatic C phases: (i) an amorphous phase comprising randomly organized aromatic rings and (ii) a crystalline phase, comprising condensed polyaromatic sheets that are turbostratically aligned (Franklin, 1951; Cohen-Ofri et al., 2006; Keiluweit et al., 2010). The concepts of aromaticity (the total proportion of aromatic C including both phases; McNaught and Wilkinson, 1997) and that of the degree of aromatic condensation (the proportion of the condensed aromatic C only; McBeath et al., 2011) relate to this two phase model. The varying extent of the two phases is believed to largely determine the charred materials' stability against degradation in the environment (Lehmann et al., 2009; Singh et al., 2012). Consequently, aromaticity and the degree of aromatic condensation of a char likely influence its sequestration potential as well as the duration during which it can provide benefits to the soil (Nguyen et al., 2010).

The two features are themselves influenced by the feedstock, and the pyrolysis conditions. The type of feedstock contributes to the aromaticity and the degree of aromatic condensation by providing different chemical structures as starting material. For example, a high amount of aromatic structures in a feedstock (e.g. lignin in wood) can promote the resulting char aromaticity (Antal and Grønli, 2003). Similarly, different precursor materials attain a high degree of aromatic condensation at different temperatures (Setton et al., 2002). The pyrolysis conditions, in particular the highest heat treatment temperature (HTT), but also residence time, O_2 availability and pressure, influence the C properties of the resulting char (Shafizadeh, 1982; Lua et al., 2004). Aromaticity has been reported to increase with HTT from 200 °C to ca. 500 °C, where maximum aromaticity values are reached. The degree of aromatic condensation showed, on the other hand, a more gradual increase with HTT from 400 °C, reaching maximum values at > 1000 °C (McBeath et al., 2011; Schneider et al., 2011).

Considering the importance of the aromatic C structure in char and its dependency on many influencing factors, it is not surprising that various attempts have been made to measure

these archetypal properties of char. A wide variety of chemical and physical methods has been used, including elemental analysis, solid state ^{13}C nuclear magnetic resonance (NMR) spectroscopy, infrared (IR) spectroscopy, pyrolysis-gas chromatography-mass spectrometry (Py-GC-MS), X-ray diffraction, near edge X-ray absorption fine-structure spectroscopy (NEXAFS), X-ray photoelectron spectroscopy and measurement of surface area, He based solid density and electrical resistivity (McBeath et al., 2011).

While the wealth of methods for aromatic structure characterization of char is fascinating, with the methods continuing to grow in number and quality, it has become increasingly difficult to compare data using different methods and to relate the findings from them. Matters are complicated by the fact that terms such as aromaticity can have multiple technique-specific meanings (McBeath et al., 2011). Moreover, from a practical point of view, researchers and practitioners may have limited resources and instrumentations and would like to optimize both insightful data acquisition and reasonable analysis cost. Efforts to compare different methods and their measurements and to put them in a common framework are therefore required, thereby guiding the interpretation of differently acquired data and suggesting suitable methods for specific analysis problems.

Here, we have used an extensive suite of seven different methods that provide 13 measurements (cf. Table 1) in a comparative study to evaluate their assessment of the aromatic structure in charred materials. A large sample set, consisting of 38 different char samples (cf. Table 2), was analyzed using each method. The objective was to show and discuss how the seven methods and their measurements capture the aromatic structures in the largely different chars and how they compare with each other. Moreover, we aimed to reveal the influence of feedstock, HTT and other pyrolysis parameters on aromaticity and degree of aromatic condensation, by statistically exploring the rich dataset from this large scale comparative study.

Material and methods

Char thermosequences

Four different feedstocks (chestnut wood, pine wood, fescue grass and rice grass) and two different pyrolysis procedures (A, 5 h residence time at HTT with continuous N_2 flow; B, 1 h residence time at HTT in a closed chamber) were used to create 38 char samples with HTT between 100 and 1000 °C, as reported in detail in two previous studies (Keiluweit et al., 2010; Schneider et al., 2011). The resulting char thermosequences (Wood-A, Grass-A, Wood-B, Grass-B) are displayed in Table 2.

Methods, measurements and derived indices

The char samples were measured using elemental analysis, mid-IR (MIR) spectroscopy, NEXAFS spectroscopy, ^{13}C NMR spectroscopy, benzene polycarboxylic acid (BPCA) analysis, lipid analysis and He pycnometry, as described in detail in the Supplementary data. Some of the methods provided more than one measurement (e.g. elemental analysis gives H/C and O/C ratios), as summarized in Table 1. Because the measurements are in widely different units and sometimes inversely proportional to each other, indices were built for comparison purposes that project the data on a common scale (0 – 1) and in the same direction (0, lowest aromaticity or lowest degree of aromatic condensation; 1, highest aromaticity or highest degree of aromatic condensation). Thus, each value x of a measurement M was transformed according to Eq. 1 to yield $M_{index_{[0-1]}}$. In the case of inversely proportional measurements, denoted [1 – 0], they were further transformed according to Eq. 2 to yield $M_{index_{[0-1]}}$. From here on, the methods and measurements are referred to by their indices (M_{index}), as listed in Table 1.

$$M_{index\ [0-1]\ or\ [\ 1-0]} = \frac{x_M - min_M}{max_M - min_M} \qquad \text{Eq. (1)}$$

$$M_{index_{[0-1]}} = 1 - M_{index_{[1-0]}} \qquad \text{Eq. (2)}$$

Data presentation and statistical analysis

The large set of original data can be found in the Supplementary data, while we focus here on the most important findings, showing only simplified data for reasons of clarity and understanding. All data analysis was conducted using the statistical software R (2011). The few missing values (ca. 5%) were imputed with the missForest algorithm (Stekhoven and Buehlmann, 2012) with an estimated normalized root mean square error of only 0.2%. Principal component analysis (PCA; Mardia et al., 1979) including biplots (Gabriel, 1971) was computed on the correlation matrix of the imputed dataset.

Results and discussion

All the methods provide measurements of physical or chemical variables linked either to aromaticity or degree of aromatic condensation, but the link between the variables and the derived aromatic features varies greatly. Measuring ring current with NMR (NMR-cond$_{index}$) is, for example, a more direct approach for assessing the degree of aromatic condensation than measuring skeletal density of char with He pycnometry (Pycno$_{index}$). However, the methods differ not only in how they provide assessment of aromatic structures but also in cost, availability and necessary expertise. Moreover, sample amount and composition can prevent the use of one method and/or promote the application of another. For these reasons, the aim was not to identify a reference method via inferential statistics or cost benefit analysis but rather to show method performance and explore qualitatively methods similarities and differences within the two categories of aromaticity and aromatic condensation. The standardized measurement results from each method (indices) are shown in full in Figs. 1 and 2 and mathematically summarized according to their resemblance in form of a PCA, in Fig. 3.

Aromaticity

Aromaticity in char is generally easier to assess than the degree of aromatic condensation (McBeath et al., 2011). Thus, more and more inexpensive methods are available for measuring aromaticity as opposed to measuring the degree of aromatic condensation (Figs. 1 and 3). In particular, the determination of elemental composition (O-C$_{index}$, H-C$_{index}$), the spectroscopic assessment of functional groups (MIR$_{index}$, NEXAFS-aroma$_{index}$, NMR-aroma$_{index}$) and the measurement of direct (BPCA$_{index}$) or indirect (TLE$_{index}$, ACL$_{index}$, PAH$_{index}$) molecular markers can yield insights into the proportion of aromatic C in chars (Table 1).

The O-C$_{index}$ and the H-C$_{index}$ are routine measurements for chars (Baldock and Smernik, 2002; Hammes et al., 2006) and an indirect measurement of their aromaticity because the proportion of C in a sample increases with HTT, as dehydration, depolymerization and volatilization take place, eventually leading to the formation of H and O depleted aromatic C structures (Keiluweit et al., 2010; Wang et al., 2013).

The O-C$_{index}$ of fresh chars depicts a characteristic trend for aromaticity measurements (Fig. 1), because it traces closely the median of all aromatic measurements and thereby shows a typical pattern for aromaticity in the samples: The proportion of aromatic rings in a sample is lowest for low temperature chars, then increases sharply between 200 and 500 °C and reaches a plateau > 600 °C. The O-C$_{index}$ also identifies low temperature wood char (e.g. Wood-B) to be more aromatic than the low-temperature grass char (e.g. Grass-B), which can be attributed to the higher lignin content of the wood feedstock (Rutherford et al., 2012). At high temperature, the wood char samples again acquire a higher C aromaticity than the grass char samples, which is probably due to higher ash content of the latter (Mukome et al., 2013).

Despite the fact that O content was assessed differently between the different thermosequences (actual measured O content for the A thermosequences vs. calculated by difference for the B thermosequences – cf. Supplementary data), similar results were obtained in both cases, indicating that the less expensive option of calculating O content by difference may be sufficient for assessing aromaticity in most freshly produced chars.

The H-C_{index} showed the lowest values for aromaticity in the lowest HTT range at 100 – 200 °C, as expected (Wang et al., 2013). Like the O-C_{index}, it also yields higher aromaticity for the lignin-rich wood char samples (Wood-B) than the lignin-poor grass char samples (Grass-B) at these low temperatures. A steep increase in aromaticity then followed from 200 – 500 °C HTT. However, highest values for H-C_{index} based aromaticity were only reached at the highest HTT (1000 °C), indicating that the H-C_{index} is not a pure measurement for aromaticity. In fact, the H-C_{index} is positioned at the edge of the aromaticity measurements in Fig. 3 (vector number 9), in relative adjacency to the aromatic condensation measurements. This also makes sense from a theoretical point of view, because H is lost during condensation of aromatic structures at high charring temperature, too (Franklin, 1951). Thus, the H-C_{index} probably indicates both an increasing amount of aromatic rings, up to ca. 500 °C HTT, and then the increasingly condensed nature of the aromatic rings, that continues to develop at higher charring temperature.

There was a slight lag in aromaticity of the Wood-B and Grass-B thermosequences vs. the Wood-A and Grass-A thermosequences with respect to HTT; the two thermosequences, which were charred for 5 h and with a N_2 flow (A) attain higher values of aromaticity at slightly lower HTT than the two thermosequences that were charred for only 1 h in closed chambers (B). This pattern was observed for most of the aromaticity measurements (cf. O-C_{index}, NMR-$aroma_{index}$, $BPCA_{index}$, TLE_{index}) and is independent of feedstock (grass vs. wood). Thus, it appears to be related to the pyrolysis method, indicating that the longer residence times of pyrolysis procedure A charred the samples more completely at the same HTT than the shorter residence times in procedure B. The slight difference in the pyrolysis procedures proved useful in this study because it allowed us to check if the various methods detect this feature.

The MIR_{index} distinguished low temperature chars from high-temperature chars with an increase in aromaticity between 300 and 500 °C, as was similarly observed by Harvey et al. (2012b). It can thus serve as a quick and inexpensive screening method for categorizing unknown char samples roughly according to their aromaticity and HTT. However, the MIR_{index} used here only qualifies as a rough estimate for aromaticity, given its large variability for chars > 400 °C, which can also be seen from the shorter length of vector 5 in Fig. 3. Moreover, the MIR_{index} seems to depend on the pyrolysis procedure in this mid- and high-temperature range, which was not reproduced by any of the other methods. The data show that MIR has the potential to measure aromaticity and possibly other HTT dependent variables, but clearly requires more research and fine tuning with respect to IR band selection and spectral data analysis.

The NEXAFS-aroma$_{index}$ has been similarly used to describe the B thermosequence chars elsewhere (Keiluweit et al., 2010) and was in the frame of the comparative study now also applied on part of the A thermosequence chars. In the case of the A thermosequence, the NEXAFS-aroma$_{index}$ increased slowly and steadily between 300 and 1000 °C. This is unlike most other aromaticity measurements that show a more pronounced increase in aromaticity over a shorter range of increasing HTT. The NEXAFS-aroma$_{index}$ also gave higher aromaticity values for the Grass-A chars than the Wood-A chars; this is in contrast to most other observations but in line with previous results from NEXAFS applications (Keiluweit et al., 2010). In the case of the B thermosequence, the NEXAFS-aroma$_{index}$ behaved unexpectedly in the low temperature range, indicating high aromaticity values for almost unaltered feedstock and showing decreasing aromaticity with increasing HTT.

Using NMR is a recently established means for assessing aromaticity of charred samples (McBeath et al., 2011). The NMR-aroma$_{index}$ determined the wood char samples in the low-temperature range (100 – 200 °C) as being more aromatic than the grass char samples, like the H-C$_{index}$ and O-C$_{index}$, and then also shows the typical increase in aromaticity between 200 and 500 °C, reaching a plateau from 600 °C for all feedstocks and pyrolysis methods, with very little variability. Since NMR measures directly the organic C bonds, it seems less sensitive to ash content, yielding equally high values for high temperature wood and grass chars. A small shift between the differently pyrolysed thermosequences (A vs. B) could also be observed where aromaticity increased, further corroborating the idea that the two pyrolysis procedures produced slightly different chars in the mid-temperature range.

The BPCA method separates and quantifies aromatic moieties that originate from condensed aromatic structures, which is why it is insensitive to lignin. Thus, the BPCA-aroma$_{index}$ scored very low for both wood and grass chars in the range up to 200 °C. It then increased steadily with HTT up to 500 °C, where maximum values were reached, and decreased slightly from 700 °C onwards. The trend at low and mid-temperatures was consistent with the other aromaticity measurements, while the slight decrease at high temperature was inconsistent with the expected high aromaticity at high HTT. This can be attributed to a method artifact from which BPCA-aroma$_{index}$ suffers: highly condensed aromatic structures are not completely converted to quantifiable BPCAs and thus, as condensation increases above 600 °C, the BPCA-aroma$_{index}$ slightly declines (Schneider et al., 2010). Still, it is able to distinguish the effects of ash content of high temperature chars (grass vs. wood) and the effect of the two different pyrolysis procedures A and B, which is why the BPCA-aroma$_{index}$ plots well within the aromaticity vector in Fig. 3.

The lipid indices (TLE$_{index}$, ACL$_{index}$, PAH$_{index}$) are indirectly linked to changes in aromaticity because the lipid proportion (e.g. TLE$_{index}$) and quality (e.g. ACL$_{index}$, PAH$_{index}$) vary with HTT and the associated changes in aromaticity. The TLE$_{index}$ showed a typical pattern for the aromaticity measurements, with low values (high extractability) at low temperatures and high values (low extractability) > 600 °C. Simple lipid extraction thus seemed to be a good proxy for aromaticity. It was able to differentiate between the two pyrolysis methods,

showing the delayed increase in aromaticity of the B thermosequences, and remained at a constant maximum > 600 °C. However, it suffers from too high index values at low HTT for all thermosequences except the Grass-A thermosequence. This is unfortunate and probably due to the generally low content of extractable lipids in woody tissue (Gocke et al., 2013).

The ACL of alkanes decreased with increasing HTT due to cracking of carbon bonds (Simoneit and Elias, 2000; Wiesenberg et al., 2009), which translates into an increasing trend in the reciprocal ACL_{index} with increasing temperature. The ACL_{index} showed the general pattern of the other aromaticity measurements, e.g. pronounced increase in the index between 200 and 600 °C, a higher lignin-derived aromaticity for woody low-temperature chars than grassy chars and the characteristic difference between the two pyrolysis procedures between 200 and 600 °C. However, while the ACL_{index} is very similar to other aromaticity measurements for the Grass-A thermosequence, it unfortunately shows a high variability between the different thermosequences and sometimes no characteristic trend was observable (e.g. for the Wood-A thermosequence). These drawbacks do not seem to depend on pyrolysis method or two types of starting material (wood vs. grass) but rather seem dependent on the individual feedstock. Thus, using ACL_{index} as an aromaticity measurement may require a careful calibration according to feedstock before conclusions can be drawn from it.

The PAH_{index} is another measurement theoretically linked to aromaticity in chars and which can be retrieved after lipid extraction (Simoneit, 2002; Yunker et al., 2002). Despite its rather straightforward concept of comparing larger with smaller PAH structures, no monotonic trend with HTT was observed. Instead, a maximum of the PAH_{index} was found at 400 – 500 °C, which interestingly correlates with total solvent-extractable PAH yield, as found in a more detailed study (Keiluweit et al., 2012). These results indicate that the relationship between PAH composition and HTT of chars is rather complex and requires more research.

Degree of aromatic condensation

We assessed the degree of aromatic condensation by investigating functional groups and atomic bonds (NMR-$cond_{index}$, NEXAFS-$cond_{index}$), quantifying molecular markers (BPCA-$cond_{index}$) and measuring the structural density ($Pycno_{index}$) of the chars (Table 1).

The NMR method is the most recent development in the field and had already afforded plausible results on one set of the chars (Wood-A thermosequence; McBeath et al., 2011). In the same study, it was shown that the degree of aromatic condensation increases more gradually with increasing HTT than aromaticity and that a high degree of condensation only occurs at high HTT. Here, the inclusion of the Grass-A, Wood-B and Grass-B thermosequences showed again a similar pattern: the degree of aromatic condensation was minimal up to 200 °C and then constantly and monotonically increased up to the highest HTT. Interestingly, the chars from the B pyrolysis procedure again lagged behind those from

the A pyrolysis procedure, indicating that the shorter pyrolysis time not only reduced the aromaticity but also the degree of aromatic condensation.

The BPCA method reproduced the NMR-cond$_{index}$ general pattern consistently, despite the large difference in methodology. The relationship between the degree of aromatic condensation and HTT was more curved than that for NMR, pointing to a slightly non-linear behavior of the BPCA-cond$_{index}$. This minor deviation is probably method inherent because it occurred reproducibly for all the thermosequences. However, it is surprising that the grass chars scored higher with respect to aromatic condensation than the wood chars at high temperature. This probably reflects the lower BPCA yield from grass chars than wood chars at high temperature (cf. Fig. 1, BPCA-aroma$_{index}$). This effect therefore has to be taken into account when the BPCA-cond$_{index}$ is used for the assessment of the degree of aromatic condensation in chars from different feedstocks.

He pycnometry represents a third, completely indepedent approach for assessing the degree of aromatic condensation. Despite its lower cost and shorter analysis time, this indirect measurement appeared to reproduce quite well the main trend from the previous, more complex and expensive aromatic condensation measurements. It depicted a rather linear increase in aromatic condensation from 300 °C up to the highest measured HTT. He pycnometry measurements in the low temperature range (< 300 °C) seem, however, to be less promising because the Pycno$_{index}$ overestimated aromatic condensation for such mild heat treatment. Besides, the Wood-B thermosequence showed unusual behavior, whereby only the highest HTT (700 °C) would be assigned as giving a condensed aromatic carbon structure.

The NEXAFS-cond$_{index}$ indicated a pronounced increase in the degree of aromatic condensation of the chars between 200 and 500 °C and a decrease above 600 °C, which is not consistent with the other aromatic condensation measurements (Fig. 3, vector 2). Both NEXAFS indices used here (NEXAFS-aroma$_{index}$ and NEXAFS-cond$_{index}$) showed some differences compared with other metrics of aromaticity and aromatic condensation. The use of simple indices derived from NEXAFS spectra is most likely limited by the fact that resonances in NEXAFS are not derived exclusively from specific functional groups but rather are a result of the entire electronic structure of the char material.

General patterns of aromatic features and implications

Applying a large suite of seven methods with 13 measurements to a diverse char sample set of four thermosequences enabled us to identify general patterns between analytical methods and char C properties.

One observable pattern was the distinction between measurements that assess aromaticity and those that assess the degree of aromatic condensation, as discussed above and shown in

Fig. 3. The differentiation was sharp and resulted in two distinct trends with HTT as depicted in Fig. 1 and Fig. 2 as the median of all measurements for each category: aromaticity increased sharply from 200 °C on, reaching maximum values at 500 – 600 °C, and stayed constant at the maximum with higher HTT (Fig. 1). The degree of aromatic condensation, on the other hand, increased smoothly from 300 °C on, reaching highest values at 1000 °C (Fig. 2). While this difference between the two categories of aromatic measures was reported elsewhere (McBeath et al., 2011), it was somewhat surprising how congruently the methods behaved within each category despite the fact that they are based on fundamentally different approaches. The O-C_{index}, for example, followed the NMR-$aroma_{index}$ with only very minor differences for all thermosequences, and the H-C_{index}, as well as the BPCA-$aroma_{index}$, also gave very similar results. Likewise, NMR-$cond_{index}$, BPCA-$cond_{index}$ and $Pycno_{index}$ were very similar for the degree of aromatic condensation for all feedstocks and pyrolysis procedures. Even the slight shift between pyrolysis procedure A and B with respect to HTT was readily detected with most of the methods (O-C_{index}, H-C_{index}, NMR-$aroma_{index}$, BPCA-$aroma_{index}$, TLE_{index}, NMR-$cond_{index}$, BPCA-$cond_{index}$, $Pycno_{index}$) reflecting both the importance of the pyrolysis conditions on the char C properties and the high sensitivity of each measurement for differences in char aromatic structure. Our observations imply that a variety of measurements are suitable for assessing the aromatic C structure of chars and that differently acquired data, e.g. from different research groups and laboratories, can be compared if it is reasonably standardized and calibrated. More comparable data interpretations of diverse published and future studies alike can lead to a more consistent and better understanding of the C structure in different chars, which, in turn, promises to illuminate the C sequestration potential of diverse chars (Wang et al.; Keiluweit et al., 2010; Harvey et al., 2012a; Singh et al., 2012).

The distinctive and reproducibly measurable trends in aromaticity and aromatic condensation as a function of HTT also allow the inverse examination of chars: if the aim is to determine the unknown HTT of a certain char, it can be estimated by measuring its aromatic C structure. A quick multiple linear regression analysis of our dataset (data not shown) indicated that it is best to combine a measurement of aromaticity with one of aromatic condensation to obtain precise HTT reconstruction estimations. Aromaticity and aromatic condensation increase over different ranges of temperature and thus yield complementary information about the char HTT. Methods that provide both aromatic measurements at the same time (e.g. NMR-$aroma_{index}$ and NMR-$cond_{index}$ or BPCA-$aroma_{index}$ and BPCA-$cond_{index}$) are thus beneficial from this point of view. However, similarly good results for HTT reconstruction were achieved by combining different methods, e.g. the O-C_{index}, which captures aromaticity, with the $Pycno_{index}$, which measures the degree of aromatic condensation. HTT reconstruction of chars may be an important application of the above methods in archeological studies (Conedera et al., 2009; Wolf et al., 2013) in addition to the more established focus on char stability in an environmental context (Nguyen et al., 2010; Al-Wabel et al., 2013).

We conclude that indirect, inexpensive and simple methods captured the aromatic structures in fresh chars similarly well as more costly and time-consuming techniques. This holds promise whereby aromaticity and the degree of aromatic condensation can be readily assessed in all kinds of char studies and with a variety of new and established methods. Thus, characterization and classification of charred materials should explicitly take these two C aromatic features into account because they are likely key to their stability against degradation in the environment as well as being highly informative about production temperatures.

Acknowledgments

Support for M.W.I.S. was also provided by the US Department of Energy (contract no. DE-AC02-05CH11231). B. H. Meier (Laboratory of Physical Chemistry ETH) made available NMR instruments. C.A.M acknowledges support from NSF EAR-0911685.

Table 1. Methods considered comparatively for assessing aromaticity and/or degree of aromatic condensation of chars (names of derived indices in bold).

Measurement principle	Method	Index (M_{index})	Measurement	Reference
Elemental composition	Elemental analysis	**O-C$_{index}$** **H-C$_{index}$**	C, H and O content (%): H/C, O/C	Baldock and Smernik (2002); Hammes et al. (2006)
Functional groups	Mid-infrared spectroscopy (MIR)	**MIR$_{index}$**	Aromaticity ratio (%): (1420 + 821) / (1510 + 1320) cm^{-1}	Wood (1988); Guo and Bustin (1998); Moore (2001)
	Near-edge X-ray absorption fine structure spectroscopy (NEXAFS)	**NEXAFS-aroma$_{index}$** **NEXAFS-cond$_{index}$**	Aromaticity ratio (%): 285 eV/ 286-288 eV Degree of condensation ratio (%): 284 eV/ 285eV	Francis and Hitchcock (1992); Agren et al. (1995); Kuznetsova et al. (2001); Brandes et al. (2008); Keiluweit et al. (2010)
	^{13}C Nuclear magnetic resonance spectroscopy (NMR)	**NMR-aroma$_{index}$**	Deconvolution on fitted spectrum with assigned aromatic peaks	McBeath et al. (2009); McBeath and Smernik (2011)
	- with sorbed ^{13}C label	**NMR-cond$_{index}$**	-Δδ (ppm): Shift of sorbed ^{13}C labelled benzene - shift of benzene	McBeath et al. (2009); McBeath and Smernik (2011)
Molecular markers	Benzene polycarboxylic acids (BPCA) analysis	**BPCA-aroma$_{index}$** **BPCA-cond$_{index}$**	Total BPCA amount per organic carbon (g kg^{-1}): BPCA/C Ratio of B6CA per total BPCA amount (%): B6CA/BPCA	Schneider et al. (2011); Wiedemeier et al. (2013)
	Lipid analysis	**TLE$_{index}$**	Total lipid extract yield (g): TLE	Wiesenberg et al. (2009)
	- *n*-alkanes	**ACL$_{index}$**	Average chain length: ACL	Wiesenberg et al. (2010)
	- polycyclic aromatic hydrocarbons	**PAH$_{index}$**	Ratio of 4-6 ring to 2-3 ring polycyclic aromatic hydrocarbons (%)	
Density	He pycnometry	**Pycno$_{index}$**	Skeletal density (g cm^{-3})	Brown et al. (2006); Brewer et al. (2009)

Table 2. Thermosequences measured with each method.

Feedstock	Pyrolysis Procedure	HTT	n	Thermosequence
Chestnut (Wood) (*Castanea sativa*)	A: 5 h HTT, N_2 flow	200 - 1000 °C	12	Wood-A
Rice (Grass) (*Oryza sativa*)		200 - 1000 °C	12	Grass-A
Pine (Wood) (*Pinus ponderosa*)	B: 1 h HTT, Closed Chamber	100 - 700 °C	7	Wood-B
Fescue (Grass) (*Festuca arundinacea*)		100 - 700 °C	7	Grass-B

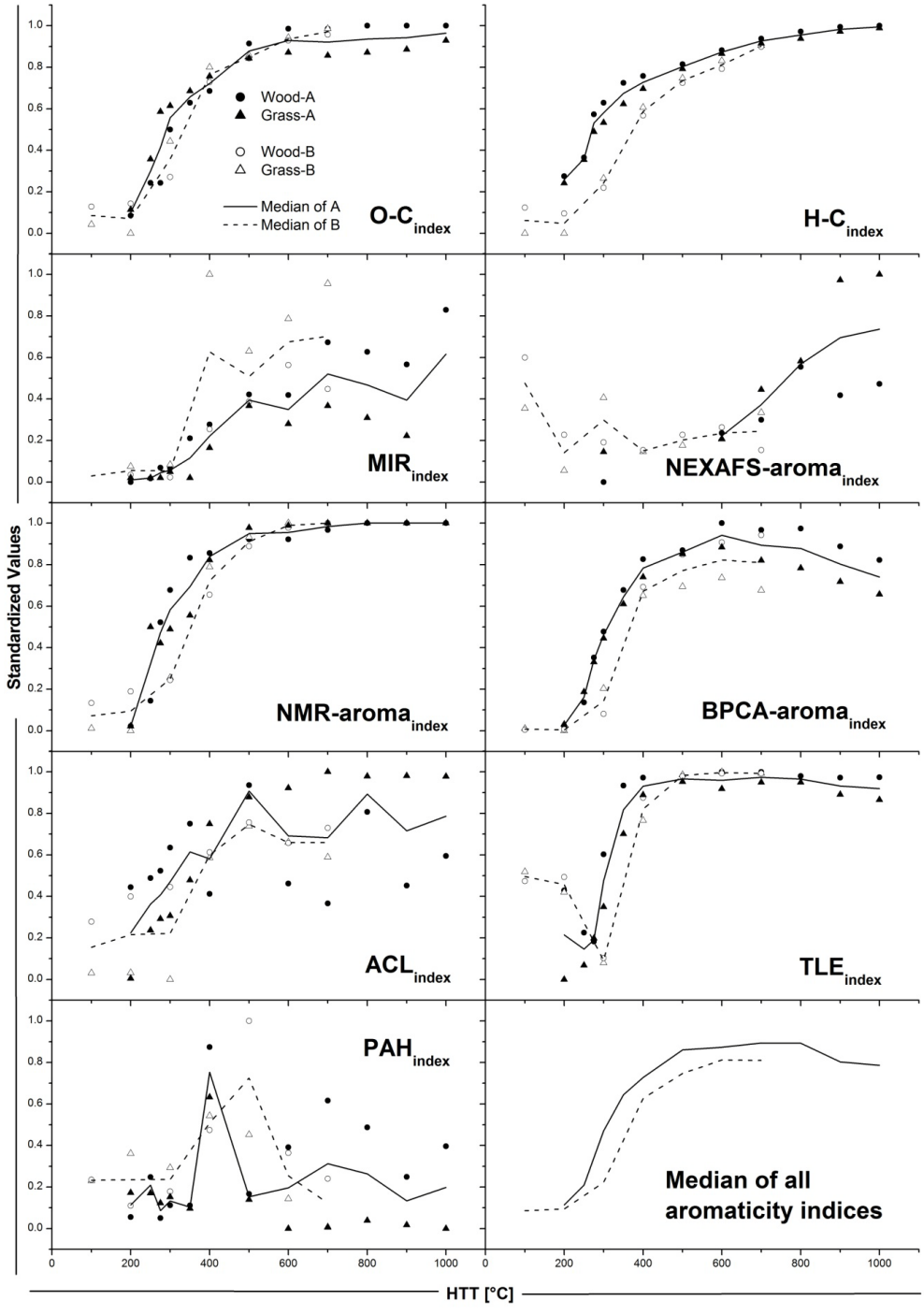

Figure 1. Char aromaticity as measured via nine different indices. The median of all the indices is shown at the lower right corner and thus describes the typical trend in aromaticity with HTT.

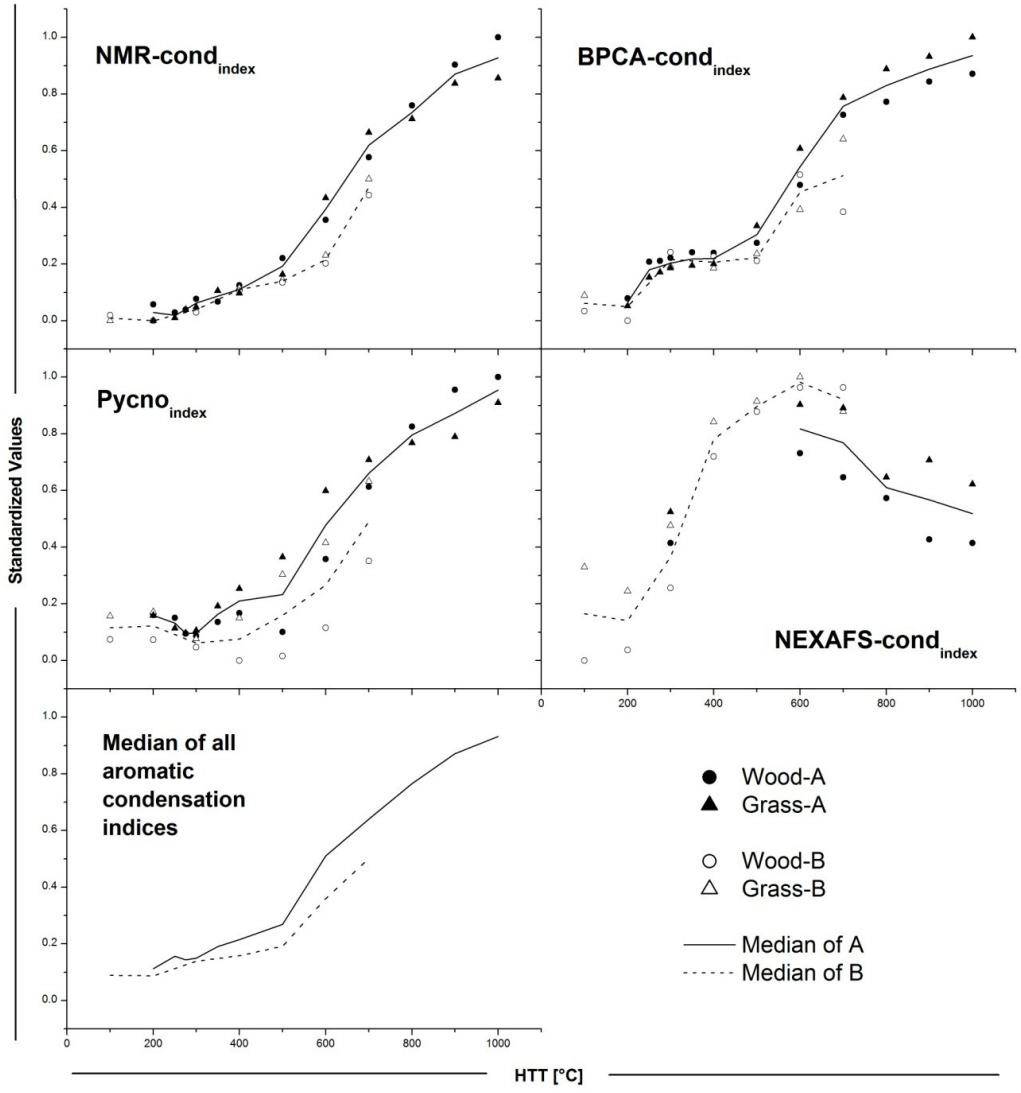

Figure 2. Degree of aromatic condensation as measured via four different indices. The median of all the aromatic condensation indices is depicted in the lower left and thus shows a typical increase in degree of aromatic condensation with HTT.

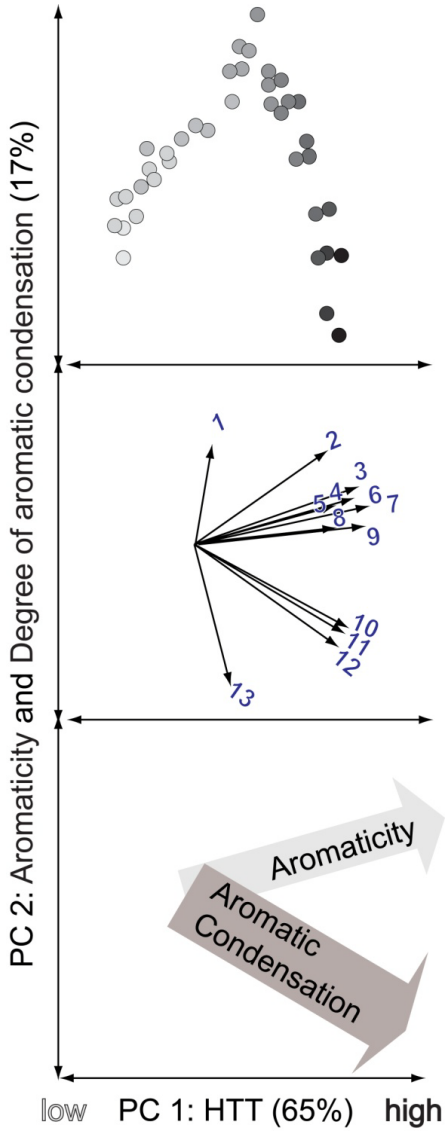

Figure 3. PCA of the large dataset generated. The first PC is projected along the HTT axis and thus differentiates the chars according to their heating temperature (top). The second PC spreads between aromaticity and the degree of aromatic condensation, showing that the char samples first become more aromatic with increasing HTT and then increase in aromatic condensation in the higher temperatures range (top). Likewise, the PCA differentiates between the different measurements (center and bottom) and groups them into typical aromaticity indices (3 – 9) and typical indices for assessing the degree of aromatic condensation (10 – 12). The numbers indicate: 1, PAHindex; 2, NEXAFS-condindex; 3, BPCA-aromaindex; 4, TLEindex; 5, MIRindex; 6, O-Cindex; 7, NMR-aromaindex; 8, ACLindex; 9, H-Cindex; 10, BPCA-condindex; 11, NMR-condindex; 12, Pycnoindex; 13, NEXAFS-aromaindex.

References

Agren, H., Vahtras, O., Carravetta, V., 1995. Near-edge core photoabsorption in polyacenes - model molecules for graphite. Chemical Physics 196, 47-58.

Al-Wabel, M.I., Al-Omran, A., El-Naggar, A.H., Nadeem, M., Usman, A.R.A., 2013. Pyrolysis temperature induced changes in characteristics and chemical composition of biochar produced from conocarpus wastes. Bioresource Technology 131, 374-379.

Antal, M.J., Grønli, M., 2003. The art, science, and technology of charcoal production. Industrial & Engineering Chemistry Research 42, 1619-1640.

Baldock, J., Smernik, R., 2002. Chemical composition and bioavailability of thermally altered Pinus resinosa (Red pine) wood. Organic Geochemistry 33, 1093-1109.

Beesley, L., Moreno-Jiménez, E., Gomez-Eyles, J.L., Harris, E., Robinson, B., Sizmur, T., 2011. A review of biochars' potential role in the remediation, revegetation and restoration of contaminated soils. Environmental Pollution 159, 3269-3282.

Biederman, L.A., Harpole, W.S., 2013. Biochar and its effects on plant productivity and nutrient cycling: a meta-analysis. GCB Bioenergy 5, 202-214.

Brandes, J., Cody, G., Rumble, D., Haberstroh, P., Wirick, S., Gelinas, Y., 2008. Carbon K-edge XANES spectromicroscopy of natural graphite. Carbon 46, 1424-1434.

Brewer, C., Schmidt Rohr, K., Satrio, J., Brown, R., 2009. Characterization of biochar from fast pyrolysis and gasification systems. Environmental progress & sustainable energy 28, 386-396.

Brown, R.A., Kercher, A.K., Nguyen, T.H., Nagle, D.C., Ball, W.P., 2006. Production and characterization of synthetic wood chars for use as surrogates for natural sorbents. Organic Geochemistry 37, 321-333.

Cohen-Ofri, I., Weiner, L., Boaretto, E., Mintz, G., Weiner, S., 2006. Modern and fossil charcoal: aspects of structure and diagenesis. Journal Of Archaeological Science 33, 428-439.

Conedera, M., Tinner, W., Neff, C., Meurer, M., Dickens, A.F., Krebs, P., 2009. Reconstructing past fire regimes: methods, applications, and relevance to fire management and conservation. Quaternary Science Reviews 28, 555-576.

Francis, J.T., Hitchcock, A.P., 1992. Inner-shell spectroscopy of a para-benzoquinone, hydroquinone, and phenol - distinguishing quinoid and benzenoid structures. Journal of Physical Chemistry 96, 6598-6610.

Franklin, R.E., 1951. Crystallite growth in graphitizing and non-graphitizing carbons. Proceedings - Royal Society. Mathematical, physical and engineering sciences 209, 196-218.

Gabriel, K.R., 1971. The biplot graphic display of matrices with application to principal component analysis. Biometrika 58, 453-467.

Glaser, B., Birk, J.J., 2012. State of the scientific knowledge on properties and genesis of Anthropogenic Dark Earths in Central Amazonia (terra preta de Índio). Geochimica et Cosmochimica Acta 82, 39-51.

Gocke, M., Kuzyakov, Y., Wiesenberg, G.L.B., 2013. Differentiation of plant derived organic matter in soil, loess and rhizoliths based on n-alkane molecular proxies. Biogeochemistry 112, 23-40.

Guo, Y., Bustin, R.M., 1998. FTIR spectroscopy and reflectance of modern charcoals and fungal decayed woods: implications for studies of inertinite in coals. International Journal of Coal Geology 37, 29-53.

Hammes, K., Smernik, R., Skjemstad, J., Herzog, A., Vogt, U., 2006. Synthesis and characterisation of laboratory-charred grass straw (Oryza saliva) and chestnut wood (Castanea sativa) as reference materials for black carbon quantification. Organic Geochemistry 37, 1629-1633.

Harvey, O., Kuo, L.-J., Zimmerman, A., Louchouarn, P., Amonette, J., Herbert, B., 2012a. An index-based approach to assessing recalcitrance and soil carbon sequestration potential of engineered black carbons (biochars). Environmental Science & Technology 46, 1415-1421.

Harvey, O.R., Herbert, B.E., Kuo, L.-J., Louchouarn, P., 2012b. Generalized Two-Dimensional Perturbation Correlation Infrared Spectroscopy Reveals Mechanisms for the Development of Surface Charge and Recalcitrance in Plant-Derived Biochars. Environmental Science & Technology 46, 10641-10650.

Keiluweit, M., Kleber, M., Sparrow, M.A., Simoneit, B.R.T., Prahl, F.G., 2012. Solvent-extractable polycyclic aromatic hydrocarbons in biochar: influence of pyrolysis temperature and feedstock. Environmental Science & Technology 46, 9333-9341.

Keiluweit, M., Nico, P.S., Johnson, M.G., Kleber, M., 2010. Dynamic molecular structure of plant biomass-derived black carbon (biochar). Environmental Science & Technology 44, 1247-1253.

Knicker, H., 2011. Pyrogenic organic matter in soil: Its origin and occurrence, its chemistry and survival in soil environments. Quaternary International 243, 251-263.

Kuznetsova, A., Popova, I., Yates, J.T., Bronikowski, M.J., Huffman, C.B., Liu, J., Smalley, R.E., Hwu, H.H., Chen, J.G.G., 2001. Oxygen-containing functional groups on single-wall carbon nanotubes: NEXAFS and vibrational spectroscopic studies. Journal of the American Chemical Society 123, 10699-10704.

Lehmann, J., Czimczik, C., Laird, D., Sohi, S., 2009. Stability of biochar in soil, in: Lehmann, J., Joseph, S. (Eds.), Biochar for environmental management: science and technology. Earthscan: London, UK, pp. 183-206.

Lehmann, J., Joseph, S., 2009. Biochar for Environmental Management - An Introduction, in: Lehmann, J., Joseph, S. (Eds.), Biochar for Environemental Management: Science and Technology. Earthscan, London, UK, pp. 1-12.

Lua, A.C., Yang, T., Guo, J., 2004. Effects of pyrolysis conditions on the properties of activated carbons prepared from pistachio-nut shells. Journal of Analytical and Applied Pyrolysis 72, 279-287.

Manyà , J., 2012. Pyrolysis for biochar purposes: a review to establish current knowledge gaps and research needs. Environmental Science & Technology 46, 7939-7954.

Mardia, K.V., Kent, J.T., Bibby, J.M., 1979. Multivariate analysis. Academic Press.

McBeath, A., Smernik, R., Plant, E., 2011. Determination of the aromaticity and the degree of aromatic condensation of a thermosequence of wood charcoal using NMR. Organic Geochemistry 42, 1194-1202.

McBeath, A.V., Smernik, R.J., 2009. Variation in the degree of aromatic condensation of chars. Organic Geochemistry 40, 1161-1168.

McNaught, A.D., Wilkinson, A., 1997. IUPAC. Compendium of Chemical Terminology., 2nd Edition ed. Blackwell Scientific Publications, Oxford.

Meyer, S., Glaser, B., Quicker, P., 2011. Technical, economical, and climate-related aspects of biochar production technologies: a literature review. Environmental Science & Technology 45, 9473-9483.

Moore, A., Owen, N., 2001. Infrared spectroscopic studies of solid wood. Applied Spectroscopy Reviews 36, 65-86.

Mukome, F.N.D., Zhang, X., Six, J., Parikh, S., Parikh, S.J., 2013. Use of chemical and physical characteristics to investigate trends in biochar feedstocks. Journal of Agricultural and Food Chemistry 61, 2196-2204.

Nguyen, B., Lehmann, J., Hockaday, W., Joseph, S., Masiello, C., 2010. Temperature sensitivity of black carbon decomposition and oxidation. Environmental Science & Technology 44, 3324-3331.

Preston, C.M., Schmidt, M.W.I., 2006. Black (pyrogenic) carbon: a synthesis of current knowledge and uncertainties with special consideration of boreal regions. Biogeosciences 3, 397-420.

R, 2011. R: A language and environment for statistical computing. R Foundation for Statistical Computing.

Rutherford, D.W., Wershaw, R.L., Rostad, C.E., Kelly, C.N., 2012. Effect of formation conditions on biochars: Compositional and structural properties of cellulose, lignin, and pine biochars. Biomass and Bioenergy 46, 693-701.

Schmidt, M.W.I., Noack, A.G., 2000. Black carbon in soils and sediments: Analysis, distribution, implications, and current challenges. Global Biogeochemical Cycles 14, 777-793.

Schneider, M.P.W., Hilf, M., Vogt, U.F., Schmidt, M.W.I., 2010. The benzene polycarboxylic acid (BPCA) pattern of wood pyrolyzed between 200 °C and 1000 °C. Organic Geochemistry 41, 1082-1088.

Schneider, M.P.W., Smittenberg, R., Dittmar, T., Schmidt, M.W.I., 2011. Comparison of gas with liquid chromatography for the determination of benzenepolycarboxylic acids as molecular tracers of black carbon. Organic Geochemistry 42, 275-282.

Setton, R., Bernier, P., Lefrant, S., 2002. Carbon molecules and materials. CRC Press.

Shafizadeh, F., 1982. Introduction to pyrolysis of biomass. Journal of Analytical and Applied Pyrolysis 3, 283-305.

Simoneit, B.R.T., 2002. Biomass burning - A review of organic tracers for smoke from incomplete combustion. Applied Geochemistry 17, 129-162.

Simoneit, B.R.T., Elias, V.O., 2000. Organic tracers from biomass burning in atmospheric particulate matter over the ocean. Marine Chemistry 69, 301-312.

Singh, B.P., Cowie, A.L., Smernik, R.J., 2012. Biochar carbon stability in a clayey soil as a function of feedstock and pyrolysis temperature. Environmental Science & Technology 46, 11770-11778.

Stekhoven, D., Buehlmann, P., 2012. MissForest--non-parametric missing value imputation for mixed-type data. Bioinformatics 28, 112-118.

Wang, T., Camps-Arbestain, M., Hedley, M., Predicting C aromaticity of biochars based on their elemental composition. Organic Geochemistry.

Wang, T., Camps-Arbestain, M., Hedley, M., 2013. Predicting C aromaticity of biochars based on their elemental composition. Organic Geochemistry 62, 1-6.

Wiedemeier, D.B., Hilf, M.D., Smittenberg, R.H., Haberle, S.G., Schmidt, M.W.I., 2013. Improved assessment of pyrogenic carbon quantity and quality in environmental samples by high-performance liquid chromatography. Journal of Chromatography A 1304, 246-250.

Wiesenberg, G.L.B., Gocke, M., Kuzyakov, Y., 2010. Fast incorporation of root-derived lipids and fatty acids into soil – evidence from a short term multiple pulse labelling experiment. Organic Geochemistry 41, 1049-1055.

Wiesenberg, G.L.B., Lehndorff, E., Schwark, L., 2009. Thermal degradation of rye and maize straw: lipid pattern changes as a function of temperature. Organic Geochemistry 40, 167-174.

Wolf, M., Lehndorff, E., Wiesenberg, G.L.B., Stockhausen, M., Schwark, L., Amelung, W., 2013. Towards reconstruction of past fire regimes from geochemical analysis of charcoal. Organic Geochemistry 55, 11-21.

Wood, D.J., 1988. Characterization of charcoals by drift. Mikrochimica Acta 2, 167-169.

Yunker, M.B., Macdonald, R.W., Vingarzan, R., Mitchell, R.H., Goyette, D., Sylvestre, S., 2002. PAHs in the Fraser River basin: a critical appraisal of PAH ratios as indicators of PAH source and composition. Organic Geochemistry 33, 489-515.

Supplementary material

Elemental Analysis: O-C$_{index}$, H-C$_{index}$

C, H and O contents of the Wood-A and Grass-A thermosequences were measured with LECO CHN-900 and LECO RO478 (Mönchengladbach, Germany) instruments, while the C and H contents of the Wood-B and Grass-B chars were measured with a Carlo Erba NA-1500 CNS analyzer (Carlo Erba Instruments, Italy) and O content was calculated by difference. H/C and O/C are used as a measurement of aromaticity, mostly in Van Krevelen diagrams (Baldock and Smernik, 2002; Hammes et al., 2006).

Mid infrared spectroscopy: MIR$_{index}$

MIR spectra were acquired using diffuse reflectance infrared Fourier transform spectroscopy. Spectra were recorded from 4000 to 400 cm^{-1} (average of 16 scans per sample at 4 cm^{-1} resolution) with a Bruker Tensor 27 (Billerica, USA) spectrometer using a powder containing 6 mg ground sample (3% of total wt.) and 194 mg KBr (97% of total wt.). Samples were homogenised in a mill using a fine ball mill (Zr) for 2 mn (frequency 25). Prior to measurement, the samples and KBr were dried at 105 °C. Assessment of aromaticity was based on four specific peaks: 1510 (lignin), 1420 (aromatic), 1320 (aliphatic) and 821 cm^{-1} (aromatic) (Wood, 1988; Guo and Bustin, 1998; Moore and Owen, 2001). Peaks were integrated using Opus 6.0 software and the ratio for aromaticity is calculated as follows: (1420 + 821) / (1510 + 1320) [cm^{-1}].

Near-edge X-ray absorption fine structure spectroscopy: NEXAFS-aroma$_{index}$, NEXAFS-cond$_{index}$

NEXAFS spectra were obtained using a scanning X-ray transmission microscope (beamline 5.3.2) at the Advanced Light Source, Berkeley, CA (Kilcoyne et al., 2003). Sample preparation, analysis and data processing were as described by Keiluweit et al. (2010). Increase in absorbance of aromatic C=C (285 eV) relative to oxygenated and aliphatic C (286-288 eV) can be used to approximate numerically the increase in aromaticity with temperature (Keiluweit et al., 2010). Marked shifts in the 1s-π^* transition band were used to identify changes in the degree of aromatic condensation at higher charring temperatures. The approach was to ratio absorbance at 284.4 eV assigned to quinones (Francis and Hitchcock, 1992), oxygenated 2- to 3-ring PAHs (Kuznetsova et al., 2001), and non-substituted 2- to 5-ring polyacenes (Agren et al., 1995) to that at 285.3 eV associated with large condensed graphene sheets (Brandes et al., 2008).

^{13}C Nuclear magnetic resonance spectroscopy: NMR-aroma$_{index}$

NMR analysis was conducted as outlined by McBeath et al. (2009; 2011). Quantification of aromatic C was carried out using a deconvolution procedure rather than the more usual approach of assigning a fixed chemical shift region (e.g. 110–160 ppm) as aromatic C. Deconvolution involved fitting each spectrum as the sum of multiple peaks of Gaussian shape, which were assigned as either aromatic or non-aromatic, based on whether or not the centre of the peak was in the range 110–165 ppm (McBeath et al., 2011).

^{13}C Nuclear magnetic resonance with sorbed ^{13}C label: NMR-cond$_{index}$

All thermosequence chars were loaded with ^{13}C labeled benzene for "ring current" analysis (McBeath and Smernik, 2009; McBeath et al., 2011). Spectra were acquired using the same acquisition conditions as with unlabeled NMR spectroscopy but fewer scans (16-128) were required. The change in chemical shift of ^{13}C labeled benzene (i.e. the chemical shift of the sorbed ^{13}C labeled benzene minus the neat chemical shift of ^{13}C labeled benzene; 128.7ppm) provides a measurement of the degree of aromatic condensation.

Benzene polycarboxylic acid analysis: BPCA-aroma$_{index}$, BPCA-cond$_{index}$

Wood-A and Grass-A thermosequence chars were measured as outlined by Schneider et al. (2011) and Wiedemeier et al. (2013). Wood-B and Grass-B thermosequence samples were prepared the same way but the separation was performed with a Waters VanGard™ pre-column (2.1x5mm, 1.7µm) and a Waters Acquity UPLC column (2.1x150mm, 1.7µm). All analyses were done in triplicate. The BPCA content normalized to C content of a sample was suggested as a measurement of aromaticity (BPCA-aroma$_{index}$) while the ratio of B6CA to total BPCA content serves as a measurement for the degree of aromatic condensation (BPCA-cond$_{index}$) (McBeath et al., 2011; Schneider et al., 2011).

Lipid analysis: TLE$_{index}$, ACL$_{index}$, PAH$_{index}$

Ca. 300 mg of sample were extracted in an ultrasonic bath with CH_2Cl_2/MeOH (93:7; v:v) at 60 °C for 15 min. After centrifugation, the supernatant was filtered and collected for five repetitions of the extraction, yielding the total lipid extract (TLE$_{index}$). Aliphatic and aromatic hydrocarbon fractions were recovered after separation via activated silica gel columns. Deuterated standards were added before alkane (ACL$_{index}$) and polycyclic aromatic hydrocarbon (PAH$_{index}$) identification and quantification via gas chromatography-mass spectrometry (GC-MS; Wiesenberg et al., 2010).

A decreasing total lipid extract yield (TLE_{index}) can indirectly indicate increasing aromaticity. With higher temperatures, plant-derived lipids become low in abundance and small molecules combine to larger molecules, whose extractability is limited. The decrease of average chain length of alkanes (ACL_{index}) can also serve as an indirect indicator of increasing aromaticity. Based on the findings of Wiesenberg et al. (2009), plant-derived long chain (> 25 C atoms) alkanes degrade and short chain (< 25 C atoms) aliphatic side chains of other lipids become increasingly important with temperature. Finally, the ratio of 4- to 6-ring PAHs divided by 2- to 3-ring PAHs (PAH_{index}) was obtained as a further measurement of aromaticity. It should theoretically account for the larger polycyclic nuclei that become available at higher temperatures.

He pycnometry: $Pycno_{index}$

Samples were analyzed for skeletal density using a Micromeritics AccuPyc 1340 Gas Pycnometer (Norcross, USA) with He as the displacement fluid. Because He can access 0.1-0.2 nm open pores, density values measured with this method reflect the density of the C skeleton of the char samples, indirectly indicating C condensation (Brown et al., 2006; Brewer et al., 2009). All values were based on five consecutive measurements of each sample. Measurement reproducibility was ± 0.0017 g/cm^3 on average. A 1 cm^3 volume chamber with calibration spheres of volume 0.1796 cm^3 was used, and the chamber volume was completely filled with sample (ca. 0.26 g) for each measurement to ensure that 30% or less of the chamber was pore space.

Additional NMR applied to part of sample set: NMR_{add}

Part of the samples was also measured using ^{13}C NMR with dipolar dephasing. We show the data from this approach (NMR_{add}) only in the Supplementary data because the results could not be included in the statistical analysis and discussion, due to an insufficient number of measured samples. Spectra were acquired with a 200 MHz Bruker DSX spectrometer (^{13}C frequency 50 MHz) equipped with a 4mm magic angle spinning (MAS) probe using a 7kHz spin rate. Quantitative NMR_{add} spectra were obtained with a direct polarization pulse sequence (DPMAS), with a 90 degree excitation pulse, followed by two pulse phase-modulated ^1H decoupling during signal acquisition, with a 90 s recycle delay between scans. Additional DPMAS spectra were acquired with ^1H-^{13}C dipolar dephasing by inserting a 50 μs dephasing delay prior to the decoupling. Based upon the behavior of aromatic model compounds, we applied a 10% intensity correction to signals in the dipolar-dephasing (DDMAS) NMR_{add} spectra to compensate for relaxation during the 50 μs delay. Background signals arising from C-containing probe and rotor components were subtracted from each spectrum. To calculate the mole fraction bridgehead carbons in a sample, we followed the algorithm established by Solum et al. (1989).

Table S1. Raw data from the different analysis methods from measuring the 38 char samples.

			Elemental Analysis		MIR	NEXAFS		NMR		BPCA		MIR	Lipid Analysis			Helium	Additional, incomplete NMR_{adc}	
Feedstock	Pyrolysis	HTT	H/C	O/C	aromatic ratio	285/286 - 288 eV	284/285 eV	aromatic C	-Δδ	BPCA/C	B6CA/BPCA	aromatic ratio	TLE	ACL	PAH ratio	Pycnometry	aromatic C	bridgehead C
		[°C]	[%]	[%]	[%]	[%]	[%]	[%]	[ppm]	[‰]	[‰]	[%]	[g]	[-]	[%]	[g cm^{-3}]	[%]	[%]
Chestnut Wood	A	200	1.32	0.66	0.63	NA	NA	12	0.3	6.0	153.39	0.63	28351	0.3	24.8	1.5101	NA	NA
Chestnut Wood	A	250	1.16	0.55	0.69	NA	NA	23	0.0	33.3	255.09	0.69	38358	1.0	24.2	1.5043	NA	NA
Chestnut Wood	A	275	0.79	0.55	0.87	NA	NA	57	0.1	85.1	257.60	0.87	40439	0.3	23.7	1.4728	NA	NA
Chestnut Wood	A	300	0.69	0.37	0.86	0.99	0.45	71	0.5	115.1	265.75	0.86	19843	0.5	22.1	1.4685	70.6	16.2
Chestnut Wood	A	350	0.52	0.28	1.36	NA	NA	85	0.4	163.1	281.02	1.36	3588	0.5	20.5	1.4959	NA	NA
Chestnut Wood	A	400	0.46	0.24	1.59	NA	NA	87	1.0	198.7	280.00	1.59	1684	3.5	25.3	1.514	NA	NA
Chestnut Wood	A	450	0.70	0.30	NA	1.28	0.70	NA	NA	192.6	289.37	NA	15834	1.5	22.7	1.4916	83.9	26.3
Chestnut Wood	A	500	0.36	0.08	2.09	NA	NA	93	2.0	208.9	307.38	2.09	1330	0.7	17.9	1.4763	NA	NA
Chestnut Wood	A	600	0.24	0.03	2.08	1.25	0.71	93	3.4	240.2	468.65	2.08	327	1.6	24.6	1.6216	93.1	37
Chestnut Wood	A	700	0.14	0.03	2.96	1.32	0.64	97	5.7	232.3	663.58	2.96	351	2.5	25.9	1.7664	94.1	47.3
Chestnut Wood	A	800	0.08	0.02	2.80	1.60	0.58	100	7.6	233.9	700.29	2.80	1295	2.0	19.7	1.8863	89	48.2
Chestnut Wood	A	900	0.04	0.02	2.59	1.45	0.46	100	9.1	213.4	756.23	2.59	1679	1.0	24.7	1.9601	84.9	44.2
Rice Grass	A	1000	0.03	0.02	3.50	1.51	0.45	100	10.1	197.7	777.91	3.50	1606	1.6	22.7	1.9853	86.1	NA
Rice Grass	A	200	1.38	0.64	0.70	NA	NA	12	-0.3	8.1	131.94	0.70	49396	0.7	31.0	1.5086	NA	NA
Rice Grass	A	250	1.18	0.47	0.70	NA	NA	55	-0.2	45.4	210.85	0.70	46039	0.7	27.7	1.4831	NA	NA
Rice Grass	A	275	0.94	0.31	0.70	NA	NA	48	0.1	79.8	226.05	0.70	39672	0.5	26.9	1.4742	NA	NA
Rice Grass	A	300	0.86	0.29	0.80	1.15	0.54	54	0.2	107.3	237.00	0.80	32258	0.7	26.7	1.4787	68.5	23.5
Rice Grass	A	350	0.70	0.24	0.70	NA	NA	60	0.8	146.8	243.89	0.70	14964	0.4	24.3	1.5278	NA	NA
Rice Grass	A	400	0.57	0.19	1.20	NA	NA	84	0.7	178.1	249.17	1.20	5763	2.5	20.5	1.5627	NA	NA
Rice Grass	A	450	0.70	0.30	NA	1.16	0.77	NA	NA	165.3	238.41	NA	12550	3.5	23.8	1.5511	74	28.8
Rice Grass	A	500	0.40	0.13	1.90	NA	NA	98	1.4	204.7	354.52	1.90	2655	0.6	18.7	1.6256	NA	NA
Rice Grass	A	600	0.27	0.11	1.60	1.22	0.85	99	4.2	212.3	570.05	1.60	4346	0.1	18.1	1.7581	93.3	46.8
Rice Grass	A	700	0.18	0.12	1.90	1.48	0.84	100	6.6	197.2	711.67	1.90	2825	0.1	17.0	1.8202	NA	NA
Rice Grass	A	800	0.14	0.11	1.70	1.63	0.64	100	7.1	188.3	791.04	1.70	2781	0.2	17.3	1.8536	82.4	41.1
Rice Grass	A	900	0.08	0.10	1.40	2.06	0.69	100	8.4	172.5	825.53	1.40	5697	0.1	17.3	1.8656	88	NA
Rice Grass	A	1000	0.05	0.07	NA	2.09	0.62	100	8.6	158.2	879.46	NA	6934	0.1	17.3	1.934	NA	NA
Pine Wood	B	100	1.59	0.63	NA	1.65	0.11	22	-0.1	1.7	118.00	NA	26148	1.0	27.1	1.4615	NA	NA
Pine Wood	B	200	1.64	0.62	0.75	1.24	0.14	27	-0.3	2.2	91.00	0.75	25198	0.5	25.4	1.4607	NA	NA
Pine Wood	B	300	1.42	0.53	0.71	1.20	0.32	32	0.0	19.9	281.00	0.71	44314	0.8	24.8	1.4458	NA	NA
Pine Wood	B	400	0.80	0.21	1.51	1.16	0.70	69	0.8	166.5	270.00	1.51	6470	1.9	22.5	1.4193	NA	NA
Pine Wood	B	500	0.52	0.13	1.97	1.24	0.83	90	1.1	203.9	257.00	1.97	1355	3.9	20.4	1.4281	NA	NA
Pine Wood	B	600	0.40	0.07	2.58	1.28	0.90	98	1.8	218.0	497.00	2.58	674	1.5	21.8	1.4846	NA	NA
Pine Wood	B	700	0.21	0.05	2.18	1.16	0.90	100	4.3	226.4	394.00	2.18	706	1.0	20.8	1.6177	NA	NA
Fescue Grass	B	100	1.81	0.69	NA	1.38	0.38	11	-0.3	3.1	161.00	NA	23946	1.0	30.6	1.5077	NA	NA
Fescue Grass	B	200	1.81	0.72	0.89	1.05	0.31	10	-0.3	0.6	NA	0.89	28789	1.5	30.6	1.5162	NA	NA
Fescue Grass	B	300	1.34	0.41	0.92	1.44	0.50	33	0.2	49.5	242.00	0.92	45501	1.2	31.0	1.4626	NA	NA
Fescue Grass	B	400	0.73	0.16	4.09	1.15	0.80	81	0.9	156.6	237.00	4.09	11806	2.2	22.8	1.5041	NA	NA
Fescue Grass	B	500	0.48	0.12	2.81	1.18	0.86	94	1.2	166.9	277.00	2.81	1019	1.8	20.7	1.5907	NA	NA
Fescue Grass	B	600	0.33	0.06	3.35	1.22	0.93	100	2.1	177.1	400.00	3.35	343	0.6	21.8	1.6543	NA	NA
Fescue Grass	B	700	0.20	0.03	3.94	1.36	0.83	100	4.9	162.7	596.00	3.94	665	0.1	22.8	1.7768	NA	NA

References of supplementary material

Agren, H., Vahtras, O., Carravetta, V., 1995. Near-edge core photoabsorption in polyacenes - model molecules for graphite. Chemical Physics 196, 47-58.

Baldock, J., Smernik, R., 2002. Chemical composition and bioavailability of thermally altered Pinus resinosa (Red pine) wood. Organic Geochemistry 33, 1093-1109.

Brandes, J., Cody, G., Rumble, D., Haberstroh, P., Wirick, S., Gelinas, Y., 2008. Carbon K-edge XANES spectromicroscopy of natural graphite. Carbon 46, 1424-1434.

Brewer, C., Schmidt Rohr, K., Satrio, J., Brown, R., 2009. Characterization of biochar from fast pyrolysis and gasification systems. Environmental progress & sustainable energy 28, 386-396.

Brown, R.A., Kercher, A.K., Nguyen, T.H., Nagle, D.C., Ball, W.P., 2006. Production and characterization of synthetic wood chars for use as surrogates for natural sorbents. Organic Geochemistry 37, 321-333.

Francis, J.T., Hitchcock, A.P., 1992. Inner-shell spectroscopy of a para-benzoquinone, hydroquinone, and phenol - distinguishing quinoid and benzenoid structures. Journal of Physical Chemistry 96, 6598-6610.

Guo, Y., Bustin, R.M., 1998. FTIR spectroscopy and reflectance of modern charcoals and fungal decayed woods: implications for studies of inertinite in coals. International Journal of Coal Geology 37, 29-53.

Hammes, K., Smernik, R., Skjemstad, J., Herzog, A., Vogt, U., 2006. Synthesis and characterisation of laboratory-charred grass straw (Oryza saliva) and chestnut wood (Castanea sativa) as reference materials for black carbon quantification. Organic Geochemistry 37, 1629-1633.

Keiluweit, M., Nico, P.S., Johnson, M.G., Kleber, M., 2010. Dynamic molecular structure of plant biomass-derived black carbon (biochar). Environmental Science & Technology 44, 1247-1253.

Kilcoyne, A.L.D., Tyliszczak, T., Fakra, S., Hitchcock, P., Franck, K., Steele, W.F., Anderson, E., Harteneck, B., Rightor, E.G., Mitchell, G.E., Hitchcock, A.P., Yang, L., Warwick, T., Ade, H., 2003. Interferometer-controlled scanning transmission X-ray microscopes at the Advanced Light Source. Journal of synchrotron radiation 10, 125-136.

Kuznetsova, A., Popova, I., Yates, J.T., Bronikowski, M.J., Huffman, C.B., Liu, J., Smalley, R.E., Hwu, H.H., Chen, J.G.G., 2001. Oxygen-containing functional groups on single-wall carbon nanotubes: NEXAFS and vibrational spectroscopic studies. Journal of the American Chemical Society 123, 10699-10704.

McBeath, A., Smernik, R., Plant, E., 2011. Determination of the aromaticity and the degree of aromatic condensation of a thermosequence of wood charcoal using NMR. Organic Geochemistry 42, 1194-1202.

McBeath, A.V., Smernik, R.J., 2009. Variation in the degree of aromatic condensation of chars. Organic Geochemistry 40, 1161-1168.

Moore, A., Owen, N., 2001. Infrared spectroscopic studies of solid wood. Applied Spectroscopy Reviews 36, 65-86.

Schneider, M.P.W., Smittenberg, R., Dittmar, T., Schmidt, M.W.I., 2011. Comparison of gas with liquid chromatography for the determination of benzenepolycarboxylic acids as molecular tracers of black carbon. Organic Geochemistry 42, 275-282.

Solum, M.S., Pugmire, R.J., Grant, D.M., 1989. C-13 solid-state NMR of Argonne premium coals. Energy & fuels 3, 187-193.

Wiedemeier, D.B., Hilf, M.D., Smittenberg, R.H., Haberle, S.G., Schmidt, M.W.I., 2013. Improved assessment of pyrogenic carbon quantity and quality in environmental samples by high-performance liquid chromatography. Journal of Chromatography A 1304, 246-250.

Wiesenberg, G.L.B., Gocke, M., Kuzyakov, Y., 2010. Fast incorporation of root-derived lipids and fatty acids into soil – evidence from a short term multiple pulse labelling experiment. Organic Geochemistry 41, 1049-1055.

Wiesenberg, G.L.B., Lehndorff, E., Schwark, L., 2009. Thermal degradation of rye and maize straw: lipid pattern changes as a function of temperature. Organic Geochemistry 40, 167-174.

Wood, D.J., 1988. Characterization of charcoals by drift. Mikrochimica Acta 2, 167-169.

Paper V

Pyrogenic molecular markers: Linking PAH with BPCA analysis

Submitted as:

Wiedemeier, D.B., Brodowski, S., Wiesenberg, G.L.B., 2014. Pyrogenic molecular markers: Linking PAH with BPCA analysis. Chemosphere (in review).

Author contributions:

D.B.W. conducted statistical analysis and wrote the paper. G.L.B.W. conducted lipid analysis and contributed to the final draft of the manuscript. S.B. conducted BPCA analysis.

Abstract

Molecular characterization of pyrogenic organic matter (PyOM) is of great interest to understand the formation and behavior of these increasingly abundant materials in the environment. Two molecular marker methods have often been used to characterize and trace PyOM: polycyclic aromatic hydrocarbon (PAH) and benzene polycarboxylic acid (BPCA) analysis. Since both methods target pyrogenic polycyclic compounds, we investigated the linkages between the two approaches using chars that were produced under controlled conditions. Rye and maize straws and their analogues charred at 300, 400 and 500 °C, respectively, were thus analyzed with both methods. Moreover, we also measured BPCAs directly on the lipid extracts, on which PAHs were analyzed, and on the respective extraction residues, too. Both methods revealed important features of the chars, in particular the increasing degree of aromatic condensation with increasing highest heating temperature (HTT). The overlap between the two methods was identified in the lipid fraction, where the proportion of B3CAs correlated with PAH abundance. The results confirmed the validity and complementarity of the two molecular marker methods, which will likely continue to play a crucial role in PyOM research due to the recent developments of compound-specific PAH and BPCA stable carbon ($\delta^{13}C$) and radiocarbon (^{14}C) isotope methods.

Introduction

Pyrogenic organic matter (PyOM) is ubiquitous in the environment (Schmidt and Noack, 2000) and relatively stable against degradation, making it part of the slow-cycling C pool (Marschner et al., 2008; Kuzyakov et al., 2014). PyOM abundance is thought to increase globally with increasing wildfire occurrence in the 21st century (Flannigan et al., 2013; Kelly et al., 2013) and as a result of industrial combustion processes and traffic (Bond et al., 2013). Moreover, it is increasingly and intentionally produced in anthropogenic biochar-systems, which have been proposed as a strategy for green energy production, C sequestration, and soil improvement (Lehmann and Joseph, 2009; Meyer et al., 2011). With increasing PyOM production and the awareness of its importance for the C cycle, attention has been drawn to characterize these materials accurately across different disciplines (Simoneit, 2002; Hammes et al., 2007). Molecular marker methods are one technique providing the opportunity to characterize PyOM. They target specifically the molecules that are produced during the combustion processes. Two different approaches are often used that both focus on the polycyclic structures typical for pyrogenic materials: i) polycyclic aromatic hydrocarbon (PAH) analysis and ii) the benzene polycarboxylic acid (BPCA) method.

PAH are small polycyclic aromatic compounds that have a long history as tracers for combustion products (Simoneit et al., 1999; Simoneit, 2002; Denis et al., 2012). They proofed to be particularly useful for the source apportionment of combustion residues in soils and sediments, for example distinguishing between contributions of biomass burning and fossil fuel (Oros and Simoneit, 2001a, b; Yunker et al., 2002; Bucheli et al., 2004). High concentrations of PAH are of environmental concern due to their mutagenic and carcinogenic properties (Boffetta et al., 1997; Wilcke, 2000). Thus, PAH have recently also been heavily investigated in the context of biochar applications (Hale et al., 2012; Hilber et al., 2012; Keiluweit et al., 2012; Oleszczuk et al., 2013; Quilliam et al., 2013). After extraction with the lipid fraction from bulk PyOM (Colmsjö, 1998; Fabbri et al., 2013), they are routinely quantified with gas or liquid chromatography.

BPCAs, on the other hand, present a workaround to quantify the abundant polycyclic PyOM structures that are larger and more complex than PAH. These more condensed aromatic C phases cannot be quantified directly as polymers using chromatographic methods. In order to analyze such pyrogenic structures, PyOM is digested with nitric acid under high temperature and pressure, which breaks the polycyclic compounds down into individual BPCAs, amenable to gas or liquid chromatography (Glaser et al., 1998; Brodowski et al., 2005; Wiedemeier et al., 2013). Pyrogenic C is thus assessed on a molecular level and can be used to estimate PyOM abundance in environmental compartments such as soils and sediments. The technique has yielded valuable insights into the slow cycling of PyOM in the pedosphere (Hammes et al., 2008; Rodionov et al., 2010) and has been helpful to illuminate the pathways of PyOM into sedimentary systems, where PyOM accounts for a quantitatively important fraction of the carbon sink (Guggenberger et al., 2008; Sánchez-García et al., 2013). The BPCA

method additionally reveals information about the aromaticity, aromatic condensation and charring temperature of the analyzed PyOM when relative yields of B3-, B4-, B5- and B6CA are compared (Schneider et al., 2011; Wiedemeier et al., 2014). These qualitative parameters are indicative for the stability of PyOM in the environment and can also help to produce suitably engineered biochars (Harvey et al., 2012a).

In this study, we investigated the link between the two molecular marker approaches. Despite having different analysis windows, both methods target a part of the characteristic PyOM polycyclic aromatic features that become increasingly condensed with higher charring temperatures (McBeath et al., 2011). The aim was to test if the conceptually feasible overlap between the small aromatic PAH moieties and the larger, condensed polycyclic structures, as indicated by BPCAs, can be assessed with the two methods when applied to real pyrogenic sample materials. We thus measured PAHs and BPCAs on two different straws (rye and maize) and their corresponding chars with highest heating temperatures (HTT) of 300, 400 and 500 °C, respectively. Moreover, we also analyzed BPCAs on the same lipid extracts, on which PAHs were measured, and determined BPCAs on the resulting extraction residues, too.

Materials and methods

Chars were produced by heating rye *(Secale cereal* L.) and maize (*Zea mays* L.) straw samples for 2 hours in a pre-heated muffle furnace at 300, 400 and 500 °C, respectively (Rennert et al., 2008). Al foil was used to limit oxidation during the charring process. Straw and char samples were subsequently milled to fine powder before chemical analysis.

Organic carbon contents were measured using elemental analysis (Leco CS 225, Mönchengladbach Germany). Lipids from all samples were extracted using the accelerated solvent extraction method (Dionex ASE 200, Sunnyvale, CA) with CH_2Cl_2/CH_3OH (93/7; v/v) as described by Wiesenberg et al. (2004; 2008; 2009). Aromatic hydrocarbons were then measured after sequential chromatographic separation (Radke et al., 1980) on GC/MS (HP 5890 Series II GC and HP 5989A mass spectrometer, Palo Alto, CA). Detailed data from the PAH analysis of the samples were reported by Wiesenberg et al. (2009), while we here used specific statistics of these results with the focus to assess the linkages between the PAH and BPCA method.

BPCAs were measured on bulk materials (the two straws and all their charred analogues) as well as on the respective products from the lipid analysis (the lipid extracts and the lipid extraction residues). The lipid extracts of the 500 °C chars did not yield enough material to be amenable for BPCA analysis. BPCAs were analyzed following the procedure reported by Brodowski et al. (2005). Method-inherent underestimation of PyOM was not corrected by any conversion factor (Schneider et al., 2010). For consistency purposes, we used gas chromatography protocols for both PAH and BPCA quantification. However, both methods

have recently been adapted to liquid chromatography, which offers an interesting alternative for the assessment of these markers, particularly in environmental samples (Denis et al., 2012; Wiedemeier et al., 2013).

Data analysis was conducted with the statistical software R (R, 2011).

Results and discussion

PAH abundance was undetectable in the straw materials, highest for the Maize 400 char and was considerable for all chars that were pyrolyzed between 300 and 500 °C (Figure 1; top). This is in line with previous studies (Brown et al., 2006; Kloss et al., 2012) and indicates the potentially problematic use of low-temperature biochars as a soil amendment due to their usually high content of harmful PAH (Keiluweit et al., 2012). Moreover, a typical pattern between the proportion of PAHs with different ring sizes and the pyrolysis temperature was observed: The proportion of small PAHs (3-ring) decreased while the contribution of higher molecular weight PAHs (4-6 ring) increased with increasing temperature (Figure 1; bottom). Similar trends have been observed in other studies (McGrath et al., 2003; Brown et al., 2006; Keiluweit et al., 2012) and point to the increasingly condensed nature of the solid PyOM residue (the char) while losses of the smaller, more volatile PAHs occur with increasing charring temperature (McGrath et al., 2003).

The BPCA method detects these large, condensed polycyclic structures of non-volatile PyOM and consequently showed increasing amounts of BPCA quantity with increasing temperature in the bulk char samples (Figure 2; black bars). Besides the total BPCA yields normalized to bulk weight, also the proportion of BPCA normalized to organic carbon increased with temperature. The latter is a measure for the aromaticity of charred materials (McBeath et al., 2011) and is consistently higher for rye-derived chars than for the maize-based char samples (Figure 2; upper number). This difference in aromaticity was partially reflected by the data obtained from the PAH analysis, as the rye chars showed higher proportions of the larger PAHs than the maize chars (Figure 1). However, the relationship between PAH ring sizes and aromaticity of PyOM are complex and not entirely resolved yet (Wiedemeier et al., 2014). The BPCA analysis furthermore yields a measure for the degree of aromatic condensation with the ratio of B6CAs to total BPCA content (Schneider et al., 2011). The aromatic condensation was very similar for both, maize and rye chars, at each respective charring temperature and comparable to previously reported values for a variety of charred materials (Schneider et al., 2011; Wiedemeier et al., 2014). It indicates that temperature is the main factor controlling condensation and that an assessment of the aromatic condensation in PyOM is possibly useful to estimate its pyrolysis temperature. Moreover, the degree of aromatic condensation in PyOM has been directly associated to its stability against degradation in the environment (Harvey et al., 2012b; Wurster et al., 2013; Fang et al., 2014). Our results in combination with previously reported data (Wiedemeier et al., 2014) therefore

support the assumption that the C sequestration potential of charred lignocellulose material is largely determined by its pyrolysis temperature (Bruun et al., 2011; Fang et al., 2014).

When lipid extraction was applied on the bulk straw and char samples, a part of the polycyclic PyOM structures was extracted with it, too, while another part remained in the extraction residue, as shown by the BPCA analysis in Figure 2 (white and striped bars, respectively). The lipid extract always comprised a much smaller part (< 10 % of bulk dry weight) than the extraction residue and became smaller for chars pyrolyzed at higher temperatures, following a trend, which has been reported for other chars, too (Wiesenberg et al., 2009; Wiedemeier et al., 2014). However, the proportion of lipid extracted PyOM increased with charring temperature (Figure 2; white bars), which is explained by the increased availability of these polycyclic structures and a concomitant decrease of other lipids with higher HTT (Wiesenberg and Brodowski, 2007; Wiesenberg et al., 2009). At the same time, the much larger (> 90 % of bulk dry weight) lipid extraction residue comprised a similar proportion of BPCA-detectable PyOM as the lipid extract, also increasing with temperature (Figure 2; striped bars).

Having a closer look at the contributions of the individual BPCAs that make up the above reported BPCA contents can reveal further qualitative information about the PyOM found in bulk samples, lipid extracts and lipid extraction residues (Figure 3). In particular, the size of the PyOM polycyclic clusters can be inferred, as the more carboxylated B6CA and B5CA must derive from larger polycyclic clusters than the less carboxylated B4- and B3CAs (Hammes et al., 2008; Schneider et al., 2010). Since the extraction residue inherited most of the bulk PyOM by mass (> 90 % of bulk dry weight), it is not surprising that it showed almost the same BPCA pattern like the bulk chars, dominated by B6- and B5CAs (Figure 3). Bulk chars and the lipid extraction residues thus mostly consisted of relatively large, condensed polycyclic sheets, comprising probably the most stable aromatic phases of the chars (Franklin, 1951; Cohen-Ofri et al., 2006; Keiluweit et al., 2010). In contrast, the lipid extractable BPCAs of both rye and maize chars across all pyrolysis temperatures were mostly composed of smaller polycyclic compounds, as indicated by the predominance of B3- and B4CAs. The larger polycyclic clusters that prevailed in the bulk samples (57 – 67 % of B5- and B6CA) thus remained in the extraction residue (57 – 64 % of B5- and B6CA) while small polycyclic compounds were preferentially released during the lipid extraction (51 – 59 % of B3- and B4CA).

The overlap between the PAH and the BPCA method consequently concerns mostly the smallest BPCA-detectable polycyclic clusters. When BPCA analysis was performed on the lipid extracts for direct comparison, we found significant logarithmic relationships ($p < 0.05$, $R^2 > 0.9$) between the proportion of B3CAs and the abundance of most PAHs that were considered in this study (Figure 4). The relationship was independent of the molecular weight of the PAHs and was equally valid for total PAH abundance. However, the proportion of B3CA was the only direct predictor of PAH abundance, while proportions of more carboxylated BPCAs in the lipid fraction showed more complicated relationships with

PAH abundance (cf. supplementary material). This is in line with theoretical considerations (Glaser et al., 1998; Dittmar, 2008), after which the majority of the abundant small PAHs (cf. Figure 1) are prone to yield B3- or B4CAs and only less abundant, larger PAH species, such as benzo[a]pyrene or larger condensed polycyclic sheets, can be oxidized into more carboxylated BPCAs. It is unfortunate that the 500 °C chars did not yield enough lipid extract for BPCA analysis, which is why the comparison of the two methods could not be conducted directly on the lipid extracts for the highest HTT of this study. However, as condensation of bulk chars increased (cf. Figure 2) but extractability of B5- and B6CA decreased with higher temperature (cf. Figure 3), a similar B3CA proportion can be expected in the 500 °C as in the 400 °C lipid extracts, correlating with the still high PAH abundances at 500 °C (cf. Figure 1). Our findings confirm that the analysis windows of the PAH and the BPCA method overlap each other within the lipid fraction. Although the linkage between the two molecular marker methods has been shown for pure chemical standards (Dittmar, 2008), to the best of our knowledge, it is the first time that the theory-based relationship was established empirically on real char samples. However, it is worth noting that no relationship could be established when both methods were applied directly on the bulk chars according to their normal protocol, as the BPCA analysis was then not limited to the lipid fraction only.

This study highlighted the similarities and differences of the two most common molecular marker methods for PyOM. Despite having minimally overlapping analysis windows and traditionally serving different research purposes, they are both highly informative for PyOM characterization as they provide valuable information about its molecular composition that is strongly linked to combustion conditions. We could demonstrate that the two molecular marker approaches find common ground when the lipid fraction is considered, which confirms the validity and theoretical assumptions of both methods. Large benefits can derive from the simultaneous application of the PAH and the BPCA method to relevant environmental sample materials. The combination of both methods can lead to a better source apportionment of PyOM in soils and sediments and illuminate the pathways and fluxes of differently sized and pyrolysed PyOM through environmental compartments. Even more information about PyOM in the environment can be retrieved from compound-specific isotopic analysis of both PAH and BPCA molecular markers (Ziolkowski and Druffel, 2010; Xu et al., 2012; Coppola et al., 2013; Slater et al., 2013; Gierga et al., 2014), which is why it is crucial to understand the here presented relationships between these two approaches.

Acknowledgements

Thilo Rennert (University of Hohenheim, Germany) is thanked for preparing and providing charred samples. We gratefully acknowledge financial support of the current study by the German Research Foundation under contract WI 2810 / 9-1.

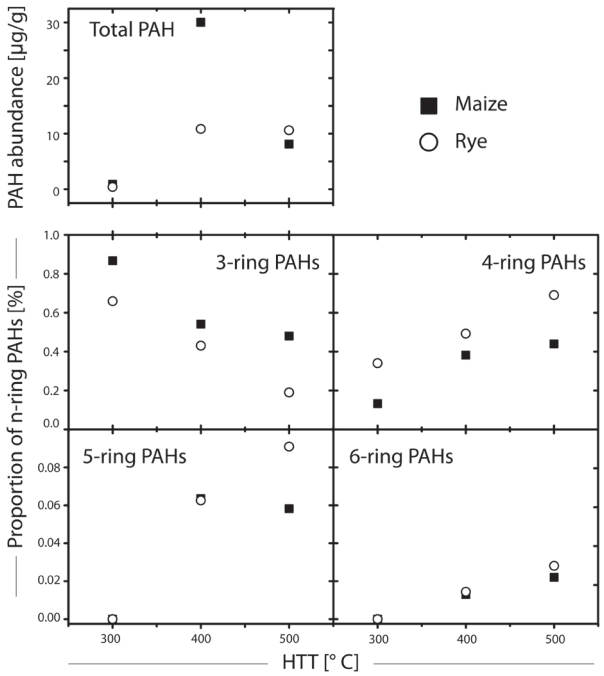

Figure 1. Absolute (top) and relative (bottom) abundance of PAHs changed with highest heating temperature (HTT). Small, 3-ring PAHs were most abundant at HTT of 300 °C and decreased with higher HTT while 4-ring PAHs became more abundant with higher HTT. The larger PAHs (5- and 6-ring) contributed a much smaller proportion to total PAH (cf. y-axis scale is stretched by a factor of 10) and their abundance increased with higher HTT, consistent with an increasing degree of aromatic condensation as revealed by BPCAs (cf. Fig. 2).

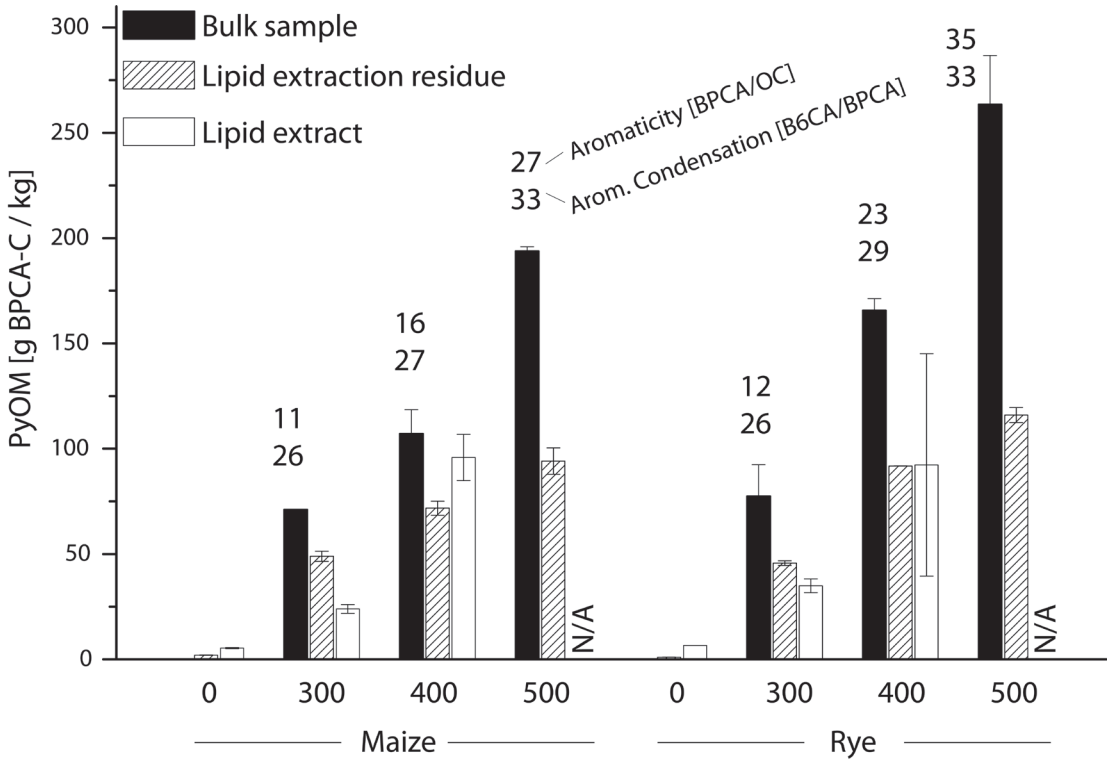

Figure 2. PyOM measured as BPCAs in the bulk materials (maize/rye straw and chars), the respective lipid extracts and the remaining lipid extraction residues. The aromaticity and degree of aromatic condensation of the bulk samples increased with increasing HTT. Likewise, the PyOM content in the lipid extracts and in the lipid extraction residues increased with increasing HTT. The lipid extracts of the chars produced at 500 °C did not yield sufficient sample amounts for BPCA analysis.

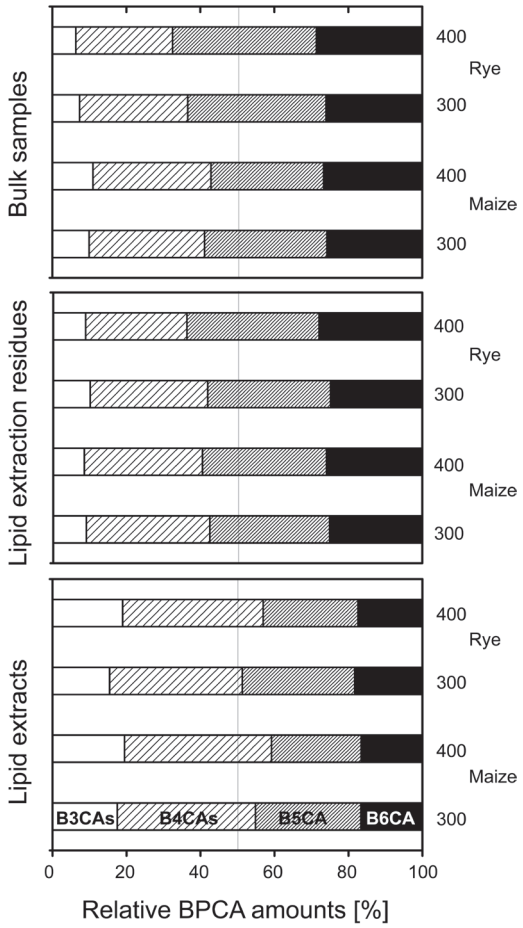

Figure 3. BPCA signatures of bulk chars, their lipid extracts and the corresponding lipid extraction residues. Larger PyOM polycyclic structures, indicated by B5CA and B6CA, were retained in the lipid extraction residues, while B3CA and B4CA, indicative of smaller polycyclic compounds, were preferentially extracted and accounted for more than 50 % of all BPCAs in the lipid extracts.

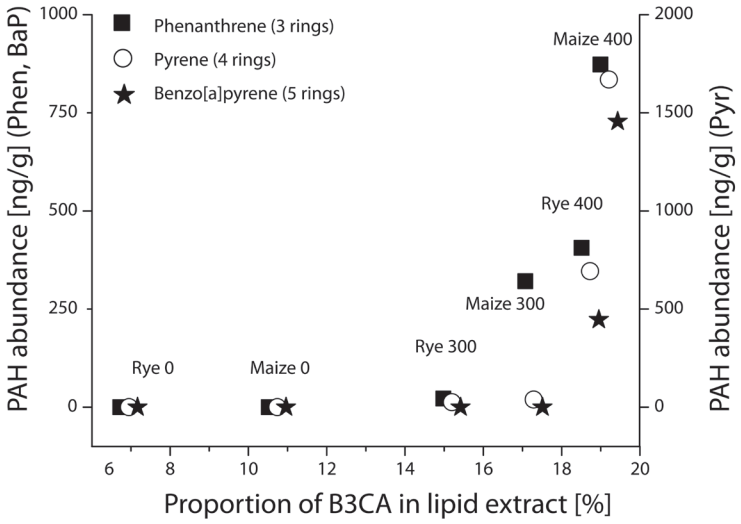

Figure 4. The proportion of B3CA in the lipid extracts correlated with PAH abundance. Data is shown for three different PAH sizes and is indicative for all PAHs considered in this study as well as for total PAH abundance. The correlation confirms that the measurement window of PAH analysis overlaps with B3CA analysis in the lipid extracts while no correlation could be found between PAHs and more carboxylated BPCAs, indicative of larger polycyclic clusters that would escape PAH analysis.

References

Boffetta, P., Jourenkova, N., Gustavsson, P., 1997. Cancer risk from occupational and environmental exposure to polycyclic aromatic hydrocarbons. Cancer Causes & Control 8, 444-472.

Bond, T.C., Doherty, S.J., Fahey, D.W., Forster, P.M., Berntsen, T., Deangelo, B.J., Flanner, M.G., Ghan, S., Kärcher, B., Koch, D., Kinne, S., Kondo, Y., Quinn, P.K., Sarofim, M.C., Schultz, M.G., Schulz, M., Venkataraman, C., Zhang, H., Zhang, S., Bellouin, N., Guttikunda, S.K., Hopke, P.K., Jacobson, M.Z., Kaiser, J.W., Klimont, Z., Lohmann, U., Schwarz, J.P., Shindell, D., Storelvmo, T., Warren, S.G., Zender, C.S., 2013. Bounding the role of black carbon in the climate system: A scientific assessment. Journal of Geophysical Research D: Atmospheres 118, 5380-5552.

Brodowski, S., Rodionov, A., Haumaier, L., Glaser, B., Amelung, W., 2005. Revised black carbon assessment using benzene polycarboxylic acids. Organic Geochemistry 36, 1299-1310.

Brown, R.A., Kercher, A.K., Nguyen, T.H., Nagle, D.C., Ball, W.P., 2006. Production and characterization of synthetic wood chars for use as surrogates for natural sorbents. Organic Geochemistry 37, 321-333.

Bruun, E.W., Hauggaard-Nielsen, H., Ibrahim, N., Egsgaard, H., Ambus, P., Jensen, P.A., Dam-Johansen, K., 2011. Influence of fast pyrolysis temperature on biochar labile fraction and short-term carbon loss in a loamy soil. Biomass and Bioenergy 35, 1182-1189.

Bucheli, T.D., Blum, F., Desaules, A., Gustafsson, Ö., 2004. Polycyclic aromatic hydrocarbons, black carbon, and molecular markers in soils of Switzerland. Chemosphere 56, 1061-1076.

Cohen-Ofri, I., Weiner, L., Boaretto, E., Mintz, G., Weiner, S., 2006. Modern and fossil charcoal: aspects of structure and diagenesis. Journal Of Archaeological Science 33, 428-439.

Colmsjö, A., 1998. Concentration and Extraction of PAHs from Environmental Samples, in: Neilson, A. (Ed.), PAHs and Related Compounds. Springer, Berlin, Germany, pp. 55-76.

Coppola, A.I., Ziolkowski, L.A., Druffel, E.R.M., 2013. Extraneous carbon assessments in radiocarbon measurements of black carbon in environmental matrices. Radiocarbon 55, 1631-1640.

Denis, E.H., Toney, J.L., Tarozo, R., Scott Anderson, R., Roach, L.D., Huang, Y., 2012. Polycyclic aromatic hydrocarbons (PAHs) in lake sediments record historic fire events: Validation using HPLC-fluorescence detection. Organic Geochemistry 45, 7-17.

Dittmar, T., 2008. The molecular level determination of black carbon in marine dissolved organic matter. Organic Geochemistry 39, 396-407.

Fabbri, D., Rombolà, A.G., Torri, C., Spokas, K.A., 2013. Determination of polycyclic aromatic hydrocarbons in biochar and biochar amended soil. Journal of Analytical and Applied Pyrolysis 103, 60-67.

Fang, Y., Singh, B., Singh, B.P., Krull, E., 2014. Biochar carbon stability in four contrasting soils. European Journal of Soil Science 65, 60-71.

Flannigan, M., Cantin, A.S., De Groot, W.J., Wotton, M., Newbery, A., Gowman, L.M., 2013. Global wildland fire season severity in the 21st century. Forest Ecology and Management 294, 54-61.

Franklin, R.E., 1951. Crystallite growth in graphitizing and non-graphitizing carbons. Proceedings of the Royal Society of London Series A 209, 196-218.

Gierga, M., Schneider, M.P.W., Wiedemeier, D.B., Lang, S.Q., Smittenberg, R.H., Hajdas, I., Bernasconi, S., Schmidt, M.W.I., 2014. Purification of fire-derived markers for μg scale isotope analysis ($\delta^{13}C$, $\Delta^{14}C$) using high-performance liquid chromatography (HPLC). Organic Geochemistry (in press).

Glaser, B., Haumaier, L., Guggenberger, G., Zech, W., 1998. Black carbon in soils: the use of benzenecarboxylic acids as specific markers. Organic Geochemistry 29, 811-819.

Guggenberger, G., Rodionov, A., Shibistova, O., Grabe, M., Kasansky, O.A., Fuchs, H., Mikheyeva, N., Zrazhevskaya, G., Flessa, H., 2008. Storage and mobility of black carbon in permafrost soils of the forest tundra ecotone in Northern Siberia. Global Change Biology 14, 1367-1381.

Hale, S.E., Lehmann, J., Rutherford, D., Zimmerman, A.R., Bachmann, R.T., Shitumbanuma, V., O'Toole, A., Sundqvist, K.L., Arp, H.P.H., Cornelissen, G., 2012. Quantifying the total and bioavailable polycyclic aromatic hydrocarbons and dioxins in biochars. Environmental Science & Technology 46, 2830-2838.

Hammes, K., Schmidt, M.W.I., Smernik, R.J., Currie, L.A., Ball, W.P., Nguyen, T.H., Louchouarn, P., Houel, S., Gustafsson, O., Elmquist, M., Cornelissen, G., Skjemstad, J.O., Masiello, C.A., Song, J., Peng, P., Mitra, S., Dunn, J.C., Hatcher, P.G., Hockaday, W.C., Smith, D.M., Hartkopf-Froeder, C., Boehmer, A., Luer, B., Huebert, B.J., Amelung, W., Brodowski, S., Huang, L., Zhang, W., Gschwend, P.M., Flores-Cervantes, D.X., Largeau, C., Rouzaud, J.N., Rumpel, C., Guggenberger, G., Kaiser, K., Rodionov, A., Gonzalez-Vila, F.J., Gonzalez-Perez, J.A., de la Rosa, J.M., Manning, D.A.C., Lopez-Capel, E., Ding, L., 2007. Comparison of quantification methods to measure fire-derived (black/elemental) carbon in soils and sediments using reference materials from soil, water, sediment and the atmosphere. Global Biogeochemical Cycles 21, GB3016.

Hammes, K., Torn, M., Lapenas, A., Schmidt, M., 2008. Centennial black carbon turnover observed in a Russian steppe soil. Biogeosciences 5, 1339-1350.

Harvey, O., Kuo, L.-J., Zimmerman, A., Louchouarn, P., Amonette, J., Herbert, B., 2012a. An index-based approach to assessing recalcitrance and soil carbon sequestration potential of engineered black carbons (biochars). Environmental Science & Technology 46, 1415-1421.

Harvey, O.R., Herbert, B.E., Kuo, L.-J., Louchouarn, P., 2012b. Generalized two-dimensional perturbation correlation infrared spectroscopy reveals mechanisms for the development of surface charge and recalcitrance in plant-derived biochars. Environmental Science & Technology 46, 10641-10650.

Hilber, I., Blum, F., Leifeld, J., Schmidt, H.P., Bucheli, T.D., 2012. Quantitative determination of PAHs in biochar: A prerequisite to ensure its quality and safe application. Journal of Agricultural and Food Chemistry 60, 3042-3050.

Keiluweit, M., Kleber, M., Sparrow, M.A., Simoneit, B.R.T., Prahl, F.G., 2012. Solvent-extractable polycyclic aromatic hydrocarbons in biochar: influence of pyrolysis temperature and feedstock. Environmental Science & Technology 46, 9333-9341.

Keiluweit, M., Nico, P.S., Johnson, M.G., Kleber, M., 2010. Dynamic molecular structure of plant biomass-derived black carbon (biochar). Environmental Science & Technology 44, 1247-1253.

Kelly, R., Chipman, M.L., Higuera, P.E., Stefanova, I., Brubaker, L.B., Hu, F.S., 2013. Recent burning of boreal forests exceeds fire regime limits of the past 10,000 years. Proceedings of the National Academy of Sciences of the United States of America 110, 13055-13060.

Kloss, S., Zehetner, F., Dellantonio, A., Hamid, R., Ottner, F., Liedtke, V., Schwanninger, M., Gerzabek, M.H., Soja, G., 2012. Characterization of slow pyrolysis biochars: Effects of feedstocks and pyrolysis temperature on biochar properties. Journal of Environmental Quality 41, 990-1000.

Kuzyakov, Y., Bogomolova, I., Glaser, B., 2014. Biochar stability in soil: Decomposition during eight years and transformation as assessed by compound-specific ^{14}C analysis. Soil Biology and Biochemistry 70, 229-236.

Lehmann, J., Joseph, S., 2009. Biochar for Environmental Management - An Introduction, in: Lehmann, J., Joseph, S. (Eds.), Biochar for Environemental Management: Science and Technology. Earthscan, London, UK, pp. 1-12.

Marschner, B., Brodowski, S., Dreves, A., Gleixner, G., Gude, A., Grootes, P.M., Hamer, U., Heim, A., Jandl, G., Ji, R., Kaiser, K., Kalbitz, K., Kramer, C., Leinweber, P., Rethemeyer, J., Schaeffer, A., Schmidt, M.W.I., Schwark, L., Wiesenberg, G.L.B., 2008. How relevant is recalcitrance for the stabilization of organic matter in soils? Journal of Plant Nutrition and Soil Science 171, 91-110.

McBeath, A., Smernik, R., Plant, E., 2011. Determination of the aromaticity and the degree of aromatic condensation of a thermosequence of wood charcoal using NMR. Organic Geochemistry 42, 1194-1202.

McGrath, T.E., Geoffrey Chan, W., Hajaligol, M.R., 2003. Low temperature mechanism for the formation of polycyclic aromatic hydrocarbons from the pyrolysis of cellulose. Journal of Analytical and Applied Pyrolysis 66, 51-70.

Meyer, S., Glaser, B., Quicker, P., 2011. Technical, economical, and climate-related aspects of biochar production technologies: a literature review. Environmental Science & Technology 45, 9473-9483.

Oleszczuk, P., Jośko, I., Kuśmierz, M., 2013. Biochar properties regarding to contaminants content and ecotoxicological assessment. Journal of Hazardous materials 260, 375-382.

Oros, D.R., Simoneit, B.R.T., 2001a. Identification and emission factors of molecular tracers in organic aerosols from biomass burning Part 1. Temperate climate conifers. Applied Geochemistry 16, 1513-1544.

Oros, D.R., Simoneit, B.R.T., 2001b. Identification and emission factors of molecular tracers in organic aerosols from biomass burning Part 2. Deciduous trees. Applied Geochemistry 16, 1545-1565.

Quilliam, R.S., Rangecroft, S., Emmett, B.A., Deluca, T.H., Jones, D.L., 2013. Is biochar a source or sink for polycyclic aromatic hydrocarbon (PAH) compounds in agricultural soils? GCB Bioenergy 5, 96-103.

R, 2011. R: A language and environment for statistical computing. R Foundation for Statistical Computing.

Radke, M., Willsch, H., Welte, D.H., 1980. Preparative hydrocarbon group type determination by automated medium pressure liquid chromatography. Analytical Chemistry 52, 406-411.

Rennert, T., Kaufhold, S., Brodowski, S., Mansfeldt, T., 2008. Interactions of ferricyanide with humic soils and charred straw. European Journal of Soil Science 59, 348-358.

Rodionov, A., Amelung, W., Peinemann, N., Haumaier, L., Zhang, X., Kleber, M., Glaser, B., Urusevskaya, I., Zech, W., 2010. Black carbon in grassland ecosystems of the world. Global Biogeochemical Cycles 24, GB3013.

Sánchez-García, L., de Andrés, J.R., Gélinas, Y., Schmidt, M.W.I., Louchouarn, P., 2013. Different pools of black carbon in sediments from the Gulf of Cádiz (SW Spain): Method comparison and spatial distribution. Marine Chemistry 151, 13-22.

Schmidt, M.W.I., Noack, A.G., 2000. Black carbon in soils and sediments: Analysis, distribution, implications, and current challenges. Global Biogeochemical Cycles 14, 777-793.

Schneider, M.P.W., Hilf, M., Vogt, U.F., Schmidt, M.W.I., 2010. The benzene polycarboxylic acid (BPCA) pattern of wood pyrolyzed between 200 °C and 1000 °C. Organic Geochemistry 41, 1082-1088.

Schneider, M.P.W., Smittenberg, R., Dittmar, T., Schmidt, M.W.I., 2011. Comparison of gas with liquid chromatography for the determination of benzenepolycarboxylic acids as molecular tracers of black carbon. Organic Geochemistry 42, 275-282.

Simoneit, B.R.T., 2002. Biomass burning -- a review of organic tracers for smoke from incomplete combustion. Applied Geochemistry 17, 129-162.

Simoneit, B.R.T., Fraser, M.P., Schauer, J.J., Nolte, C.G., Oros, D.R., Elias, V.O., Rogge, W.F., Cass, G.R., 1999. Levoglucosan, a tracer for cellulose in biomass burning and atmospheric particles. Atmospheric Environment 33, 173-182.

Slater, G.F., Benson, A.A., Marvin, C., Muir, D., 2013. PAH fluxes to Siskiwit revisted: Trends in fluxes and sources of pyrogenic PAH and perylene constrained via radiocarbon analysis. Environmental Science and Technology 47, 5066-5073.

Wiedemeier, D.B., Abiven, S., Hockaday, W.C., Keiluweit, M., Kleber, M., Pyle, L.A., Masiello, C.A., McBeath, A.V., Nico, P.S., Schneider, M.P.W., Smernik, R.J., Wiesenberg, G.L.B., Schmidt, M.W.I., 2014. Aromaticity and aromatic condensation of chars. Organic Geochemistry (in review).

Wiedemeier, D.B., Hilf, M.D., Smittenberg, R.H., Haberle, S.G., Schmidt, M.W.I., 2013. Improved assessment of pyrogenic carbon quantity and quality in environmental samples by high-performance liquid chromatography. Journal of Chromatography A 1304, 246-250.

Wiesenberg, G.L.B., Brodowski, S., 2007. Veränderungen der Zusammensetzung und Überlagerung von Lipiden und Black Carbon infolge der Verkohlung von Pflanzenmaterial. Mitteilungen der Deutschen Bodenkundlichen Gesellschaft 110, 315-316.

Wiesenberg, G.L.B., Lehndorff, E., Schwark, L., 2009. Thermal degradation of rye and maize straw: lipid pattern changes as a function of temperature. Organic Geochemistry 40, 167-174.

Wiesenberg, G.L.B., Schmidt, M.W.I., Schwark, L., 2008. Plant and soil lipid modifications under elevated atmospheric CO2 conditions: I. Lipid distribution patterns. Organic Geochemistry 39, 91-102.

Wiesenberg, G.L.B., Schwark, L., Schmidt, M.W.I., 2004. Improved automated extraction and separation procedure for soil lipid analyses. European Journal of Soil Science 55, 349-356.

Wilcke, W., 2000. Polycyclic aromatic hydrocarbons (PAHs) in soil — A review. Journal of Plant Nutrition and Soil Science 163, 229-248.

Wurster, C.M., Saiz, G., Schneider, M.P.W., Schmidt, M.W.I., Bird, M.I., 2013. Quantifying pyrogenic carbon from thermosequences of wood and grass using hydrogen pyrolysis. Organic Geochemistry 62, 28-32.

Xu, L., Zheng, M., Ding, X., Edgerton, E.S., Reddy, C.M., 2012. Modern and fossil contributions to polycyclic aromatic hydrocarbons in PM 2.5 from North Birmingham, Alabama in the Southeastern U.S. Environmental Science and Technology 46, 1422-1429.

Yunker, M.B., Macdonald, R.W., Vingarzan, R., Mitchell, R.H., Goyette, D., Sylvestre, S., 2002. PAHs in the Fraser River basin: a critical appraisal of PAH ratios as indicators of PAH source and composition. Organic Geochemistry 33, 489-515.

Ziolkowski, L., Druffel, E., 2010. Aged black carbon identified in marine dissolved organic carbon. Geophysical Research Letters 37, L16601.

Supplementary material

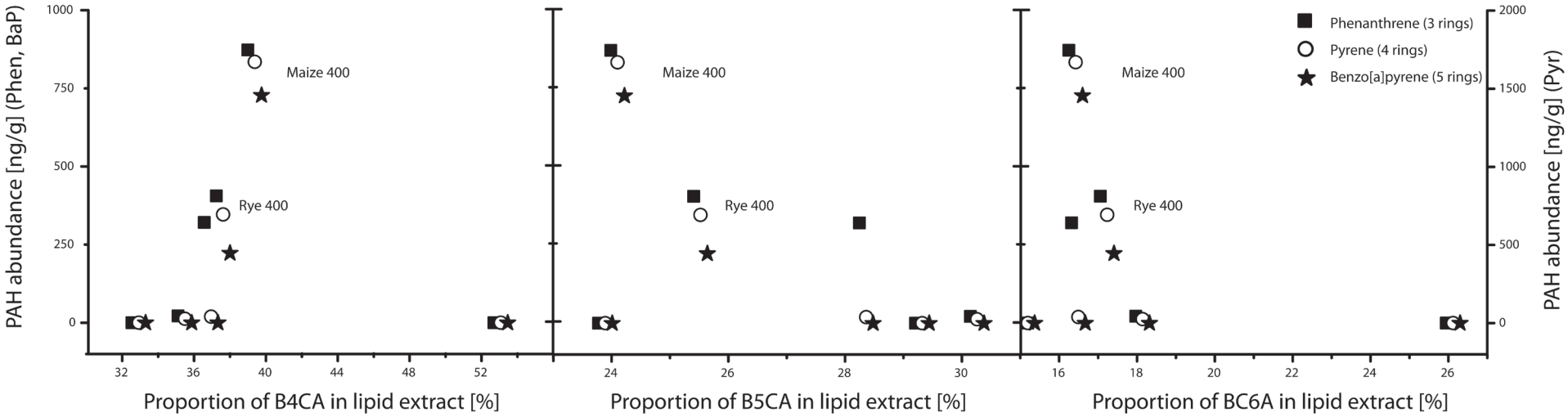

Table S1. The proportions of B4-, B5- and B6CA in the lipid extracts did not show any consistent relationships with PAH abundance of phenanthrene (Phen), benzo[a]pyrene (BaP) or pyrene (Pyr) that were measured in the same lipid extracts. This is in contrast to the proportions of B3CA in the lipid extracts, which showed strong logarithmic relationships with all measured PAH (cf. main article).

Curriculum vitae

Research Experience

04.2010 – present **Research assistant**
University of Zürich, Soil Science and Biogeochemistry (CH)
in collaboration with ETH Zurich (CH), University of Bern (CH), CSIRO Adelaide (AU) and ANU Canberra (AU)

- Method development for PyC characterization
- Molecular marker and isotopic analysis
- Statistical analysis of multivariate data
- Scientific writing and presentation
- Teaching duties in soil science, biogeochemistry and ethics

09.2008 – 09.2009 **Research assistant**
Swiss Federal Inst. for Forest, Snow and Landscape Research (CH)
in collaboration with Sokoine University Morogoro (TZ)

- Reconstruction of vegetation dynamics in subtropical Eastern-Africa with C and N isotopes in soil organic matter

Education

04.2010 – present **PhD in Physical Geography**
University of Zürich, Soil Science and Biogeochemistry

- PhD project: "Geochemical tools for PyC characterization and quantification"
  (Prof. Michael W. I. Schmidt, UZH)
- Research stays at ANU and CSIRO (AU)
- Postgraduate diploma in statistics, ETH

09.2007 – 09.2009 **MSc in Physical Geography**
University of Zürich, Soil Science and Biogeochemistry

- MSc thesis: "Vegetation dynamics in the Tanzanian savanna: evidence from stable isotopes in soil organic matter"
  (Dr. Frank Hagedorn, WSL)
- Research stay at Sokoine University (TZ)

10.2003 – 09.2007 **BSc in Geography**
University of Zürich, Remote Sensing Laboratories

- BSc thesis: "Thermal hyperspectral remote sensing"
  (Dr. Mathias Kneubühler, UZH)
- Minor in Economics, UZH
- Exchange semester at ETH Lausanne

09. 1999 – 07.2003 **High School Wohlen (Latin Matura)**

- High school exchange year in Oregon (USA)
- Bilingual high school (German/French)

Research awards

- Best presentation at Intl. Soil Organic Matter workshop (SOM 5), Ascona, 2012.
- Young Scientist Travel Award by ESF (European Science Foundation) Network MOLTER, 2011.

Peer-reviewed publications

- **Wiedemeier DB**, Brodowski S, Wiesenberg GLB (2014) Pyrogenic molecular markers: Linking PAH with BPCA analysis. *Chemosphere* (in review).
- McFarlane KJ, Mambelli S, Porras RC, **Wiedemeier DB**, Murphy L, Orans K, Dawson TE, Torn MS (2014) Contrasting belowground carbon budgets for coast redwood forest and adjacent prairie. *Journal of Geophysical Research: Biogeosciences* (in review).
- **Wiedemeier DB,** Abiven S, Hockaday WC, Keiluweit M, Kleber M, Pyle LA, Masiello CA, McBeath AV, Nico PS, Schneider MPW, Smernik RJ, Wiesenberg GLB, Schmidt MWI (2014) Aromaticity and degree of aromatic condensation of chars. *Organic Geochemistry* (in review).
- Gierga M, Schneider MPW, **Wiedemeier DB,** Lang SQ, Smittenberg RH, Hajdas I, Bernasconi S, Schmidt MWI (2014) Purification of fire-derived markers for μg scale isotope analysis ($\delta^{13}C$, $\Delta^{14}C$) using high-performance liquid chromatography (HPLC). *Organic Geochemistry* (in press).
- **Wiedemeier DB**, Hilf MD, Smittenberg RH, Schmidt MWI (2013) Improved assessment of pyrogenic carbon quantity and quality in environmental samples by high-performance liquid chromatography. *Journal of Chromatography A* 1304, 246-250.
- **Wiedemeier DB,** Bloesch U, Hagedorn F (2012) Stable forest-savanna mosaic in north-western Tanzania: local-scale evidence from $\delta^{13}C$ signatures and ^{14}C ages of soil fractions. *Journal of Biogeography* 39, 247-257.

Conference contributions

Oral presentations

- **Wiedemeier DB,** Hilf MD, Smittenberg RH, Schmidt MWI. Improved assessment of pyrogenic carbon quantity and quality in soils by liquid chromatography. Bodenkundliche Gesellschaft Schweiz (BGS) Jahrestagung, Reckenholz, Switzerland. Feb 7-8, 2013.
- **Wiedemeier DB,** Hilf MD, Schmidt, MWI. Improved quantification of pyrogenic carbon in soils by a HPLC-DAD method. 4th international Congress of the European Confederation of Soil Science Societies (EUROSOIL), Bari, Italy. Jul 2– 6, 2012.
- **Wiedemeier DB,** Hilf MD, Smittenberg RH, Schmidt MWI. Improved quantification of pyrogenic carbon in environmental samples – the use of HPLC to quantify BPCAs in matrix samples. European Geoscience Union (EGU) – General Assembly 2012, Vienna, Austria. Apr 22– 27, 2012.

- **Wiedemeier DB,** Colombaroli D, Haberle SG, Krull ES, Schmidt MWI. New molecular marker and spectroscopic tools for reconstructing wildfire history. 18th International Union for Quaternary Research (INQUA) Congress, Bern, Switzerland. Jul 21– 27, 2011.

Poster presentations

- **Wiedemeier DB,** Abiven S, Hockaday WC, Keiluweit M, Kleber M, Pyle LA, Masiello, CA, McBeath AV, Nico PS, Schneider MPW, Smernik RJ, Wiesenberg GLB, Schmidt, MWI. Aromaticity and the degree of aromatic condensation of pyrogenic carbon. American Geoscience Union (AGU) Fall Meeting, San Francisco, USA. Dec 9-13, 2013.
- **Wiedemeier DB,** Abiven S, Hockaday WC, Keiluweit M, Kleber M, Pyle LA, Masiello, CA, McBeath AV, Nico PS, Schneider MPW, Smernik RJ, Wiesenberg GLB, Schmidt MWI. Aromaticity and the degree of aromatic condensation of chars. 26th International Meeting on Organic Geochemistry (IMOG), Tenerife, Spain. Sep 16-20, 2013.
- **Wiedemeier DB,** Hilf MD, Smittenberg RH, Schmidt MWI. Improved assessment of pyrogenic carbon in soils by liquid chromatography. Jahrestagung der Deutschen Bodenkundlichen Gesellschaft 2013, Rostock, Germany. Sep 7– 12, 2013.
- **Wiedemeier DB,** Abiven S, Hockaday WC, Keiluweit M, Kleber M, Pyle LA, Masiello CA, McBeath AV, Nico PS, Schneider MPW, Smernik R, Schmidt MWI. A method comparison to infer charring temperature, aromaticity and the degree of condensation of pyrogenic carbon. European Geoscience Union (EGU) – General Assembly 2013, Vienna, Austria. Apr 7– 12, 2013.
- **Wiedemeier DB,** Hilf MD, Smittenberg RH, Schmidt MWI. Improved assessment of pyrogenic carbon quantity and quality in soils by liquid chromatography. European Geoscience Union (EGU) – General Assembly 2013, Vienna, Austria. Apr 7– 12, 2013.
- **Wiedemeier DB,** Hilf MD, Schmidt MWI. Improved quantification of pyrogenic carbon in soils and sediments by a HPLC-DAD method. 5th International Workshop on Soil and Sedimentary Organic Matter Stabilization and Destabilization (SOM5), Ascona, Switzerland. Oct 7– 11, 2012.
- **Wiedemeier DB,** Haberle SG, Krull ES, Schmidt MWI. New molecular marker and spectroscopic tools for reconstructing wildfire history. 25th International Meeting on Organic Geochemistry (IMOG), Interlaken, Switzerland. Sep 18 –23, 2011.
- **Wiedemeier DB,** Haberle SG, Krull ES, Schmidt MWI. New molecular marker and spectroscopic tools for reconstructing wildfire history. European Geoscience Union (EGU) – General Assembly 2011, Vienna, Austria. Apr 3– 8, 2011.
- **Wiedemeier DB,** Haberle SG, Krull ES, Schmidt MWI. New molecular marker and spectroscopic tools for reconstructing wildfire history from sedimentary records. 16th Australian Geochemistry Conference (AOGC), Canberra, Australia. Dec 7 – 10, 2010.

Acknowledgements

It is a rare privilege to do one of the most exciting jobs on earth: scientific research. However, this thesis would not have been possible without the various and solid support from many people. I am very grateful for the enjoyable personal and scientific environment that surrounded me during my doctoral studies.

Michael Schmidt is thanked for being a great mentor and supervisor ever since my times as an undergraduate student. I was very glad to profit from Michael's broad research experience during e.g. discussions of manuscripts, refinements of presentations or considerations about the next steps of the project. Moreover I benefitted from his large scientific network and could count on his support whenever necessary.

Guido Wiesenberg is thanked for bringing additional scientific expertise and complementary data and perspectives into my PhD project. One of his specialities, the lipid analysis, proofed to be of high value in even two of the above presented papers. Moreover, I highly appreciated that he was always available for valuable discussions, providing rapid and competent feedback at any time (of the day).

Michael Hilf is thanked for his valuable technical inputs during the development and tuning of the improved BPCA method. Moreover, I was always glad for various less scientific discussions during long hours of laboratory work and his dedicated contribution of smoked cigarettes for teaching purposes.

Samuel Abiven is thanked for contributing many creative ideas to my PhD work, which led to the collaboration in one of the above papers and fostered another two ongoing projects with foreign researchers. Moreover, I always appreciated all kinds of statistical and other small talks with him.

Rienk Smittenberg is thanked for his valuable technical and conceptual contributions to the improved BPCA method.

Simon Haberle is thanked for organizing a fruitful research stay with productive field work at the ANU in Australia and for providing precious sediment sample materials.

Jens Leifeld and **Willy Tinner** are thanked for their constructive inputs during PhD committee meetings and for getting me into contact with other researchers.

Further co-authors and collaborators are thanked for the productive collaboration on various occasions, including: **Daniele Colombaroli, Merle Gierga, Bill Hockaday, Marco Keiluweit, Markus Kleber, Evelyn Krull, Carrie Masiello, Anna McBeath, Karis McFarlane, Peter Nico, Lacey Pyle, Max Schneider** and **Ron Smernik.**

Furthermore, all the past and present members of the Soil Science and Biogeochemistry group and associated groups are thanked for creating a very pleasant and inspiring working environment: **Dolores Asensio, Conradin Burga, Beatriz Gonzalez Dominguez, Marco Griepentrog, Ulrich Hanke, Alexander Heim, Anett Hofmann, Bruno Kägi, Bernardo Maestrini, Angela Maurer, Barbara Pichler, Nicolas Roduner, Sandra Röthlisberger, Claudia Schreiner, Corinne Schweri, Nimisha Singh, Kavita Srivastava, Mirjam Studer** and **Ivan Woodhatch.**

Special thanks go to my sister **Jeanine** and my parents **Christa** and **Beat** for trusting in me and supporting me throughout the years, and I would also like to thank my other relatives, in particular Götti **Benno,** Gotti **Marie-Therese** and **Grossmami**.

Moreover, I want to thank **Lucie** for spending lots of delightful and entirely unscientific times together.

"Man kann die Wahrheit nicht ins Feuer werfen – sie ist das Feuer."

Friedrich Dürrenmatt